12-17-2015

Heavy p-Block Analogues of Dithiazolyl Radicals

Thao Thi Phuong Tran
University of Windsor

HEAVY p-BLOCK ANALOGUES OF DITHIAZOLYL RADICALS

By

THAO THI PHUONG TRAN

A Dissertation
Submitted to the Faculty of Graduate Studies
through the Department of Chemistry & Biochemistry
in Partial Fulfillment of the Requirements for
the Degree of Doctor of Philosophy
at the University of Windsor

Windsor, Ontario, Canada

2015

Heavy p-Block Analogues of Dithiazolyl Radicals

by

Thao Tran

APPROVED BY:

_____

P. Ragogna, External Examiner
Western University

_____

D. Northwood
Mechanical, Automotive & Materials Engineering

_____

C. Macdonald
Department of Chemistry & Biochemistry

_____

S. Loeb
Department of Chemistry & Biochemistry

_____

J. Rawson, Advisor
Department of Chemistry & Biochemistry

December 14, 2015

DECLARATION OF ORIGINALITY

I hereby certify that I am the sole author of this thesis and that no part of this thesis has been published or submitted for publication except where indicated otherwise in this thesis.

I certify that, to the best of my knowledge, my thesis does not infringe upon anyone's copyright nor violate any proprietary rights and that any ideas, techniques, quotations, or any other material from the work of other people included in my thesis, published or otherwise, are fully acknowledged in accordance with the standard referencing practices. Furthermore, to the extent that I have included copyrighted material that surpasses the bounds of fair dealing within the meaning of the Canada Copyright Act, I certify that I have obtained a written permission from the copyright owner(s) to include such material(s) in my thesis and have included copies of such copyright clearances to my appendix.

I declare that this is a true copy of my thesis, including any final revisions, as approved by my thesis committee and the Graduate Studies office, and that this thesis has not been submitted for a higher degree to any other University or Institution.

ABSTRACT

This thesis commences with an introduction to the chemistry and materials properties of dithiazolyl radicals and a review of previous research on the isolobal heterocyclic phosphorus-containing derivatives, particularly dithiaphospholes and diazaphospholes.

P-chloro-1,3,2-benzo-dithiaphospholes were prepared from the condensation of PCl_3 and 1,2-benzodithiols in good yield. Reduction afforded $2c,2e^-$ P-P σ-bonded dimers containing a formal P^{II} oxidation state which were characterised by X-ray diffraction. Re-oxidation generates the crystallographically characterised *P*-halogeno-1,3,2-benzo-dithiaphospholes. The synthesis and structural characterisation of the isolobal *P*-chloro-1,3,2-benzodiazaphospholes, $C_6H_4(NR)_2PCl$ (R = H, Me, Et, COMe, COOMe) is described. The outcome of attempted reductive coupling was found to be sensitive to reaction conditions, affording the P^{II} dimer alongside other decomposition products characterised by X-ray diffraction.

Functionalisation of the *P*-chloro group by salt metathesis and/or condensation was used to prepare a series of poly-cyclic structures containing two or more diazaphosphole, dithiaphosphole and dithia-arsole rings linked via bridging units which were characterised by X-ray diffraction. The paddle-wheel molecules $N(C_7H_6S_2Pn)_3$ (Pn = P, As) were prepared by a stepwise condensation of $Li[N(SiMe_3)_2]$ with *P*-chloro-dithiaphosphole and *As*-chloro-dithia-arsole whereas the bis-triamide $C_6H_4(NR[C_6H_4(NR)_2P])_2$ was prepared from condensation of the *P*-chloro-diazaphosphole with *ortho*-$C_6H_4(NHR)_2$.

Treatment of *P*-chloro-dithiaphospholes or *P*-chloro-benzodiazaphospholes with MCl_3 (M = Al, Ga) generated a series of two-coordinate phosphenium cations whose structures were determined by X-ray crystallography. This methodology was extended to prepare the heavier dithia-arsenium and dithia-stibenium cations and the structure of the first benzodithia-arsenium cation is reported. These cations

are Lewis acidic and form a series of 1:1 complexes with Ph_3E (E= P, As, Sb) which are characterised by multinuclear NMR. The dithiaphosphenium cation (as its $GaCl_4^-$ salt) also forms adducts with dioxane and propylene oxide but is an efficient catalyst for the cationic ring opening polymerisation (CROP) of THF to form poly(THF), $[O(CH_2)_4]_n$. The conversion rate and yield is sensitive to reaction conditions. Notably the corresponding $AlCl_4^-$ salt did not polymerise THF due to reformation of the *P*-chloro-dithiaphosphole and formation of the adduct, $AlCl_3 \cdot 2THF$. The related arsenium and stibenium cations show limited activity as reagents for the CROP of THF.

DEDICATION

I dedicate my dissertation to my Mom, my Dad, and my Family who have been loving me unconditionally, and guiding me to live a more fulfilling and more meaningful life.

ACKNOWLEDGEMENTS

First of all, I would like to express my highest gratitude to Professor Jeremy Rawson for granting me the opportunity to work in his group. I sincerely appreciate his guidance, help, support, patience, and friendship through my years of graduate study. I am grateful for his training in EPR spectroscopy (even if my samples were invariably silent!), single crystal X-ray diffraction, X-ray structure solution and refinement as well as computational chemistry. His assistance in collecting single crystal X-ray data, and completing structure solution and refinement is highly acknowledged. I also appreciate his great help in revising my thesis. I am especially thankful for his open-minded working styles in giving me total freedom environment to explore the phosphorus chemistry. Without his talent and encouragement, I could hardly approach and comprehend these new research areas.

I am indebted to the current and previous members of the Rawson group. Dr. John Hayward and Dr. Muhammad Usman Anwar worked tirelessly to take care of the labs so that I have a clean and joyful workplace. Dr. Anwar is also acknowledged for showing me how to use the diffractometer, for helping me collect some single crystal X-ray data and do some preliminary structure solution. I would like to thank Adam Dunmore (Outstanding Scholar and 410 student) for his collaborative work and contributions to Chapter 3. Other group members are acknowledged for their help and making graduate studies a great and memorable time.

I am grateful to my current and past committee members Professor Holger Eichhorn, Professor Ricardo Aroca, Professor Charles Macdonald, Professor Stephen Loeb, and Professor Derek Northwood, who have given me continuous support, help, and valuable feedback.

I would like to thank the Natural Sciences and Engineering Research Council of Canada, University of Windsor, the Department of Chemistry & Biochemistry for the support in funding, administration, and maintenances of chemistry instruments.

I would like to show appreciation towards Dr. Zhuo Wang for training me in air-sensitive techniques in my chemistry, Dr. Matthew Revington for his training on NMR spectrometer, Dr. Janeen Auld for undertaking mass spectroscopy and elemental analysis for some samples, Mr. Tuan Hoang for collecting powder X-ray data, Ms. Elizabeth Kickham and Ms. Marlene Bezaire for preparing the paperwork, and Mr. Al Ditchburn for repairing broken glassware.

Most importantly, I would like to express greatest gratitude to my parents and my family for their continuous support, their care, their love, and their encouragement, and providing me with the meaning and purpose of life.

TABLE OF CONTENTS

LIST OF TABLES

LIST OF FIGURES

LIST OF SCHEMES

LIST OF APPENDICES

LIST OF ABBREVIATIONS/SYMBOLS

3Cn	3-center non-Lewis orbital
6-31G*+	split-valence double-zeta basis set with polarization and diffuse Gaussian functions
6-311G*+	split-valence triple-zeta basis set with polarization and diffuse Gaussian functions
^{o}	degrees
Å	Ångström
ATR	attenuated total reflectance
AROP	Anionic Ring Opening Polymerisation
a.u.	atomic unit, 1 a.u. = 627.5 kcal/mol
a_X	hyperfine coupling constant to nucleus X
bm	broad, medium
B3LYP	Becke, 3-parameter, Lee-Yang-Parr functional
BBDTA	Benzo-bis(1,3,2-dithiazolyl) radical
BD & BD*	2-center bond & 2-center antibond
C_{3v}	local 3-fold symmetry
^{o}C	Celsius
cf.	*confer* (compare)
CROP	Cationic Ring-Opening Polymerization
Cp	cyclopentadienyl
δ	chemical shift (NMR) or atomic partial charge (DFT calculation)

d	doublet (in NMR) or bond length (in crystal)
dd	doublet of doublet
DFT	Density Functional Theory
DTA	Dithiazolyl radical
DTDA	Dithiadiazolyl radical
E(2)	energy of second order perturbations within an NBO analysis
E(NL)-E(L)	Energy difference between donor (L) and acceptor (NL) orbitals
ECP	Effective Core Potential
e.g.	*exempli gratia* (for example)
endo/exo	endocyclic/exocyclic
EPR	Electron Paramagnetic Resonance
Et	ethyl
et al.	*et alia* (and others)
eV	electron Volt
F(L,NL)	the Fock matrix element between L and NL NBO orbitals
FT	fourier transform
g	gram or g value in EPR spectroscopy
G_{tot} & ΔG_{dim}	Total Gibbs free energy & Gibbs free energy change in dimerization
H_{tot} & ΔH_{dim}	Total enthalpy & enthalpy change in dimerization
ΔH_{f298}	enthalpy change at 298 K
h	hour(s)

HOMO	Highest Occupied Molecular Orbital
Hz/MHz	Hertz/Megahertz
$\{^1H\}$	proton decoupled
i.e.	*id est* (it is)
IR	Infrared
^{i}Pr	isopropyl
J	NMR coupling constant
K	Kelvin
kJ	kilojoule
L/NL	Lewis/non-Lewis donor-acceptor type
LACV3P	triple-zeta basis set developed at Los Alamos National Laboratory
LP	1-center valence lone pair
LUMO	Lowest Unoccupied Molecular Orbital
LV	unfilled valence non-bonding orbital of "lone vacancy"
m	multiplet (in NMR spectrum) or medium (in IR spectrum)
mL	milliliter
mmol	millimole
mM	millimole per liter
Me	methyl
MeCN	acetonitrile
Mes*	2,4,6-$C_6H_2(^tBu)_3$

M_n	number-average molecular weight of polymer
MO	molecular orbital
MS	Mass Spectrometry
MW	Molecular Weight
NBO	Natural Bond Orbital
NHCs	*N*-heterocyclic carbenes
NHPs	*N*-heterocyclic phospheniums
NMR	Nuclear Magnetic Resonance
P	primitive unit cell
PDI	Poly-dispersity Index
Pn	pnictogen element (group 15 element)
ppm	parts per million
Ph	Phenyl
PXRD	Powder X-Ray Diffraction
R^2	goodness-of-fit of linear regression
R	alkyl or aryl
ROMP	Ring Opening Metathesis Polymerisation
ROP	Ring Opening Polymerization
RROP	(free) Radical Ring Opening Polymerisation
RT	room temperature
σ^3-Pn	neutral tricoordinate pnictogen

σ_m & σ_p	Hammett parameters (*meta* and *para* substituted benzene rings)
$\sigma_{dia}/\sigma_{para}/\sigma_{neigh}/\sigma_{other}$	diamagnetic shielding/paramagnetic shielding/neighbouring group shielding/other effects shielding constants
s	singlet (in NMR spectrum) or strong (in IR spectrum)
SOMO	Single Occupied Molecular Orbital
t	triplet (in NMR spectrum)
TOF-MS	Time-of-flight Mass Spectrometry
^{t}Bu	*tert*-Butyl
THF	Tetrahydrofuran
U_{tot} & ΔU_{dim}	Total internal energy & internal energy change in dimerization
υ_{max} (cm^{-1})	IR absorption frequency
w	weak (in IR spectrum)
ZPE	Zero Point Energy

CHAPTER 1

GENERAL INTRODUCTION

1.1 Introduction

1.1.1 Overview of research: Phosphorus-containing materials and their analogues

This dissertation presents studies on the synthesis, characterization, exploration, and catalytic properties of new five-membered heterocylic materials based on phosphorus and other heavy *p*-block group 15 elements (arsenic and antimony). Phosphorus is often considered as "*a carbon copy of carbon*" due to the similar reactivity and bonding associated with these two elements.[1] This similarity arises out of the diagonal relationship between these elements which leads to similar electronegativities (χ_C 2.55; χ_P 2.19) and bond enthalpies to a range of elements (*e.g.* C-O 358 kJ mol^{-1}; P-O 335 kJ mol^{-1}; C-Cl and P-Cl at 327 and 326 kJ mol^{-1}, respectively; C-F 485 kJ mol^{-1}; and P-F 490 kJ mol^{-1}).[2] Although the P-P bond (209 kJ mol^{-1}) is somewhat weaker than C-C (346 kJ mol^{-1}), there is still a propensity for P-based compounds to catenate. This is highlighted by the many forms of elemental P including white phosphorus (P_4), red and black phosphorus.[3] In addition, many other cyclic and acyclic catena-phosphorus compounds are known.[4] While π-bonding between the lighter main group elements (B, C, N, O) is well established and the strength of π-bonding for these light atoms is comparable with σ-bonding, the more diffuse nature of the 3*p* orbitals is typically considered to lead to weaker π-bonding and a tendency to oligomerise. As a consequence multiple bonding for the heavier *p*-block elements is generally less common. Indeed it was not until 1981 that the first compound containing a P=P double bond, Mes*P=PMes*, was reported by Yoshifuji.[5] The use of sterically protecting groups to inhibit oligomerisation has also been employed to generate As=As, Sb=Sb and Bi=Bi bonds.[6] Since then other multiple bonds to phosphorus have been reported, including phospha-alkynes, RC≡P.[7]

Besides the well-defined examples of simple homoleptic E=E multiple bonds, a range of π-conjugated P-containing heterocycles are known. Amongst some of the most common are those related *via* formal isolobal substitution of RC by P within conventional all-carbon aromatics such as $C_5H_5^-$ and C_6H_6. For example a range of 'metallocenes' based on the $(^tBuC)_3P_2^-$ anion have been reported by Nixon[8] and P-rich analogues of benzenes, exemplified by tri-*t*-butyl-1,3,5-triphosphabenzene, $(^tBuC)_3P_3$ have been reviewed.[9] Although the degree of heteroaromaticity still remains under some debate,[10] an examination of the series of P-substituted aromatics expose a group of well-correlated thermodynamic, structural, and chemical properties. Nowadays the aromaticity has been explicitly noted in phosphorus-containing 6π systems.[10a] A widespread series of heterophospholes including O, S, Se, and N heteroatoms have been found to exhibit heteroaromaticity and significant aromatic stabilization energy.[10a,11]

Similar to other elements of the third period, phosphorus possesses diffuse valence orbitals leading to longer bonds and more polarisable electron density which stabilise longer-range bonding interactions through dispersion forces or significant bonding at distances at or beyond the conventional P-P bond length (2.20Å).[2]

The overall aim of this research is to combine several topics following current trends of heterocyclic chemistry, focusing on several isolobal π-delocalised structures which build upon dithiaphospholyl **A**, diazaphospholyl **B**, and some arsenic/antimony analogues of **A**. These structures are isolobal with 1,3,2-dithiazolyl (DTA) radicals **C** which have been known to possess some interesting magnetic properties which are discussed in the next section.[12]

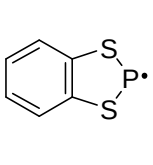

Benzo-1,3,2-dithiaphospholyl radical

A

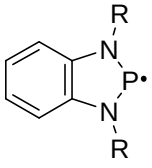

Benzo-1,3,2-diazaphospholyl radical

B

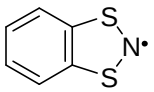

Benzo-1,3,2-dithiazolyl (DTA) radical

C

1.1.2 Physical properties of dithiazolyl (DTA) radicals

Developments in sulfur–nitrogen chemistry have made significant contributions in the synthesis of molecular materials. In the last few decades thiazyl (S/N containing) and selenazyl (Se/N containing) radicals have attracted particular attention as building blocks for both conducting and magnetic materials,[12c,13] as well as paramagnetic ligands in coordination[14] and organometallic chemistry.[14b] For example, work by Oakley has focused on the use of thiazyl and selenazyl radicals as conducting materials, achieving true metallic behaviour with conductivities up to 10^2 S/cm for selected pristine and doped radical systems.[15] Within the Rawson group the family of dithiadiazolyl (DTDA) radicals has been studied as building blocks for molecule-based magnets with magnetic ordering up to 70 K.[12c,14a,16] These DTDA radicals have also been used as paramagnetic ligands in coordination chemistry and as building units in photoconductors.[14a,17]

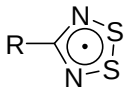

Dithiadiazolyl (DTDA) radical

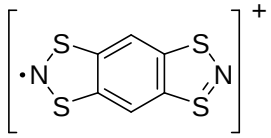

Benzo-bis(1,3,2-dithiazolyl) diradical (BBDTA)

The closely-related 1,3,2-DTA radicals **C** have also been investigated.[12,14a,15a,18] The DTA radical **C** was originally reported by Wolmershauser[19] and subsequent studies by Passmore[20] indicated that N-N σ-bond formation was unfavourable and **C** is found to exist in equilibrium with its π*-π* dimer, $(\mathbf{C})_2$ in solution. In the solid state **C** adopts a multi-centre π*-π* diamagnetic dimer motif with close intra-dimer S···S contacts ($d_{S\cdots S}$ = 3.1752(8) Å) although heating generates a poorly defined paramagnetic phase which undergoes long range antiferromagnetic order below 13 K.[18c,21] Other derivatives of these radicals also exhibit bulk magnetic order with the tetrachlorogallate salt of the radical cation $BBDTA^{+\bullet}$ exhibiting ferromagnetism below 7 K,[22] whereas [BBDTA][$FeCl_4$] is a ferrimagnet below 44 K.[23] However it is the propensity for many DTA derivatives to exhibit bistability, in which they undergo a first order phase transition between a diamagnetic dimer motif and a paramagnetic monomer which has attracted particular

attention as this can occur at/near room temperature, with spin switching driven by heat, light, and pressure.[12c,24] This behaviour offers the potential for switchable materials for data storage. In addition, the 7π-electron 1,3,2-dithiazolyl (DTA) radicals also form conducting charge-transfer salts.[18a]

There has been a considerable body of work dedicated to the expansion of these families of sulfur–nitrogen radicals. Pioneering research on heterocyclic C/N/S chemistry by Banister,[25] Roesky,[26] Passmore,[20] Oakley,[27] Chivers[28] and Rawson[12c,d] *inter alia* initiated the development of many thiazyl-based radical ring systems. Recent work by Oakley has shown that the magnetic anisotropy of these radicals can be substantially enhanced by the inclusion of heavy *p*-block elements[15c,29] since the spin-orbit coupling constant scales as Z^4 (Z denotes the nuclear charge).[30] As a consequence, while light atom radicals (C/N/O) are expected to give little magnetic anisotropy and behave as 'Heisenberg' spin systems with small coercive fields, replacement of these lighter *p*-block elements such as C, N, O by heavier *p*-block elements such as P, S are highly desirable to develop radicals with larger magnetic anisotropy necessary to form permanent magnets.

1.1.3 Dithiaphospholes - Analogues of DTA structures

Inorgano-phosphorus chemistry has been entirely revitalized through the discovery and development of stable phosphorus derivatives since the beginning of the 1970's. There are many types of phosphorus-containing heterocyclic structures. These include trivalent phosphorus atoms which bear a lone-pair with representative coordination numbers of two or three, to pentavalent ones exhibiting general coordination numbers between four and six. In addition, low valent P^I chemistry has become an established field.[11] Among five-membered heterocycles containing mixed group 14, 15, and 16 elements, those with phosphorus and sulfur have gained less attention than the ones with phosphorus and oxygen due to their synthetic limitations.[31] However the benzo-1,3,2-dithiaphosphole **A** can be considered as a heavier *p*-block analogue of the benzo-1,3,2-DTA radical **C** through isovalent replacement of N by its heavier pnictogen congener, P. Indeed these form two examples within a larger series of similar bicyclic structures containing a five-membered heterocycle [C_2S_2Pn] (Pn = group 15 elements N, P, As, Sb).

1.1.3.1 Syntheses of dithiaphospholes

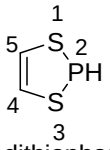

1,3,2-dithiaphosphole

S1

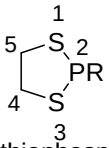

1,3,2-dithiaphospholane

S2

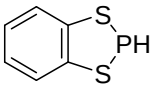

Benzo-1,3,2-dithiaphosphole

S3

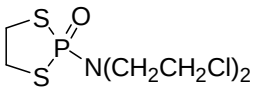

S4

1,3,2-dithiaphosphole **S1** is closely related to the 1,3,2-dithiaphospholane **S2** (R = H) which was first synthesized by Arbuzov and Zoroastrova in 1952.[32] Benzo-1,3,2-dithiaphosphole **S3**, originally named 1,3-dithia-2-phosphaindan, was initially prepared in 1960 by Campbell and Way in a stereochemical examination of the optical stability induced only by three-covalent phosphorus-containing compounds.[33] The 1,3,2-dithiaphospholane-2-oxide derivatives **S4** containing >PN($CH_2CH_2C1)_2$ side-chain have been studied due to their potential activity as neoplasm (tumor or abnormal tissue) inhibitors.[32c,34]

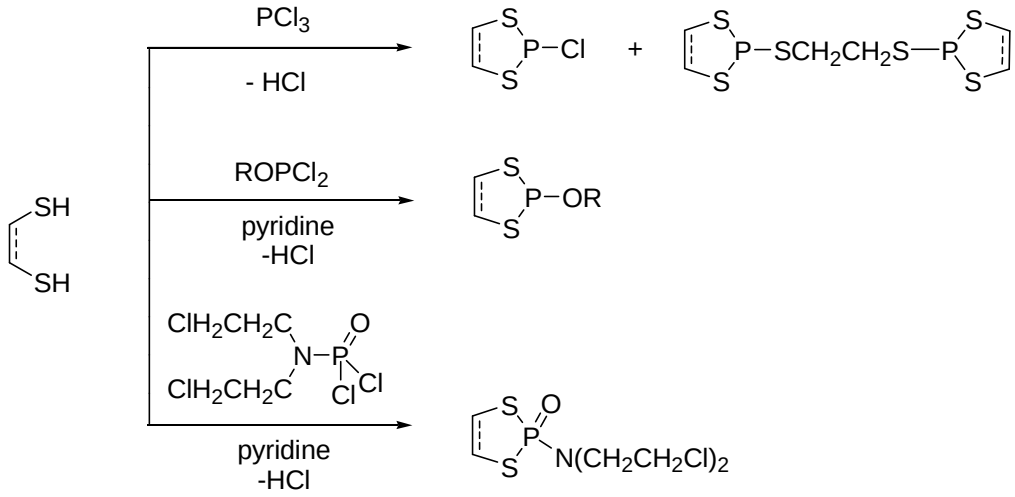

Scheme 1.1. Syntheses of monocyclic 1,3,2-dithiaphosphole derivatives.[32c]

Generally, the dithiaphosphole heterocycle is generated *via* ring-closure condensation between a dithiol and a phosphorus halide derivative with the HCl by-product eliminated by heating or the addition of a base.[32c,35] Most of these heterocycles have developed from

commercially available 1,2-ethanedithiol, 1,2-ethenedithiol, benzene-1,2-dithiol and toluene-3,4-dithiol starting materials (Schemes 1.1 and 1.2).

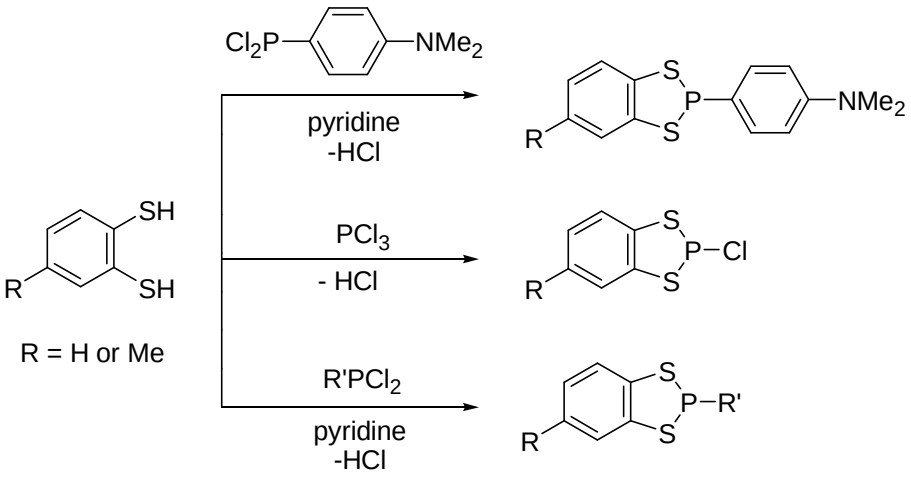

Scheme 1.2. Syntheses of bicyclic 1,3,2-dithiaphosphole derivatives.[35]

1.1.3.2 Chemical reactivities of dithiaphospholes

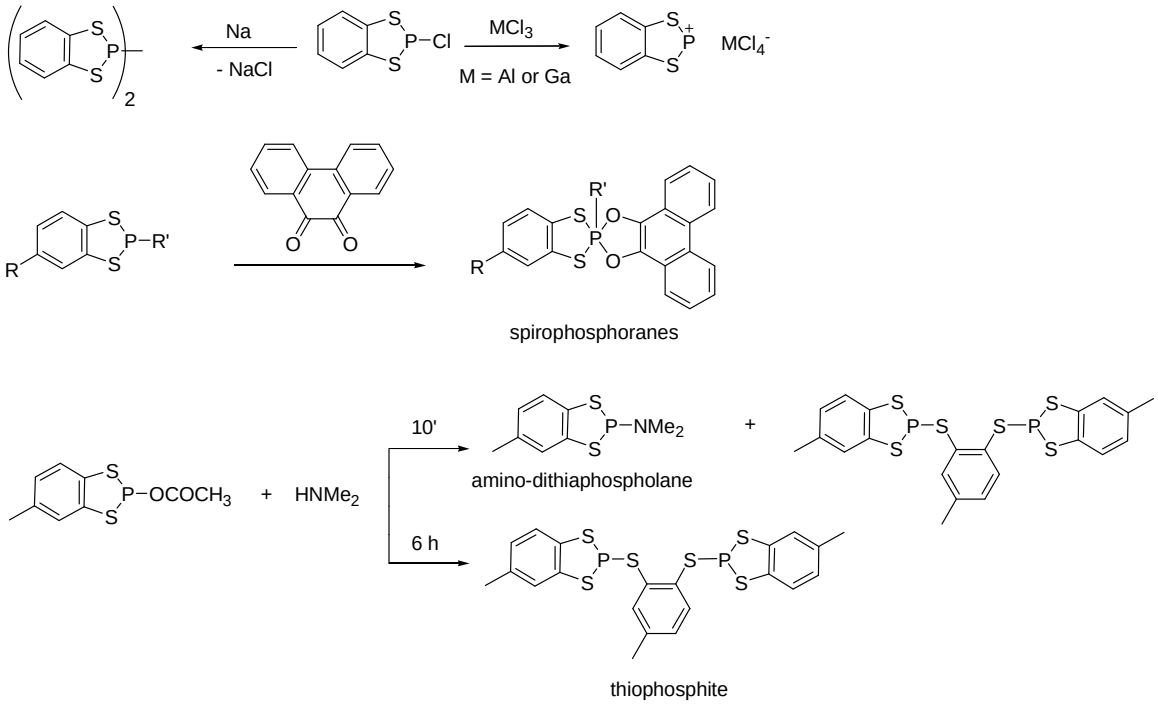

Scheme 1.3. Chemical reactivities of the dithiaphosphole family.[35-36]

Dithiaphospholes have been investigated as starting materials to synthesize other P-containing heterocycles such as the 2-coordinate phosphenium cation,[36a,b] low oxidation state P^{II} systems,[35] new sulfur-containing spirophosphoranes, amino-dithiaphospholane,[36c] and diphosphite[36c] (Scheme 1.3). However the chemistry of these heterocycles is not well explored, and predominantly stems from a few studies by Baudler[35] in the 1970's and Burford[36a,b,36d-f] in the 1980's. In many cases a mixture of products was obtained with a paucity of structural data with compounds predominantly characterised by NMR spectroscopy.

The lone pair associated with the P^{III} centre offers potential Lewis base behaviour, *e.g.* for coordination to softer transition metals and a small number of studies have recently focused on dithiaphospholanes as ligands, for example the complexes **S5** – **S7**.[37] Notably both the complexes **S5** and **S6** catalyze the etherification between propargylic alcohols and methanol or ethanol (8–48 h, 90 ^{o}C, 40–85% isolated yields).[37a]

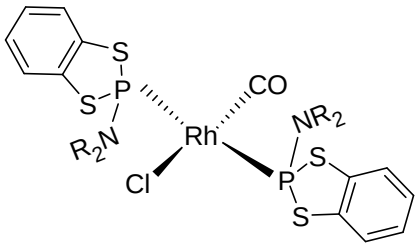

S5

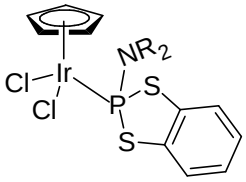

S6

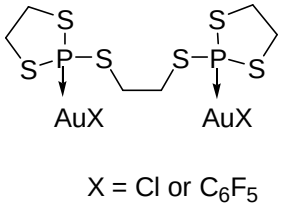

S7

1.1.4 Diazaphospholes - Isolobal Analogues of DTA Structures

Heterocycles comprising phosphorus–nitrogen frameworks are considered to be one of the oldest inorganic rings ever known, and they have attracted applications as precursors for inorganic polymers (polyphosphazenes),[38] powerful bases, nucleophiles, or catalysts in inorganic synthesis.[39]

Diazaphospholes comprise a five-membered ring containing one phosphorus and two functionalised nitrogen atoms. These represent a more thoroughly examined group of heterophospholes than the dithiaphospholes described in the last section. However,

research on neutral monocyclic 1,3,2-diazaphosphole **N1** which is proposed as a transient species has not been fully developed so far. In contrast, its ionic derivatives such as anion **N2** and cation **N3** are more stable and have been synthesized.[40] The synthesis of cyclic phosphenium cation **N3** can be readily accessed by P-hydride abstraction of **N4**.[41]

Pilgram and Korte[42] are credited for their initial discovery of an anellated azaphosphole. In 1963 they reported the synthesis of the first diazaphosphole, *N*-phenyl-1,3,2-benzodiazaphosphole **N5**, from condensation between *N*-phenyl-1,2-diaminobenzene and triphenylphosphite at 150–180 °C. Even though this compound was later found to undergo oligomerization,[43] their discovery was farsighted in terms of signifying the possibility of the involvement of two-coordinate, trivalent phosphorus in cyclic delocalization thereby affording aromatic stabilization.

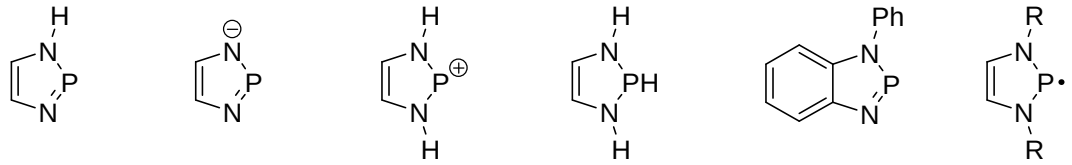

N1 **N2** **N3** **N4** **N5** **N6**

There is not a standardized nomenclature for organophosphorus compounds due to the co-existence of several more or less systematic classifications. The parent neutral heterocycle **N1** always appears to be designated as a 1,3,2-diazaphosphole and the anion **N2** is named as a 1,3,2-diazaphospholide. The neutral *N*-heterocyclic phosphine **N4** has been called either a 2,3-dihydro-1,3,2-diazaphosphole or 1,3,2-diazaphospholene while its completely saturated heterocycle is then named as 1,3,2-diazaphospholidine. Cation **N3** can be categorized as a derivative of **N4** and can therefore be designated as either a 1,3,2-diazaphospholium or 1,3,2-diazaphospholenium ion.[10b] In addition, the dicoordinate phosphorus cations (>P^+) like **N3** are also referred to as phosphenium cations.[31b,36a,b,44] In this thesis ions of type **N3** will be referred to as phosphenium cations for consistency. Covalently bound precursors such as derivatives of **N4** where P-H is replaced by P-X will be described as *P*-chloro phospholes etc. In addition the radicals derived from reduction of these phospholes wil be described as phospholyl radicals. The corresponding radical

N6 can be considered to be isolobal with the DTA radical through replacement of (i) S by N-R and (ii) N by P and both can be classified as five-membered heterocyclic 7π-electron radicals.[12c,45]

1.1.4.1 Syntheses of diazaphosphole derivatives

Synthesis of *C*-alkyl-substituted or benzo-fused five-membered-ring diazaphospholes can be typically achieved *via* a [4+1] cyclo-condensation between an electrophilic P and a nucleophilic C_2N_2 building block. Amongst these neutral 1,3,2-diazaphospholes, the *P*-halogeno-substituted diazaphospholes are available *via* condensation of 1,2-diamines with PX_3. For example, the single-ring 2-chloro-1,3,2-diazaphosphole has been produced by means of condensation between diaminomaleonitrile and PCl_3 (Scheme 1.4).[46] Such *P*-halogeno-diazaphospholes have been used as precursors for further reactions such as coupling reductions, halide substitutions, and halide abstractions.[40]

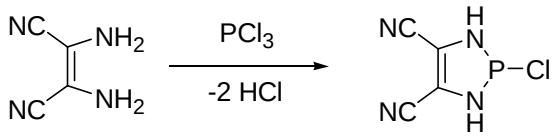

Scheme 1.4. Synthesis of monocyclic 2-chloro-1,3,2-diazaphosphole.

Additionally, α-diimines are the most common starting materials toward the syntheses of monocyclic diazaphosphole derivatives. They can undergo base-activated reactions with PCl_3 to form 2,4-dichloro-1,3,2-diazaphospholes. On the other hand, they can be transformed into di-lithio-diamines *via* two-electron reduction (by Li, Na, or Mg), followed by condensation with PCl_3[44d] or $RPCl_2$[44d,47] to form diazaphospholes (Scheme 1.5).

Similarly, benzannulated 1,3,2-diazaphospholes are readily obtained from *N*,*N*′-disubstituted *o*-phenylenediamines *via* base-promoted condensation with PCl_3 or $RPCl_2$.[48]

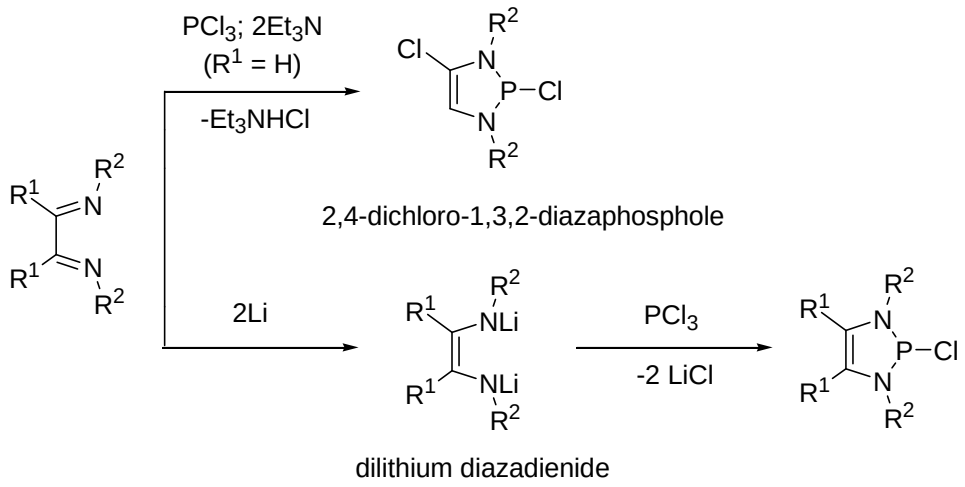

Scheme 1.5. Syntheses of monocyclic 1,3,2-diazaphosphole derivatives from diimines.[44d,47]

1.1.4.2 Chemical reactivities of diazaphosphole derivatives

P-functionalized 1,3,2-diazaphospholes (X = Cl, Br, I) have attracted significant interest due to their distinctive reactivity which can be attributed to the bond/no-bond resonance (covalent *vs* ionic resonance) forms (Scheme 1.6).[49]

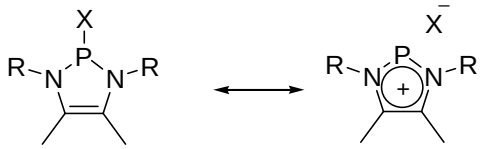

Scheme 1.6. The bond/no-bond resonance forms of *P*-functionalized 1,3,2-diazaphospholes.

The unique P-X bonding in *P*-functionalized 1,3,2-diazaphospholes is characterized by considerable n(N)-σ*(P-X) hyperconjugation, leading to strong polarization of the P-X bond in the sense $^{\delta+}P-X^{\delta-}$.[49] Surprisingly, this induced polarization is preserved even when P and X have similar electronegativities (X = H, P (χ_P = 2.1)).[41,47b,49] The majority of publications regarding the chemical reactivities of 1,3,2-diazaphospholes and their derivatives have focused on substitution of functional groups at the C, N, and P atoms of these heterocycles. The reactivities related to P-X bonds have been extensively studied

and *P*-halogeno-diazaphospholes are commonly utilized as starting materials[45] which facilitate substitution of the *P*-bound halogen by another halogen,[47b] hydrogen,[41,47a] phosphino,[50] amino,[51] or alkoxy groups[52] (Scheme 1.7). Many *P*-chloro-diazaphosphole derivatives are air and moisture sensitive, showing both oxidation to P(V) and hydrolysis of the P-Cl bond.[53]

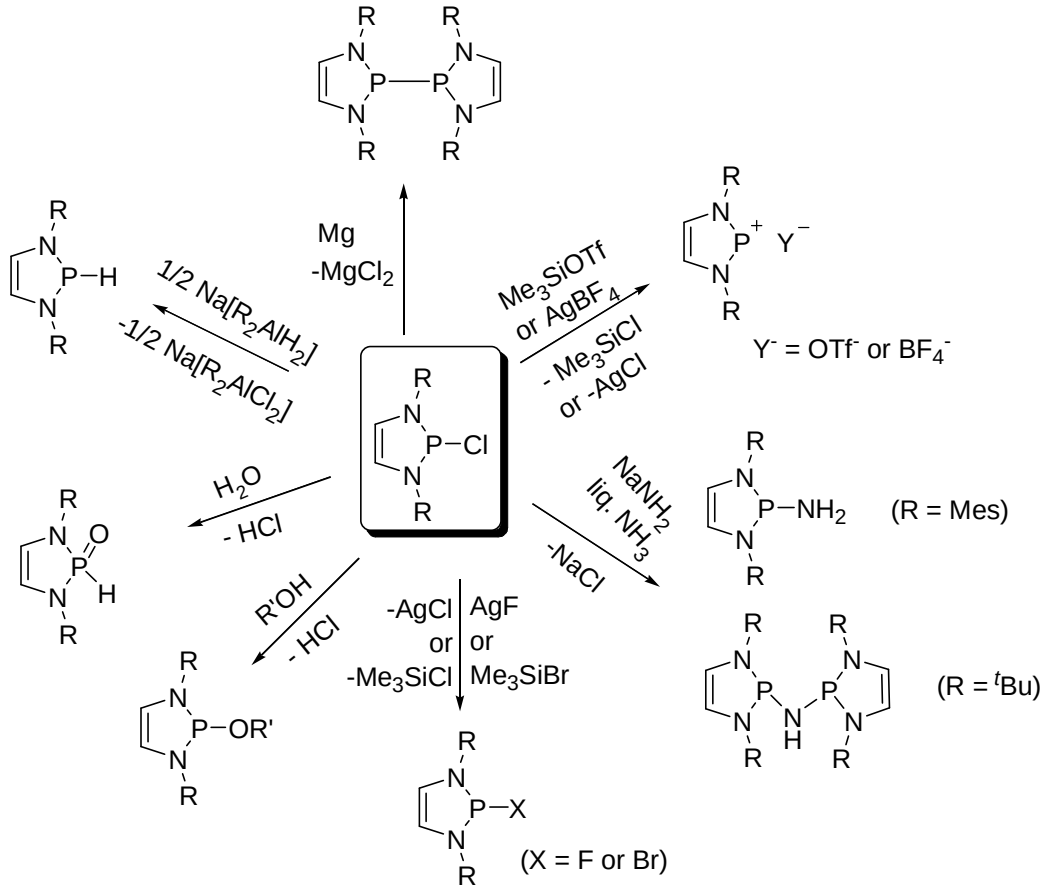

Scheme 1.7. Reactivities of *P*-chloro-1,3,2-diazaphospholes.[41,47,50-53]

1.1.5 Phosphenium (R_2P^+), arsenium (R_2As^+), and stibenium (R_2Sb^+) ions

Phosphines (PH_3, RPH_2, R_2PH) have been considered as conventional ligands particularly for low oxidation state metals due to (i) their lone-pair donor capacity; (ii) the availability of low-lying P-C σ* orbitals which offer some π-acceptor characteristics and (iii) the ability to fine-tune both the steric and electronic properties of the phosphine.[54] As a consequence phosphines are amongst the armoury of strong field ligands used in

organometallic chemistry in which the steric and electronic nature of the phosphine can be systematically tuned.[44a,55]

In recent decades, singlet carbenes have attracted significant interest in coordination chemistry and organometallics as alternatives to phosphines due to their strong σ-donor character and tunable π-acceptor character.[56] In particular Arduengo's development of *N*-heterocyclic carbenes (NHCs) has been rapidly deployed in a range of active catalysts including the Grubbs-II catalysts for olefin metathesis.[57] The relationship between carbenes, their heavier silylene congeners and the isoelectronic phosphenium cations, which are simply attained by treatment of R_2PCl with $AlCl_3$,[11] offers a series of singlet carbene-analogues which simultaneously offer a lone pair of electrons and a formally vacant *p* orbital.[44e] Replacement of the carbene C by isolobal P^+ leads to a phosphenium cation capable of acting as a poor σ-donor but strong π-acceptor (Figure 1.1).[44e,56e,58] Similarly, replacement of C by Si leads to silylenes which offer a softer donor set to the metal center.[59]

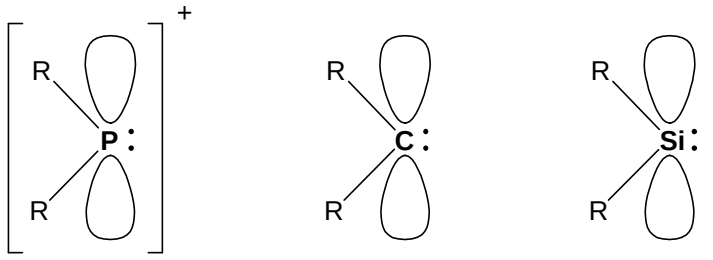

Figure 1.1. The parallel between the singlet states of phosphenium cations, carbenes, and silylenes.

Such isolobal analogies provide a drive to establish novel synthetic methodologies which may lead to new structures, bonding, and chemical reactivities.[60] Phosphenium (R_2P^+), arsenium (R_2As^+), and stibenium (R_2Sb^+) ions have been shown to exhibit amphoteric properties as either Lewis acids or prospective Lewis bases because they offer both a lone pair of electrons and a vacant *p* orbital.[44a,44e,61] Here the steric and electronic effects of the R groups coupled with the ability to tune the 'hardness' of the group 15 element, offers a potentially strong chemical diversity in Lewis acid/base character as a potential ligand.

Their Lewis acidic nature was first illustrated by the formation of phosphenium-phosphane adducts in which phosphanes act as Lewis bases in the research of Schultz and Parry.[62] For instance, the cation Ph_2P^+ acts as a Lewis acid regardless of the existence of lone-pair electrons at the phosphorus atom.[44c] Since the mid-1970s, phosphenium ion chemistry has attracted progressively more interest from chemists. These species have proved to be very useful reagents with versatile reactivity due to their electrophilic character. Conversely, the phosphorus lone pair is attributed to their reactivity toward azides, and to exhibit a rich coordination chemistry.[44e,63]

1.1.5.1 General synthesis of phosphenium, arsenium, and stibenium cations

The simplest models of coordination chemistry can be constructed by the combination of electron-rich pnictogen centers and electron-deficient group 13 centers (*e.g.* donor-acceptor bond $R_3N\rightarrow BX_3$). Examples of phosphorus coordination chemistry are well-known (*e.g.* $R_3P\rightarrow EX_3$).[64] For chlorophosphines, although P→E coordination [*e.g.* $R_2(Cl)P\rightarrow ECl_3$; E = Al or Ga] has been detected in some examples,[65] the Lewis acidic ECl_3 ($AlCl_3$ or $GaCl_3$) favours interaction with the chlorine center of the chlorophosphine, resulting in heterolytic cleavage of the P-Cl bond to yield phosphenium salts R_2P^+.[44e] In addition, the naturally weak-donor potential of halophosphines[66] and the heterolytic lability[62] of P-X bonds permit the generation of new interesting structures instead of formation of a coordinate P→E bond.

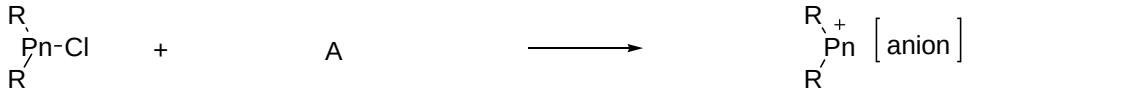

Pn = P/As/Sb Halide abstracting agent [anion] = $[AlCl_4]^-$; $[GaCl_4]^-$; $[OSO_2CF_3]^-$

Scheme 1.8. General synthesis of phosphenium, arsenium, and stibenium cations.

1.1.5.2 N-*heterocyclic cations*

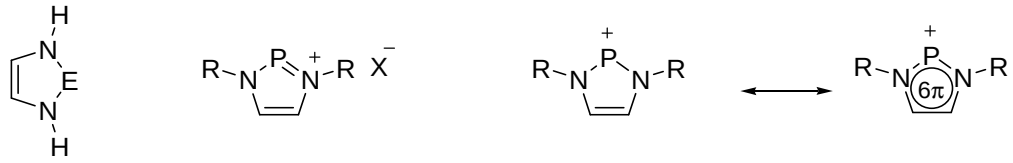

N7 **N8** **N9** **N10**

The five-membered heterocyclic systems **N7** (E = N^+, P^+, As^+, Sb^+) have flourished as a consequence of the discovery of stable carbene (**N7**, E = C:) in the early 1990s. These N-heterocyclic carbenes are powerful nucleophiles, and have great contributions in coordination chemistry as well as in catalysis.[56c] Although the cyclic phosphenium cation **N7** (E = P^+) was discovered (in 1972)[67] before the carbene analogue, its significance was not widely appreciated. However, the numerous and valuable applications of carbenes have aroused an uninterrupted pursuit of isoelectronic inorganic replacements from other elements in groups 13–16.[40]

Recently, the 6π-aromatic 1,3,2-diazaphosphenium ions (**N9**, **N10**) symbolized cyclic phosphenium cations have intrigued chemists since they are isoelectronic with the well-known and heavily utilised family of Arduengo carbenes. The solid state structure of **N8** (R = ^{t}Bu, X = Cl) reveals a P···Cl distance (2.715(2) Å)[44d] shorter than the sum of the van der Waals radii (3.55 Å)[68] but notably longer than those of representative covalent P–Cl bonds (PCl_3 2.043 Å,[69] Mes*NPCl 2.142(4) Å,[70] Mes* = $C_6H_2{}^tBu_3$-2,4,6). This compound undergoes autoionisation in solution and is a regular observation for non-metals and certain phosphenium salts in which anion–cation interactions are less than the sum of the van der Waals radii, and appear somewhat insensitive to the structural characteristics of the cation or anion.[71] Clearly solvation of the cation and anion in polar solvents compensate the cleavage of the P-X bond. The bonding, structure, reactivities and aromatic nature of *N*-heterocyclic phosphenium cations have currently become the themes of experimental and theoretical research.[44b,44d,44f,g,47b,72]

1.1.5.3 S-heterocyclic phosphenium cations

Calculations have revealed that the π-bond strengths of P=N (44 kcal·mol^{-1}) are comparable to those of P=S (40 kcal·mol^{-1}).[73] This theoretical analysis supports the fact that aromatic structures containing $[S_2P]^+$ as well as their analogues ($[S_2As]^+$, $[S_2Sb]^+$) might also offer alternatives to N-heterocyclic stabilised phosphenium cations. These species are believed to gain their stability based on two principles: i) their 6π-electron count follow the Hückel 4*n*+2 rule; ii) the π-delocalization of the positive charge over the aromatic framework,[74] although this occurs *via* 2*p*-3*p* π-bonding in *N*-heterocyclic phospheniums (NHPs) and *via* 3*p*-3*p* π-bonding in S-heterocyclic phospheniums.[36] For diazaphosphenium cations the P-N bonds are polarised $P^{\delta+}$-$N^{\delta-}$ (Pauling electronegativities of P and N are 2.19 and 3.04 respectively), leaving much of the positive charge on the P-centre. This makes the P centre an efficient Lewis acid, but rather poor Lewis base. Conversely the electronegativity of S (2.58), whilst larger than that of P, is less than that of N and is expected to lead to poorer Lewis acidity but better Lewis-base character.

S8

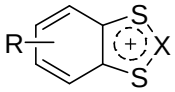

S9

X = P/As/Sb

Despite the fact that monocyclic 1,3,2-dithiaphosphenium $C_2S_2P^+$ cations (**S8**) theoretically adopt planar aromatic structures, their salts have not been isolated yet.[75] The inclusion of a benzene ring into the two-carbon backbone can afford extensive stability in 1,3,2-benzodithiaphosphenium ions and heavier atom analogues (**S9**). The 1,3,2-benzodithiaphosphenium ions are considered as 10π-heteronaphthalenic cations which are stabilized by pπ-pπ bonding between P(III) and S. Crystallographic studies by Burford on $[C_6H_4S_2P][AlCl_4]$ reveals this heterocycle adopts planar geometry.[36a,b,36d,e] The shortening of the P-S bond with respect to $C_6H_4S_2P$-Ph reflects stabilisation by 3*p*π-3*p*π bonding, providing insight into the capacity for π-bonding between these heavier

main group elements. The isolobal nature of these SHPs in relation to the more thoroughly studied NHPs indicate these systems may offer some potential Lewis acid/base character.[31b,36a,b,36d-f] Although several S-E-S (E = P, As, Sb) salts have been isolated as air-sensitive, yellow-to-orange crystalline solids, studies of their structures and chemical reactivity are limited.[36a,b,36e]

1.1.6 Ring-opening polymerization

Ring-opening polymerization (ROP) has become one of the most important methods to produce polymers in the latter half of the 20th century.[76] ROP has proved to be a valuable route to polymers with very specific, and controllable properties. This process can be classified as a chain-growth polymerization in which monomer units consecutively add into an active chain at its terminal end to form a longer polymer chain (Scheme 1.9).[76a,b,76d,77]

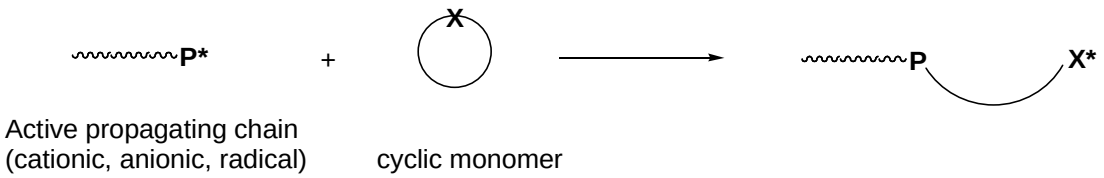

Scheme 1.9. A generic ring-opening polymerization process.

However, ROP is much more complicated in reality because many stages are involved such as initiation, chain growth, and termination as well as accompanying side reactions.[76-78] ROPs are categorized according to the type of initiator used. These are broadly described as cationic ROPs, anionic ROPs, and radical ROPs. Cyclic monomers for ROPs are diverse and include cyclic olefins **M1**, ethers **M2**, thioethers **M3**, amines **M4**, lactones **M5**, thiolactones **M6**, lactams **M7**, and many other heterocycles with one or more heteroatoms in therings.[76d] The driving force for ROP is the relief of ring strain or steric repulsion between atoms at the reactive center. Consequently, the enthalpy change in ROP is negative, following a similar trend in other types of polymerization. In conclusion, the reactivity of cyclic monomers towards polymerization depends on the ability to release the ring strain. Therefore, ROP rarely occurs with cyclic monomers

possessing little or no ring strain.[77] Relevant to this thesis is the cationic ring-opening polymerisation process (CROP) which is discussed in more detail below.

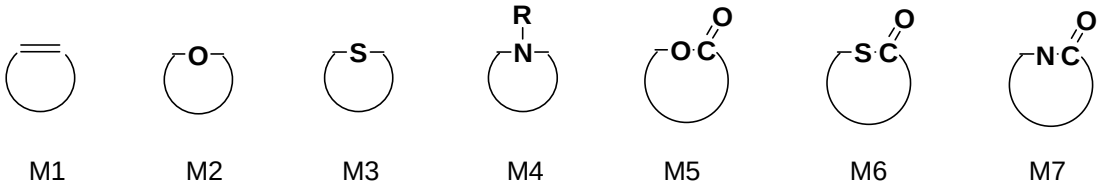

M1 M2 M3 M4 M5 M6 M7

Cationic ring-opening polymerization (CROP)

Cationic ring-opening polymerization (CROP) is a polymerization process characterized by employing cationic initiators and involves positively charged intermediates. Several important industrial polymers such as polyacetals, polytetrahydrofurans, poly(3,3-bis(chloro-methyl)oxetanes), polysiloxanes, and polymers of ethyleneimine and poly(phosphazenes) are synthesized by these methods.[76d] CROP reactions are often relatively time-consuming processes with slow kinetics. Reaction times are regularly in the order of hours even at higher temperatures. In some cases, the reaction rate can be improved significantly up to 400 fold with microwave assistance.[76d,78b]

Initiation. CROP can be typically initiated by electrophilic agents such as Brønsted acids (HCl, H_2SO_4, $HClO_4$, etc.), Lewis acids ($AlCl_3$, $BF_3 \cdot OEt_2$, $TiCl_4$, etc.), carbenium ions, onium ions, and photo-initiators.[76a,b,76d,e,77,79] Here donation of a lone pair to the electron-poor initiator leads to initial ring-opening of the cyclic monomer (Scheme 1.10).[76b,78a,79b]

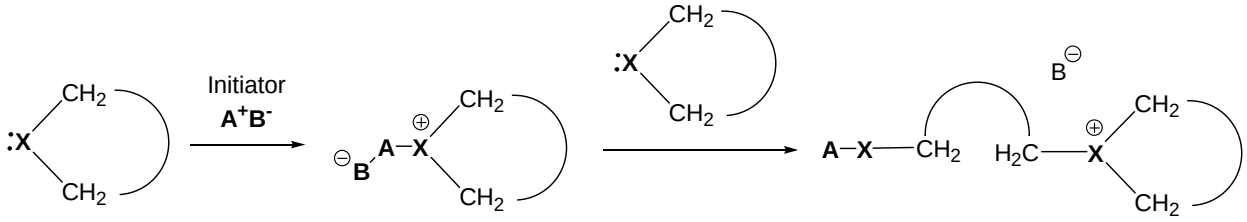

X = O; N; S
cyclic monomer

Scheme 1.10. Initiation process in ring-opening polymerization.

CROP of heterocyclic monomers frequently necessitates another reagent, which serves as a co-initiator (*e.g.* an alkyl halide or water), alongside a Lewis acid.[76e,79b,80] BF_3 and its precursor $BF_3 \cdot OEt_2$ are the most commonly Lewis acids utilized in CROP. Nevertheless, if these activators are employed in the polymerization of THF, the presence of cationogenic compounds (*e.g.* acid halides) is mandatory. This indicates that the active species is not the parent Lewis acid itself (BF_3) but the R^+ alkyl cation generated *via* halide abstraction from R-X.[76d] The Lewis acid PF_5 has been comprehensively studied for the CROP of THF, and its mechanism is supported by both ^{19}F and ^{31}P NMR spectroscopy.[81] In this case the PF_4^+ cation appears as the initiator, reacting with THF to form an oxonium ion (Figure 1.2).

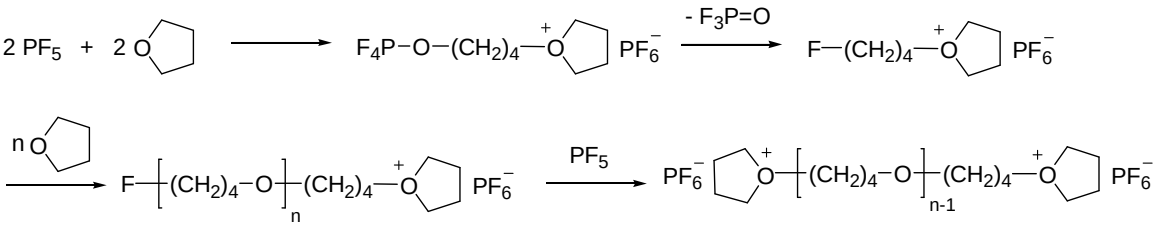

Figure 1.2. Mechanism of the CROP of THF by PF_5 (chain growth from both ends).

Chain growth. In the chain growth process the initial species formed is, itself, sufficiently Lewis acidic to react with another monomer unit to generate an equivalent Lewis acid centre which can continue to propagate the reaction. The active species for chain growth in CROPs are typically oxonium, sulfonium, ammonium or phosphonium cations.[76d]

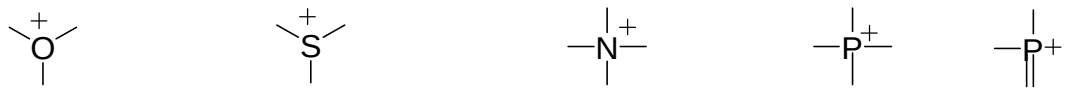

oxonium sulfonium ammonium phosphonium

One of the suggested mechanisms for CROP implements the addition of a monomer molecule to the cationic centre of an active chain *via* an S_N1 or S_N2 mechanism.[76e] The stability of the active cationic species determines which of the two mechanisms is

predominant. For instance, CROP will typically undergo S_N1 type mechanisms if the positive charge is stabilized by electron-donating groups.[76a]

Conventionally, CROP of some heterocyclic monomers, particularly cyclic ethers such as THF and oxetane, can be considered as a "living" process at appropriate temperatures and monomer concentrations. That means the process occurs without termination.[77d,e] Compared to step growth polymerization, chain-growth CROPs provide significant advantages to manage the average molecular weight, affording well-defined average molecular weights (MW) and poly-dispersity indices (PDI) close to 1.0, reflecting a narrow distribution of polymer molecular weights around the mean.[78b] Such 'living' polymerisation processes afford PDI close to 1.0 whereas step polymerisation afford PDI ~ 2 and addition PDI can often be as high as 10, reflecting broad distributions of molecular weight.[76d,e,77,79]

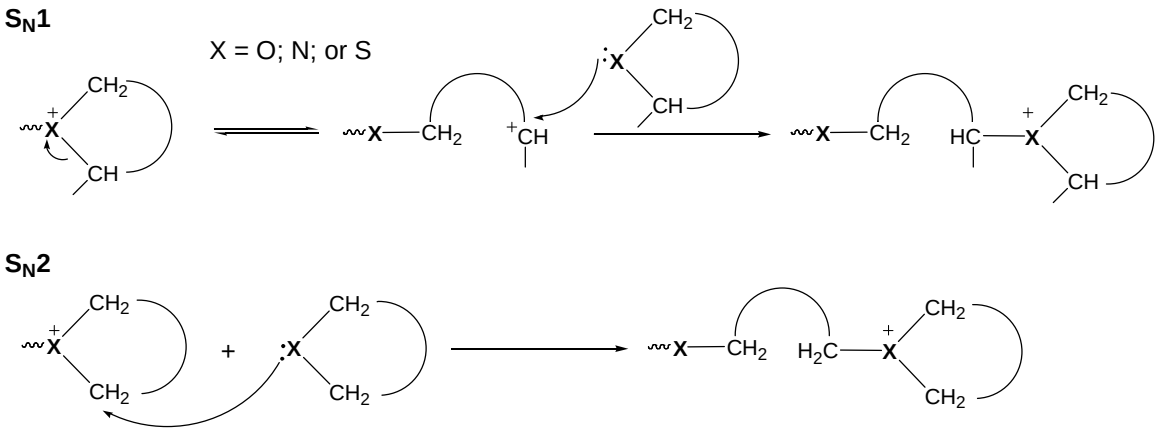

Figure 1.3. Suggested S_N1 and S_N2 mechanisms for chain growth in a CROP reaction.

Termination. For CROP reactions, the addition of a Lewis base efficiently quenches the growth process and 'termination reagents' such as phenoxy anions, phosphines might be deliberately added for quantitative or qualitative analysis,[82] or polyanions can also be utilized to synthesize block copolymers.[78d] These polyanions effectively (cross)link individual polymer chains. In many cases these termination reagents can be of the form X-H where the X group terminates the chain growth process, liberating H^+ (Scheme 1.11).[76b,76d,77]

In the absence of a terminating reagent, termination can take place in intra- or inter-molecular fashions when monomers are almost entirely consumed. At that point, the active end can "backbite" the chain, generating a macrocycle. Additionally, alkyl chain transfer is also a potential process where the active end is extinguished by transferring an alkyl chain to another polymer molecule.[76d]

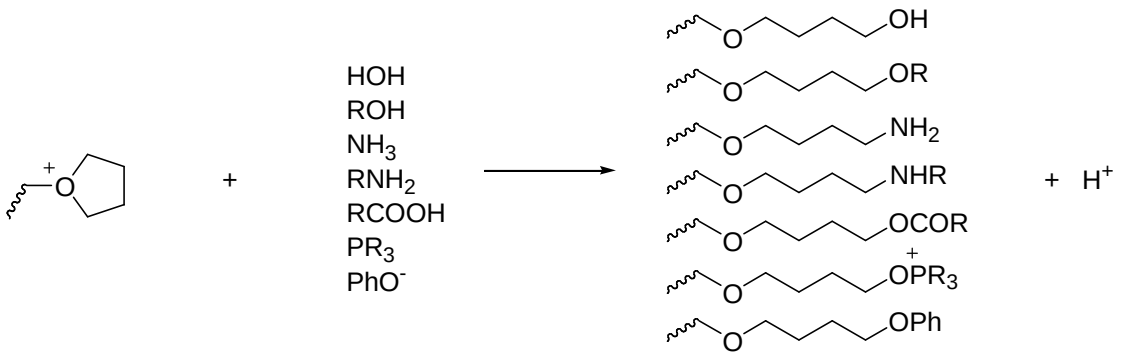

Scheme 1.11. Examples of termination process in the CROP of THF.

1.1.7 Persistent and stable radicals of the heavier main group 15 elements

The exploration of stable radical chemistry has attracted significant attention from researchers in the last two–three decades as building blocks for the design of molecule-based materials such as conductors, and magnets.[12c] The first main group radical, $S_3N_2^{+\bullet}$, in the form of $S_6N_4Cl_2$, was originally prepared in the 1800s by Demarcay,[83] but the concept of 'organic' compounds containing odd numbers of electrons was first proposed by Gomberg's proposal of a trivalent carbon in his radical, $Ph_3C^{\bullet}$ in 1900.[84] The isolation and characterization of persistent radicals of the heavier group 14 and 15 elements was not extensively carried out until the 1960s.[85] Although the chemistry of radicals based on heavier *p*-block group 15 is less established than those of group 16, the structural and chemical diversity of these radicals (especially both P(III) and P(V)) has been characterised.[85-86] Some categories of phosphorus-based radicals have been investigated. Multiple examples of pure σ-radicals where the unpaired electron is localized and sterically protected include phosphinyls $[R_2P]^{\bullet}$ and phosphoranyls $[R_4P]^{\bullet}$.[87,88] In addition π-based P-radicals have been reported in which the unpaired electron is stabilized by π-

delocalization over several nuclei, such as 1,3-diphospha-allyls $[(RP)_2CR]^{\bullet}$,[89] diphosphanyls $[R_2PPR]^{\bullet}$,[90] and $[(CH)_2(NR)_2P]^{\bullet}$.[45]

1.1.8 Stabilization strategies for radicals

Typically radicals are reactive and will undergo self-dimerisation according to the process:

$$R^{\bullet} + R^{\bullet} \rightarrow R{-}R$$

Two key strategies have generally been utilized to stabilise main group radicals:

i) π-delocalisation of the unpaired electron over several atoms in the molecules containing electronegative elements. This approach reduces electron density on any one atom making conventional '2 centre, 2 electron' (2*c*,2*e*) covalent bonding less favourable. In such cases, the unpaired electron typically occupies a low-lying weakly antibonding singly-occupied molecular orbital (SOMO) and is exemplified by the families of 7π S/N and Se/N radicals.[45] Despite the π-conjugation which disfavours 2*c*,2*e* bonding, many such π-radicals still dimerise through a so-called 'pancake bond', *i.e.* a multi-centre, two electron bond (*mc*,2*e*).[91] Such 'pancake bonds' are clearly discriminated from van der Waals forces by the short nature of the intra-dimer contacts which are substantially less than the sum of the van der Waals radii and the propensity for atoms to adopt specific 'eclipsed' geometries reflecting a strong orientational preference[91] rather than the conventional 'staggered' geometry of a π–π interaction such as that seen in graphite where the C of one ring is located over the centre of the π-system of the next layer.

ii) Kinetic and thermodynamic stabilization can be achieved using sterically demanding groups close to the radical center. This protects the radical centre through unwanted reactivity and hampers dimerization through reducing the degree of orbital overlap at the longer distances enforced by the bulky substituents.[85] Structural studies have identified that $R_2E\bullet$ monomers (E = P, As) associate in the solid state to form dimers R_2EER_2 with short 2*c*,2*e* E–E bonds, *e.g.* the 7π P-based *N*-heterocyclic radicals $[(CH)_2(NR)_2P]^{\bullet}$ (R = ^{t}Bu; R = mesityl; R = 2,6-diisopropylphenyl) are dimers in the solid

state[47] but readily dissociate *via* low-energy P–P bond cleavage in solution (*e.g.* $[(CH)_2(NMe)_2P]^{\bullet}$ has a dimerization energy (ΔE) of ~ 3 kJ mol^{-1}).[45] In addition such radicals can be sufficiently stable to be identified in the gas phase by electron diffraction, *e.g.* $\{(Me_3Si)_2CH\}_2E^{\bullet}$ (E = P, As).[92] In reality, the tendency of radical dimerization *via* covalent bonding often makes isolation of these radicals difficult, particularly for elements with inherently large E-E bond energies.[12c]

1.1.9 General procedures for syntheses and characterizations

All reactions in this dissertation were carried out under an inert nitrogen atmosphere, using standard Schlenk techniques or in an inert-atmosphere nitrogen-filled glove box (MBraun Labmaster 130) with typical water levels less than 7 ppm and oxygen levels less than 2 ppm. All glassware was oven-dried at 125 ^{o}C for a minimum of 4 h prior to use. High purity solvents (Aldrich) were additionally dried and deoxygenated by passing through molecular sieve and copper catalyst columns using an Innovative Technology Solvent Purification System.

Nuclear Magnetic Resonance (NMR) spectra were recorded at room temperature in deuterated solvents on Bruker Avance 300 and 500 MHz spectrometers. Chemical shifts (δ) and coupling constant magnitudes, |J|, are given in ppm and Hz, respectively. Chemical shifts are relative to $SiMe_4$ and referenced to the residual solvent signal (^{1}H, ^{13}C) or relative to an external standard (^{11}B, $Et_2O \cdot BF_3$; ^{19}F, $CFCl_3$; ^{31}P, 85% H_3PO_4).

Melting points were obtained on samples sealed in glass capillaries under dry nitrogen using an EZ OptiMelt Automated Melting Point System (Stanford Research Systems).

Elemental analysis was obtained by using a Perkin Elmer 2400.

Infrared (IR) spectra were recorded on a Bruker Alpha-P ATR FT-IR spectrometer with Opus software.

Mass spectrometry (MS) were recorded on a Micromass LCT Classic, using electrospray ionization operating in positive mode. All sample solutions were introduced in to the

instrument by a syringe pump. The software used to simulate isotope distribution patterns was MassLynx version 3.5.

Single crystal X-ray diffraction studies were performed using a Bruker SMART APEX diffractometer equipped with a Bruker Kryo-flex cryostream device and Mo-Kα radiation or on a Bruker Duo diffractometer equipped with an Oxford cryostream device using Mo-Kα radiation. Crystals were examined in paratone oil and mounted on a goniometer head using a cryo-loop. Data were typically collected at 173 K and processed using SAINTPLUS with absorption corrections applied using SADABS or TWINABS. Structures were solved by direct methods and refined using full-matrix least squares within SHELXTL. All non-H atoms were refined anisotropically and H atoms added at calculated positions and refined using a riding model. A summary of structural information including unit cell parameters and final residuals are tabulated in the Appendices.

Powder X-ray diffraction was carried out on a Bruker D8 Discover powder diffractometer equipped with an Oxford Cryosystems cryostream device and Cu-Kα radiation (40 kV, 40 mA) source. Samples were sealed in glass capillary tubes to avoid air/moisture contact during experiment. The step size was 0.02° and the counting time was 0.3 s for each step. Diffraction patterns were recorded in the range $5 \leq 2\theta \leq 45^{o}$.

1.2 Conclusions and Outlook

The above review in the field of phosphorus based materials to-date demonstrates that the research on the five-membered heterocyclic diazaphosphole ring systems (section 1.1.4),[40,44b,46-47,49,51,72,93] is significantly more established than the isolobal dithiaphosphole ring systems (section 1.1.3).[43,48b] Nevertheless, the reactivity profiles of both heterocycles reveal potentially similar behaviour centered on the heterocyclic phosphenium ions which are common to both systems. The status of the monocyclic N/P chemistry has now reached some degree of maturity. Nevertheless, the achievements accomplished in this field so far show that besides conventionally predictable chemical behaviors of typical phosphines, they also exhibit some unexpected reactivity trends

associated with the low valent phosphenium, P^+ centre or potential to generate P-based radicals.

In Chapter 2 of this thesis, the chemistry of dithiaphospholes and the formal P^{II} derivatives formed *via* $1e^-$ reduction are described, whereas Chapter 3 focuses on new contributions to the field of diazaphospholes. Chapter 4 describes the synthesis, characterisation and chemistry of novel phosphenium and arsenium cations, while Chapter 5 examines the reactivity of the Pn-Cl bond to transfer diazaphosphole, dithiaphosphole and dithia-arsole units in order to construct more complex polycyclic systems. Chapter 6 concludes with an examination of the ability of phosphenium, arsenium and stibenium cations to promote the CROP of THF.

1.3 References

1. Bansal, R. K., Phosphorous Heterocycles I. In *Topics in Heterocyclic Chemistry*, Springer Berlin Heidelberg: 2009; Vol. 20, pp 1-31.

2. Housecroft, C. E.; Sharpe, A. G., *Inorganic Chemistry 3rd Edition*. Pearson, Harlow UK: **2008**.

3. Greenwood, N. N.; Earnshaw, A., 12 - Phosphorus. In *Chemistry of the Elements (Second Edition)*, Greenwood, N. N.; Earnshaw, A., Eds. Butterworth-Heinemann: Oxford, 1997; pp 473-546.

4. (a) Baudler, M., *Angew. Chem. Int. Ed. Engl* **1982**, *21* (7), 492-512; (b) Baudler, M., *Angew. Chem. Int. Ed. Engl* **1987**, *26* (5), 419-441; (c) Baudler, M.; Glinka, K., *Chem. Rev.* **1993**, *93* (4), 1623-1667; (d) Baudler, M.; Glinka, K., *Chem. Rev.* **1994**, *94* (5), 1273-1297; (e) Haiduc, I., The Chemistry of Inorganic Ring Systems. Wiley-Interscience: 1970; pp 82-150.

5. Yoshifuji, M.; Shima, I.; Inamoto, N.; Hirotsu, K.; Higuchi, T., *J. Am. Chem. Soc.* **1981**, *103* (15), 4587-4589.

6. (a) Cowley, A. H.; Lasch, J. G.; Norman, N. C.; Pakulski, M., *J. Am. Chem. Soc.* **1983**, *105* (16), 5506-5507; (b) Tokitoh, N.; Arai, Y.; Sasamori, T.; Okazaki, R.; Nagase, S.; Uekusa, H.; Ohashi, Y., *J. Am. Chem. Soc.* **1998**, *120* (2), 433-434; (c) Tokitoh, N.; Arai, Y.; Okazaki, R.; Nagase, S., *Science* **1997**, *277* (5322), 78-80.

7. Arif, A. M.; Barron, A. R.; Cowley, A. H.; Hall, S. W., *J. Chem. Soc., Chem. Commun.* **1988**, (3), 171-172.

8. (a) Nixon, J. F., *Chem. Rev.* **1988**, *88* (7), 1327-1362; (b) Cloke, F. G. N.; Green, J. C.; Hitchcock, P. B.; Nixon, J. F.; Suter, J. L.; Wilson, D. J., *Dalton Trans.* **2009**, (7), 1164-1171; (c) Clendenning, S. B.; Hitchcock, P. B.; Lappert, M. F.; Merle, P. G.; Nixon, J. F.; Nyulászi, L., *Chem. Eur. J.* **2007**, *13* (25), 7121-7128.

9. Falconer, R. L.; Russell, C. A., *Coord. Chem. Rev.* **2015**, *297–298*, 146-167.

10. (a) Nyulászi, L., *Chem. Rev.* **2001**, *101* (5), 1229-1246; (b) Bansal, R. K.; Drabowicz, J., Phosphorous Heterocycles II. In *Topics in Heterocyclic Chemistry*, Bansal, R. K., Ed. Springer Berlin Heidelberg: 2010; Vol. 21, pp 1-207; (c) Krygowski, T. M.; Cyranski, M. K., Aromaticity in Heterocyclic Compounds. In *Topics in Heterocyclic Chemistry*, Krygowski, T. M.; Cyranski, M. K., Eds. Springer Berlin Heidelberg: 2009; Vol. 19, pp 39-53.

11. Mathey, F., *Angew. Chem. Int. Ed.* **2003**, *42* (14), 1578-1604.

12. (a) Alberola, A.; Collis, R. J.; Humphrey, S. M.; Less, R. J.; Rawson, J. M., *Inorg. Chem.* **2006**, *45* (5), 1903-1905; (b) Alberola, A.; Eisler, D. J.; Harvey, L.; Rawson, J. M., *Cryst. Eng. Comm* **2011**, *13* (6), 1794-1796; (c) Rawson, J. M.; Alberola, A.; Whalley, A., *J. Mater. Chem.* **2006**, *16* (26), 2560-2575; (d) Rawson, J. M.; McManus, G. D., *Coord. Chem. Rev.* **1999**, *189* (1), 135-168.

13. (a) Hicks, R. G., The Synthesis and Characterization of Stable Radicals Containing the Thiazyl (SN) Fragment and Their Use as Building Blocks for

Advanced Functional Materials. In *Stable Radicals*, John Wiley & Sons, Ltd: 2010; pp 317-380; (b) Hicks, R. G., Stable Radicals: Fundamentals and Applied Aspects of Odd-Electron Compounds. Hicks, R. G., Ed. Wiley: 2010; Vol. 9-10, pp 317-404.

14. (a) Preuss, K. E., *Dalton Trans.* **2007**, *0* (23), 2357-2369; (b) Preuss, K. E., *Coord. Chem. Rev.* **2015**, *289–290* (0), 49-61.

15. (a) Yu, X.; Mailman, A.; Lekin, K.; Assoud, A.; Robertson, C. M.; Noll, B. C.; Campana, C. F.; Howard, J. A. K.; Dube, P. A.; Oakley, R. T., *J. Am. Chem. Soc.* **2012**, *134* (4), 2264-2275; (b) Leitch, A. A.; Yu, X.; Winter, S. M.; Secco, R. A.; Dube, P. A.; Oakley, R. T., *J. Am. Chem. Soc.* **2009**, *131* (20), 7112-7125; (c) Robertson, C. M.; Leitch, A. A.; Cvrkalj, K.; Reed, R. W.; Myles, D. J. T.; Dube, P. A.; Oakley, R. T., *J. Am. Chem. Soc.* **2008**, *130* (26), 8414-8425.

16. Banister, A. J.; May, I.; Rawson, J. M.; Smith, J. N. B., *J. Organomet. Chem.* **1998**, *550* (1–2), 241-253.

17. (a) Fatila, E. M., Coordination of 1,2,3,5-Dithiadiazolyl Radical Ligands to Paramagnetic Metal Ions: a Framework for Molecule Based Magnets. University of Guelph, **2013**; (b) Iwasaki, A.; Hu, L.; Suizu, R.; Nomura, K.; Yoshikawa, H.; Awaga, K.; Noda, Y.; Kanai, K.; Ouchi, Y.; Seki, K.; Ito, H., *Angew. Chem. Int. Ed. Engl.* **2009**, *48* (22), 4022-4024.

18. (a) Awaga, K.; Umezono, Y.; Fujita, W.; Yoshikawa, H.; Cui, H.; Kobayashi, H.; Staniland, S. S.; Robertson, N., *Inorg. Chim. Acta* **2008**, *361* (14–15), 3761-3770; (b) Barclay, M.; Cordes, T. W.; George, A. A.; Haddon, N. C.; Oakley, R. T.; Palstra, R. T. M.; Patenaude, T. W.; Reed, G. W.; Richardson, R. F.; Zhang, J. H., *Chem. Commun.* **1997**, *0* (9), 873-874; (c) Fujita, W.; Awaga, K., *Chem. Phys. Lett.* **2004**, *388* (1–3), 186-189; (d) Alberola, A.; Burley, J.; Collis, R. J.; Less, R. J.; Rawson, J. M., *J. Organomet. Chem.* **2007**, *692* (13), 2750-2760; (e) Awere, E. G.; Burford, N.; Mailer, C.; Passmore, J.; Schriver, M. J.; White, P. S.; Banister,

A. J.; Oberhammer, H.; Sutcliffe, L. H., *J. Chem. Soc., Chem. Commun.* **1987**, *0* (2), 66-69.

19. Wolmershauser, G.; Schnauber, M.; Wilhelm, T., *J. Chem. Soc., Chem. Commun.* **1984**, (9), 573-574.

20. Burford, N.; Passmore, J.; Schriver, M. J., *J. Chem. Soc., Chem. Commun.* **1986**, 140-142.

21. Fujita, W.; Awaga, K.; Nakazawa, Y.; Saito, K.; Sorai, M., *Chem. Phys. Lett.* **2002**, *352* (5–6), 348-352.

22. Fujita, W.; Awaga, K., *Chem. Phys. Lett.* **2002**, *357* (5–6), 385-388.

23. Fujita, W.; Awaga, K.; Takahashi, M.; Takeda, M.; Yamazaki, T., *Chem. Phys. Lett.* **2002**, *362* (1–2), 97-102.

24. (a) Brusso, J. L.; Clements, O. P.; Haddon, R. C.; Itkis, M. E.; Leitch, A. A.; Oakley, R. T.; Reed, R. W.; Richardson, J. F., *J. Am. Chem. Soc.* **2004**, *126* (26), 8256-8265; (b) Brusso, J. L.; Clements, O. P.; Haddon, R. C.; Itkis, M. E.; Leitch, A. A.; Oakley, R. T.; Reed, R. W.; Richardson, J. F., *J. Am. Chem. Soc.* **2004**, *126* (45), 14692-14693.

25. Banister, A. J., *Nature Phys. Sci.* **1972**, *237*, 92-93.

26. Krebs, B.; Henkel, G.; Pohl, S.; Roesky, H. W., *Chem. Ber.* **1980**, *113*, 2802-2813.

27. Oakley, R. T., *Prog. Inorg. Chem.* **1988**, (36), 299-391.

28. Chivers, T., Five-membered Carbon–Nitrogen–Chalcogen Ring Systems: from Radicals to Functional Materials In *A Guide to Chalcogen-Nitrogen Chemistry*, World Scientific: 2005; Vol. 12, pp 212-239.

29. (a) Winter, S. M.; Hill, S.; Oakley, R. T., *J. Am. Chem. Soc.* **2015**, *137* (11), 3720-3730; (b) Winter, S. M.; Oakley, R. T.; Kovalev, A. E.; Hill, S., *Phys. Rev. B* **2012**, *85* (9), 94430-94441.

30. van Eldik, R.; Stochel, G., Inorganic Photochemistry. In *Advances in inorganic chemistry*, Elsevier Science: 2011; Vol. 63, pp 50-55.

31. (a) Tangour, B.; Malavaud, C.; Boisdon, M. T.; Barrans, J., *Phosphorus Sulfur Silicon Relat. Elem.* **1989**, *45* (3-4), 189-195; (b) Cameron, T. S.; Linden, A., *Phosphorus Sulfur Silicon Relat. Elem.* **1989**, *41* (1-2), 75-81; (c) Gololobov, Y. G.; Gusar, N. I.; Chaus, M. P., *Tetrahedron* **1985**, *41* (4), 793-799; (d) Poutasse, C. A.; Day, R. O.; Holmes, R. R., *J. Am. Chem. Soc.* **1984**, *106* (13), 3814-3820.

32. (a) Arbuzov, A. E.; Zoroastrova, V. M., *Chem. Abstr.* **1953**, (47), 4833-4839; (b) Arbuzov, A. E.; Zoroastrova, V. M., *lzvest. Akad. Nauk. S.S.S.R. Otdel. Khim. Nauk.* **1952**, (48), 453-458; (c) Mann, F. G.; Weissberger, A., The Chemistry of Heterocyclic Compounds, Heterocyclic Derivatives of Phosphorous, Arsenic, Antimony and Bismuth. John Wiley & Sons: 2009; Vol. 1, pp 11-150.

33. Campbell, I. G. M.; Way, J. K., *J. Chem. Soc. (Resumed)* **1960**, (0), 5034-5041.

34. (a) Arnold, V. H.; Bourseaux, F.; Brock, N., *Arzneimittel. Forsch.* **1961**, (11), 143-156; (b) Arnold, V. H.; Bourseaux, F.; Brock, N., *Chem. Abstr.* **1961**, (55), 16816-16823.

35. Baudler, M.; Moog, A.; Glinka, K.; Kelsch, U., *Z. Naturforsch., B* **1973**, *28*, 363-369.

36. (a) Burford, N.; Royan, B. W.; Linden, A.; Cameron, T. S., *J. Chem. Soc., Chem. Commun.* **1988**, *0* (13), 842-844; (b) Burford, N.; Royan, B. W.; Linden, A.; Cameron, T. S., *Inorg. Chem.* **1989**, *28* (1), 144-150; (c) Burgada, R., *Bull. Soc. Chim. Fr.* **1975**, *9* (10), 2207-2212; (d) Burford, N.; Royan, B. W.; White, P. S., *J. Am. Chem. Soc.* **1989**, *111* (10), 3746-3747; (e) Burford, N.; Royan, B. W., *J.*

Chem. Soc., Chem. Commun. **1989**, *0* (1), 19-21; (f) Burford, N.; Parks, T. M.; Royan, B. W.; Richardson, J. F.; White, P. S., *Can. J. Chem.* **1992**, *70* (3), 703-709.

37. (a) Costin, S.; Sedinkin, S. L.; Bauer, E. B., *Tetrahedron Lett.* **2009**, *50* (8), 922-925; (b) Strasser, C. E.; Cronje, S.; Schmidbaur, H.; Raubenheimer, H. G., *J. Organomet. Chem.* **2006**, *691* (22), 4788-4796.

38. Mark, J. E.; Allcock, H. R.; West, R., *Inorganic polymers 2nd Edn* Oxford University Press: New York, **2005**.

39. Verkade, J. G.; Urgaonkar, S., Proazaphosphatrane. In *Encyclopedia of Reagents for Organic Synthesis*, John Wiley & Sons, Ltd: 2001.

40. Gupta, N., Recent Advances in the Chemistry of Diazaphospholes. In *Phosphorus Heterocycles II*, Bansal, R. K., Ed. Springer Berlin Heidelberg: 2010; Vol. 21, pp 175-206.

41. Gudat, D.; Haghverdi, A.; Nieger, M., *Angew. Chem.* **2000**, *112* (17), 3211-3214.

42. Pilgram, K.; Korte, F., *Tetrahedron* **1963**, *19* (1), 137-141.

43. Nitcheu, S. K.; Malavaud, C., *Tetrahedron* **1993**, *49* (21), 4651-4658.

44. (a) Abrams, M. B.; Scott, B. L.; Baker, R. T., *Organometallics* **2000**, *19* (24), 4944-4956; (b) Benko, Z.; Burck, S.; Gudat, D.; Nieger, M.; Nyulaszi, L.; Shore, N., *Dalton Trans.* **2008**, (36), 4937-4945; (c) Burford, N.; Ragogna, P. J.; McDonald, R.; Ferguson, M. J., *J. Am. Chem. Soc.* **2003**, *125* (47), 14404-14410; (d) Carmalt, J. C.; Lomeli, V., *Chem. Commun.* **1997**, *0* (21), 2095-2096; (e) Cowley, A. H.; Kemp, R. A., *Chem. Rev.* **1985**, *85* (5), 367-382; (f) Denk, M. K.; Gupta, S.; Lough, A. J., *Eur. J. Inorg. Chem.* **1999**, *1999* (1), 41-49; (g) Denk, M. K.; Gupta, S.; Ramachandran, R., *Tetrahedron Lett.* **1996**, *37* (50), 9025-9028.

45. Edge, R.; Less, R. J.; McInnes, E. J. L.; Muther, K.; Naseri, V.; Rawson, J. M.; Wright, D. S., *Chem. Commun.* **2009**, *0* (13), 1691-1693.

46. (a) Karaghiosoff, K.; Majoral, J. P.; Meriem, A.; Navech, J.; Schmidpeter, A., *Tetrahedron Lett.* **1983**, *24* (21), 2137-2140; (b) Schmidpeter, A.; Karaghiosoff, K., *Z. Naturforsch., B: Chem. Sci.* **1981**, *36* (10), 1273-1276.

47. (a) Burck, S.; Gudat, D.; Nieger, M.; Du Mont, W.-W., *J. Am. Chem. Soc.* **2006**, *128* (12), 3946-3955; (b) Gudat, D.; Haghverdi, A.; Hupfer, H.; Nieger, M., *Chem. Eur. J.* **2000**, *6* (18), 3414-3425.

48. (a) Wieber, M.; Mulfinger, O.; Wunderlich, H., *Z. Anorg. Allg. Chem.* **1981**, *477* (6), 108-112; (b) Jennings, W. B.; Randall, D.; Worley, S. D.; Hargis, J. H., *J. Chem. Soc., Perkin Trans. 2* **1981**, (10), 1411-1416.

49. Gudat, D., *Acc. Chem. Res.* **2010**, *43* (10), 1307-1316.

50. (a) Burck, S.; Gudat, D.; Nieger, M., *Angew. Chem.* **2004**, *116* (36), 4905-4908; (b) Burck, S.; Hajdók, I.; Nieger, M.; Bubrin, D.; Schulze, S.; Gudat, D., *Z. Naturforsch., B* **2009**, *64b*, 63-72.

51. Burck, S.; Gudat, D.; Lissner, F.; Nättinen, K.; Nieger, M.; Schleid, T., *Z. Anorg. Allg. Chem.* **2005**, *631* (13-14), 2738-2745.

52. (a) Kibardin, A. M.; Gryaznova, T. V.; Pudovik, A. N., *Zh. Org. Khim.* **1996**, *66*, 372-375; (b) Kibardin, A. M.; Gryaznova, T. V.; Musin, R. Z.; Pudovik, A. N., *Zh. Org. Khim.* **1993**, *63*, 39-41.

53. Kibardin, A. M.; Gryaznova, T. V.; Gryaznov, P. I.; Pudovik, A. N., *Zh. Org. Khim.* **1996**, *66*, 1452-1454.

54. (a) Klanberg, F.; Muetterties, E. L., *J. Am. Chem. Soc.* **1968**, *90* (12), 3296-3297; (b) Hayter, R. G., *Inorg. Chem.* **1963**, *2* (5), 932-935.

55. (a) Burford, N.; Clyburne, J. A. C.; Bakshi, P. K.; Cameron, T. S., *Organometallics* **1995**, *14* (4), 1578-1585; (b) Tan, C.; Wang, P.; Liu, H.; Zhao, X.-L.; Lu, Y.; Liu, Y., *Chem. Commun.* **2015**, *51* (54), 10871-10874; (c) Burford, N.; Cameron, T. S.; LeBlanc, D. J.; Phillips, A. D.; Concolino, T. E.; Lam, K.-C.; Rheingold, A. L., *J. Am. Chem. Soc.* **2000**, *122* (22), 5413-5414; (d) Reed, R.; Réau, R.; Dahan, F.; Bertrand, G., *Angew. Chem., Int. Ed. Engl.* **1993**, *32* (3), 399-401.

56. (a) Schuster, O.; Yang, L.; Raubenheimer, H. G.; Albrecht, M., *Chem. Rev.* **2009**, *109* (8), 3445-3478; (b) Melaimi, M.; Soleilhavoup, M.; Bertrand, G., *Angew. Chem. Int. Ed.* **2010**, *49* (47), 8810-8849; (c) Bourissou, D.; Guerret, O.; Gabbaï, F. P.; Bertrand, G., *Chem. Rev.* **2000**, *100* (1), 39-92; (d) Herrmann, W. A., *Angew. Chem. Int. Ed. Engl.* **2002**, *41* (8), 1290-1309; (e) Tuononen, H. M.; Roesler, R.; Dutton, J. L.; Ragogna, P. J., *Inorg. Chem.* **2007**, *46* (25), 10693-10706.

57. (a) Huang, J.; Schanz, H.-J.; Stevens, E. D.; Nolan, S. P., *Organometallics* **1999**, *18* (25), 5375-5380; (b) Scholl, M.; Trnka, T. M.; Morgan, J. P.; Grubbs, R. H., *Tetrahedron Lett.* **1999**, *40* (12), 2247-2250.

58. Caputo, C. A.; Price, J. T.; Jennings, M. C.; McDonald, R.; Jones, N. D., *Dalton Trans.* **2008**, (26), 3461-3469.

59. (a) Denk, M.; Lennon, R.; Hayashi, R.; West, R.; Belyakov, A. V.; Verne, H. P.; Haaland, A.; Wagner, M.; Metzler, N., *J. Am. Chem. Soc.* **1994**, *116* (6), 2691-2692; (b) Ghadwal, R. S.; Roesky, H. W.; Merkel, S.; Stalke, D., *Chem. Eur. J.* **2010**, *16* (1), 85-88.

60. Burford, N.; Ragogna, P. J., *J. Chem. Soc., Dalton Trans.* **2002**, *0* (23), 4307-4315.

61. (a) Porter, K. A.; Willis, A. C.; Zank, J.; Wild, S. B., *Inorg. Chem.* **2002**, *41* (24), 6380-6386; (b) Althaus, H.; J. Breunig, H.; Lork, E., *Chem. Commun.* **1999**, *0*

(19), 1971-1972; (c) Kilah, N. L.; Weir, M. L.; Wild, S. B., *Dalton Trans.* **2008**, *0* (18), 2480-2486.

62. Kopp, R. W.; Bond, A. C.; Parry, R. W., *Inorg. Chem.* **1976**, *15* (12), 3042-3046.

63. Gudat, D., *Coord. Chem. Rev.* **1997**, *163* (0), 71-106.

64. Norman, N. C.; Pickett, N. L., *Coord. Chem. Rev.* **1995**, *145* (0), 27-54.

65. Burford, N.; Cameron, T. S.; LeBlanc, D. J.; Losier, P.; Sereda, S.; Wu, G., *Organometallics* **1997**, *16* (21), 4712-4717.

66. Alton, E. R.; Montemayor, R. G.; Parry, R. W., *Inorg. Chem.* **1974**, *13* (9), 2267-2270.

67. Fleming, S.; Lupton, M. K.; Jekot, K., *Inorg. Chem.* **1972**, *11* (10), 2534-2540.

68. Bondi, A., *J. Phys. Chem.* **1964**, *68* (3), 441-451.

69. Pauling, L., *The Nature of the Chemical Bond and the Structure of Molecules and Crystals: An Introduction to Modern Structural Chemistry*. Cornell University Press: **1960**.

70. Burford, N.; Losier, P.; Macdonald, C.; Kyrimis, V.; Bakshi, P. K.; Cameron, T. S., *Inorg. Chem.* **1994**, *33* (7), 1434-1439.

71. (a) Niecke, E.; Nieger, M.; Reichert, F., *Angew. Chem. Int. Ed. Engl.* **1988**, *27* (12), 1715-1716; (b) Burford, N.; Mason, S.; Spence, R. E. H.; Whalen, J. M.; Richardson, J. F.; Rogers, R. D., *Organometallics* **1992**, *11* (6), 2241-2250.

72. (a) Burck, S.; Gudat, D.; Nättinen, K.; Nieger, M.; Niemeyer, M.; Schmid, D., *Eur. J. Inorg. Chem.* **2007**, *2007* (32), 5112-5119; (b) Sauers, R. R., *Tetrahedron* **1997**, *53* (7), 2357-2364.

73. Schmidt, M. W.; Truong, P. N.; Gordon, M. S., *J. Am. Chem. Soc.* **1987**, *109* (17), 5217-5227.

74. Bansal, R. K.; Grupta, N.; Collier, S. J., Product class 15: dithiaphospholes and their analogues. 2004; Vol. 13, pp 641-646.

75. MacLennan, M. T.; Darvesh, K. V., *Can. J. Chem.* **1995**, *73* (4), 544-549.

76. (a) Coulembier, O.; Dubois, P.; Raquez, J. M., Handbook of Ring-Opening Polymerization. Wiley-VCH, Weinheim, Bergstraße: 2008; (b) Grath James, E. M., Ring-Opening Polymerization: Introduction. In *Ring-Opening Polymerization*, American Chemical Society: 1985; Vol. 286, pp 1-22; (c) Jayakannan, M.; Ramakrishnan, S., *Macromol. Rapid Commun.* **2001**, *22* (18), 1463-1473; (d) Nuyken, O.; Pask, S., *Polymers* **2013**, *5* (2), 361-403; (e) Penczek, S.; Kubisa, P., Cationic Ring-Opening Polymerization. In Ring-Opening Polymerization. Brunelle, D.J., Ed. ed.; Hanser Publishers: Munich, Germany: 1993; pp 13-86.

77. Young, R. J.; Lovell, P. A., Introduction to Ring-Opening Polymerization. In *Introduction to Polymers, Third Edition*, Taylor & Francis: 2011; pp 169-189.

78. (a) Bednarek, M.; Biedroń, T.; Kahłużyński, K.; Kubisa, P.; Pretula, J.; Penczek, S., *Macromol. Symp.* **2000**, *157* (1), 1-12; (b) Kamber, N. E.; Jeong, W.; Waymouth, R. M.; Pratt, R. C.; Lohmeijer, B. G. G.; Hedrick, J. L., *Chem. Rev.* **2007**, *107* (12), 5813-5840; (c) Navarro-Llobet, D., Studies of the ring-opening polymerization of cyclic ethers and esters by coordinate catalysis. 3054367, Indiana University, Ann Arbor, **2002**; (d) Richards, D. H., Ring-Opening Polymerization in the Synthesis of Block Copolymers. In *Ring-Opening Polymerization*, American Chemical Society: 1985; Vol. 286, pp 87-95.

79. (a) Ravve, A., Ring-Opening Polymerizations. In *Principles of Polymer Chemistry*, Springer New York: 2012; pp 253-327; (b) Kubisa, P., Cationic

Polymerization of Heterocyclics. In Cationic Polymerizations. Matyjaszewski, K., Ed, Ed. Marcel Dekker: New York, NY, USA: 1996; pp 437-553.

80. Kennedy, J. P.; Marechal, E., Carbocationic Polymerization. John Wiley & Sons: New York, NY, USA: 1982; pp 95-97.

81. Hoene, R.; Reichert, K.-H. W., *D. Makromol. Chem.* **1976**, *177* (12), 3545-3570.

82. (a) Matyjaszewski, K.; Penczek, S., *D. Makromol. Chem.* **1981**, *182* (6), 1735-1742; (b) Saegusa, T.; Matsumoto, S.-I., *J. Polym. Sci. A Polym. Chem.* **1968**, *6* (6), 1559-1565.

83. Demarcay, E., *Compt. Rend.* **1881**, *92*, 726-728.

84. Gomberg, M., *J. Am. Chem. Soc.* **1900**, *22* (11), 757-771.

85. Power, P. P., *Chem. Rev.* **2003**, *103* (3), 789-810.

86. Armstrong, A.; Chivers, T.; Boeré, R. T., The Diversity of Stable and Persistent Phosphorus-Containing Radicals. In *Modern Aspects of Main Group Chemistry*, American Chemical Society: 2005; Vol. 917, pp 66-80.

87. (a) Gynane, M. J. S.; Hudson, A.; Lappert, M. F.; Power, P. P., *J. Chem. Soc., Chem. Commun.* **1976**, *0* (16), 623-624; (b) Gynane, M. J. S.; Hudson, A.; Lappert, M. F.; Power, P. P.; Goldwhite, H., *J. Chem. Soc., Dalton Trans.* **1980**, (12), 2428-2433.

88. Marque, S.; Berchadsky, Y.; Bertrand, P.; Fournel, A.; Tordo, P.; Lang, K.; Moussavi, M.; Belorizky, E., *J. Phys. Chem. A* **1997**, *101* (31), 5640-5645.

89. Canac, Y.; Baceiredo, A.; Schoeller, W. W.; Gigmes, D.; Bertrand, G., *J. Am. Chem. Soc.* **1997**, *119* (32), 7579-7580.

90. Loss, S.; Magistrato, A.; Cataldo, L.; Hoffmann, S.; Geoffroy, M.; Röthlisberger, U.; Grützmacher, H., *Angew. Chem. Int. Ed.* **2001**, *40* (4), 723-726.

91. Preuss, K. E., *Polyhedron* **2014**, *79*, 1-15.

92. (a) Bezombes, J.-P.; Borisenko, K. B.; Hitchcock, P. B.; Lappert, M. F.; Nycz, J. E.; Rankin, D. W. H.; Robertson, H. E., *Dalton Trans.* **2004**, *0* (13), 1980-1988; (b) Hinchley, S. L.; Morrison, C. A.; Rankin, D. W. H.; Macdonald, C. L. B.; Wiacek, R. J.; Voigt, A.; Cowley, A. H.; Lappert, M. F.; Gundersen, G.; Clyburne, J. A. C.; Power, P. P., *J. Am. Chem. Soc.* **2001**, *123* (37), 9045-9053.

93. Burck, S.; Forster, D.; Gudat, D., *Chem. Commun.* **2006**, (26), 2810-2812.

CHAPTER 2

BENZO-1,3,2-DITHIAPHOSPHOLYLS: HEAVY *p*-BLOCK ANALOGUES OF THE BENZO-1,3,2-DITHIAZOLYL RADICAL

2.1 Introduction

2.1.1 Benzodithiaphosphole chemistry

The synthesis of *P*-chloro-1,3,2-benzodithiaphosphole [**1**]Cl was first reported by Baudler and coworkers from the reaction of benzene dithiol with PCl_3 in ether.[1] Treatment of [**1**]Cl with a Lewis acid, MCl_3 (M = Al, Ga) was reported to afford the dithiaphosphenium salt [**1**][MCl_4] which was crystallographically characterised.[2] The related dithiaphosphenium salt [**1**][OTf] was prepared from [**1**]Cl and AgOTf. The cationic phosphenium cation $\mathbf{2}^+$ were reported to form adducts with pyridine.[3] The related *P*-phenyl-dithiaphospholes [**1**]Ph and [**2**]Ph were prepared from the corresponding dithiol and $PhPCl_2$ and could be oxidized with ortho-quinones such as ortho-chloranil or phenanthrenequinone to the spirocyclic P^V compounds.[4] Baudler indicated that reduction of [**1**]Cl with elemental Na in xylene yielded the dimer $(\mathbf{1})_2$ which exhibited a broad ^{31}P solution NMR spectrum, potentially indicative of paramagnetic broadening.[1] However, the structures of [**1**]Cl or $(\mathbf{1})_2$ or related derivatives have not been reported nor has the chemical reactivity and properties of dimer $(\mathbf{1})_2$ been investigated. A summary of the known 1,3,2-dithiaphosphole chemistry is shown in Scheme 2.1. The isoelectronic relationship between N and P means that 1,3,2-benzodithiaphospholes potentially possess structures similar to those of the isoelectronic DTA radicals which exhibit unusual magnetic propeties and which inspired us to investigate their heavier *p*-block congeners.

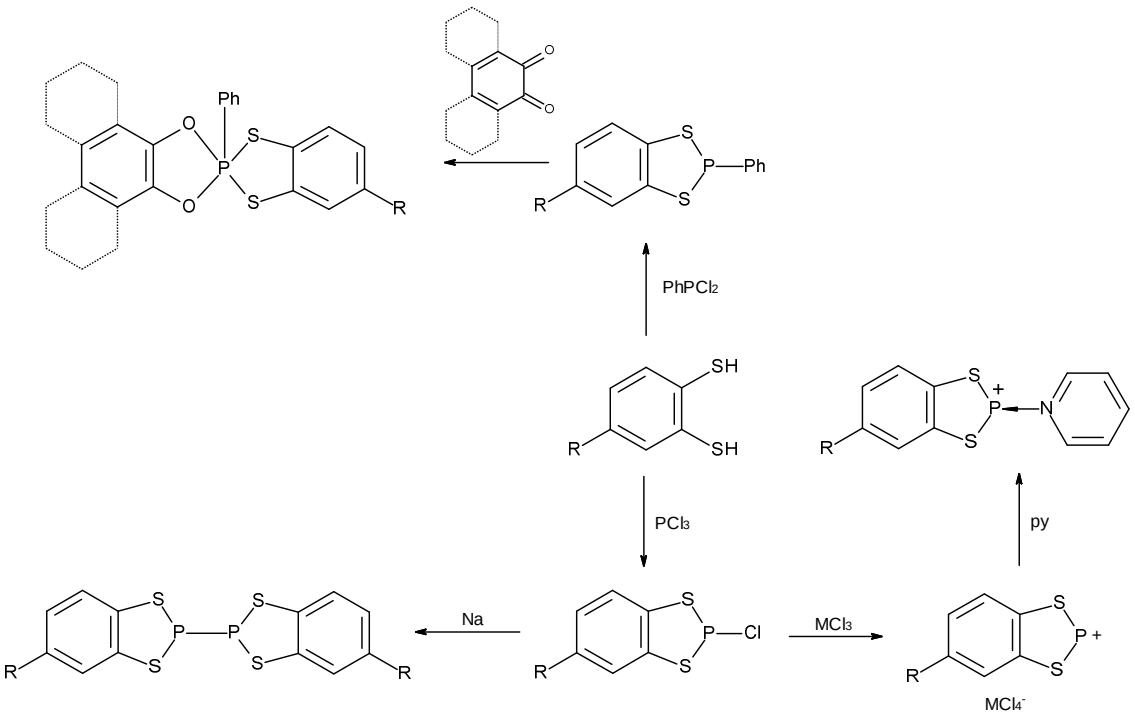

Scheme 2.1. A schematic summary of the known 1,3,2-dithiaphosphole chemistry (R = H, Me).

2.1.2 Project aims

The inclusion of heavier *p*-block elements into the framework of radical **3** can lead to increased magnetic anisotropy through larger spin-orbit coupling[5] and improved dimensionality in their electronic structure.[6] This has led us to pursue synthetic routes to heavier *p*-block analogues of **3** in order to probe trends in structure, bonding and reactivity. Here the synthesis, structural and computational studies on the dithiaphospholyl dimer $(\mathbf{1})_2$ are reported which is related to $[C_2S_2N]$ framework by isoelectronic replacement of N by P.

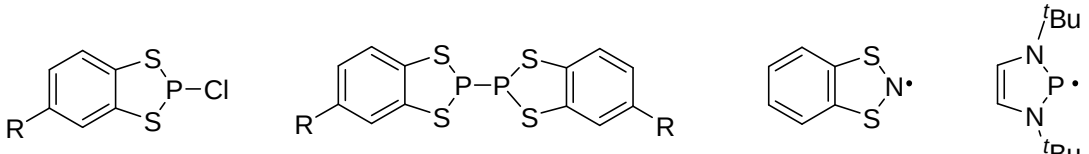

[**1**]Cl (R = H) $(\mathbf{1})_2$ (R = H)

[**2**]Cl (R = CH_3) $(\mathbf{2})_2$ (R = CH_3) **3** **3'**

Recent collaboration work between Rawson and Wright has shown that the analogous species **3'** in which S is replaced by isolobal ^{t}Bu-N forms a σ-bonded dimer in the solid state (**3'**)$_2$ but dissociates in solution *via* homolytic P-P bond cleavage to generate radical **3'**.[7] A comparison of the properties of **1** in relation to isoelectronic **3** and **3'** was therefore targetted. Herein the syntheses and structural studies on [**1**]Cl and (**1**)$_2$ are addressed. In addition the syntheses of [**2**]Cl and (**2**)$_2$ are described and (**2**)$_2$ is shown to readily undergoes oxidative P-P bond cleavage to afford [**2**]X. The structures of [**2**]Cl, [**2**]Br and [**2**]I have been determined by single crystal and powder X-ray diffraction (PXRD).

2.2 Results and Discussion

2.2.1 Synthesis and characterization of [1]Cl and [2]Cl

The synthesis of [**1**]Cl broadly followed the protocols first described by Baudler[1] with some minor modifications (Scheme 2.2). Condensation between benzene-dithiol and PCl_3 affords spectroscopically pure [**1**]Cl as a colourless oil at high yield, consistent with previous literature. Reaction of toluene-dithiol with PCl_3 occurs under similar conditions to give pure [**2**]Cl as a viscous oil. Storage of these oily products at -20 ^{o}C and then at room temperature for several days in the glove-box yields [**1**]Cl and [**2**]Cl as analytically pure poly-crystalline solids. The ^{31}P NMR spectra of [**1**]Cl and [**2**]Cl exhibit singlets at 158.5 and 161.4 ppm respectively.

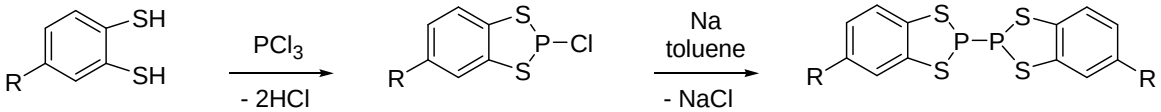

R = H or CH_3

[**1**]Cl (R = H)

[**2**]Cl (R = CH_3)

(**1**)$_2$ (R = H)

(**2**)$_2$ (R = CH_3)

Scheme 2.2. Synthesis of [1]Cl, [2]Cl, (1)$_2$ and (2)$_2$.

Structure and bonding in [1]Cl

A poly-crystalline sample of [**1**]Cl was grown from cooling its colorless oil for 1 day at -20 ^{o}C and leaving at RT for several days in the glove-box. The well-resolved powder

X-ray diffraction pattern measured at 110 K (Figure 2.1) was indexed on the monoclinic space group $P2_1/n$ using DICVOL.[8] The structure was initially solved using a rigid body refinement and a simulated annealing method (DASH),[9] based on the geometry-optimised gas-phase structure (B3LYP/6-31G*+) of [**1**]Cl. Subsequent refinement of the heavy atom positions (S/P/Cl) afforded a modest improvement in the final profile (Figure 2.1).

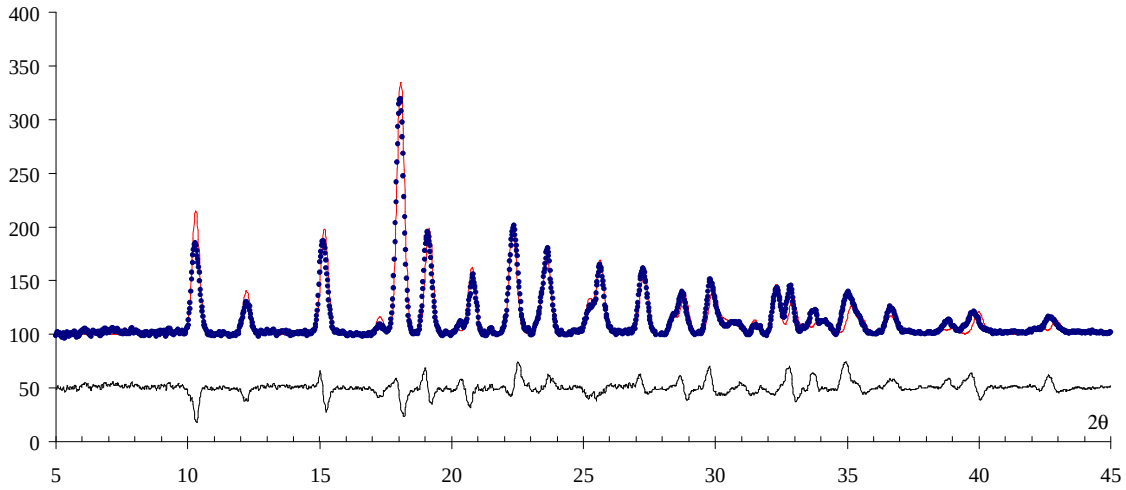

Figure 2.1. X-ray powder diffraction pattern (+) profile (—) and difference (—) for [**1**]Cl at 223 K, based on the monoclinic space group $P2_1/n$ (a = 6.013 , b = 17.026, c = 8.000 Å, β = 97.71°).

Subsequently a small shard cut from a poly-crystalline bundle was used for a single crystal study which confirmed the molecular geometry and space group (monoclinic, $P2_1/n$) of [**1**]Cl identified from the initial powder diffraction studies. The single crystal data permitted a full geometry refinement and the structure of [**1**]Cl is shown in Figure 2.2. The structure clearly reveals a covalent P-Cl bond [2.1037(9) Å] a little longer than that observed for PCl_3 (2.043 Å)[10] and a geometry akin to the phenyl derivative [**1**]Ph in which the phenyl ring is also covalently bonded and displaced out of the ring plane.[2b,c] This is markedly different from the bonding in isovalent [**3**]Cl which is considerably ionic with the closest cation···anion contacts being S···Cl at 3.120 Å.[11] This can be attributed to the difference in bond polarity within this pair of heterocycles ($^{\delta+}$S—N$^{\delta-}$ *vs*

$^{\delta-}$S—P $^{\delta+}$) which leads to delocalisation of the positive charge in [**3**]Cl over two S atoms. Based on Fajan's rules,[12] the reduced partial charge on each S atom leads to reduced covalency and hence an ionic structure. The P-S bonds (2.0864(8)-2.0880(7) Å) are longer than those in [**1**][$AlCl_4$] (mean 2.016(2) Å)[2b,c] suggesting P-S single bond character in [**1**]Cl but some multiple bond character in [**1**][$AlCl_4$]. Unlike the planar $\mathbf{1}^+$ cation in [**1**][$AlCl_4$], the five-membered C_2S_2P ring is folded about the S-S vector with the C_2S_2 and PS_2 planes forming an angle of 28.35°. These observations support the previous thesis[2b,c] that planarity optimises p_π-p_π bonding between the heavier *p*-block elements leading to bond shortening.

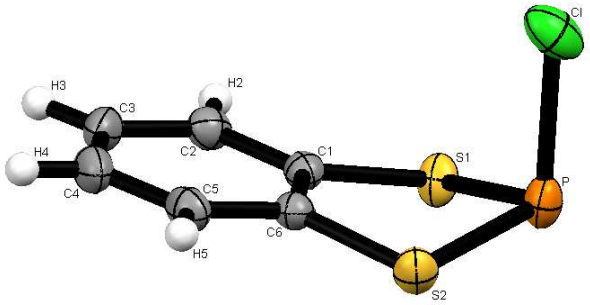

Figure 2.2. Molecular structure of [**1**]Cl determined from single crystal X-ray diffraction. Thermal ellipsoids for non-H atoms drawn at the 50% probability level. Selected heterocyclic bond lengths and angles are: P-Cl 2.1037(9), P-S1 2.0879(7), P-S2 2.0864(8), C1-S1 1.761(2), S2-C6 1.765(2), C1-C6 1.391(3) Å; S1-P-S2 95.39(3); S1-P-Cl 101.49(3), S2-P-Cl 101.66(3) C1-S1-P 99.44(6), C6-S2-P 99.37(6), S1-C1-C6 118.9(1), S2-C6-C1 118.7(1) °.

Covalent bonding of P to Cl therefore occurs at the expense of disruption to the π-system. Indeed an Natural Bond Orbital (NBO) analysis (based on DFT B3LYP/6-311G*+ calculations)[13] of $C_6H_4S_2PCl$ and $[C_6H_4S_2P]^+$ confirms this assumption with the dominant resonance form of [**1**]Cl exhibiting single bonds from P to both S and Cl. Conversely the $[C_6H_4S_2P]^+$ cation reflects significant p_π-p_π bonding between P and S atoms (A detailed comparison is provided in Chapter 4).

2.2.2 Synthesis of (1)$_2$ and (2)$_2$ and structure of (1)$_2$

Reduction of [**1**]Cl and [**2**]Cl in Na/toluene afforded (**1**)$_2$ and (**2**)$_2$, respectively, as off-white/pale yellow microcrystalline solids. These reactions were monitored by $^{31}P\{^1H\}$ NMR to follow the progress of the reaction with the reduction products (**1**)$_2$ and (**2**)$_2$ appearing at 38.3 and 40.6 ppm respectively. However the rate of reduction appeared variable even when using seemingly similar reaction conditions. In particular it was found that the rates of the reductions are sensitive to the size of the sodium pieces employed. Initial reactions required 2–4 days to ensure complete reduction (monitored by ^{31}P NMR). However pre-treatment of a suspension of sodium metal in toluene in a microwave (100 ^oC, 20 minutes) proved efficient to form a fine sodium dispersion which affords consistently shorter reaction times (2 days). This suggests a heterogeneous reduction process in which the rate of reaction depends upon the surface area of the sodium metal.

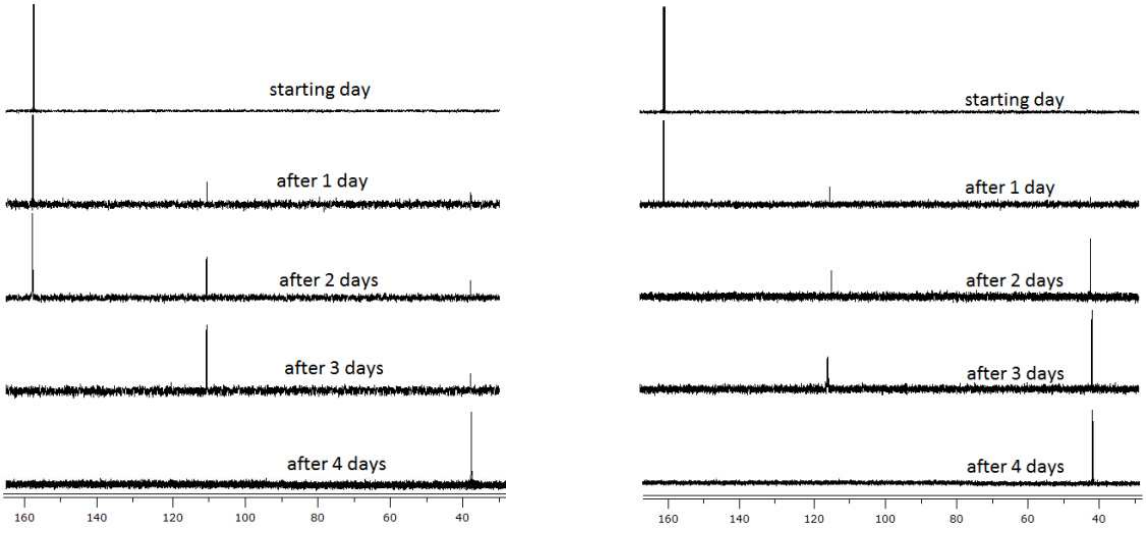

Figure 2.3. $^{31}P\{^1H\}$ NMR studies of reductions of [**1**]Cl (left) and [**2**]Cl (right) with Na metal in toluene at reflux.

^{31}P NMR studies reveal that reductions of [**1**]Cl and [**2**]Cl with Na metal in toluene proceed *via* build up of an unknown intermediate ($\delta_P \sim 113$ ppm) prior to conversion to $(\mathbf{1})_2$ and $(\mathbf{2})_2$, respectively.

EPR studies on $(\mathbf{1})_2$ and $(\mathbf{2})_2$ in both the solid state and solution at room temperature indicated both $(\mathbf{1})_2$ and $(\mathbf{2})_2$ were EPR silent consistent with complete dimerization at ambient temperature. Variable temperature studies to 110 ^{o}C also failed to lead to thermal dissociation, indicating a large exothermic dimerization energy.

2.2.2.1 Structure of $(\mathbf{1})_2$

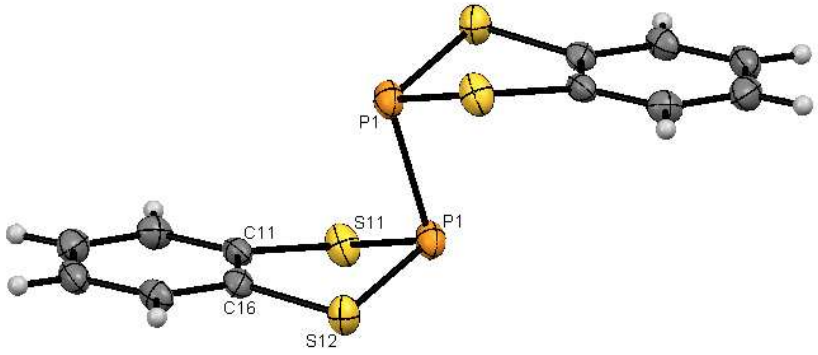

Figure 2.4. Crystal structure of $(\mathbf{1})_2$. Thermal ellipsoids for non-H atoms drawn at 50% probability. Selected heterocyclic bond lengths and angles are P1-S11 2.1003(13), P1-S12 2.1056(14), P1-P1′ 2.233(2), S11-C11 1.770(3), S12-C16 1.769(3), C11-C16 1.398(5) Å; S11-P1-S12 95.95(5), C11-S11-P1 97.55(12), C16-S12-P1 97.10(12), S11-C11-C16 118.7(3), S12-C16-C11 119.7(3)

Crystalline $(\mathbf{1})_2$ was formed by slow evaporation of a toluene solution to afford a polycrystalline mass. The structure of $(\mathbf{1})_2$ proved particularly problematic to determine due to persistent twinning. Nevertheless, a satisfactory solution could be determined in the monoclinic space group $P2_1/n$ with half a molecule in the asymmetric unit with the structure of $(\mathbf{1})_2$ located about an inversion centre (Figure 2.4). The P-P bond length (2.233(2) Å) is comparable with that observed for other alkyl and aryl diphosphanes, R_2P-PR_2 (2.20 – 2.31 Å),[11,14] indicating dimerization *via* a formal P-P single bond rather

than the multi-centre 2e^- 'pancake bonding' interaction seen for DTA radicals.[15] The heterocyclic geometry of (**1**)$_2$ is very similar to that of [**1**]Cl, though the P-S bonds (2.1003(13) and 2.1056(14) Å) are a little longer than in [**1**]Cl consistent with a formal reduction in oxidation state from P^{III} to P^{II} and the fold of the heterocyclic ring is marginally larger at 33.03°. Similar folding was observed in the isoelectronic $[C_6H_4P_2Sb]_2^{4-}$ tetra-anion (28.21 – 29.04°) in which dimerisation occurs *via* Sb-Sb bond formation.[16] Clearly folding of the ring from coplanarity is a direct reflection of P-X covalency (see [**1**]Cl and *vide infra*).

2.2.2.2 Theoretical calculations

Density functional theory (DFT)[17] studies (B3LYP/6-31G*+) revealed excellent agreement between the gas-phase geometry-optimised structure of (**1**)$_2$ and the crystal structure (Figure 2.5). Calculations (including a zero-point energy correction, ZPE) on (**1**)$_2$ and the radical $C_6H_4S_2P^{\bullet}$ formed by homolytic cleavage of the P-P bond indicated that whilst dissociation is unfavourable in the gas phase (B3LYP/6-31G*+: ΔH = +119 kJ/mol; B3LYP/6-311G*+: ΔH = +120 kJ/mol) the bond enthalpy of the P-P bond is less than the average P-P bond dissociation enthalpy (~ 210 kJ/mol).[18] Nevertheless, this dimerisation enthalpy is considerably larger than that observed in the isovalent benzodithiazolyl radical **3** (ΔH_{dim} ~ 0 kJ/mol).[19] Whilst the P-P bond length in the isolobal diazaphosphole dimer (**3'**)$_2$ (2.2439(3) Å) is comparable with (**1**)$_2$, dissociation of (**3'**)$_2$ to radical **3'** occurs in solution, indicating the importance of steric factors in the latter case. Similar ZPE-corrected gas-phase calculations (UB3LYP/6-31G*+) reveal ΔH_{dim} to be substantially lower (-60 kJ/mol) for formation of (**3'**)$_2$ consistent with this difference in behaviour.

The propensity for **1** to dimerise in relation to **3** would appear to arise from the differing electronegativities of P and N in relation to S. The more electropositive elements will offer larger coefficients to the (antibonding) SOMO (Figure 2.6). Thus for **1** the greatest electron density resides at P favouring a 2*c*,2e^- σ-bond interaction whereas for **3** it is more evenly distributed over the two S atoms, favouring a 4*c*,2e^- π*-π* interaction at S.[19-20]

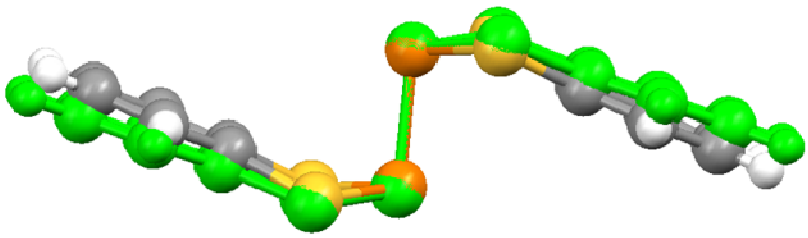

Figure 2.5. Overlay of the crystal structure of $(\mathbf{1})_2$ (coloured by element) and the DFT geometry-optimised structure (green).

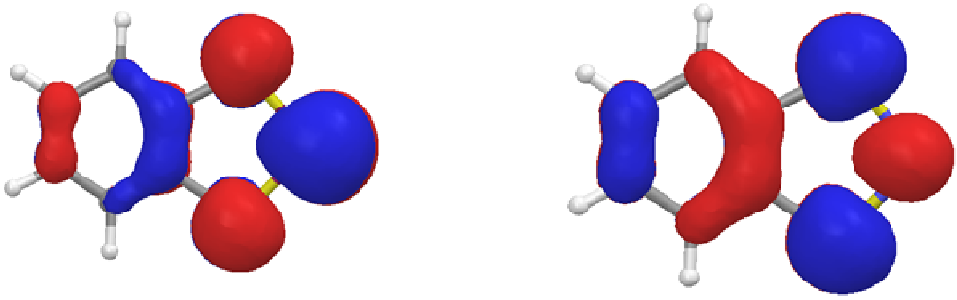

Figure 2.6. Singly occupied MO's of **1** (left) and **3** (right) illustrating the redistribution of electron density from P in **1** to S in **3**.

2.2.2.3 Structure of $(\mathbf{2})_2$

The structure of $(\mathbf{2})_2$ is potentially more complex due to the asymmetry induced by the presence of the methyl group. Thus both '*cis*' and '*trans*' forms of $(\mathbf{2})_2$ could potentially exist. In addition the '*cis*' arrangement has a pair of optical enantiomers.

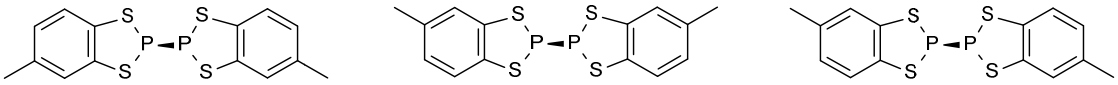

Figure 2.7. '*Cis*' isomers of $(\mathbf{2})_2$ (left and centre) and '*trans*' isomer (right).

Compound $(\mathbf{2})_2$ was analytically pure by ^{31}P NMR (δ_P 40.6 ppm) and microanalysis but attempts to grow suitable crystals for X-ray diffraction persistently proved unsuccessful. Whilst PXRD studies on $(\mathbf{2})_2$ confirmed its crystallinity (Figure 2.8), attempts to solve the

structure of $(\mathbf{2})_2$ have, to date, proved unsuccesful. Nevertheless the similarity in properties (^{31}P NMR chemical shift and lack of EPR spectrum even at elevated temperatures) indicates a structure analogous to $(\mathbf{1})_2$.

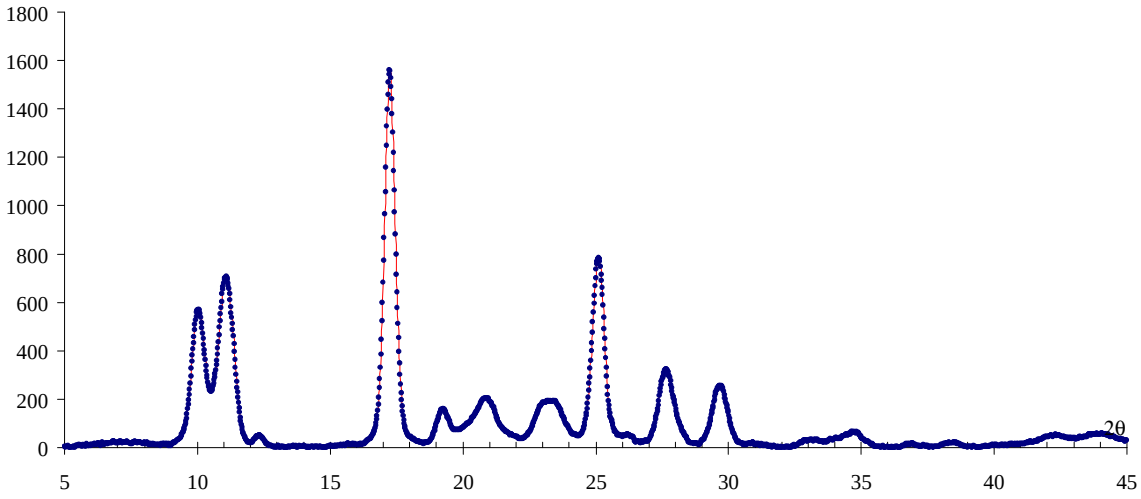

Figure 2.8. PXRD pattern of $(\mathbf{2})_2$.

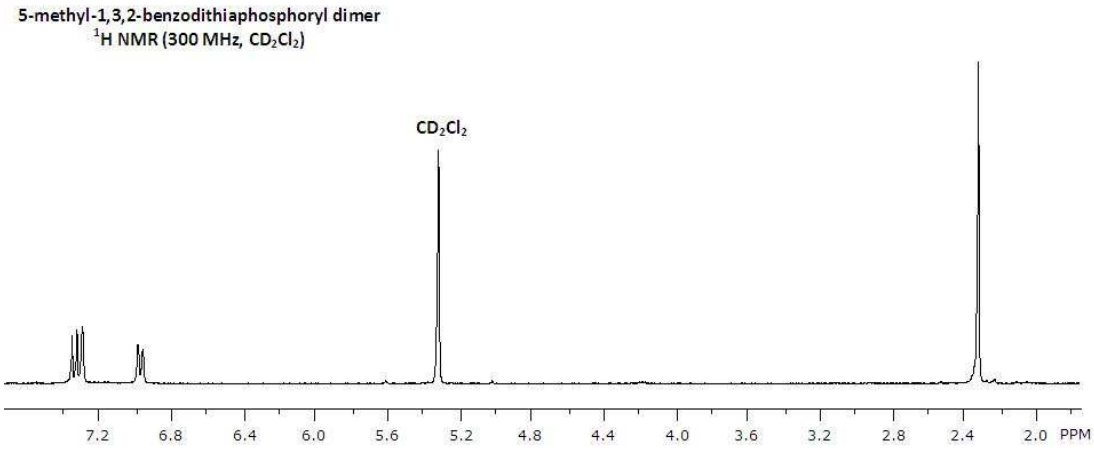

Figure 2.9. ^{1}H NMR spectrum of $(\mathbf{2})_2$.

While ^{1}H NMR spectroscopy will not distinguish between the pair of optical isomers, resolution of a mixture of '*cis*' and '*trans*' isomers may be possible. However a ^{1}H NMR study of $(\mathbf{2})_2$ (Figure 2.9) reveals only one singlet for the CH_3 groups (δ_H 2.31 ppm). It is

therefore believed that either (a) there is only one isomer formed or (b) if several isomers exist both the ^{1}H methyl resonances and ^{31}P NMR resonances happen to be coincident.

2.2.3 Oxidation of (2)$_2$

Oxidation of (**2**)$_2$ with SO_2Cl_2, Br_2 and I_2 all proceed smoothly at 0^{o}C in 2-3 hours to provide quantitative yields of [**2**]X (X = Cl, Br, I) which were isolated after workup as air and moisture sensitive white-to-yellow solids. They were characterized by microanalytical data, X-ray crystallography, and ^{31}P and ^{1}H NMR spectroscopy.

Crystal structures of [2]Cl, [2]Br and [2]I

Single-crystal X-ray structure determinations were performed for compounds [**2**]X (X = Cl; Br; I). The structures of [**2**]X (X = Br and I) were determined by X-ray diffraction and found to be isomorphous with [**2**]Cl, all adopting the monoclinic space group *P2$_1$/c*.

Table 2.1. Selected bond lengths [Å] and angles [°] for [**1**]Cl, [**2**]X, [**2**][$GaCl_4$],[a] and (**1**)$_2$. Fold angle [°] is the angle between [SCCS] and [SPS] planes.

	P-X	**P-S**	**S-C**	**C-C**	**S-P-S**	**Fold angle**
[**1**]Cl	2.1037(9)	2.0879(7)	1.761(2)	1.391(3)	95.39(3)	28.35
		2.0864(8)	1.765(2)			
[**2**]Cl	2.1103(7)	2.0932(7)	1.767(2)	1.390(2)	95.43(2)	26.06
		2.0921(6)	1.766(2)			
[**2**]Br	2.304(3)	2.079(3)	1.772(9)	1.39(1)	96.1(1)	24.27
		2.078(3)	1.761(9)			
[**2**]I	2.5687(8)	2.0861(9)	1.759(3)	1.395(4)	96.16(4)	19.62
		2.090(1)	1.757(2)			
[**2**][$GaCl_4$][a]	-	2.027(2)	1.736(6)	1.409(8)	98.37(8)	0.83
		2.033(2)	1.749(5)			
(**1**)$_2$	-	2.1003(13)	1.770(3)	1.398(5)	95.95(5)	33.03
		2.1056(14)	1.769(3)			

[a]*Data from Chapter 4*

Important bond lengths, and bond angles are summarized in Table 2.1 and compared with structural data obtained for (**1**)$_2$ and [**1**][$GaCl_4$] (see Chapter 4). The molecular structures of [**2**]Cl, [**2**]Br and [**2**]I are presented in Figures 2.10 – 2.12.

Whilst there are some small variations in heterocyclic bond lengths and angles in [**2**]Cl, [**2**]Br and [**2**]I, there are no marked trends which can be discerned between these structures. However there are the expected increases in P-X bond length on descending the halogen group consistent with the increasing covalent radius of the halogen and the P-X bond lengths are comparable with conventional P-X bonds (P-Cl 2.03 Å, P-Br 2.22 Å and P-I 2.55 Å),[21] and there is a steady decrease in the fold angle between C_2S_2 and S_2P planes on replacing Cl (26.06°) by Br (24.27°) and I (19.62°). This may indicate a reduction in covalency and a move towards more ionic bonding, *cf* $\mathbf{2}^+$ which is essentially planar. However the shortening of the P-S bond associated with multiple bonding in $\mathbf{2}^+$ is not evident in the P-S bond lengths in the series [**2**]Cl, [**2**]Br and [**2**]I.

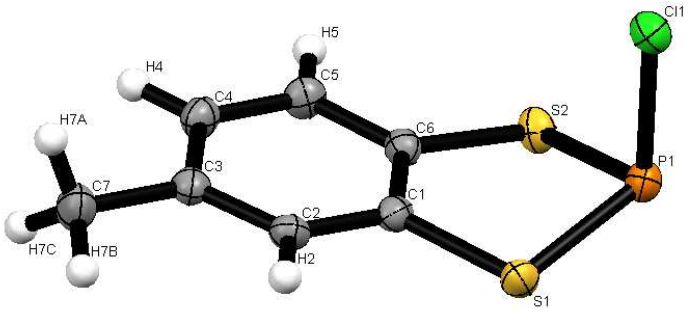

Figure 2.10. Crystal structure of [**2**]Cl with thermal ellipsoids for non-H atoms drawn at the 50% probability level.

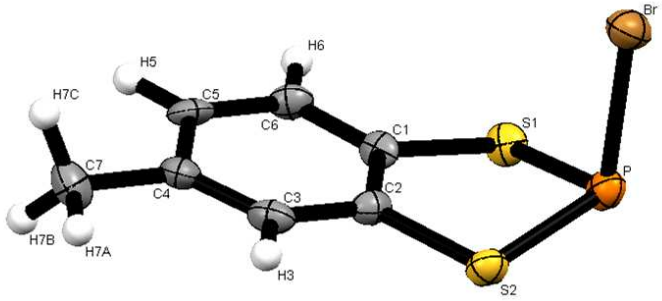

Figure 2.11. Crystal structure of [**2**]Br with thermal ellipsoids for non-H atoms drawn at the 50% probability level.

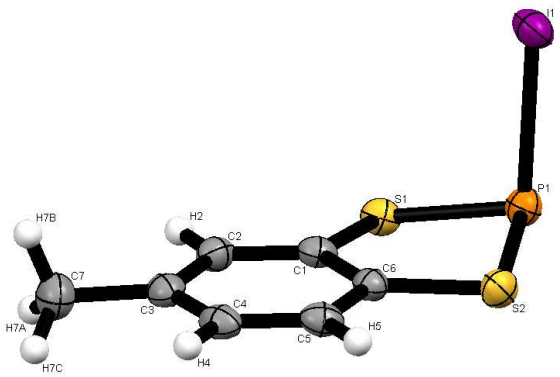

Figure 2.12. Crystal structure of [**2**]I with thermal ellipsoids for non-H atoms drawn at the 50% probability level.

2.2.4 $^{31}P\{^{1}H\}$ NMR studies

The shielding constant σ can be broken down into diamagnetic shielding (σ_{dia}), paramagnetic shielding (σ_{para}), neighbouring group shielding (σ_{neigh}) and other effects (σ_{other}). For ^{1}H NMR, the chemical shift is mostly dominated by the diamagnetic shielding which is related to the electron density and hence sensitive to the electron withdrawing/releasing groups attached to the H nucleus. Conversely for other nuclei other contributions can be significant. The paramagnetic shielding arises from motion of electrons between ground state and excited state orbitals and is therefore closely related to the energy of low-lying states. The paramagnetic shielding is not due to unpaired electrons but merely relates to the fact that the effect of paramagnetic shielding is opposite to diamagnetic shielding. Neighbouring group effects arise from the effect of the magnetic moments generated by neighbouring atoms or groups, of which the ring current effect in deshielding ^{1}H nuclei is an example. Other effects can be the nature of the environment, hydrogen bonding, the effect of a paramagnetic ion etc.

Given the complexity of possible factors (such as oxidation state and valency) associated with phosphorus, it is perhaps surprising that ^{31}P NMR chemical shifts provide any useful information. Nevertheless for a series of structurally closely related structures such as phosphines, R_3P, empirical correlations can be made. For example for tertiary phosphines

$\delta_P = -62 + \Sigma\sigma_R$ where σ_R is a constant for a specific R group.[22] The additive nature of the chemical shielding effects for different groups can therefore be used in a chemically meaningful way. For example the ^{31}P NMR data of [**2**]X all reveal singlets whose chemical shifts cover the range of 155–164 ppm. When descending the halogen group (Cl → Br → I), their δ_P values do not follow a simple order just based on electronegativity arguments: [**2**]Cl (δ_P 161.4 ppm), [**2**]Br (δ_P 163.6 ppm), [**2**]I (δ_P 155.4 ppm) but the order of chemical shifts among [**2**]X compounds is directly comparable to the trend in the PX_3 series;[23] PCl_3 (δ_P 220 ppm), PBr_3 (δ_P 228 ppm) and PI_3 (δ_P 178 ppm), indicating the dominance of paramagnetic shielding over diamagnetic shielding in these systems. Conversely the chemical shift of [**1**]Cl is shifted by about 2-3 ppm with respect to [**2**]Cl reflecting the more subtle neighbour group effect in which the electron-donating methyl group leads to a shielding of ca 2-3 ppm. Such remote effects on ^{31}P chemical shift have been previously observed and shown to follow a Hammett style correlation.[24]

The reduction products $(\mathbf{1})_2$ and $(\mathbf{2})_2$ which contain P-P bonds (with a formal P oxidation state of +2) both reveal singlets in their ^{31}P NMR spectra in the region 38 – 41ppm, significantly shifted from their P^{III} precursors.

Table 2.2. $^{31}P\{^1H\}$ NMR chemical shift of the synthetic compounds.

Compound	**[1]Cl**	**$(1)_2$**	**[2]Cl**	**[2]Br**	**[2]I**	**$(2)_2$**
δ_P (ppm)	158.5	38.3	161.4	163.6	155.4	40.6

The ^{31}P chemical shifts of primary phosphines have been shown to follow the empirical law $\delta_P = -62 + \Sigma\sigma_{para}$ where σ_{para} refer to paramagnetic shielding effects for each of the three R groups attached to the phosphine. From the reported ^{31}P NMR data for PX_3 (X = F,Cl, Br, I, NMe_2, OMe and SMe, Ph) we can derive σ_{para} values for each substituent. These are presented in Table 2.3.

Table 2.3. σ_{para} values for each substituent derived from the reported ^{31}P NMR data of PR_3.

Group	**F**	**Cl**	**Br**	**I**	**OMe**	**NMe_2**	**SMe**	**Ph**
^{31}P (δ) PR_3	98	220	228	178	140	122	126	-6
σ_{para}	53.3	94	96.3	80	67.3	61.5	62.5	18.7

Using these paramagnetic shielding constants we can estimate the ^{31}P NMR chemical shift range of [**1**]X and [**2**]X derivatives. Thus for $(RS)_2PCl$ a chemical shift of 157 ppm is calculated (*cf.* [**2**]Cl at 161 ppm). Similarly [**2**]Br is computed in the range 159 ppm and observed at 164 ppm while [**2**]I is calculated at 143 ppm and observed at 155pm. Notably the groups further from the ^{31}P centre will have a secondary effect and, for example, the introduction of a methyl group leads to a shift of 2-3 ppm when comparing [**1**]Cl and [**2**]Cl. In Chapter 5 [**2**]$N(SiMe_3)_2$ is observed upfield at 94 ppm. The calculated value for [**2**]NMe_2 is 124 ppm. Although there is less good agreement between observed and calculated ^{31}P chemical shifts the $SiMe_3$ group can be considered electron-accepting which would have a deshielding effect in comparison to methyl.

In this context it is noteworthy that the ^{31}P NMR data for P_2Br_4 (146 ppm) and P_2I_4 (107 ppm) provide a σ_{para} value for a P substituent in the region 9 – 16 ppm, from which $(\mathbf{1})_2$ would be estimated around 73–76 ppm which is a significant deviation from observation. This likely arises from the fact that for such P_2R_4 groups changing the R substituent simultaneously changes both the primary coordination sphere of the ^{31}P centre as well as the electronics of the substituent PR_2 group. While both Br and I can be considered electron-withdrawing, the π-donating S centre would lead to a significant shielding effect. While some aspects of the ^{31}P chemical shifts of these systems appear predictable, such approaches should clearly be treated with caution.

2.3 Conclusions

The 1,3,2-dithiaphospholylium salts and 1,3,2-dithiaphospholyl ‘radicals’ are heavy *p*-block analogs of the 1,3,2-dithiazolylium and 1,3,2-dithiazolyl radicals respectively.

However the difference in bond polarity of the S—N and S—P bonds afforded by the different electronegativities of N and P with respect to S leads to marked differences in the structures of both cations and neutral species. For $\mathbf{1}^+$ the increased positive charge on the single P centre, favours covalent 2*c*, 2*e*$^-$ P-X bond formation (X = Cl, Br, I) whereas the distribution of positive charge over two S atoms in 1,3,2-dithiazolylium salts leads to more ionic bonding with close cation…anion contacts to the S atoms. This difference in electronegativity also means that the SOMO of **1** has the largest coefficient at P favouring 2*c*, 2*e*$^-$ dimerisation through irreversible σ-bond formation whereas the SOMO of **3** has larger coefficients on S and adopts a weak, multi-centre, reversible π*-π* bonding interaction which maximises spatial overlap at the S atoms.

2.4 Experimental

All reagents were used as received without any further purification unless otherwise noted; benzene dithiol, PCl_3, $CDCl_3$, C_6D_6, CD_2Cl_2, SO_2Cl_2, Br_2, I_2, and Na (Sigma-Aldrich), toluene dithiol (Acros).

2.4.1 Synthesis of P-chloro-1,3,2-benzodithiaphosphole, [1]Cl

A solution of 1,2-benzenedithiol (2.00 g; 14.1 mmol) in CH_2Cl_2 (20 mL) was added dropwise to a solution of PCl_3 (1.94 g; 14.1 mmol) in CH_2Cl_2 (20 mL). The reaction mixture was heated at reflux under N_2 at 40 ^oC for 1 h, and then stirred for a further 12 h at room temperature. The solution was evaporated *in vacuo* to afford a colourless oil which, when stored at -20 ^oC, yielded colorless crystals of [**1**]Cl (2.673 g, 92%).

^{1}H NMR (300 MHz, $CDCl_3$): δ_H 7.66-7.69 (m, 2H, aromatic CH-CS-CS-CH); 7.29-7.35 (m, 2H, aromatic CH-CH).

^{31}P{^{1}H} NMR (121.5 MHz, $CDCl_3$): δ_P 158.5 (s).

Found ($C_6H_4S_2PCl$ requires): C = 35.04% (34.87); H = 2.23% (1.95).

Melting point: 44-45 ^oC.

2.4.2 Synthesis of benzo-1,3,2-dithiaphospholyl dimer, (1)$_2$

A suspension of [**1**]Cl (1.00 g; 4.84 mmol) and finely chopped Na (0.30 g; 13.0 mmol) in toluene (20 mL) was stirred at 100 ^{o}C for 4 days. The mixture reaction was filtered and the filtrate evaporated *in vacuo* to afford a yellow solid. Recrystallization by slow evaporation of a toluene solution afforded very pale yellow crystals of (**1**)$_2$. Yield: 0.413 g (50%).

^{1}H NMR (500 MHz, $CDCl_3$): δ_H 7.34-7.37 (m, 4H, aromatic CH-CS-CS-CH), 7.25-7.29 (m, 4H, aromatic CH-CH).

^{31}P{^{1}H} NMR (202.5 MHz, $CDCl_3$): δ_P 38.3 (s).

Found ($C_{12}H_8P_2S_4$ requires): C = 43.19% (42.09); H = 2.90% (2.36).

Melting point: 224-225 ^{o}C.

2.4.3 Synthesis of P-chloro-5-methyl-1,3,2-benzodithiaphosphole, [2]Cl

A solution of toluene-3,4-dithiol (1.00 g; 6.4 mmol) in CH_2Cl_2 (10 mL) was added dropwise to a solution of phosphorous trichloride (0.88 g; 6.4 mmol) in CH_2Cl_2 (10 mL). The reaction mixture was heated at reflux under N_2 at 40 ^{o}C for 1 h, and then stirred for a further 12 h at room temperature. The solution was evaporated *in vacuo* to afford a colourless oil. Storage at -20 ^{o}C afforded colorless crystals of *P*-chloro-5-methyl-1,3,2-benzodithiaphosphole. Yield: 1.363 g (96%).

^{1}H NMR (300 MHz, C_6D_6): δ_H 6.98 (d, $^{3}J_{HH}$ = 8.1 Hz, 1H, aromatic CH); 6.82 (s, 1H, aromatic CH); 6.48 (d, $^{3}J_{HH}$ = 8.1 Hz, 1H, aromatic CH); 1.80 (s, 3H, CH_3).

^{13}C NMR (75.5 MHz, CD_2Cl_2) δ_C 138.01, 137.30, 134.47, 128.06, 126.55 (d, $^{2}J_{PC}$ = 5.5 Hz, 1C, aromatic SC), 125.74 (d, $^{2}J_{PC}$ = 5.4 Hz, 1C, aromatic SC), 21.03.

^{31}P{^{1}H} NMR (202.5 MHz, C_6D_6): δ_P 161.4 (s).

Found ($C_7H_6S_2PCl$ requires): C = 38.16% (38.10); H = 2.87% (2.74).

Melting point: 40-41 ^{o}C.

2.4.4 Synthesis of 5-methyl-1,3,2-benzodithiaphospholyl dimer, (2)$_2$

A suspension of 5-methyl-1,3,2-benzodithiaphospholium chloride(1.07 g; 4.85 mmol) and finely chopped Na (0.30 g; 13.0 mmol) in toluene (20 mL) was stirred at 100 ^{o}C for 4 days. The mixture reaction was filtered and the filtrate evaporated *in vacuo* to afford a yellow solid. Recrystallization by slow evaporation of a toluene solution afforded very pale yellow crystals of 5-methyl-1,3,2-benzodithiaphospholyl dimer. Yield: 0.631 g (70%).

^{1}H NMR (300 MHz, CD_2Cl_2): δ_H 7.35 (d, $^{3}J_{HH}$ = 8.1 Hz, 2H, aromatic CH); 7.31 (s, 2H, aromatic CH); 6.98 (d, $^{3}J_{HH}$ = 8.1 Hz, 2H, aromatic CH); and 2.31 (s, 6H, CH_3).

^{31}P{^{1}H} NMR (202.5 MHz, $CDCl_3$): δ_P 40.6 (s).

Found ($C_{14}H_{12}S_4P_2$requires): C = 45.48% (45.39); H = 3.34% (3.27).

Melting point: 221-222 ^{o}C.

2.4.5 Halogenation of (2)$_2$

2.4.5.1 With SO_2Cl_2

To a solution of 5-methyl-1,3,2-benzodithiaphospholyl dimer (40 mg; 0.11 mmol) in toluene (5 mL) at 0 ^{o}C under N_2 was added dropwise 0.35 mL of fresh-prepared sulfuryl chloride solution (227 mg SO_2Cl_2 in 5 mL CH_2Cl_2). The reaction mixture was stirred at 0 ^{o}C for 2 h. Solvent was removed *in vacuo*, and colourless oil was stored at -20 ^{o}C to give colourless crystals of *P*-chloro-5-methyl-1,3,2-benzodithiaphosphole. Yield: 42 mg (88%).

^{1}H NMR (300 MHz, C_6H_6): δ_H 6.98 (d, $^{3}J_{HH}$ = 8.1 Hz, 1H, aromatic CH); 6.82 (s, 1H, aromatic CH); 6.48 (d, $^{3}J_{HH}$ = 8.1 Hz, 1H, aromatic CH); 1.80 (s, 3H, CH_3).

^{31}P{^{1}H} NMR (202.5 MHz, C_6D_6): δ_P 161.4 (s).

Melting point: 40-41 ^{o}C.

2.4.5.2 With Br_2

To a solution of 5-methyl-1,3,2-benzodithiaphospholyl dimer (57 mg; 0.15 mmol) in toluene (5 mL) at 0 ^{o}C under N_2 was added dropwise 0.88 mL of fresh-prepared bromine solution (153 mg Br_2 in 5 mL CH_2Cl_2). The reaction mixture was stirred at 0 ^{o}C for 2 h. Solvent was removed *in vacuo* to give yellow solid which was recrystallized in CH_2Cl_2 to afford yellow crystals of *P*-bromo-5-methyl-1,3,2-benzodithiaphosphole. Yield: 58 mg (70%).

^{1}H NMR (500 MHz, C_6D_6): δ_H 7.03 (d, $^{3}J_{HH}$ = 8 Hz, 1H, aromatic CH); 6.87 (s, 1H, aromatic CH); 6.55 (d, $^{3}J_{HH}$ = 8 Hz, 1H, aromatic CH); 1.86 (s, 3H, CH_3).

^{31}P{^{1}H} NMR (202.5 MHz, C_6D_6): δ_P 163.6 (s).

Found ($C_7H_6S_2PBr$ requires): C = 31.70% (31.71); H = 2.30% (2.28).

Melting point: 55-56 ^{o}C.

2.4.5.3 With I_2

To a solution of 5-methyl-1,3,2-benzodithiaphospholyl dimer (48 mg; 0.13 mmol) in toluene (3 mL) at 0 ^{o}C under N_2 was added dropwise a solution of I_2 (33mg; 0.13 mmol) in toluene (2 mL). The reaction mixture was stirred at 0 ^{o}C for 2.5 h. Solvent was removed *in vacuo* to give a yellow solid which was recrystallized in CH_2Cl_2 to afford yellow crystals of *P*-iodo-5-methyl-1,3,2-benzodithiaphosphole. Yield: 55 mg (68%).

^{1}H NMR (500 MHz, C_6D_6): δ_H 6.95 (d, $^{3}J_{HH}$ = 8 Hz, 1H, aromatic CH); 6.79 (s, 1H, aromatic CH); 6.48 (d, $^{3}J_{HH}$ = 8 Hz, 1H, aromatic CH); 1.79 (s, 3H, CH_3).

^{31}P{^{1}H} NMR (202.5 MHz, C_6D_6): δ_P 155.4 (s).

Melting point: 79-81 ^{o}C.

Found ($C_7H_6IPS_2$ requires): C = 26.65% (26.94); H = 2.09% (1.94).

2.4.6 Crystallography

Powder X-ray diffraction studies on [**1**]Cl and $(\mathbf{2})_2$ were undertaken on a Bruker D8 Discover powder diffractometer equipped with an Oxford Cryosystems cryostream device and Cu-Kα radiation. Data were collected at 0.02^o intervals with counting times of 0.3 s in the range $5 \leq 2\theta \leq 45^o$. The unit cell of [**1**]Cl was determined from indexing 15 peaks ($\theta < 30^o$) using DICVOL[8] and the structure of [**1**]Cl was solved using DASH[9] implementing a Z-matrix based on a geometry optimised (B3LYP/6-31G*+)[13] gas phase structure from within Jaguar.[25] In the latter stages the C-S, S-P and P-Cl bond lengths and angles were refined to afford a modest improvement in fit to the diffraction profile.

Single crystal structure determinations of [**1**]Cl, $(\mathbf{1})_2$, [**2**]Cl, [**2**]Br and [**2**]I were determined on a Bruker APEX three circle diffractometer using a Bruker cryoflex cooler. Data were processed using SAINT[26] and an absorption correction applied using SADABS (TWINABS for $(\mathbf{1})_2$).[27] Structures were solved and refined against F^2 within SHELXTL.[28] Crystallographic summaries of these structures are presented in Appendix 1.

2.4.7 Theoretical calculations

Full geometry optimizations of closed-shell species were undertaken in Jaguar,[25] using Density Functional Theory with the B3LYP functional[29] and 6-31G*+ or 6-311 G*+ basis set and a closed shell singlet configuration. Calculations of the gas phase energetics of dimerisation process were based on the energies of the closed shell singlet $(\mathbf{1})_2$ and open shell doublet **1** and included appropriate zero point energy corrections.

Table 2.4. Energies of monomer and dimer, and the energy changes associated with the dimerization processes (2 monomer → dimer).

	U_{tot} (hartrees)	H_{tot} (hartrees)	G_{tot} (hartrees)	ΔU_{dim} (kJ/mol)	ΔH_{dim} (kJ/mol)	ΔG_{dim} (kJ/mol)
1•[a]	-1368.704516	-1368.703572	-1368.748262	-116.202	-118.656	-55.260
$(\mathbf{1})_2$[a]	-2737.453725	-2737.452781	-2737.517778			
1•[b]	-1368.820264	-1368.819320	-1368.863924	-117.218	-119.673	-57.442
$(\mathbf{1})_2$[b]	-2737.685612	-2737.684668	-2737.749941			
2•[b]	-1408.116651	-1408.115707	-1408.165696	-116.581	-119.036	-55.123
$(\mathbf{2})_2$[b(trans)]	-2816.278141	-2816.277197	-2816.352593			
2•[b]	-1408.116651	-1408.115707	-1408.165696	-116.592	-119.044	-56.181
$(\mathbf{2})_2$[b(cis-1)]	-2816.278145	-2816.277200	-2816.353000			
2•[b]	-1408.116651	-1408.115707	-1408.165696	-116.581	-119.036	-57.879
$(\mathbf{2})_2$[b(cis-2)]	-2816.278141	-2816.277197	-2816.353653			

[a]6-31G*+ basis set; [b]6-311 G*+ basis set; [dim]Dimerization
Total internal energy, U_{tot}; total enthalpy, H_{tot}; total Gibbs free energy, G_{tot}

2.5 References

1. Baudler, M.; Moog, A.; Glinka, K.; Kelsch, U., *Z. Naturforsch., B* **1973**, *28*, 363-369.

2. (a) Burford, N.; Passmore, J.; Schriver, M. J., *J. Chem. Soc., Chem. Commun.* **1986**, 140-142; (b) Burford, N.; Royan, B. W.; Linden, A.; Cameron, T. S., *J. Chem. Soc., Chem. Commun.* **1988**, *0* (13), 842-844; (c) Burford, N.; Royan, B. W.; Linden, A.; Cameron, T. S., *Inorg. Chem.* **1989**, *28* (1), 144-150.

3. (a) Payrastre, C.; Madaule, Y.; Wolf, J. G.; Kim, T. C.; Mazières, M.-R.; Wolf, R.; Sanchez, M., *Heteroat. Chem.* **1992**, *3* (2), 157-162; (b) Bansal, R. K.; Grupta, N.; Collier, S. J., Product class 15: dithiaphospholes and their analogues. 2004; Vol. 13, pp 641-646.

4. (a) Day, R. O.; Sau, A. C.; Holmes, R. R., *J. Am. Chem. Soc.* **1979**, *101* (14), 3790-3801; (b) Sau, A. C.; Holmes, R. R., *J. Organomet. Chem.* **1978**, *156* (1), 253-258.

5. Winter, S. M.; Oakley, R. T.; Kovalev, A. E.; Hill, S., *Phys. Rev. B* **2012**, *85* (9), 94430-94441.

6. Luzon, J.; Campo, J.; Palacio, F.; McIntyre, G. J.; Rawson, J. M.; Less, R. J.; Pask, C. M.; Alberola, A.; Farley, R. D.; Murphy, D. M.; Goeta, A. E., *Phys. Rev. B* **2010**, *81* (14), 144429(12).

7. Edge, R.; Less, R. J.; McInnes, E. J. L.; Muther, K.; Naseri, V.; Rawson, J. M.; Wright, D. S., *Chem. Commun.* **2009**, *0* (13), 1691-1693.

8. Boultif, A.; Louer, D., *J. Appl. Cryst.* **2004**, *37* (5), 724-731.

9. David, W. I. F.; Shankland, K.; van de Streek, J.; Pidcock, E.; Motherwell, W. D. S.; Cole, J. C., *J. Appl. Cryst.* **2006**, *39* (6), 910-915.

10. Pauling, L., *The Nature of the Chemical Bond and the Structure of Molecules and Crystals: An Introduction to Modern Structural Chemistry*. Cornell University Press: **1960**.

11. Cambridge Crystallographic Database (ConQuest) 21 October 2008.

12. Fajans, K., *Z. Naturwiss.* **1923**, *11* (10), 165-172.

13. (a) Gudat, D.; Haghverdi, A.; Hupfer, H.; Nieger, M., *Chem. Eur. J.* **2000**, *6* (18), 3414-3425; (b) Reed, A. E.; Weinstock, R. B.; Weinhold, F., *J. Chem. Phys.* **1985**, *83* (2), 735-746.

14. Bruno, I. J.; Cole, J. C.; Edgington, P. R.; Kessler, M.; Macrae, C. F.; McCabe, P.; Pearson, J.; Taylor, R., *Acta Cryst., B* **2002**, *58* (3 Part 1), 389-397.

15. Preuss, K. E., *Polyhedron* **2014**, *79*, 1-15.

16. García, F.; Less, R. J.; Naseri, V.; McPartlin, M.; Rawson, J. M.; Wright, D. S., *Angew. Chem.* **2007**, *119* (41), 7973-7976.

17. (a) Becke, A. D., *Phys. Rev. A* **1988**, *38* (6), 3098-3100; (b) Becke, A. D., *J. Chem. Phys.* **1993**, *98* (7), 5648-5652.

18. Housecroft, C. E.; Sharpe, A. G., *Inorganic Chemistry 3rd Edition*. Pearson, Harlow UK: **2008**.

19. Rawson, J. M.; Alberola, A.; Whalley, A., *J. Mater. Chem.* **2006**, *16* (26), 2560-2575.

20. Awere, E. G.; Burford, N.; Mailer, C.; Passmore, J.; Schriver, M. J.; White, P. S.; Banister, A. J.; Oberhammer, H.; Sutcliffe, L. H., *J. Chem. Soc., Chem. Commun.* **1987**, *0* (2), 66-69.

21. Lide, D. R., *CRC Handbook of Chemistry and Physics (88th 2007-2008 edition)*. CRC Press: **2007**.

22. Kühl, O., *Phosphorus-31 NMR Spectroscopy: A concise introduction for the synthetic organic and organometallic chemist*. Springer-Verlag: **2008**.

23. (a) Gutowsky, H. S.; McCall, D. W., *J. Chem. Phys.* **1954**, (22), 162-164; (b) Emsley, J. W.; Feeney, J.; Sutcliffe, L. H., *High Resolution Nuclear Magnetic Resonance Spectroscopy*. Elsevier Science: **2013**.

24. Jiang, Z. H.; Argyropoulos, D. S.; Granata, A., *Magn. Reson. Chem.* **1995**, *33*, 375 - 382.

25. Jaguar, version 7.9, Schrödinger, LLC, New York, NY, 2012.

26. Bruker SAINT, Bruker AXS, Madison, WI, USA.

27. SADABS 2012/1 or TWINABS, Bruker AXS, Madison, WI, USA.

28. SHELXTL, Bruker AXS, Madison, WI, USA.

29. Tirado-Rives, J.; Jorgensen, W. L., *J. Chem. Theory Comput.* **2008**, *4* (2), 297-306.

CHAPTER 3

BENZODIAZAPHOSPHOLES: TOWARDS DIAZAPHOSPHOLYL RADICALS

3.1 Introduction

3.1.1 Benzodiazaphospholyl radicals – Bicyclic C_2N_2P systems

Acyclic tetrakis(dialkylamino)diphosphanes of common structure $(R_2N)_2P–P(NR_2)_2$ have periodically been examined throughout the past few decades.[1] The alliance of prospectively reactive P–N and P–P bonds provides a diversity of chemical reactivity and the sterically hindered bisphosphanes can go through reversible homolytic cleavage to afford phosphanyl radicals.[1a,b,2]

Only a few five-membered mono-heterocyclic diphosphanes of structure $[(CH)_2(NR)_2P]_2$ have been reported to date.[3] A report in 2009 showed that the symmetrical species $[(CH)_2(NR)_2P]_2$ (R = ^{t}Bu; R = mesityl; R = 2,6-diisopropylphenyl) dissociated at room temperature to afford P-based 7π radicals. These radicals are obtained *via* low-energy P–P bond cleavage, driven by entropy coupled with a combination of electronic delocalization within the C_2N_2P framework coupled with steric stabilization.[3d]

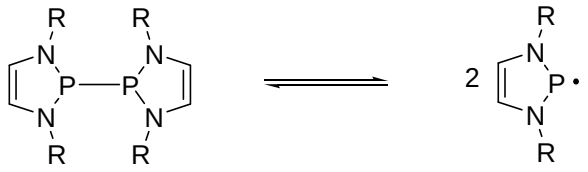

3.1.1.1 Solid-state structures of $[(CH)_2(NR)_2P]_2$ dimers

Three derivatives $[(CH)_2(NR)_2P]_2$ (R = ^{t}Bu; R = mesityl; R = 2,6-di-isopropylphenyl) have been determined crystallographically and exist as *trans*-oid dimers in the solid state to minimize steric hindrance between the bulky substituents R groups on the four heterocyclic nitrogen atoms.[3d] The bulky R groups create a substantial increase in the P–P bond length, from 2.2439(8) Å (R = ^{t}Bu), to 2.324(2) Å (R = mesityl), to mean 2.33Å (R

= 2,6-di-isopropylphenyl) in comparison to a typical P-P bond (2.21 Å).[4] When the R group becomes increasingly sterically demanding, additional structural distortions occur such as puckering of the rings, and the twisting of the R substituents out of the heterocyclic plane. The twisting of the P–P bond away from the centro symmetric arrangement can also occur to avoid the steric clash between the five-member $[(CH)_2(NR)_2P]$ ring units.[3d] In addition five derivatives with a saturated backbone, $[(CH_2)_2(NR)_2P]_2$ have been reported (R = 2,6-di-methylphenyl, 2,6-di-disopropyl-phenyl, mesityl, butyl and 2-t-butyl-phenyl).[3a,3c,5] Selected structures are presented in Figure 3.1.

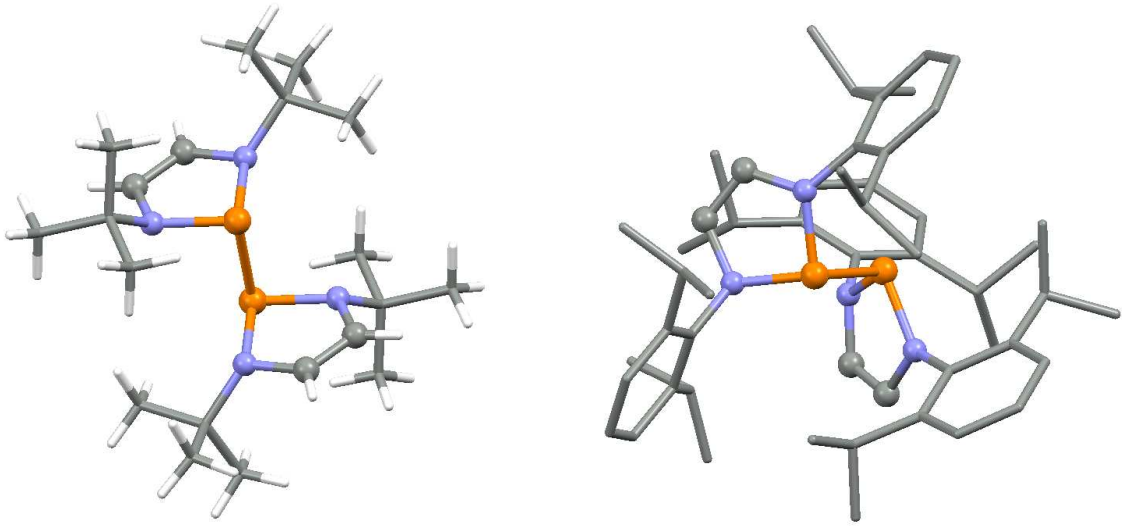

Figure 3.1. Structures of two unsaturated diazaphospholyl dimers: centrosymmetric $[(CH)_2(N^tBu)_2P]_2$ (left) and twisted $[(CH)_2(N(^iPr_2C_6H_3))_2P]_2$ (right).

3.1.1.2 EPR spectroscopy

The dimers $[(CH)_2(NR)_2P]_2$ (R = ^{t}Bu; R = mesityl; R = 2,6-diisopropylphenyl) are all EPR-silent in the solid state because of the presence of P–P bonds. At 353 K the colourless toluene solution (R = ^{t}Bu) turns faint yellow, heralding the dissociation of the P-P bonded dimer to form two radicals. The EPR spectrum reveals a 1:1 doublet of 1:2:3:2:1 quintets [a_P = 41 G, 2 × a_N = 5.8 G] at g = 2.00088, in agreement with hyperfine coupling to one phosphorus and two equivalent nitrogen nuclei. Additional ^{1}H coupling to substituents (^{t}Bu) or to heterocyclic C–H atoms was not detected. This is in contrast to

related indium complexes, $[(CH)_2(NR)_2In]$ which display hyperfine coupling to ^{1}H, ^{14}N and indium isotopes (^{113}In and ^{115}In, both $I = {}^{9}/_{2}$).[6]

The dimers with longer P–P bonds appear to dissociate more readily in solution, consistent with bond weakening. The dimer $[(CH)_2(NR)_2P]_2$ (R = mesityl) possesses an analogous structure and the radical can also be detected by EPR spectroscopy at 315 K, [g = 2.0178, a_P = 40 G, 2 × a_N = 5.2 G] and the bulkiest derivative (R = 2,6-di-isopropylphenyl) shows considerable dissociation at room temperature [g = 2.0248, a_P = 42 G, 2 × a_N = 5.4 G].[3d]

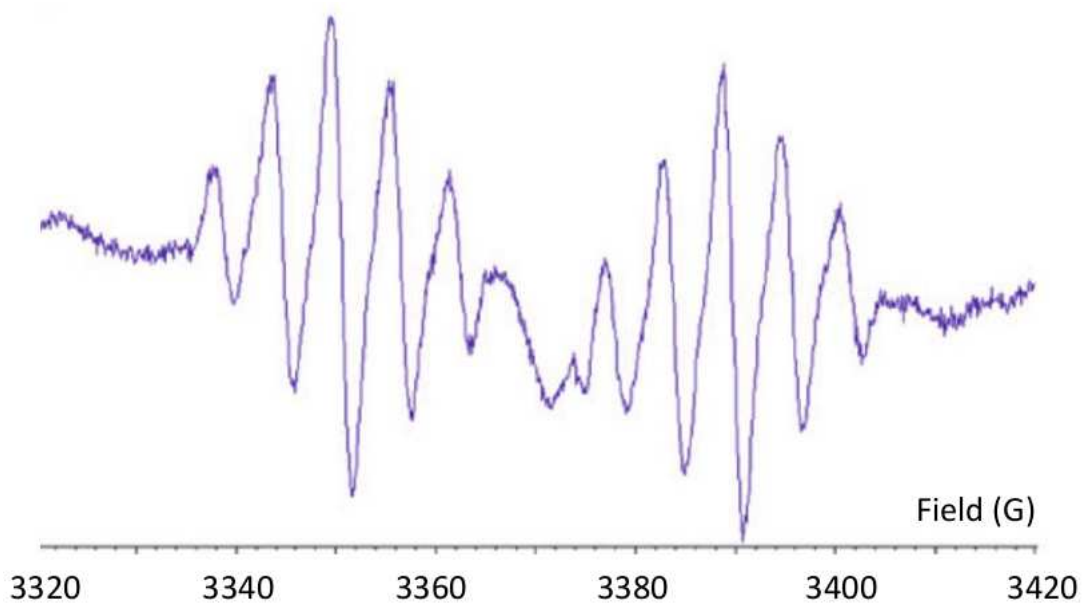

Figure 3.2. EPR spectrum of $[(CH)_2(N^tBu)_2P]_2$ in toluene at 353 K.[3d] Adapted from reference {3d} with permission of The Royal Society of Chemistry.

3.1.1.3 Syntheses of symmetrical [1,3,2]diazaphospholyl dimers

The most common general synthetic method to prepare diazaphospholyl dimers is the reductive coupling of 2-chloro-1,3,2-diazaphospholes, regularly offering moderate yields (40 - 60%).[3]

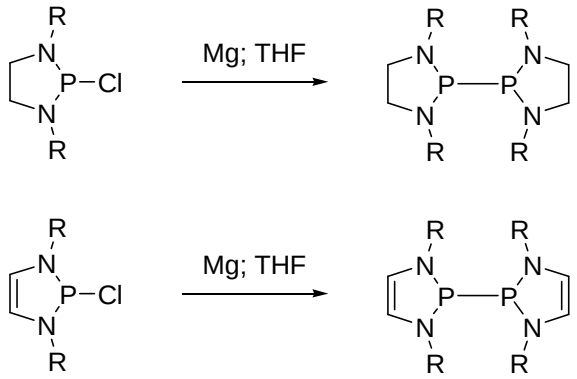

Scheme 3.1. Syntheses of symmetrical [1,3,2]diazaphospholyl dimers.

A recently improved synthetic approach describes a time-saving, consecutive "one-pot" synthesis from ethane-1,2-diamines or 1,4-diazabutadienes.[3c,5] This route offers high selectivity and high yields because it reduces the loss of products due to unexpected hydrolysis. However, in some cases *N*-heterocyclic secondary phosphanes ($C_2H_2(NR)_2PH$ or $C_2H_4(NR)_2PH$) are generated alongside, or instead of, the target diazaphospholyl radical dimer.[5]

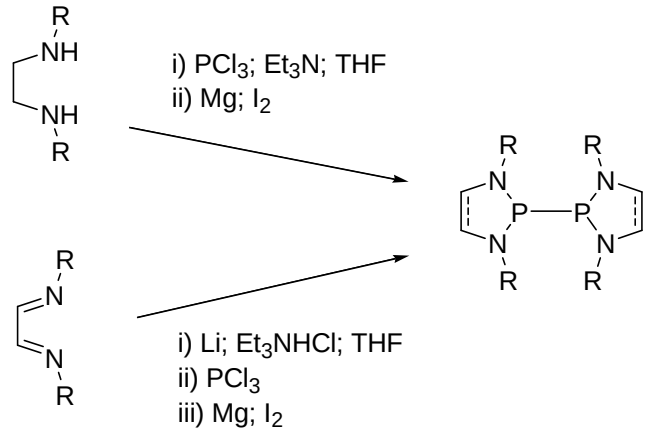

Scheme 3.2. One-pot syntheses of P-P dimers.

3.1.2 Project aims

Our research interest has been focused on new classes of persistent radicals which are isoelectronic with the well known DTA radicals. In Chapter 2, replacement of N by

isovalent P was undertaken but led to P-P σ-bond formation with a lack of tunable steric protection near the reactive P centre. Here we replace the S atoms in the dithiaphospholyls by isolobal NR, providing the opportunity for both extended π-conjugation to the benzo-fused substituent and sterically-tunable R groups at N.[3d,7] The $[C_2(NR)_2P]$ framework is therefore similarly expected to be a 7π-electron radical system (or 11π if the benzo-fused bicyclic system is considered) and the effect of extended π-delocalisation can be compared with steric protection as a method to inhibit dimerization. Notably in both the dithiaphospholyl (C_2S_2P) radicals and diazaphospholyls ($C_2(NR)_2P$), the electronegativity differences afford similar bond polarities *viz* $^{\delta-}S-P^{\delta+}$ and $^{\delta-}N-P^{\delta+}$ such that the electropositive P-centre will contribute more to the SOMO in both cases. This will favour localised 2*c*,2*e* P-P bonds (as identified above), although the differences in electronegativity are anticipated to create some differences in charge and electron distributions between the diazaphospholyl heterocycle (N/P) compared to dithiazolyl (S/N) and dithiaphospholyl (S/P) counterparts.

3.2 Results and Discussion

3.2.1 Syntheses of P-chloro-benzodiazaphospholes

An adaptable synthetic methodology was devised to access benzo-fused diazaphospholes. In these processes, the readily available *ortho*-phenylenediamine, $C_6H_4(NH_2)_2$, was used as starting material. Treatment of *o*-phenylenediamine with methyl chloroformate or acetyl chloride according to the literature protocol[8] afforded the intermediate *N*,*N*′-dimethylcarbamate- and *N*,*N*′-diacetyl-*o*-phenylenediamine in high yields (64-70%, Scheme 3.3). Their structures were confirmed by NMR spectroscopy and X-ray diffraction (Figure 3.3). These intermediates were reduced using $LiAlH_4$ to afford *N*,*N*′-dimethyl- and *N*,*N*′-diethyl-substituted-*o*-phenylenediamine in good yield (70-76%) using a literature method.[9]

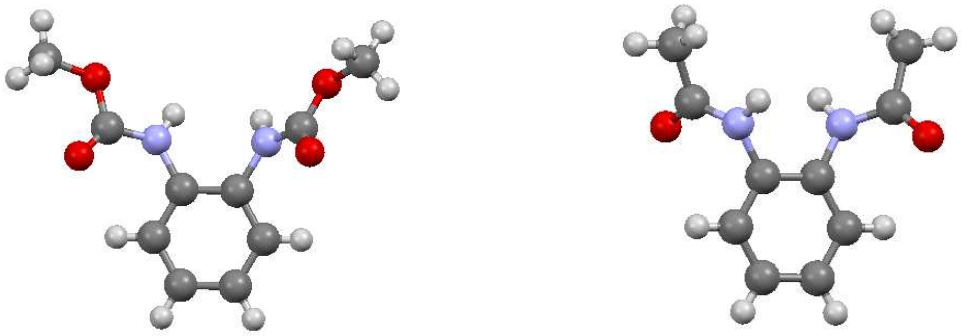

Figure 3.3. Molecular structures of the intermediates *N*,*N*′-dimethylcarbamate- (left) and *N*,*N*′-diacetyl-*o*-phenylenediamines (right).

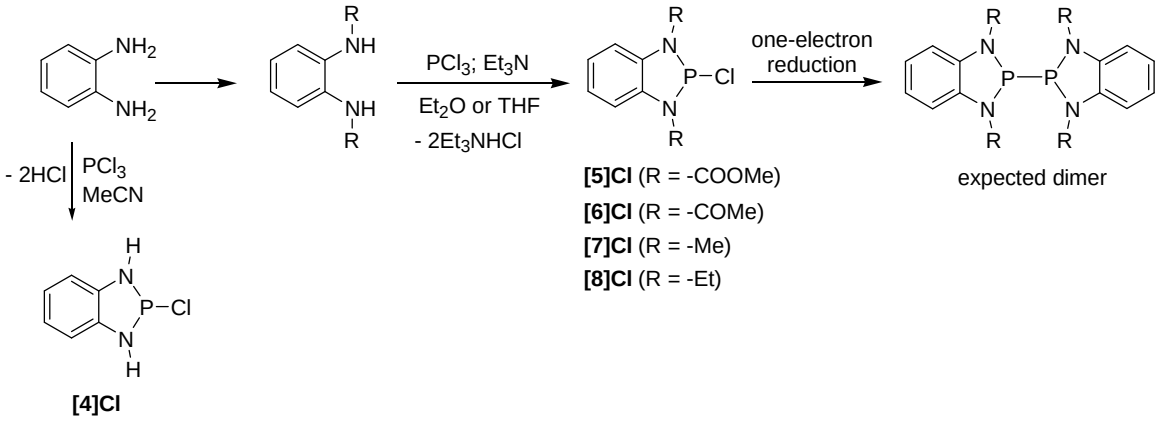

Scheme 3.3. Synthesis of *P*-chloro-*N*,*N*′-substituted diazaphospholes and dimers.

In comparison to the direct ring closure reactions of benzene and toluene dithiols with PCl_3 to afford [**1**]Cl and [**2**]Cl, *P*-chloro-*N*,*N*′-substituted precursors were generated by condensation of the diamine precursors with PCl_3 in the presence of Et_3N to remove the HCl by-product (as $Et_3N{\cdot}HCl$), otherwise the *o*-phenylenediamine itself proved sufficiently strong to act as a base. Each of the *P*-chloro-benzodiazaphospholes ([**5**]Cl, [**6**]Cl, [**7**]Cl and [**8**]Cl) was isolated in high yields (80-88%) from the corresponding amine, although the parent *P*-chloro derivative [**4**]Cl could be synthesized directly from the condensation between *o*-phenylenediamine and PCl_3 in MeCN in the absence of Et_3N in medium yield (47%). Condensation between *N*,*N*′-dimethyl-*o*-phenylenediamine and

PBr_3 was carried out using a similar protocol to give [**7**]Br as a green powder in moderate yield (43%).

The *P*-chloro-benzodiazaphospholes ([**5**]Cl, [**6**]Cl, and [**7**]Cl) are off-white to pale yellow solids which are thermally stable, but very sensitive to moisture and air. Crystals of [**5**]Cl and [**6**]Cl were obtained from recrystallization by slow evaporation of saturated CH_2Cl_2 solutions under N_2. Crystals of [**7**]Cl were grown similarly by slow evaporation of acetonitrile solutions under N_2.

For comparison, condensation between *N,N′*-diethyl-diaminobenzene and $POCl_3$ yielded a purple solid [**8**]OCl (39%),[10] which was recrystallized by slow evaporation of acetonitrile solution to obtain suitable crystals for X-ray diffraction. Unlike the P^{III} derivatives, this P(V)-containing heterocycle, like previously reported derivatives, appears air stable.[11]

3.2.2 Structures of [5]Cl, [6]Cl, [7]Cl[10] and [8]OCl[10]

The crystal structures of [**5**]Cl, [**6**]Cl, [**7**]Cl[10] and [**8**]OCl[10] were determined by X-ray diffraction. The crystallographic data are listed in Appendix 3. All four compounds crystallised with one molecule in the asymmetric unit. Compound [**5**]Cl crystallised in the monoclinic space group $P2_1/c$ (Figure 3.4), crystals of [**6**]Cl crystallised in the triclinic space group *P-1* (Figure 3.4), [**7**]Cl crystallised in the orthorhombic space group $P2_12_12_1$ with one molecule in the asymmetric unit (Figure 3.5). The related P(V) compound [**8**]OCl crystallises in the orthorhombic space group *Pbca* (Figure 3.5). Relevant geometric parameters for these four compounds are presented in Table 3.1.

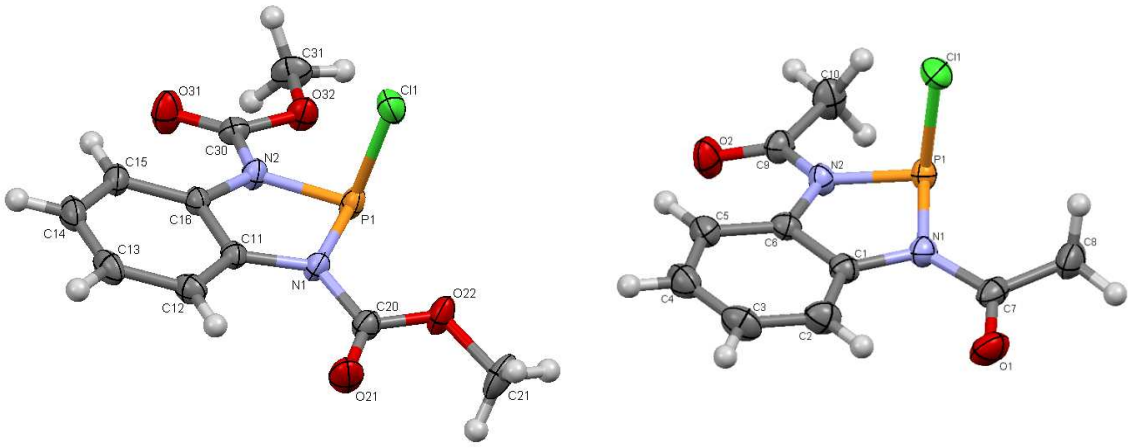

Figure 3.4. Molecular structures of [**5**]Cl (left) and [**6**]Cl (right) determined from single crystal X-ray diffraction with thermal ellipsoids for non-H atoms drawn at 50% probability.

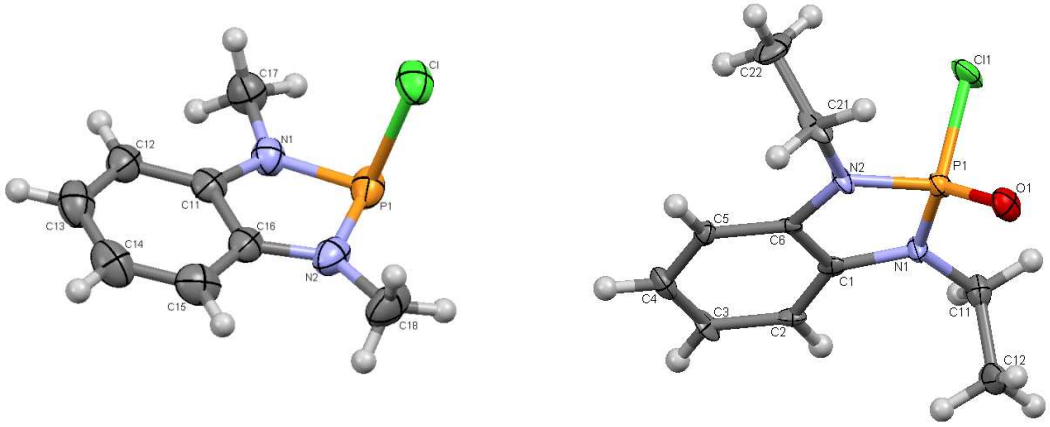

Figure 3.5. Molecular structures of [**7**]Cl (left) and [**8**]OCl (right) determined from single crystal X-ray diffraction with thermal elipsoids of non-H atoms drawn at 50% probability.[10]

Table 3.1. Selected bond lengths [Å], bond angles and fold angles [°] for [**5**]Cl, [**6**]Cl, [**7**]Cl,[10] and [**8**]OCl.[10]

	P-Cl	**P-N**	**N-C**	**C-C**	**N-P-N**	**Fold angle**
[**5**]Cl	2.1210(9)	1.709(2) 1.713(2)	1.418(2) 1.417(2)	1.399(2)	88.63(8)	10.36
[**6**]Cl	2.1267(6)	1.715(1) 1.709(1)	1.436(2) 1.429(2)	1.399(2)	89.93(6)	13.37
[**7**]Cl[10]	2.297(1)	1.668(2) 1.669(3)	1.398(3) 1.401(3)	1.399(3)	90.4(1)	12.32
[**7**][$GaCl_4$][a,10]	-	1.650(2) 1.654(2)	1.384(2) 1.385(2)	1.397(2)	91.33(7)	1.46
[**8**]OCl[10]	2.038(2)	1.651(5) 1.661(5)	1.412(8) 1.410(8)	1.390(8)	94.2(3)	2.60

[a]*Data from Chapter 4*

The heterocyclic geometries of these compounds are broadly similar to those of the dithiaphosphole systems in which the P-Cl bonding is better represented in a covalent rather than ionic manner. The P-Cl bonds in [**5**]Cl, [**6**]Cl and [**7**]Cl (2.1210(9) – 2.297(1) Å) are a little longer than conventional P^{III}-Cl bonds, *e.g.* PCl_3 (2.043 Å),[12] but significantly shorter than the sum of the van der Waals radii (3.55 Å).[13] Notably the P-Cl bond lengths are somewhat shorter than the values reported for $[(CR^2)_2(NR^1)_2P]Cl$[14] mono-heterocycles in which P^{III}-Cl bond lengths fall in the range 2.243(1) to 2.692(4) Å. It has been shown that most *N*-heterocyclic phosphines $[(CR^2)_2(NR^1)_2P]X$ (X = Cl, H, P) experience some degree of P-X bond polarization which is reflected in bond lengthening, a decrease in covalent bond order and a build up of charge separation $P^{\delta+}\cdots X^{\delta-}$, reflecting increased bond ionicity.[14-15] Such behaviour is similar to the S/P heterocycles (described in Chapter 2) and other monocyclic diazaphospholes.[16] Thus the P-Cl bonds in the current series would appear somewhat more covalent than the non-benzo-fused analogues.

The skeletal geometry of [**7**]Cl is in agreement with the observation that the C and N atoms can adopt an sp^2 hybrid geometry with approximate-120° bond angles (Figure 3.6), affording efficient π-conjugation. Conversely, S and P, in line with the heavier *p*-block

elements, exhibit less tendency to hybridize, preferring geometries close to 90°. A regular planar 5-membered ring exhibits internal angles of 108° and both a decrease in the C-N-P bond angle from the ideal value (120°) to 113.5-113.7° and expansion of C-S-P from 90° to 99.4° can be considered to generate some degree of ring strain,[17] which can in part be alleviated by folding (at the expense of reduced conjugation). The small angles at both S and P lead to significant strain which is, in part, relieved by significant folding for the dithiaphospholes (26.06 – 28.35°). In the case of the *P*-chloro-benzodiazaphosphole rings, the angle at N is much closer to ideality, reducing strain and affording a heterocyclic ring where the degree of folding is much reduced (10.36-13.37°). Indeed, if distortion from planarity can be considered a measure of ring strain in these systems, then the diazaphospholes would appear less strained than the corresponding dithiaphospholes.

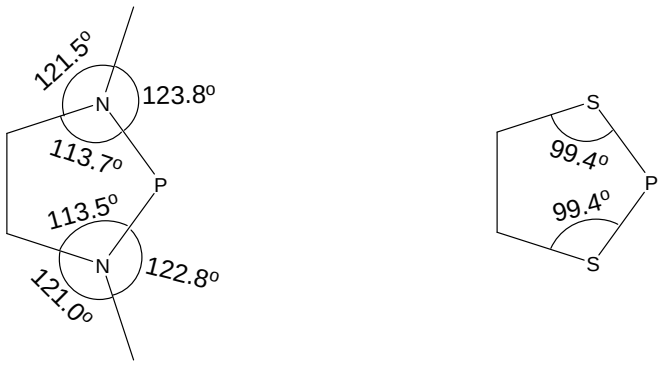

Figure 3.6. Comparison between bond angles of N and S atoms in heterocycles based on the crystallographic data for [**1**]Cl and [**7**]Cl[10].

Substituents on the N atoms affect endocyclic P-N and N-C bond lengths to some extent (< 3%). Within the series [**5**]Cl, [**6**]Cl and [**7**]Cl the P-N bond lengths in [**5**]Cl and [**6**]Cl are the same within error (3 standard deviations) but slightly longer than those observed in [**7**]Cl. This may be due to the change in the electronic effects of the R substituent where the ketone and ester C=O groups act as π-electron withdrawing whereas the alkyl group in [**7**]Cl is σ-electron releasing. These bond lengths and angles are comparable to reported values for other diazaphospholes (P-N 1.79 ± 0.07 Å; N-C 1.46 ± 0.06 Å; C=C 1.36 ± 0.07 Å; N-P-N 89.31 - 92.29°; P-N-C 113.18°).[14,16a,18]

The "envelope shape" of the five-membered ring in [**7**]Cl possesses longer P-N and N-C bonds than those observed in the planar $\mathbf{7}^+$ cation in [**7**][$GaCl_4$] (Chapter 4). This behaviour is similar to the trends observed in the dithiaphosphole/dithiaphosphenium, C_2S_2P, ring (see Chapter 2). Both are consistent with bond shortening in the cation and can be rationalized in terms of ring planarity which optimizes p_π bonding within the C_2N_2P ring, leading to shorter bonds. Additionally, it has been proposed that the attachment of halogen atom on P causes P-N and C-N bond lengthening due to the disruption of π-system, permitting the P atom to distort out of C_2N_2 plane.[19]

3.2.3 Spectroscopic studies on benzodiazaphospholes

3.2.3.1 Infrared (IR) spectra

A comparison of the IR spectra of *P*-halogeno-benzodiazaphospholes with their corresponding *N,N'*-substituted-*o*-phenylenediamine precursors reveal diagnostic changes which can be used to probe the condensation reaction between the diamines and PCl_3 or PBr_3. Specifically the absence of N-H stretching frequencies (3312 cm^{-1} of $C_6H_4(NHCOOMe)_2$ and $C_6H_4(NHEt)_2$, 3230 cm^{-1} of $C_6H_4(NHCOMe)_2$, and 3343 cm^{-1} of $C_6H_4(NHMe)_2$) in *P*-halogen-benzodiazaphospholes are diagnostic evidence for formation of the $[C_2N_2P]X$ heterocycles (X = Cl or Br). Notably the absence of a ν_{N-H} vibration also reflects the absence of the $[Et_3NH]Cl$ by-product.

3.2.3.2 Nuclear Magnetic Resonance (NMR) spectra

The identification and characterization of all products were systematically carried out by multinuclear NMR spectroscopy.

a. ^{1}H NMR

The absence of N-H protons of *N,N'*-substituted-*o*-phenylenediamine precursors in samples of *P*-halogen-benzodiazaphospholes could also be detected by ^{1}H NMR spectroscopy. The positions of the NH proton (in solvent $CDCl_3$) in the precursor

substrates were variable, *e.g.* δ_H 7.47 ppm for $C_6H_4(NHCOOMe)_2$, δ_H 8.58 ppm for $C_6H_4(NHCOMe)_2$, δ_H 3.27 ppm for $C_6H_4(NHMe)_2$ and δ_H 3.32 ppm for $C_6H_4(NHEt)_2$.

In addition, the ^{1}H NMR spectra of some compounds (such as [**4**]Cl, [**7**]Cl, and [**7**]Br) reveal a single resonance for the *N,N′*-hydrogen or *N,N′*-methyl substituents which is split into a doublet due to a coupling to the ^{31}P center. In [**4**]Cl δ_H 7.72 ppm (d, $^2J_{PH}$ = 23.7 Hz, 2H, NH), in [**7**]Cl δ_H 2.67 ppm (d, $^3J_{PH}$ = 12.1 Hz, 6H, NCH_3), and in [**7**]Br δ_H 3.37 ppm (d, $^3J_{PH}$ = 13.1 Hz, 6H, NCH_3). The J_{PH} coupling values are consistent with those in their corresponding ^{31}P ^{1}H-coupled NMR spectra discussed below. These observations substantiate the condensation reaction between *N,N′*-substituted-*o*-phenylenediamines and PCl_3 or PBr_3 to generate new P/N heterocyclic compounds.

b. ^{13}C NMR

While the resonances for all carbon-13 atoms in *N,N′*-substituted-*o*-phenylenediamine precursors appear as singlets in ^{13}C NMR spectra, the ^{13}C NMR spectra of the *P*-chloro-benzodiazaphospholes are more complex due to ^{13}C-^{31}P coupling affording doublets reflecting either $^2J_{PC}$ or $^3J_{PC}$ coupling. For example [**5**]Cl exhibits two doublets due to $^2J_{PC}$ coupling; δ_C 152.02 ppm (d, $^2J_{PC}$ = 14.3 Hz, PN**C**O), 131.46 ppm (d, $^2J_{PC}$ = 9.7 Hz, heterocyclic PN**C**). For [**6**]Cl three doublets are detected; δ_C 168.79 ppm (d, $^2J_{PC}$ = 23.1 Hz, PN**C**O), 132.52 ppm (d, $^2J_{PC}$ = 7.9 Hz, heterocyclic PN**C**), 25.93 ppm (d, $^3J_{PC}$ = 15.8 Hz, CH_3). Similarly two doublets are recorded in [**7**]Cl (δ_C 137.19 ppm (d, $^2J_{PC}$ = 12.8 Hz, heterocyclic PN**C**), 29.37 ppm (d, $^2J_{PC}$ = 17.7 Hz, PN**C**H_3).

c. ^{31}P NMR

^{31}P NMR spectra offer particularly diagnostic values with specific chemical shift ranges for N/P heterocycles which are also sensitive to the diverse types of *N,N′*-substituent. The pyramidal starting materials PCl_3 and PBr_3 exhibit peaks at δ_P 220 ppm and δ_P 228 ppm respectively. After condensation the ^{31}P NMR spectra reveal diagnostic singlets in the ^{31}P{^{1}H} NMR spectra with chemical shifts in the range 120–175 ppm, depending upon the halogen and *N,N′*-substituents. As with the starting materials the *P*-bromo derivatives

occur at a higher chemical shift than the corresponding chloro derivatives, *e.g.* [**7**]Br (~ 173 ppm) > [**7**]Cl (~ 153 ppm). These values are comparable to the dithiaphospholes, [**1**]Cl (δ_P 158.5 ppm), [**2**]Cl (δ_P 161.4 ppm), [**2**]Br (δ_P 163.6 ppm), [**2**]I (δ_P 155.4 ppm), reflecting similar chemical environments across the series of S_2PX and N_2PX compounds. Replacement of the halogen by N or O donors (section 3.2.4) leads to further shifts with P-O and P-N compounds occurring in the range 104-94 ppm. The ^{31}P NMR spectrum of P(V)-containing [**8**]OCl displays a singlet at 21 ppm, clearly distinct from the three-coordinate P^{III} derivatives but comparable to the P(V) hydrolysis product of [**7**]Cl (15.3 ppm, section 3.2.6).

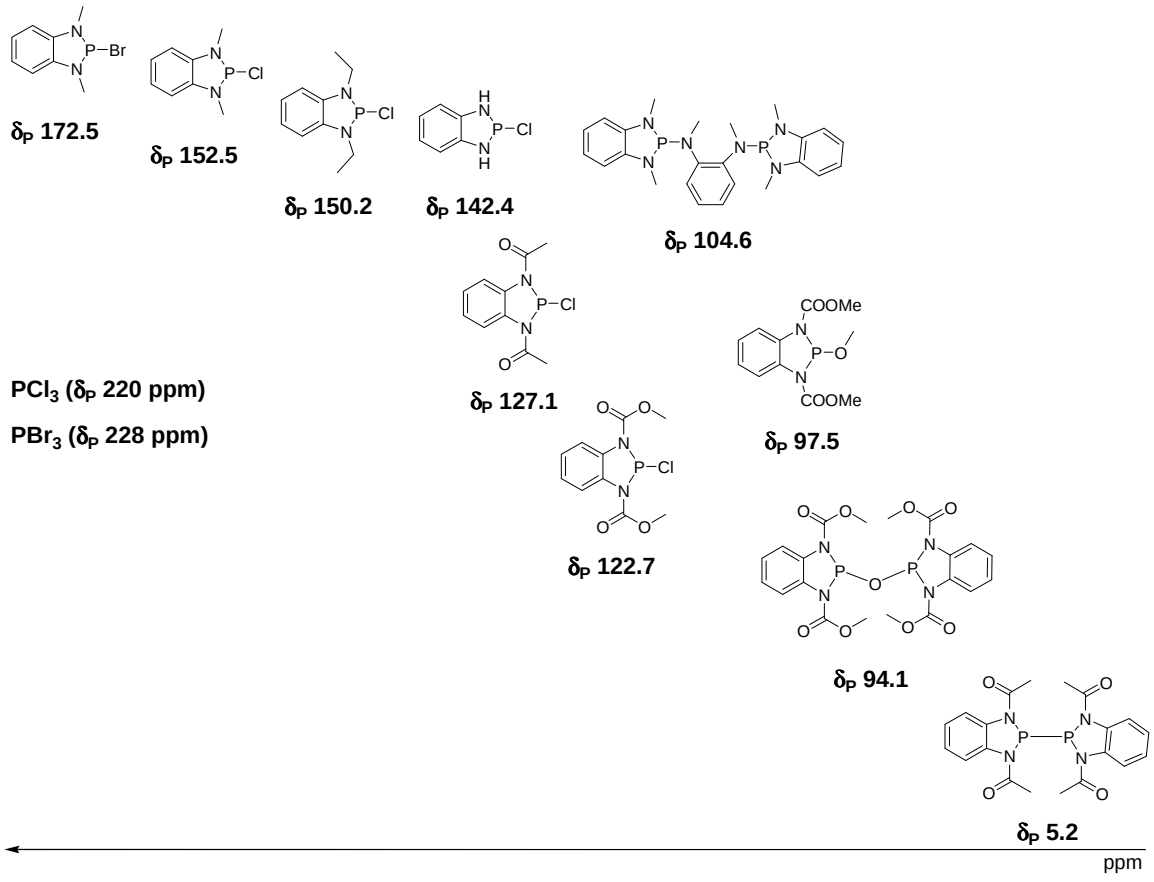

Figure 3.7. $^{31}P\{^1H\}$ NMR chemical shifts of *N,N′*-substituted-1,3,2-benzodiazaphospholes prepared in this chapter.

The $^{31}P\{^{1}H\}$ NMR chemical shifts of tri-coordinate phosphorus compounds prepared in this thesis containing the C_2N_2P ring are presented in Figure 3.7.

Using a similar methodology to that described in Chapter 2 we can estimate the ^{31}P NMR chemical shift based on the paramagnetic shielding constants. For example for an N_2PCl coordination geometry (using NMe_2 for N) the ^{31}P chemical shift is predicted to be δ_P = -62 + (61.5 × 2) + 94 = +155 ppm (*cf* experimental: [**7**]Cl at 152.5 ppm).

Notably the *N,N′*-substituents affect the chemical shift. Broadly speaking there is a correlation between the Hammett parameter for the N-substituent and the ^{31}P chemical shift (Table 3.2). However the electron-donating alkyl groups lead to a downfield shift whereas electron-withdrawing groups lead to an upfield shift. Whilst this appears counter-intuitive, as described in Chapter 2, conventional diamagnetic shielding effects are typically less important than the paramagnetic shielding contribution for ^{31}P NMR spectra.

Table 3.2. Correlation between ^{31}P NMR chemical shift and Hammett parameter σ for the exocyclic R group bound to N.

Group	**COMe**	**COOMe**	**H**	**Et**	**Me**
Hammett σ	0.50	0.45	0.0	-0.15	-0.17
δ_P	127.1	122.7	142.4	150.2	152.5

Depending on the *N,N′*-substituents, the ^{1}H coupled ^{31}P NMR spectra display signals with splitting patterns due to the coupling between ^{31}P (I = 1/2) and ^{1}H (I = 1/2). In the *P*-halogeno-benzodiazaphosphole system,both $^{2}J_{PH}$ and $^{3}J_{PH}$ coupling can be detected. Thus, while most of single-phosphorus-containing compounds exhibit a singlet in both ^{31}P NMR and $^{31}P\{^{1}H\}$NMR, a triplet can be resolved for [**4**]Cl (δ_P 142.4 ppm, $^{2}J_{PH}$ = 23.7 Hz) and septets for both [**7**]Cl (δ_P 152.5 ppm, $^{3}J_{PH}$ = 12.1 Hz) and [**7**]Br (δ_P 172.5 ppm, $^{3}J_{PH}$ = 13.1 Hz) (Figure 3.8).

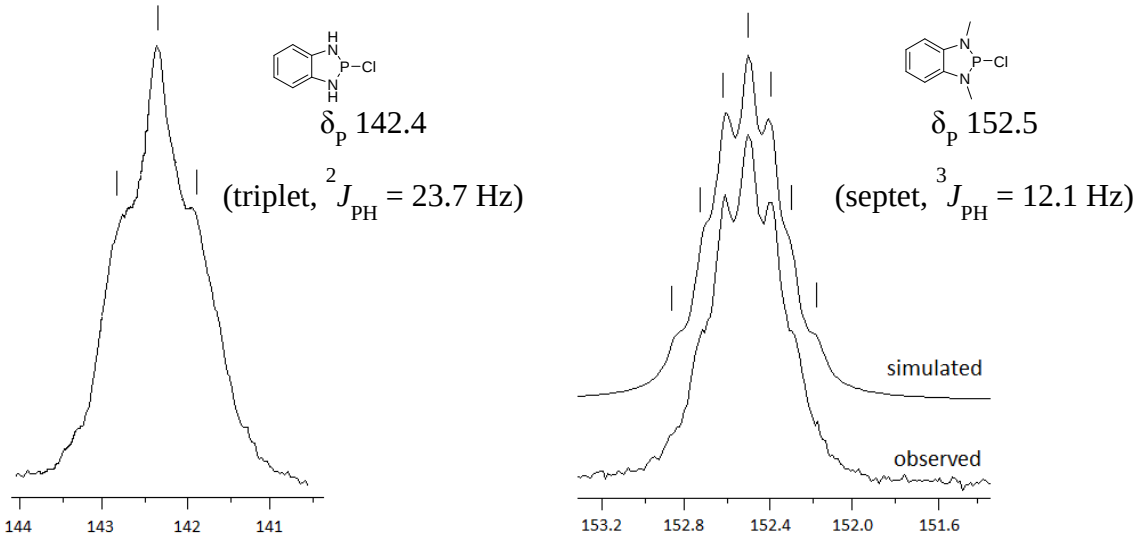

Figure 3.8. Splitting patterns of signals in the ^{1}H coupled ^{31}P NMR spectra of [**4**]Cl (left) and [**7**]Cl (right, simulation was made with SpinWorks 3.1.7).

3.2.4 Reductions of P-chloro-diazaphospholes

The reductive coupling of *P*-chloro-diazaphospholes was attempted under a variety of conditions (*e.g.* different solvents and reducing metals) but proved significantly more challenging than the dithiaphosphole syntheses described in Chapter 2. The progress of these chemical reactions was monitored by ^{31}P{^{1}H} NMR and the reaction terminated when a new single ^{31}P–containing product could be identified. Most attempted reductions appeared "complete" after 24h at reflux in MeCN or THF (*i.e.* afford only one singlet) but longer reaction times (4 – 11 days) were required for toluene. A summary of the reaction outcomes is presented in Table 3.3.

^{31}P{^{1}H} NMR studies of the reduction process

Akin to S/P heterocyclic systems, the coupling reductions of N/P compounds appear to be multi-step reactions which occur *via* unknown intermediates.

Table 3.3. Results of coupling reductions of *P*-chloro-*N,N′*-substituted diazaphospholes.

Starting material	**δ_P (ppm) of $C_6H_4(NR)_2PCl$**	**Reducing reagents**	**Product (yield %)**	**δ_P (ppm) of product**
[**5**]Cl	122.7	Mg/Toluene Reflux, 11 days	White needle crystals (59%)*	94.1
[**5**]Cl	122.7	Mg/MeCN Reflux, 1 day	Yellow needle crystals	99.1
[**5**]Cl	122.7	Na/THF Reflux, 1 day	Yellow solid	141.3
[**5**]Cl	122.7	Mg/I_2/Toluene Reflux, 1 day	White needle crystals (27%)*	97.5
[**6**]Cl	127.1	Mg/I_2/Toluene Reflux, 1 day	Yellow plate crystal (75%)	5.2
[**6**]Cl	127.1	Mg/THF Reflux, 1 day	Yellow solid	91.7
[**6**]Cl	127.1	Mg/MeCN Reflux, 1 day	Off-white solid	101.2
[**7**]Cl	152.5	Mg/Toluene Reflux, 4 days	Brown solid	17.0
[**7**]Cl	152.5	Na/Toluene Reflux, 3 days	Pale yellow crystals (72%)*	104.6
[**8**]Cl	150.2	Mg/Toluene Reflux, 4 days	Black gel	14.9
[**8**]Cl	150.2	Na/Toluene Reflux, 4 days	Black gel	103.0

* indicates successful crystal structure determination.
Mg/I_2 indicates trace quantities of I_2 as activator for the Mg surface.

The ^{31}P NMR of (**1**)$_2$ and (**2**)$_2$,[20] exhibit singlets in the region δ_P 38-41 ppm whereas the starting materials [**1**]Cl and [**2**]Cl can be observed around δ_P 158-162 ppm. Given the similar chemical shifts of [**1**]Cl and the *P*-chloro-diazaphospholes, successful reduction

was expected to lead to diazaphospholyl dimers characterized by ^{31}P chemical shifts in the *ca*. 0 – 20 ppm region.

Among numerous studies of these N/P heterocyclic reductions, four reactions were found to undergo similar reactivity to the S/P systems: reduction of [**5**]Cl by Mg/Toluene, [**6**]Cl by Mg/I_2/Toluene, [**7**]Cl by Mg/Toluene, and[**8**]Cl by Mg/Toluene. In each case one new major singlet emerging in the upfield area around 0-20 ppm which can be tentatively assigned to (**5**)$_2$ (δ_P 1 ppm), (**6**)$_2$ (δ_P 5 ppm), (**7**)$_2$ (δ_P 17 ppm), and (**8**)$_2$ (δ_P 15 ppm), respectively. In each case the change in chemical shifts between starting materials and corresponding products are shifted upfield by *ca.*120-135 ppm but these products were often contaminated with starting material or other intermediate evidenced by $^{31}P\{^1H\}$ NMR.

The reduction of [**5**]Cl in Mg/Toluene yielded [**5**]$_2$O containing the P-O-P bridging unit and which was characterised by X-ray diffraction (section 3.2.5.2). The former is believed to be generated through oxidation of (**5**)$_2$. ^{31}P NMR studies of this reaction reveal initial formation of a major product at *ca.*1 ppm, proposed to be (**5**)$_2$, after 2 days (Figure 3.9) which after reaction for a further 9 days afforded selectively [**5**]$_2$O (^{31}P δ 94.1 ppm) presumably *via* oxidation over the extended reaction time.

The presence of I_2 in the reaction mixture has an unanticipated effect on the one-day-reduction of [**5**]Cl by Mg/Toluene, yielding a different product (δ_P 97.5 ppm) whose ^{31}P NMR spectrum remained unchanged after a further three days. [The I_2 was added to facilitate cleaning of the Mg surface to try and increase reaction rate]. The structure was subsequently determined to be [**5**]OMe by X-ray diffraction (section 3.2.5.4). Unsurprisingly [**5**]$_2$O and [**5**]OMe have similar chemical shifts. The formation of [**5**]OMe must arise from a metal-catalysed de-esterification of the ester group with the resultant methoxide anion displacing the chloride group by nucleophilic substitution.

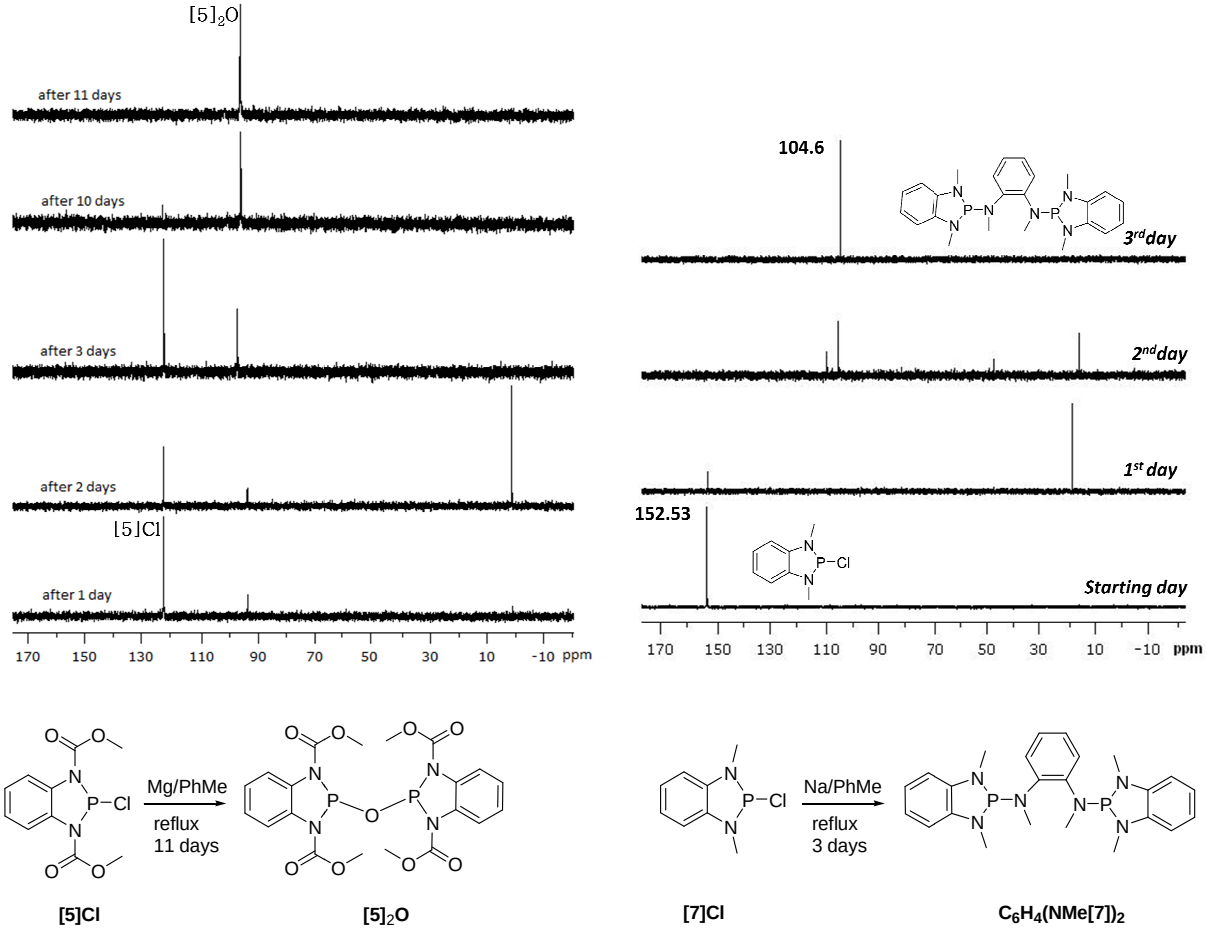

Figure 3.9. ^{31}P NMR spectra of the reduction of [**5**]Cl (left) and [**7**]Cl (right), both of which appear to proceed *via* the dimer $(\mathbf{5})_2$ or $(\mathbf{7})_2$ which appears around 0 – 20 ppm.

Reduction of [**7**]Cl (Na/Toluene) followed an alternative reaction pathway. After 24h a single peak was detected around 20 ppm (Figure 3.9), consistent with initial formation of $(\mathbf{7})_2$ which after 3 days was replaced by a singlet at 104.6 ppm, a position diagnostic of three-coordinate P. Subsequent recrystallization and structure determination (section 3.2.5.3) revealed it to be $C_6H_4(NMe)_2P\text{-}NMeC_6H_4NMe\text{-}P(NMe)_2C_6H_4$ presumably afforded by thermal degradation of $(\mathbf{7})_2$.

The reductions of the *P*-chloro-*N*,*N'*-dialkyl-diazaphospholes [**7**]Cl and [**8**]Cl afford analogous results in terms of ^{31}P chemical shifts either in reduction by Mg/Toluene or by

Na/Toluene. Thus reduction with Mg/Toluene affords products which appear as singlets around 15-17 ppm, consistent with formation of (**7**)$_2$ and (**8**)$_2$. Conversely reduction with Na/Toluene afforded singlets around 103-105 ppm, consistent with $C_6H_4(NR)_2P$-NRC_6H_4NR-$P(NR)_2C_6H_4$. Although all attempts to prepare suitable crystals for X-ray structure determination failed, the ^{31}P chemical shift (δ_P 103.0 ppm) is very close to that observed for $C_6H_4(NMe[\mathbf{7}])_2$ (δ_P 104.6 ppm), suggesting [**8**]Cl is reduced by Na/Toluene to give a bis-triamide structure.

The formation of species such as $C_6H_4(NMe[\mathbf{7}])_2$ and $C_6H_4(NEt[\mathbf{8}])_2$ is noteworthy since previous studies found that reaction between 2-chloro-4-methyl-1,3-di-tert-butyl-[1,3,2]diazaphosphorinane and metallic Na(K) in *o*-xylene at 110 °C under Würtz coupling conditions does not afford P-P dimer as expected[21,22] but leads to a disproportionation and ring-opening to generate a bis-triamide (Scheme 3.4).[3b]

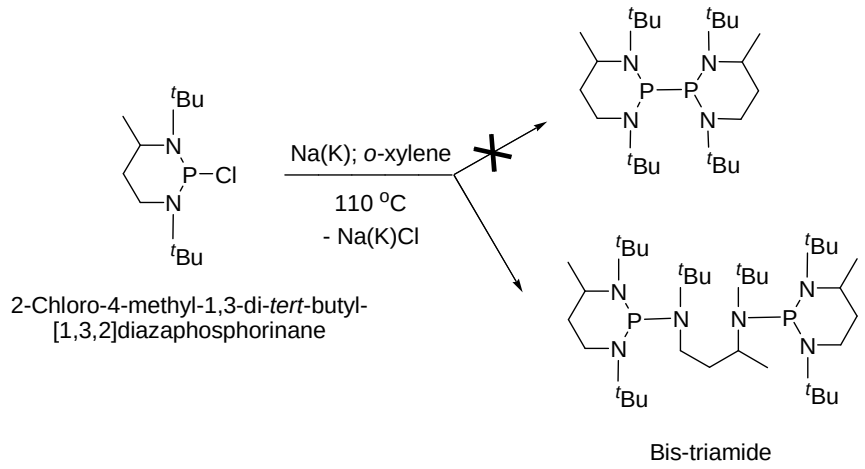

Scheme 3.4. Reduction of 2-chloro-4-methyl-1,3-di-tert-butyl-[1,3,2]diazaphosphorinane by Na(K) in *o*-xylene at 110 °C.[3b]

3.2.5 Structures and bonding in the reduced products

*3.2.5.1 Crystal structure of (**6**)$_2$*

Yellow plate crystals of (**6**)$_2$ were obtained by slow evaporation of a saturated toluene solution under N_2 atmosphere. The compound crystallises in the triclinic space group *P-1* with half a molecule in the asymmetric unit. The structure was severely twinned but clearly revealed the molecular connectivity (Figure 3.10).

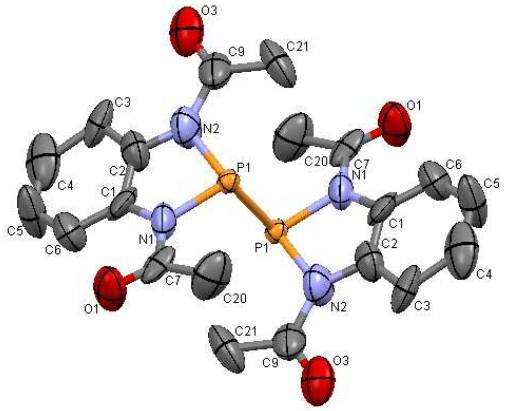

Figure 3.10. Crystal structure of (**6**)$_2$ with thermal elipsoids plotted at 50% probability. H atoms omitted for clarity. Selected heterocyclic bond lengths and angles are: P1-P1 2.1598(3), P1-N1 1.7126(2), P1-N2 1.8068(2), C1-C2 1.3277(2), C1-N1 1.4263(2), C2-N2 1.3584(2) Å; N1-P1-N2 86.17, N1-P1-P1 100.79, N2-P1-P1 103.83, P1-N1-C1 111.72, P1-N2-C2 111.98, N1-C1-C2 112.75, N2-C2-C1 112.68^o.

The structure of dimer (**6**)$_2$ is similar to (**1**)$_2$ and P-P dimers of the monocyclic $[(CH)_2(NR)_2P]_2$ system,[3d] adopting a *trans*-oid geometry in the solid state so as to minimize steric repulsion between (COMe) groups on N atoms. The dimer exibits a P–P bond length of 2.1598(3) Å, a little shorter than the P–P bonds for other alkyl and aryl diphosphanes, $R_2P\text{-}PR_2$ (2.20 – 2.31 Å) in the literature,[3d,4,23] which is not unexpected given the significantly larger steric effecs associated with the larger R groups necessary to protect the P centre. Dimerization in (**6**)$_2$ follows the trend of (**1**)$_2$, occuring by means of a formal P-P single bond rather than a multi-centre 2e^- 'pancake bonding' interaction as observed in DTA radicals.[24]

The heterocyclic geometry of $(\mathbf{6})_2$ is very similar to that of [**6**]Cl, but the fold of the ring is larger at 19.10° in comparison to that in [**6**]Cl (13.37°). The same observation is also noted between [**1**]Cl and $(\mathbf{1})_2$ (see Chapter 2). While P-N (1.7126(2)-1.8068(2) Å) bond lengths in $(\mathbf{6})_2$ are longer than those in precuror [**6**]Cl (P-N 1.709(1)-1.715(1) Å), the endocyclic C-N (1.3584(2)-1.4263(2) Å) and C-C (1.3277(2) Å) are shorter than those in [**6**]Cl (C-N 1.429(2)-1.436(2), C-C 1.399(2) Å). The N-P-N angle decreases from 89.93(6)° (in [**6**]Cl) to 86.17° (in $(\mathbf{6})_2$), consistent with the elongation in P-N bond lengths.

Theoretical calculations

Density functional theory (DFT) studies were undertaken to probe the nature of the frontier orbitals, and to calculate the dimerization energy of $(\mathbf{6})_2$.[25] The model heterocyclic radical $C_6H_4(NCOMe)_2P^{\bullet}$ and $(\mathbf{6})_2$ systems were geometry-optimized at the triple zeta UB3LYP and B3LYP/6-311G*+[3d] level of theory respectively.

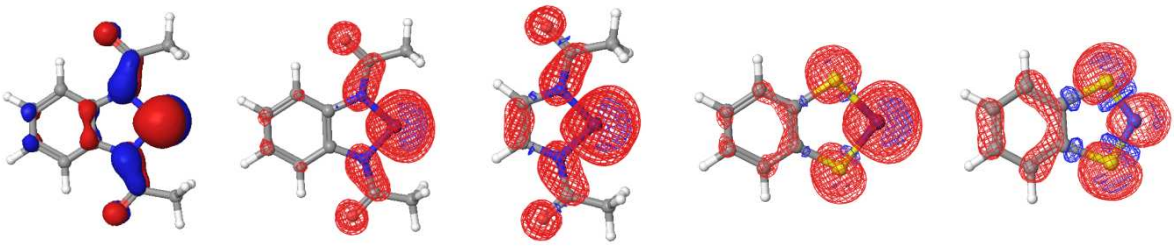

a **b** **c** **d** **e**

Figure 3.11. SOMO of $\mathbf{6}^{\bullet}$ (a), and spin density distributions in the heterocycle of $\mathbf{6}^{\bullet}$ (b), $\mathbf{(CH)_2(NCOMe)_2P^{\bullet}}$ (c), $\mathbf{C_6H_4S_2P^{\bullet}}$ (d), and $\mathbf{C_6H_4S_2N^{\bullet}}$ (e).

The Singly Occupied Molecular Orbital (SOMO) of $\mathbf{6}^{\bullet}$ reveals unpaired electron density located mainly on the heterocyclic C_2N_2P ring with greatest electron density at the P atom (Figure 3.11). This feature is similar to the $(CH)_2(NR)_2P^{\bullet}$[3d] and C_2S_2P ring systems (Chapter 2), though it is notable that there is additional π-delocalisation of electron density to the exocyclic COMe group in addition to π-delocalisation to the benzo-fused ring.

A comparison of the spin density distributions within the series $C_6H_4S_2N^{\bullet}$, $C_6H_4S_2P^{\bullet}$, $C_6H_4(NCOMe)_2P^{\bullet}$ (Table 3.4) reveals that replacement of N by P leads to a significant increase in spin density on the pnictogen (from 56% to 73%). Further replacement of S by NCOMe leads to a further increase in spin density at P suggesting that dimerization *via* Pn-Pn σ-bond formation is more favourable in the order $C_6H_4(NCOMe)_2P^{\bullet}$ > $C_6H_4S_2P^{\bullet}$ >> $C_6H_4S_2N^{\bullet}$. While EPR studies clearly reveal the stability of $C_6H_4S_2N^{\bullet}$ in solution, both P-based systems are EPR silent consistent with much greater association energies. In order to examine the effect of extended conjugation both $C_6H_4(NCOMe)_2P^{\bullet}$ and $C_2H_2(NCOMe)_2P^{\bullet}$ were examined. Surprisingly the benzo-fused ring, rather than leading to enhanced delocalisation, leads to a greater localisation of spin density at P (77% *cf* 73% for $C_2H_2(NCOMe)_2P^{\bullet}$). Seemingly the role of the benzo substituent does little to enhance radical stability and the electronic/steric factors of the RN functionality are likely to be more influential on dimerization than extended conjugation.

Table 3.4. Atomic charges and atomic spin densities from Mulliken population analysis of the five-membered heterocycles in some radicals.

$C_6H_4S_2N^{\bullet}$	**N**	**S**	**S**	**C_{endo}**	**C_{endo}**
Atom charge	-0.22659	0.25725	0.25699	-0.14710	-0.14744
Atom spin	0.55582	0.20635	0.20630	-0.01425	-0.01400
Sum of atomic spin		94.022%			
$C_6H_4S_2P^{\bullet}$	**P**	**S**	**S**	**C_{endo}**	**C_{endo}**
Atom charge	-0.13968	0.02175	0.02148	0.01176	0.01208
Atom spin	0.73387	0.12131	0.12126	-0.00225	-0.00233
Sum of atomic spin		97.186%			
$C_6H_4(NCOMe)_2P^{\bullet}$	**P**	**N**	**N**	**C_{endo}**	**C_{endo}**
Atom charge	0.11576	-0.23911	-0.23783	0.11908	0.12027
Atom spin	0.77073	0.01982	0.01932	0.00217	0.00110
Sum of atomic spin		81.314%			
$(CH)_2(NCOMe)_2P^{\bullet}$	**P**	**N**	**N**	**C_{endo}**	**C_{endo}**
Atom charge	0.19049	-0.20718	-0.20616	-0.14883	-0.15054
Atom spin	0.72777	0.02009	0.01953	0.02594	0.02606
Sum of atomic spin		81.894%			

DFT calculations on the dimer $(\mathbf{6})_2$ are consistent with the formation of a σ-bonded 2c–$2e^-$ P–P dimer *via* a *trans*-cofacial π*–π* interaction (Figure 3.12). This is confirmed by an NBO analysis (Figure 3.12) which reveals that all the bond orders within the heterocycle in $(\mathbf{6})_2$ can be considered single bonds. While the exocyclic P-P bond order (0.89) is somewhat less than the heterocyclic bond orders (0.96 – 0.97), it is close to that expected for a single bond.

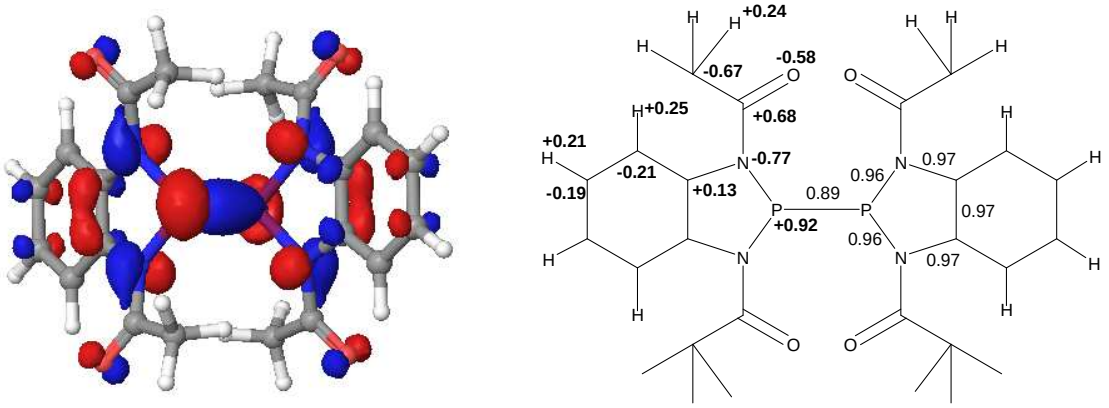

Figure 3.12. Bonding interaction between radicals in the HOMO of $(\mathbf{6})_2$ (left) with NBO charges and bond orders (right).

Zero-point energy corrected thermodynamic calculations based on the dimer $(\mathbf{6})_2$ and radical $\mathbf{6}^{\bullet}$ reveal a gas-phase P-P bond dissociation enthalpy (ΔH) of 99 kJ/mol at the B3LYP/6-311G*+ level. This is smaller than that reported in $(\mathbf{1})_2$ at the same level of theory, but significantly larger than that of $[(CH)_2(NMe)_2P]_2$ (~ 3 kJ/mol, calculations on the dimer $[(CH)_2(NMe)_2P]_2$ at the B3LYP/6-31G level).[3d] The computational result is in agreement with EPR spectra, which are all silent in xylene solution and in solid state at room temperature and even up to 110 ^oC due to the presence of strong P–P bonded dimers (ΔH_{dim} ~ -100 kJ/mol).

*3.2.5.2 Crystal structure of [**5**]$_2$O*

White needle crystals of $[C_6H_4(NCOOCH_3)_2P]_2O$ were obtained by slow evaporation of its CH_2Cl_2 solution under a N_2 atmosphere. The compound crystallises in the monoclinic

space group *C2/c* with half a molecule in the asymmetric unit (Figure 3.13) with O(10) located on a 2-fold rotation axis.

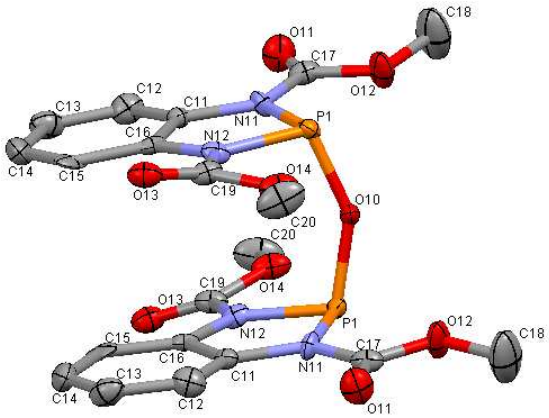

Figure 3.13. Crystal structure of [**5**]$_2$O with thermal elipsoids plotted at 50% probability. H atoms omitted for clarity. Selected heterocyclic bond lengths and angles are: P1-O10 1.630(3), P1-N11 1.745(6), P1-N12 1.737(7), N11-C11 1.42(1), N12-C16 1.412(9), C11-C16 1.376(9), N11-C17 1.373(9), N12-C19 1.385(8), C17-O11 1.189(8), C19-O13 1.20(1), C17-O12 1.33(1), C19-O14 1.339(9), O12-C18 1.43(1), O14-C20 1.440(8) Å; P1-O10-P1 147.0(5), O10-P1-N11 103.4(3), O10-P1-N12 104.9(3), N11-P1-N12 86.5(3), P1-N11-C17 119.9(5), P1-N12-C19 119.9(5), P1-N11-C11 115.6(5), P1-N12-C16 116.2(5), N12-C16-C11 111.0(6), N11-C11-C16 110.7(6)^o.

The O-bridged compound [**5**]$_2$O has a P-O bond length of 1.630(3) Å, typical for a P-O single bond (1.63 Å),[23] and P-O-P bridge angle of 147.0(5)^o. The rather obtuse angle (>120^o) is rather unexpected but may be due to packing effects; typically the exocyclic P-X bond appears near-orthogonal to the heterocyclic plane but with two heterocycles attached to the exocyclic O atom a conventional sp^3 or sp^2 O atom (109 – 120^o) would lead to significant steric repulsion between rings. Electronic effects cannot entirely be ruled out in order to optimize π-bonding but the P-O bond length itself mitigates against significant multiple bond character. The heterocyclic ring planes in the P-O-P compound appear to be almost planar with fold angles of only 3.06^o, considerably lesser than that of [**5**]Cl (10.63^o). The N-P-O bond angle 104.1(8)^o is akin to those of the tetrameric O-

bridged macrocycle [{P(μ_2-N^{t}Bu}$_2$(μ_2-O)]$_4$ (P-O 1.654-1.665 Å; N-P-O mean 102.6^o).[26] Generally, the phosphorus atoms in [**5**]$_2$O inherit the pyramidal geometry at P of [**5**]Cl. The sum of the bond angles at P (294.8^o) is about 2% larger than the one of the corresponding chloride starting material [**5**]Cl but still closer to the values expected for a non-hybridized P centre (270^o) rather than classical sp^3 hybrid (328^o).

Unfortunately the quality of the structure determination for [**5**]$_2$O was poor affording large errors on the geometric parameters. Nevertheless, while the heterocyclic geometry appears similar to that of [**5**]Cl, the P-N bond lengths in [**5**]$_2$O (1.737(7)-1.745(6) Å) appear marginally longer than those in [**5**]Cl (P-N 1.709(2)-1.713(2) Å). The N-P-N angle (86.5(3)^o) is slightly smaller than that of [**5**]Cl (88.63(8)^o).

Theoretical calculations

Natural Bond Orbital (NBO) analysis provides an efficient method to examine intra-/inter-molecular bonding interactions, charge transfer, and conjugative interactions in molecular systems.[27] The NBO process breaks down the multi-centre delocalised bonding interactions associated with delocalised MOs and reconstructs it in terms of a 'best' classical Lewis structure derived from localised 2*c*,2e^- bonds and lone pairs. Deviations from the localised Lewis structure are then taken into account through second-order effects which are described in terms of interactions between filled (donor) Lewis-type NBOs and empty (acceptor) non-Lewis NBOs, *i.e.* a hyperconjugation effect. The strength of these interactions, in terms of their interaction stabilization energy, is derived through a second order perturbation theory.[28] For each donor (i) and acceptor NBO (j) the stabilization energy E(2) associated with electron delocalization between donor and acceptor is estimated as $E(2) = \Delta E_{ij} = q^i F(i,j)/(E_j-E_i)$ (where q^i is the orbital occupancy, E_j and E_i are diagonal elements and F(i,j) is the off-diagonal NBO Fock matrix element).[29] Higher E(2) values indicate stronger interaction between electron donors and electron acceptors, and more extensive conjugation of the whole system. Selected perturbation energies of donor-acceptor interactions in [**5**]$_2$O are summarized in Table 3.5.

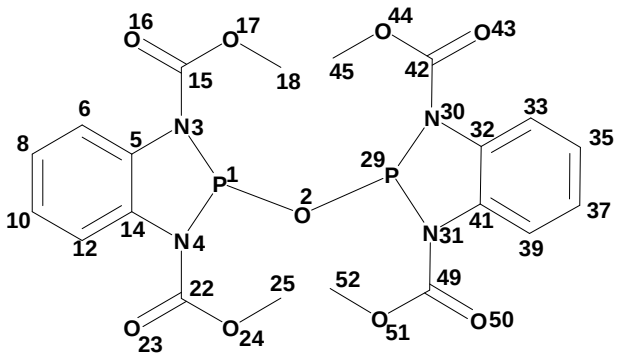

Figure 3.14. NBO atom labelling scheme for $[\mathbf{5}]_2O$.

Table 3.5. Summary of second-order perturbation theory analysis of the Fock matrix in NBO basis for $[\mathbf{5}]_2O$, showing second order contributions with E(2) > 50 kcal/mol.

Donor (L) NBO	**Acceptor (NL) NBO**	**E(2)** kcal/mol	**E(NL)-E(L)** a.u.	**F(L,NL)** a.u.
47. LP(3) O2	137. BD*(1) P1-O2	106.19	0.99	0.289
48. LP(1) N3	158. BD*(2) C15- O16	56.94	0.28	0.112
47. LP(3) O2	136. LV (2) P29	135.90	0.85	0.304
69. BD(1) P1-O2	136. LV (2) P29	72.67	0.51	0.172
59. LP(1) N30	191. BD*(2) C42- O43	56.94	0.28	0.112

E(2): means energy of hyperconjugation interaction; L: Lewis; NL: non-Lewis
E(NL)-E(L): Energy difference between donor (L) and acceptor (NL) NBO orbitals
F(L,NL): the Fock matrix element between L and NL NBO orbitals
LP: 1-center valence lone pair; LV: unfilled valence nonbonding orbital of "lone vacancy"
BD: 2-center bond; BD*: 2-center antibond

An NBO analysis of the bonding in $[\mathbf{5}]_2O$ reveals the best resonance model can be considered as $[\mathbf{5}^+][\mathbf{5}O^-]$ with a formal P-O single covalent bond within one fragment and a dative covalent bond from the O to the cationic P centre in the second fragment $\mathbf{5}^+$ (Table 3.6). The NBO analysis reveals 3 lone pairs on O consistent with >P-O$^-$ and a P-O single bond of *p* character on O with a charge on O of -1.12370. Covalency between the two fragments is evident from the second order perturbation analysis which reveals the dominant second order contribution is electron donation of an O lone pair to the vacant *p*-orbital on the phosphenium centre (135 kcal/mol) and delocalisation of the P-O covalent

bond to the phosphenium centre (73 kcal/mol). These large second order perturbations indicate defficiences in a localised bonding view of [**5**]$_2$O. Other significant delocalisations (> 50 kcal/mol) relate to (a) π-delocalisation of the *p*-orbital lone pair on N to the C=O π* orbital consistent with a conventional 3*c*,4*e*$^-$ bonding view of an amide functional group and (b) delocalisation of a bridging O lone pair to the P-O σ* orbital. The net effect of this interaction (weakening the P1-O2 bonding) and the lone pair donation to the vacant *p*-orbital on P29 leads to similar net bonding effects between the P atoms and central O within the molecule.

Table 3.6. Natural Bond Orbital Analysis of selected localized orbitals in [**5**]$_2$O.

Bond orbital	**Coefficients / Hybrids**
LP (1) P1	s (68.09%) p 0.47 (31.89%) d 0.00 (0.02%)
LP (1) O2	s (12.49%) p 7.01 (87.50%) d 0.00 (0.01%)
LP (2) O2	s (0.00%) p 1.00 (99.99%) d 0.00 (0.01%)
LP (3) O2	s (87.47%) p 0.14 (12.49%) d 0.00(0.04%)
LP (1) P29	s (68.09%) p 0.47 (31.89%) d 0.00(0.02%)
BD (1) P1-O2	(13.99%) 0.3740*P1 s (11.07%) p 7.89 (87.35%) d 0.14(1.58%) (86.01%) 0.9274*O2 s (0.00%) p 1.00 (99.97%) d 0.00(0.02%)
LP (1) N3	s (0.01%) p 1.00 (99.99%) d 0.00(0.00%)
LP (1) N30	s (0.01%) p 1.00 (99.99%) d 0.00 (0.00%)

LP: 1-center valence lone pair; BD: 2-center bond.

*3.2.5.3 Crystal structure of C_6H_4(NMe[**7**])$_2$*

Pale yellow crystals of C_6H_4(NMe[**7**])$_2$ were formed by cooling a saturated toluene solution to -20 ^{o}C in the freezer. The compound crystallises in the monoclinic space group *C2/c* with half a molecule in the asymmetric unit located about a crystallographic 2-fold axis (Figure 3.15).

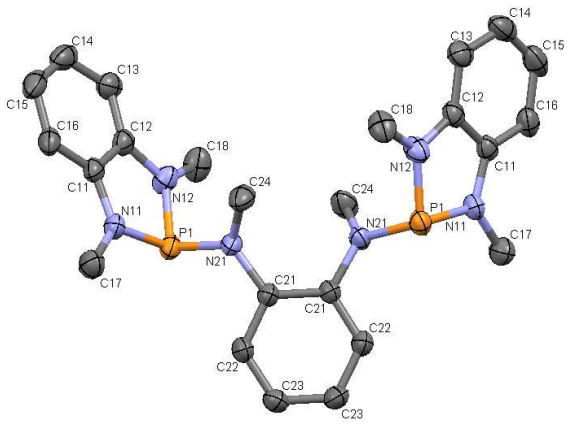

Figure 3.15. Crystal structure of $C_6H_4(NMe[\mathbf{7}])_2$. Thermal elipsoids plotted at 50% probability and H atoms omitted for clarity. Selected heterocyclic bond lengths and angles are: P1-N11 1.714(1), P1-N12 1.713(1), P1-N21 1.699(1), N11-C11 1.388(2), N12-C12 1.390(2), C11-C12 1.402(2), N11-C17 1.450(2), N12-C18 1.449(2), N21-C24 1.461(2), N21-C21 1.426(2), C21-C21 1.414(2) Å; N11-P1-N12 88.12(6), N11-P1-N21 104.53(6), N12-P1-N21 105.69(6), P1-N11-C11 115.3(1), P1-N12-C12 115.2(1), N11-C11-C12 110.7(1), C11-C12-N12 110.7(1), C12-C11-N11 110.7(1), P1-N12-C18 122.4(1), P1-N11-C17 123.0(1), C12-N12-C18 122.0(1), C11-N11-C17 121.6(1), P1-N21-C24 122.6(1), P1-N21-C21 118.18(9), C24-N21-C21 118.1(1), N21-C21-C21 122.5(1)^o.

The endocyclic P-N (1.713(1)-1.714(1) Å) bonds are longer than those in starting material [**7**]Cl (1.668(2)-1.669(3) Å) with the remaining C-N and C-C bonds being the same within experimental error. The new exocyclic P-N bonds (1.699(1) Å) are a little shorter than the endocyclic P-N bond lengths (1.713(1)-1.714(1) Å). Both P-N_{exo} and P-N_{endo} bond lengths fall in the ranges between conventional P=N (1.54-1.63 Å)[30] and P-N (1.71-1.73Å)[31] bonds.

In $C_6H_4(NMe[\mathbf{7}])_2$, the N-P-N bond angle (88.12^o) becomes smaller in comparison to the N-P-N (90.4^o) of [**7**]Cl and certainly strained with respect to the non-hybridised expected angles of 90^o. Moreover, it is worth noting that the [C_2N_2P] heterocycles are almost planar with fold angles of just 1.57^o, substantially less than that found in [**7**]Cl (12.32^o),

suggesting an interplay between ring strain and π-delocalisation. Although the total of bond angles at P atoms (298.3°) is slightly larger than that of the chloride starting material [**7**]Cl, the phosphorus atoms in $C_6H_4(NMe[\mathbf{7}])_2$ still preserve their pyramidal shape (*cf* non-hybridised sum expected at 270° and sp^3 hybrid at 328.5°).

The exocyclic N21 atom is almost coplanar with its three bonded atoms (P1,C21 and C24), displaced just 0.094 Å from the plane. All bond angles around N21 atoms are close to 120° (P1-N21-C24 122.6(1), P1-N21-C21 118.18(9), C24-N21- C21 118.1(1)).

Theoretical calculations

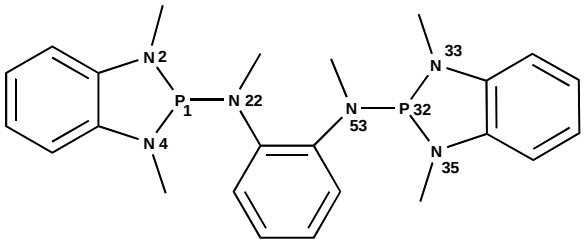

Figure 3.16. NBO atom labelling scheme for $C_6H_4(NMe[\mathbf{7}])_2$.

Table 3.7. Summary of second-order perturbation theory analysis of the Fock matrix in NBO basis for $C_6H_4(NMe[\mathbf{7}])_2$.

Donor (L) NBO	**Acceptor (NL) NBO**	**E(2)** kcal/mol	**E(NL)-E(L)** a.u.	**F(L,NL)** a.u.
42. LP (1) N2	126. BD*(1) P1- N22	10.75	0.45	0.062
43. LP (1) N4	126. BD*(1) P1-N22	11.14	0.44	0.063
44. LP (1) N22	124. BD*(1) P1- N2	7.45	0.43	0.051
44. LP (1) N22	125. BD*(1) P1- N4	6.85	0.43	0.049
46. LP (1) N33	165. BD*(1) P32-N53	10.75	0.45	0.062
47. LP (1) N35	165. BD*(1) P 32-N53	11.14	0.44	0.063
48. LP (1) N53	163. BD*(1) P32- N33	7.45	0.43	0.051
48. LP (1) N53	164. BD*(1) P32-N35	6.85	0.43	0.049

E(2): means energy of hyperconjugation interaction; L: Lewis; NL: non-Lewis
E(NL)-E(L): Energy difference between donor (L) and acceptor (NL) NBO orbitals
F(L,NL): the Fock matrix element between L and NL NBO orbitals
LP: 1-center valence lone pair; BD*: 2-center antibond

An NBO analysis of $C_6H_4(NMe[\mathbf{7}])_2$ reveals single bond heterocyclic geometry consistent with the expected Lewis structure. The selected perturbation energies of donor-acceptor interactions in $C_6H_4(NMe[\mathbf{7}])_2$ are summarized in Table 3.7. Unlike $[\mathbf{5}]_2O$ which indicated significant second order perturbation arising from lone pair donation from the lone pair on the bridging O back to the heterocycle, the energies of second order interactions are all substantially lower (< 15 kcal/mol).

*3.2.5.4 Crystal structure of [**5**]OMe*

Colourless needle crystals of [**5**]OMe suitable for single X-ray diffraction were prepared by slow evaporation of a concentrated toluene solution. [**5**]OMe crystallises in the orthorhombic space group *Pnma* with the molecule located on a mirror plane with half a molecule in the asymmetric unit (Figure 3.17).

The unique heterocyclic P-N (1.746(1) Å) bond length is longer than those of the precursor [**5**]Cl (P-N 1.709(2)-1.713(2) Å), but other heterocyclic distances are equivalent within error. The N-P-N angle reduces from 88.63^o (in [**5**]Cl) to 86.94^o and the ring becomes closer to planarity with a fold angle of just 3.09^o, significantly smaller than that of [**5**]Cl (10.63^o). Overall, the P atom conserves the pyramidal geometry with its total angle of 295^o which is greater than that of [**5**]Cl (288^o). The exocyclic P-O bond length (1.601(2) Å) is shorter than that in $[\mathbf{5}]_2O$ (1.630(3) Å) and a typical P-O single bond (1.63 Å).[23] This may reflect some degree of π-donation from the methoxy lone pair to the heterocyclic ring weakening P-N bonding character. In order to probe this interaction B3LYP/6-311G*+/NBO calculations were undertaken, analogous to those used to examine $[\mathbf{5}]_2O$.

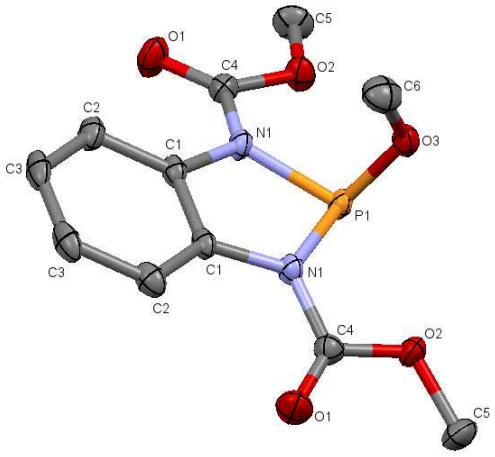

Figure 3.17. Crystal structure of [**5**]OMe with thermal elipsoids drawn at the 50% probability level and H atoms omitted for clarity. Selected heterocyclic bond lengths and angles are: P1-N1 1.746(1), P1-O3 1.601(2), O3-C6 1.442(4), N1-C1 1.422(2), C1-C1 1.396(2) Å; N1-P1-N1 86.94(7), O3-P1-N1 103.85(8), P1-N1-C1 115.7(1), P1-N1-C4 119.9(1), C1-N1-C4 123.3(1), N1-C1-C1 110.7(1)^{o}.

Theoretical calculations

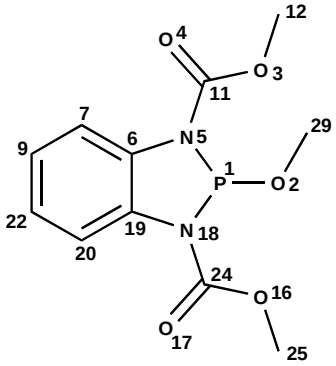

Figure 3.18. NBO atom labelling scheme for [**5**]OMe.

An NBO analysis of [**5**]OMe reveals the anticipated localised structure around the N_2POMe component. The only significant second order perturbations reflect further π–delocalisation of the multicentre bonding within the phenylene ring, reflecting the

inadequacy of the localised structure for a delocalised system. Clearly the exo methoxy group does not appear to affect changes in the C/N/P ring geometry *via* π-donation.

Table 3.8. Summary of second-order perturbation theory analysis of the Fock matrix in NBO basis for [**5**]OMe, showing second order contributions with E(2) > 50 kcal/mol.

Donor (L) NBO	**Acceptor (NL) NBO**	**E(2)** kcal/mol	**E(NL)-E(L)** a.u.	**F(L,NL)** a.u.
35. LP (1) C20	100. BD*(2) N18-C19	96.25	0.05	0.136
74. 3Cn(1) C7-C9-C22	84. BD*(2) N5-C6	204.23	0.06	0.095

E(2): means energy of hyperconjugation interaction; L: Lewis; NL: non-Lewis
E(NL)-E(L): Energy difference between donor (L) and acceptor (NL) NBO orbitals
F(L,NL): the Fock matrix element between L and NL NBO orbitals
LP: 1-center valence lone pair; BD*: 2-center antibond; 3Cn: 3-center NL orbital

3.2.6 Stability of P-chloro-benzodiazaphospholes in air/moisture

The fact that *P*-chloro-benzodiazaphospholes are considerably sensitive to air/moisture was readily apparent during NMR spectroscopy studies. On exposure to air, P-Cl bond in [**7**]Cl is swiftly hydrolysed. Conceptually this can be considered as a condensation reaction, generating [**7**]OH, with elimination of HCl. Subsequent rearrangement *via* a 1,2-H atom transfer lead to net oxidation of P^{III} to P^{V} with formation of the P(=O)H unit (Scheme 3.5). This conclusion is supported by the proton-coupled ^{31}P NMR spectra, which reveal a significant coupling between the P and the adjacent H ($^{1}J_{PH}$ = 646.8 Hz) and a coupling to the N-CH_3 group ($^{3}J_{PH}$ = 9.3 Hz) affording a doublet of septets, whereas the broad-band proton-decoupled, $^{31}P\{^{1}H\}$ NMR spectrum appeared as a singlet (δ_P 15.3 ppm). This was matched by a corresponding ^{1}H NMR spectrum in which the large $^{1}J_{PH}$ coupling appears as apparent singlets around 7.6 and 9.8 ppm but is really a doublet at ca 8.7 ppm.

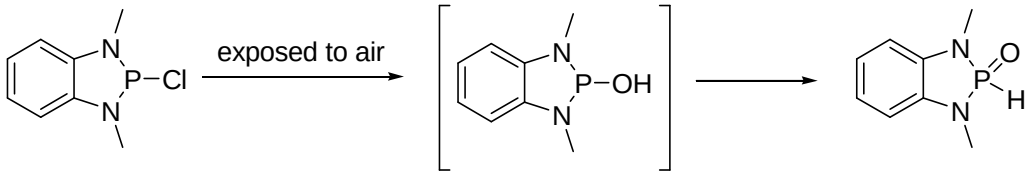

Scheme 3.5. Hydrolysis/oxidization process of [**7**]Cl.

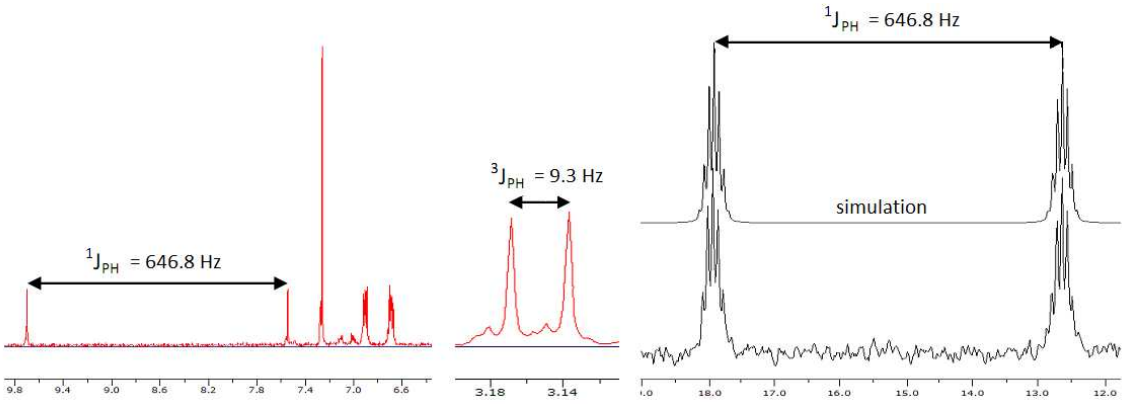

Figure 3.19. (left and middle) ^{1}H NMR spectra of the hydrolysis product of [**7**]Cl illustrating the $^1J_{PH}$ and $^3J_{PH}$ coupling; (right) corresponding ^{31}P NMR spectrum with simulation (SpinWorks 3.1.7).[10]

3.3 Conclusions

Crystallographic and spectroscopic investigations have led to a detailed picture of the structure and bonding in the family of bicyclic 1,3,2-benzodiazaphospholes. Generally, the structures and bonding situation of these bicyclic systems resemble those of the monocyclic 1,3,2-diazaphospholes. The structure of the chloride 'salts' comprise covalent P-Cl bonds with pyramidal P centres. The extent of folding of the heterocycle seems sensitive to the substituent X and, to a lesser extent, the R group bonded to the heterocyclic N atom. These rings are sensitive to air/moisture affording P(V) systems in the form of P(=O)H bonds. Reductions of *P*-halogeno-benzodiazaphospholes appears to initially form the benzodiazaphospholyl dimers which are readily re-oxidized to the P-O-P bridged systems or undergo degradation to form complex structures in which the ring is bridged by an *ortho*-phenylenediamine unit.

3.4 Experimental

All reagents were used as received without any further purification unless otherwise noted; methyl chloroformate, 1,2-phenylenediamine, pyridine, Et_3N, $LiAlH_4$, PCl_3, PBr_3, $CDCl_3$, C_6D_6, CD_2Cl_2, Na (Sigma-Aldrich), Mg (Strem Chemicals).

3.4.1 Preparation of $C_6H_4(NH)_2PCl$, [4]Cl[32]

Modified procedure: A solution of PCl_3 (2.54 g, 18.50 mmol) in MeCN (20 mL) was added dropwise to a solution of $C_6H_4(NH_2)_2$ (2.00 g, 18.50 mmol) in MeCN (20 mL). A yellow precipitate immediately formed. The mixture was then stirred at reflux overnight and the resultant orange solid was filtered off. The yellow filtrate was dried *in vacuo* to afford a yellow solid which was stirred in pentane (10 mL) for 1 hour. The solvent was decanted, and the product was dried *in vacuo*. Yield: 1.51 g (47%).

^{1}H NMR (300 MHz, CD_3CN) δ_H 7.72 (d, $^2J_{PH}$ = 23.7 Hz, 2H, NH), 7.14-7.17 and 6.98-7.01 (dd and dd, $^3J_{HH}$ = 5.9 Hz , $^4J_{HH}$ = 3.2 Hz, AA′BB′, aromatic CH).

^{13}C NMR (75.5 MHz, CD_3CN) δ_C 135.22 (d, $^2J_{PC}$ = 10.7 Hz, PNC), 122.24, 113.41.

^{31}P{^{1}H} NMR (121.5 MHz, CD_3CN) δ_P 142.37 (s).

^{31}P NMR (121.5 MHz, CD_3CN) δ_P 142.36 (t, $^2J_{PH}$ = 23.7 Hz).

IR ν_{max} (cm^{-1}): 2995 (mb), 2802 (mb), 2589 (mb), 1594 (m), 1527 (m), 1492 (m), 1368 (m), 1277 (m), 1264 (m), 1210 (m), 1186 (w), 1005 (m), 910 (m), 889 (m), 748 (s), 593 (m), 489 (m), 443 (m).

Found ($C_6H_4(NH)_2PCl$ requires): C = 40.93% (41.76); H = 3.42% (3.50); N = 15.62% (16.23).

Melting point: 133-134 ^oC.

3.4.2 Preparation of N,N'-dimethylcarbamato-benzodiamine $C_6H_4(NHCOOCH_3)_2$[8]

Methyl chloroformate (31.50 mL, 0.408 mol) was added dropwise to a cold suspension of 1,2-phenylenediamine (20.05 g, 0.185 mol), pyridine (44.80 mL, 0.556 mol) and chloroform (200 mL) in an ice bath. The reaction mixture was left to stir overnight at RT. The volatiles were then removed under vacuum from the orange solution to provide a thick orange liquid that was washed with ethyl acetate (200 mL). The organic layer was extracted with water (200 mL), and then extracted with saturated sodium chloride solution (200 mL). The resulting organic layer was dried over magnesium sulfate and the volatiles were pumped off under vacuum to afford a dark orange solid. The crude product was re-crystallized in ethanol to yield pale peach crystals (28.61 g, 70%).

^{1}H NMR (300 MHz, $CDCl_3$) δ_H 7.47 (s, 2H, NH), 7.14-7.18 (m, 4H, ring C_6H_4), 3.77 (s, 6H, $COOCH_3$).

^{13}C NMR(75.5 MHz, $CDCl_3$) δ_C 155.43, 129.94, 125.91, 124.43, 52.89.

IR ν_{max} (cm^{-1}): 3312 (bm), 2959 (w), 1728 (m), 1683 (m), 1606 (m), 1520 (s), 1462 (m), 1432 (m), 1310 (m), 1265 (m), 1233 (s), 1060 (s), 1046 (m), 957 (w), 871 (w), 830 (w), 770 (m), 753 (m), 704 (m), 561 (bm), 466 (m).

Melting point: 156-157 °C.

3.4.3 Preparation of P-chloro-N,N'-dimethylcarbamato-1,3,2-benzodiazaphosphole $C_6H_4(NCOOCH_3)_2PCl$, [5]Cl

A solution of $C_6H_4(NHCOOCH_3)_2$ (5.00 g, 22.3 mmol) and Et_3N (6.50 mL, 46.6 mmol) in THF (40 mL) was added dropwise to a solution of PCl_3 (2.50 mL, 28.7 mmol) in THF (20 mL) at 0 ^oC. The reaction mixture was then warmed to room temperature and stirred overnight. The mixture was filtered to give a yellow solution and the solvent removed *in vacuo* to afford an off-white solid. Yield: 5.67 g (88%). Suitable crystals for X-ray diffraction were obtained from slow evaporation of a CH_2Cl_2 solution.

^{1}H NMR (300 MHz, $CDCl_3$) δ_H 8.04-8.07 (m, 2H, ring C_6H_4), 7.18-7.22 (m, 2H, ring C_6H_4), 4.00 (s, 6H, $COOCH_3$).

^{13}C NMR (75.5 MHz, $CDCl_3$) δ_C 152.02 (d, $^2J_{PC}$ = 14.3 Hz, PNCO), 131.46 (d, $^2J_{PC}$= 9.7 Hz, heterocyclic PNC), 124.65 (s, aromatic), 117.05 (s, aromatic), 54.46 (s, CH_3).

^{31}P{^{1}H} NMR (121.5 MHz, $CDCl_3$) δ_P 122.73 (s).

IR ν_{max} (cm^{-1}): 2978 (w), 2946 (w), 2602 (m), 2497 (m), 1752 (m), 1729 (m), 1681 (m), 1608 (w), 1545 (m), 1522 (m), 1481 (m), 1298 (m), 1268 (m), 1035 (m), 1017 (m), 956 (m), 776 (m), 752 (m), 510 (m), 492 (m).

Found ($C_{10}H_{10}O_4N_2PCl$ requires): C = 42.09% (41.61); H = 3.49% (3.49); N = 9.75% (9.71).

Melting point: 134-135 °C.

3.4.4 Preparation of N,N'-dimethyl-1,2-diaminobenzene $C_6H_4(NHCH_3)_2$[9]

A solution of $C_6H_4(NHCOOCH_3)_2$ (10.02 g, 44.69 mmol) in dry THF (130 mL) was added dropwise to a cold suspension of $LiAlH_4$ (5.11 g, 134.65 mmol) in dry THF (120 mL) in an ice bath. The resulting grey solution was stirred at room temperature for 1 h then at reflux overnight. The mixture was cooled to 0 ^{o}C, and then water (10 mL), 10% NaOH (15 mL) and water (30 mL) were added slowly dropwise to the reaction, respectively. The solution was allowed to stir overnight at room temperature under nitrogen. The reaction mixture was filtered, and the residue extracted with warm THF (200 mL). The filtrate and extracts were dried *in vacuo* to give an oily solution. Addition of 10% HCl (210 mL) made the oily solution turn red. The aqueous phase was washed with CH_2Cl_2 (3 × 130 mL), basified with 10% NaOH (270 mL), and extracted with CH_2Cl_2 (3 × 150 mL). The organic phase was dried over anhydrous $MgSO_4$, and the solvent was removed under vacuum to yield a red oil (4.63 g, 76%).

^{1}H NMR (300 MHz, $CDCl_3$) δ_H 6.82-6.85 (m, 2H, aromatic CH), 6.67-6.70 (m, 2H, aromatic CH), 3.27 (s, 2H, NH), 2.86 (s, 6H, NCH_3).

^{13}C NMR (75.5 MHz, $CDCl_3$) δ_C 138.69, 119.40, 110.82, 31.40.

IR ν_{max} (cm^{-1}): 3343 (wb, NH), 3050 (w, CH), 2980 (w), 2939 (w), 2877 (w), 2804 (w), 2607 (w), 1700 (w), 1600 (m), 1560 (w), 1510 (s), 1476 (m), 1439 (m), 1419 (w), 1340 (w), 1305 (w), 1261 (s), 1223 (m), 1163 (s), 1124 (m), 1092 (w), 1039 (m), 945 (w), 897 (w), 826 (w), 732 (vs).

Found ($C_8H_{12}N_2$ requires): C = 70.25% (68.52); H = 8.26% (11.50); N = 20.40% (19.98).

3.4.5 Preparation of P-chloro-N,N′-dimethyl-1,3,2-benzodiazaphosphole $C_6H_4(NCH_3)_2PCl$, [7]Cl[33]

Modified procedure: A solution of $C_6H_4(NHCH_3)_2$ (2.40 g, 17.6 mmol) and Et_3N (6.20 mL, 44.5 mmol) in dry THF (25 mL) was added dropwise to a cold solution of PCl_3 (2.00 mL, 22.9 mmol) in dry THF (25 mL) under nitrogen. The purple mixture was allowed to stir overnight at room temperature and filtered to afford a yellow solution. The solvent was removed *in vacuo* to give a yellow powder (yield: 2.92 g, 83%) which was recrystallized from dry acetonitrile to afford crystals suitable for single X-ray diffraction.

^{1}H NMR (300 MHz, C_6D_6) δ_H 6.87-6.91 and 6.49-6.52 (dd and dd, $^{3}J_{HH}$ = 5.88 Hz, $^{4}J_{HH}$ = 3.1 Hz, AA′BB′, aromatic CH), 2.67 (d, $^{3}J_{PH}$ = 12.1 Hz, 6H, NCH_3).

^{13}C NMR (125.8 MHz, $CDCl_3$) δ_C 137.19 (d, $^{2}J_{PC}$ = 12.8 Hz, heterocyclic PNC), 121.27 (s, aromatic), 110.02 (s, aromatic), 29.37 (d, $^{2}J_{PC}$ = 17.7 Hz, $PNCH_3$).

^{31}P{^{1}H} NMR (121.5 MHz, $CDCl_3$) δ_P 152.53 (s).

^{31}P NMR (202.5 MHz, $CDCl_3$) δ_P 152.58 (septet, $^{3}J_{PH}$ = 12.1 Hz)

IR ν_{max} (cm^{-1}): 3059 (w), 2962 (w), 2925 (w), 2820 (w), 2603 (w), 2498 (w), 1592 (w), 1478 (m), 1460 (m), 1444 (m), 1275 (m), 1197 (m), 1118 (m), 1047 (m), 1024 (m), 922 (w), 886 (m), 747 (s), 692 (m), 543 (m), 507 (w), 489 (w), 466 (w), 440 (w), 394 (s).

Found ($C_8H_{12}N_2$ requires): C = 47.46% (47.90); H = 5.15% (5.02); N = 13.61% (13.96).

Melting point: 121-122 °C.

3.4.6 Preparation of P-bromo-N,N′-dimethyl-1,3,2-benzodiazaphosphole $C_6H_4(NCH_3)_2PBr$, [7]Br

A solution of $C_6H_4(NHCH_3)_2$ (2.105 g, 15.5 mmol) and Et_3N (6.50 mL, 46.6 mmol) in dry THF (15 mL) was added dropwise to a cold solution of PBr_3 (1.60 mL, 17.0 mmol) in dry THF (5 mL) under nitrogen. The purple mixture was allowed to stir at 0 °C for 1 h. The solid was filtered off to afford a brown solution. The volatiles were removed *in vacuo* to give a green powder. Yield: 1.63 g (43%).

^{1}H NMR (300 MHz, $CDCl_3$) δ_H 7.09-7.12 and 6.98-7.01 (dd and dd, $^{3}J_{HH}$ = 5.85 Hz, $^{4}J_{HH}$ = 3.2 Hz, $^{5}J_{HH}$ = 0.7 Hz, AA′BB′, aromatic CH), 3.37 (d, $^{3}J_{PH}$ = 13.1 Hz, 6H, NCH_3).

^{13}C NMR (125.8 MHz, $CDCl_3$) δ_C 137.5, 122.2, 110.7, 30.0.

^{31}P{^{1}H}NMR (121.5 MHz, $CDCl_3$) δ_P 172.43 (s).

^{31}P NMR (121.5 MHz, $CDCl_3$) δ_P 172.50 (septet, $^{3}J_{PH}$ = 13.1 Hz).

IR ν_{max} (cm^{-1}): 2964 (w), 2922 (w), 2675 (w), 1733 (w), 1591 (w), 1478 (m), 1456 (m), 1296 (m), 1274 (m), 1214 (m), 1195 (m), 1121 (m), 1046 (m), 1025 (m), 887 (s), 867 (m), 746 (s), 692 (m), 542 (w), 507 (w), 469 (m), 440 (m).

Melting point: 129-130 °C.

3.4.7 Preparation of N,N′-diacetyl-o-phenylenediamine $C_6H_4(NHCOCH_3)_2$[8]

Acetyl chloride (29.0 mL, 0.408 mol) was added dropwise to a cold suspension of 1,2-phenylenediamine (20.15 g, 0.186 mol), pyridine (44.80 mL, 0.556 mol) and chloroform (300 mL) in an ice bath. The orange solution was left to stir overnight at room temperature. The volatiles were then removed under vacuum from the orange solution to provide a thick orange liquid that was washed with ethyl acetate (200 mL). The organic layer was extracted with water (200 mL), and then extracted with saturated sodium chloride solution (200 mL). The resulting organic layer was dried over $MgSO_4$ and the

volatiles were removed under vacuum to afford an orange solid. The crude product was re-crystallized from ethanol to yield small beige crystals (22.92 g, 64%).

^{1}H NMR (300 MHz, $CDCl_3$) δ_H 8.58 (s, 2H, NH), 7.26-7.30 (m, 2H, aromatic CH), 7.15-7.21 (m, 2H, aromatic CH), 2.09 (s, 6H, $COCH_3$).

^{13}C NMR (75.5 MHz, $CDCl_3$) δ_C 170.03, 130.48, 126.02, 125.47, 23.67.

IR ν_{max} (cm^{-1}): 3230 (w), 3015 (w), 1665 (m), 1607 (w), 1525 (m), 1460 (m), 1367 (m), 1311 (s), 1275 (m), 1245 (m), 1036 (w), 971 (m), 858 (w), 764 m), 708 (m), 681 (m), 603 (m), 561 (m), 532 (m), 475 (w), 459 (w).

Melting point: 174-175 °C.

3.4.8 Preparation of P-chloro-N,N'-dimethylcarbamato-1,3,2-benzodiazaphosphole $C_6H_4(NCOCH_3)_2PCl$, [6]Cl

A solution of $C_6H_4(NHCOCH_3)_2$ (5.00 g, 26.0 mmol) and Et_3N (7.50 mL, 53.8 mmol) in THF (40 mL) was added dropwise to a solution of PCl_3 (2.50 mL, 28.7 mmol) in THF (20 mL) at 0 ^{o}C. The reaction mixture was then warmed up to room temperature, and stirred overnight. The mixture was filtered to give a yellow solution. The solvent was removed *in vacuo* to afford a pale yellow solid. Yield: 5.65 g (85%). Crystals suitable for X-ray diffraction were obtained by slowly evaporating a saturated CH_2Cl_2 solution.

^{1}H NMR (300 MHz, $CDCl_3$) δ_H 8.22-8.25 (m, 2H, ring C_6H_4), 7.21-7.26 (m, 2H, ring C_6H_4), 2.65 (d, $^{4}J_{PH}$ = 5.4 Hz, 6H, $COCH_3$).

^{13}C NMR (75.5 MHz, $CDCl_3$) δ_C 168.79 (d, $^{2}J_{PC}$ = 23.1 Hz, PNCO), 132.52(d, $^{2}J_{PC}$ = 7.9 Hz, heterocyclic PNC), 125.48 (s, aromatic), 118.98 (s, aromatic), 25.93 (d, $^{3}J_{PC}$ = 15.8 Hz, CH_3).

^{31}P{^{1}H} NMR (121.5 MHz, $CDCl_3$) δ_P 127.10 (s).

IR ν_{max} (cm^{-1}): 2920 (w), 1662 (m), 1564 (m), 1538 (m), 1398 (m), 1345 (m), 1204 (w), 1102 (m), 987 (w), 931 (w), 841 (w), 788 (w), 740 (m), 648 (w), 589 (m).

Found ($C_{10}H_{10}O_4N_2PCl$ requires): C = 46.79% (46.80); H = 4.03% (3.93); N = 10.83% (10.92).

Melting point: 105-106 °C.

3.4.9 Preparation of N,N'-diethyl-phenylene-1,2-diamine, $C_6H_4(NHEt)_2$[9]

A solution of $C_6H_4(NHCOCH_3)_2$ (10.05 g, 52.28 mmol) in dry THF (150 mL) was dispensed dropwise to a cold suspension of $LiAlH_4$ (5.15 g, 135.7 mmol) in dry THF (120 mL) in an ice bath. The resulting grey solution was stirred at room temperature for 1 h then at reflux overnight. The mixture was cooled to 0 ^oC and then water (10 mL), 10% NaOH (15 mL) and water (30 mL) were added slowly dropwise to the reaction, respectively. The solution was allowed to stir overnight at room temperature under nitrogen. The reaction mixture was filtered, the residue extracted with warm THF (200 mL) and the volatiles removed from the filtrate *in vacuo* to give an oily solution. Addition of 10% HCl (210 mL) made the oily solution turn red. The aqueous phase was washed with CH_2Cl_2 (3 × 130 mL), 10% NaOH (270 mL) added and extracted with CH_2Cl_2 (3 × 150 mL). The organic phase was dried over anhydrous $MgSO_4$, and the solvent was removed under vacuum to yield a dark red brown oil (6.01 g, 70%).

^{1}H NMR (300 MHz, $CDCl_3$) δ_H 6.78-6.81 (m, 2H, aromatic CH), 6.67-6.70 (m, 2H, aromatic CH), 3.32 (s, 2H, NH), 3.15 (q, $^3J_{HH}$ = 7.2 Hz, 4H, NCH_2), 1.32 (t, $^3J_{HH}$ = 7.2 Hz, 6H, CH_3).

^{13}C NMR (121.5 MHz, $CDCl_3$) δ_C 137.45, 119.10, 111.44, 38.94, 15.19.

IR ν_{max} (cm^{-1}): 3312 (bm), 2959 (w), 1728 (m), 1674 (m), 1607 (m), 1520 (s), 1462 (m), 1310 (m), 1265 (m), 1233 (s), 1060 (s), 753 (m), 704 (m), 466 (m).

Found ($C_8H_{12}N_2$ requires): C = 74.72% (73.13); H = 8.37% (9.82); N = 17.07% (17.06).

3.4.10 Preparation of P-chloro-N,N'-diethyl-1,3,2-benzodiazaphosphole, $C_6H_4(NEt)_2PCl$, [8]Cl

A solution of $C_6H_4(NHEt)_2$ (2.90 g, 17.66 mmol) and Et_3N (7.25 mL, 52.0 mmol) in THF (20 mL) was added dropwise to a solution of PCl_3 (2.30 mL, 26.36 mmol) in THF (20 mL) at 0 ^oC. The reaction mixture was then warmed up to room temperature and stirred overnight. The mixture was filtered to give a brown solution.The solvent was removed *in vacuo* to afford a black gel. Yield: 3.22 g (80%).

^{1}H NMR (300 MHz, $CDCl_3$) δ_H 7.06-7.07 (m, 2H, aromatic CH), 6.94-6.98 (m, 2H, aromatic CH), 3.27 (q, $^3J_{HH}$ = 7.2 Hz, 4H, NCH_2), 1.37 (t, $^3J_{HH}$ = 7.2 Hz, 6H, CH_3).

^{13}C NMR (125.8 MHz, $CDCl_3$) δ_C 136.8, 121.3, 110.6, 38.9, 14.3.

^{31}P{^{1}H} NMR (121.5 MHz, $CDCl_3$) δ_P 150.22 (s).

IR ν_{max} (cm^{-1}): 2984 (w), 2939 (w), 2892 (w), 1599 (w), 1486 (s), 1471 (m), 1377 (m), 1356 (m), 1263 (s), 1176 (m), 1104 (m), 1086 (m), 1055 (m), 1001 (m), 900 (m), 781 (m), 750 (s), 686 (m), 539 (s), 515 (s), 432 (m).

3.4.11 Reductive coupling of $C_6H_4(NMe)_2PCl$ by Na to form $C_6H_4(NMe[7])_2$

A suspension of $C_6H_4(NMe)_2PCl$ (0.29 g; 1.45 mmol) and finely chopped Na (0.10 g; 4.35 mmol) in toluene (20 mL) was stirred at 100 ^oC for 3 days. The mixture reaction was filtered and the filtrate evaporated *in vacuo* to afford a yellow solid. Recrystallization by storing toluene solution in the fridge at -20 ^oC afforded very pale yellow crystals of $C_6H_4(NMe(\mathbf{7}))_2$. Yield: 0.162 g (72%).

^{1}H NMR (300 MHz, CD_2Cl_2): δ_H 6.78-6.90 (m, 6H, aromatic CH-CH), 6.63-6.71 (m, 6H, aromatic CH-CN-CN-CH), and 3.10-3.13 (d, $^3J_{PH}$ = 9.6 Hz, 18H, N-CH_3).

^{31}P{^{1}H} NMR (202.5 MHz, $CDCl_3$): δ_P 104.6 (s).

Found ($C_{12}H_8P_2S_4$ requires): C = 62.02% (62.06); H = 6.84% (6.51); N = 17.95% (18.09).

Melting point: 82-83 ^{o}C.

3.4.12 Reduction of $C_6H_4(NCOOMe)_2PCl$ by Mg/Toluene to form $[5]_2O$

A suspension of $C_6H_4(NCOOCH_3)_2PCl$ (0.50 g, 1.73 mmol) and Mg powder (0.50 g, 20.6 mmol) in toluene (30 mL) was stirred at reflux in 11 days. $^{31}P\{^1H\}$ NMR was used to monitor the reaction. At completion, the reaction mixture was filtered and the filtrate evaporated *in vacuo* to afford a white solid. Recrystallization by slow evaporation of a CH_2Cl_2 solution afforded white needle crystals of $[C_6H_4(NCOOCH_3)_2P]_2O$. Yield: 0.265 g (59%).

^{1}H NMR (300 MHz, $CDCl_3$) δ_H 7.96 (m, 2H, aromatic CH), 7.10-7.18 (m, 2H, aromatic CH), 3.87 (s, 6H, $COOCH_3$).

^{13}C NMR (75.5 MHz, $CDCl_3$) δ_C 152.92 (d, $^2J_{PC}$ = 15.6 Hz, PNCO), 131.67 (d, $^2J_{PC}$ = 9.5 Hz, heterocyclic PNC), 124.05 (s, aromatic), 116.46 (s, aromatic), 54.02 (s, CH_3).

^{31}P{^{1}H} NMR (121.5 MHz, $CDCl_3$) δ_P 94.06 (s).

Found ($[C_6H_4(NCOOCH_3)_2P]_2O$ requires): C = 47.55% (45.99); H = 4.37% (3.86); N = 10.36% (10.73).

Melting point: 158-159 ^{o}C.

3.4.13 Reduction of [5]Cl by Mg/Toluene/I_2 to form [5]OMe

A suspension of $C_6H_4(NCOOMe)_2PCl$ (0.50 g, 1.73 mmol), Mg powder (0.50 g, 20.6 mmol), and several crystals of I_2 in toluene (10 mL) was stirred at reflux overnight. $^{31}P\{^1H\}$ NMR indicated the starting material $C_6H_4(NCOOMe)_2PCl$ was consumed and a new singlet appeared at *ca.* 98 ppm. All solids were filtered off, the toluene was removed from the filtrate *in vacuo* to give a white solid. Yield: 0.132 g (26.8%). Recrystallization by slow evaporation of its toluene solution afforded colorless needle crystals of [**5**]OMe for single X-ray diffraction.

^{1}H NMR (300 MHz, C_6D_6) δ_H 8.39-8.42 and 6.95-6.98 (dd and dd, $^{3}J_{HH}$ = 6.1 Hz, $^{4}J_{HH}$ = 3.4 Hz, AA'BB', aromatic CH), 3.38 (s, 6H, $COOCH_3$), 2.83 (d, $^{3}J_{PH}$ = 9.0 Hz, 3H, $POCH_3$).

^{13}C NMR (75.5 MHz, C_6D_6) δ_C 153.47, 133.22, 123.93, 116.30, 53.00, 50.68.

^{31}P{^{1}H} NMR (121.5 MHz, C_6D_6) δ_P 97.52 (s).

IR ν_{max} (cm^{-1}): 2961 (w), 1722 (m), 1482 (m), 1436 (m), 1360 (m), 1296 (m), 1260 (m), 1199 (m), 1083 (m), 1018 (m), 988 (m), 799 (m), 760 (m), 734 (m), 534 (m), 480 (m).

Found ($C_6H_4(NCOOMe)_2POMe$ requires): C = 46.12% (46.49); H = 4.44% (4.61); N = 9.28% (9.86).

Melting point: 127-128 °C.

3.4.14 Reduction of $C_6H_4(NCOMe)_2PCl$ by Mg/Toluene/I_2

A suspension of $C_6H_4(NCOMe)_2PCl$ (0.50 g, 1.95 mmol), Mg powder (0.50 g, 20.6 mmol), and several crystals of I_2 in toluene (10 mL) was stirred at reflux overnight. $^{31}P\{^{1}H\}$ NMR indicated starting material $C_6H_4(NCOMe)_2PCl$ was almost consumed and a new phosphorus species formed (singlet 5.17 ppm). All solids were filtered off, and the filtrate evaporated *in vacuo* to afford a lemon yellow solid. Yield: 0.322 g (74.7%). Recrystallization by slow evaporation of a toluene solution afforded yellow plate crystals suitable for single X-ray diffraction.

^{1}H NMR (300 MHz, $CDCl_3$) δ_H 8.23-8.26 (m, 2H, ring C_6H_4), 7.23-7.25 (m, 2H, ring C_6H_4), 2.64 (d, $^{4}J_{PH}$ = 5.7 Hz, 6H, $COCH_3$).

^{13}C NMR (75.5 MHz, $CDCl_3$) δ_C 168.66 (d, $^{2}J_{PC}$ = 22.9 Hz, PNCO), 132.78 (s, heterocyclic PNC), 125.56 (s, aromatic), 118.98 (s, aromatic), 25.81 (d, $^{3}J_{PC}$ = 15.5 Hz, CH_3).

^{31}P{^{1}H} NMR (121.5 MHz, $CDCl_3$) δ_P 5.17 (s).

IR ν_{max} (cm^{-1}): 2922 (w), 1703 (m), 1683 (m), 1479 (m), 1365 (m), 1254 (m), 1169 (m), 1060 (m), 1022 (m), 1002 (m), 881 (m), 784 (m), 754 (m), 736 (m), 561 (m), 469 (m), 418 (m).

Found ($[C_6H_4(NCOMe)_2P]_2$ requires): C = 54.84% (54.30); H = 4.93% (4.56); N = 12.90% (12.67).

Melting point: 100-101 ^oC.

3.5 References

1. (a) Bezombes, J.-P.; Borisenko, K. B.; Hitchcock, P. B.; Lappert, M. F.; Nycz, J. E.; Rankin, D. W. H.; Robertson, H. E., *Dalton Trans.* **2004**, *0* (13), 1980-1988; (b) Bezombes, J.-P.; Hitchcock, P. B.; Lappert, M. F.; Nycz, J. E., *Dalton Trans.* **2004**, (4), 499-501; (c) Domańska-Babul, W.; Chojnacki, J.; Matern, E.; Pikies, J., *J. Organomet. Chem.* **2007**, *692* (17), 3640-3648; (d) Grubba, R.; Ponikiewski, L.; Chojnacki, J.; Pikies, J., *Acta Crystallogr. Sect. E* **2009**, *65* (9), 2214-2223; (e) Grubba, R.; Wisniewska, A.; Baranowska, K.; Matern, E.; Pikies, J., *Dalton Trans.* **2011**, *40* (9), 2017-2024.

2. Gynane, M. J. S.; Hudson, A.; Lappert, M. F.; Power, P. P.; Goldwhite, H., *J. Chem. Soc., Dalton Trans.* **1980**, (12), 2428-2433.

3. (a) Giffin, N. A.; Hendsbee, A. D.; Roemmele, T. L.; Lumsden, M. D.; Pye, C. C.; Masuda, J. D., *Inorg. Chem.* **2012**, *51* (21), 11837-11850; (b) Nifantiev, E. E.; Vyazankin, N. S.; Sorokina, S. F.; Vorobieva, L. A.; Vyazankina, O. A.; Bravo-Zhivotovsky, D. A.; Bekker, A. R., *J. Organomet. Chem.* **1984**, *277* (2), 211-225; (c) Puntigam, O.; Hajdók, I.; Nieger, M.; Niemeyer, M.; Strobel, S.; Gudat, D., *Z. Anorg. Allg. Chem.* **2011**, *637* (7-8), 988-994; (d) Edge, R.; Less, R. J.; McInnes, E. J. L.; Muther, K.; Naseri, V.; Rawson, J. M.; Wright, D. S., *Chem. Commun.* **2009**, *0* (13), 1691-1693.

4. (a) Bruno, I. J.; Cole, J. C.; Edgington, P. R.; Kessler, M.; Macrae, C. F.; McCabe, P.; Pearson, J.; Taylor, R., *Acta Cryst., B* **2002**, *58* (3 Part 1), 389-397; (b) Cambridge Crystallographic Database (ConQuest) 21 October 2008.

5. Puntigam, O.; Förster, D.; Giffin, N. A.; Burck, S.; Bender, J.; Ehret, F.; Hendsbee, A. D.; Nieger, M.; Masuda, J. D.; Gudat, D., *Eur. J. Inorg. Chem.* **2013**, *2013* (12), 2041-2050.

6. Allan, C. J.; Cooper, B. F. T.; Cowley, H. J.; Rawson, J. M.; Macdonald, C. L. B., *Chem. Eur. J* **2013**, *19* (43), 14470-14483.

7. Power, P. P., *Chem. Rev.* **2003**, *103* (3), 789-810.

8. Davis, M. C., *Synth. Commun.* **2007**, *37* (12), 2079-2089.

9. Gendler, S.; Zelikoff, A. L.; Kopilov, J.; Goldberg, I.; Kol, M., *J. Am. Chem. Soc.* **2008**, *130* (7), 2144-2145.

10. Dunmore, A., Cooperation work in 59-410: Synthesis and Reactivity of Benzodiazaphospholes: Towards Diazaphospholyl Radicals. University of Windsor, Windsor, **2014**.

11. Gholivand, K.; Shariatinia, Z.; Pourayoubi, M.; Farshadian, S., *Z. Naturforsch.* **2005**, *60b*, 1021 - 1026.

12. Pauling, L., *The Nature of the Chemical Bond and the Structure of Molecules and Crystals: An Introduction to Modern Structural Chemistry*. Cornell University Press: **1960**.

13. Bondi, A., *J. Phys. Chem.* **1964**, *68* (3), 441-451.

14. Burck, S.; Gudat, D.; Nättinen, K.; Nieger, M.; Niemeyer, M.; Schmid, D., *Eur. J. Inorg. Chem.* **2007**, *2007* (32), 5112-5119.

15. Gudat, D., *Acc. Chem. Res.* **2010**, *43* (10), 1307-1316.

16. (a) Burck, S.; Gudat, D.; Nieger, M., *Angew. Chem. Int. Ed.* **2004**, *43* (36), 4801-4804; (b) Gudat, D.; Haghverdi, A.; Hupfer, H.; Nieger, M., *Chem. Eur. J.* **2000**, *6* (18), 3414-3425.

17. Cowley, A. H.; Kemp, R. A., *Chem. Rev.* **1985**, *85* (5), 367-382.

18. Abrams, M. B.; Scott, B. L.; Baker, R. T., *Organometallics* **2000**, *19* (24), 4944-4956.

19. Gudat, D.; Haghverdi, A.; Hupfer, H.; Nieger, M., *Chemistry – A European Journal* **2000**, *6* (18), 3414-3425.

20. (a) See Chapter 2; (b) Baudler, M.; Moog, A.; Glinka, K.; Kelsch, U., *Z. Naturforsch., B* **1973**, *28*, 363-369.

21. Komlev, I. V.; Zavalishina, A. I.; Chernikevich, I. P.; Predvoditelev, D. A.; Nifantiev, E. E., *Zh. Obshch. Khim.* **1972**, (42), 802-807.

22. Nifantiev., E. E.; Sorokina, S. F.; Vorobieva, L. A.; Borisenko, A. A., *Dokl. Akad. Nauk SSSR* **1982**, (263), 900-910.

23. Lide, D. R., *CRC Handbook of Chemistry and Physics (88th 2007-2008 edition)*. CRC Press: **2007**.

24. Preuss, K. E., *Polyhedron* **2014**, *79*, 1-15.

25. (a) Becke, A. D., *Phys. Rev. A* **1988**, *38* (6), 3098-3100; (b) Becke, A. D., *J. Chem. Phys.* **1993**, *98* (7), 5648-5652.

26. (a) Doyle, E. L.; Garcia, F.; Humphrey, S. M.; Kowenicki, R. A.; Riera, L.; Woods, A. D.; Wright, D. S., *Dalton Trans.* **2004**, (5), 807-812; (b) Gonzalez Calera, S.; Eisler, D. J.; Goodman, J. M.; McPartlin, M.; Singh, S.; Wright, D. S., *Dalton Trans.* **2009**, (8), 1293-1296.

27. Snehalatha, M.; Ravikumar, C.; Hubert Joe, I.; Sekar, N.; Jayakumar, V. S., *Spectrochim. Acta Mol. Biomol. Spectrosc.* **2009**, *72* (3), 654-662.

28. James, C.; Raj, A. A.; Reghunathan, R.; Jayakumar, V. S.; Joe, I. H., *J. Raman Spectrosc.* **2006**, *37* (12), 1381-1392.

29. Weinhold, F., *Discovering Chemistry With Natural Bond Orbitals*. Wiley: **2012**.

30. Miqueu, K.; Sotiropoulos, J.-M.; Pfister-Guillouzo, G.; Rudzevich, Valentyn L.; Gornitzka, H.; Lavallo, V.; Romanenko, Vadim D., *Eur. J. Inorg. Chem.* **2004**, *2004* (11), 2289-2300.

31. Zeiss, W.; Schwarz, W.; Hess, H., *Angew. Chem., Int. Ed. Engl.* **1977**, *16* (6), 407-408.

32. Bratulescu, G., *Rev. Roum. Chim.* **2007**, *52(5)*, 467-469.

33. Jennings, W. B.; Randall, D.; Worley, S. D.; Hargis, J. H., *J. Chem. Soc., Perkin Trans. 2* **1981**, (10), 1411-1416.

CHAPTER 4

SYNTHESIS AND LEWIS ACIDITY OF PHOSPHENIUM, ARSENIUM AND STIBENIUM CATIONS

4.1 Introduction

4.1.1 Heterocyclic phosphenium, arsenium, and stibenium cations

Monoheterocyclic phosphenium, arsenium, and stibenium cations $(CH)_2(N^tBu)_2E^+$ (E = P/As/Sb) are isoelectronic with the analogous group 14 carbenes and silylenes.[1] Theoretically they all possess six π electrons. Therefore, they drive appealing questions regarding electron delocalization within the rings. Provided that there is a formal positive charge located on the phosphorus, or arsenic, or antimony centre, these cations might be expected to display more extensive delocalization than their neutral group 14 counterparts.[2]

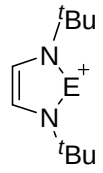

E = P/As/Sb

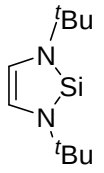

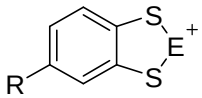

R = H or CH_3

Bi-cyclic frameworks incorporating $[S_2E^+]$ such as $C_6H_4S_2E^+$ and $C_7H_6S_2E^+$ are considered as 10π–cationic hetero-naphthalenic systems because they are related to naphthalene *via* their common 10π electron count.[3] Their electronic structures include n*p*π-3*p*π (*n*= 3, 4, 5) bonding between the heavier group 15 elements (P/As/Sb) and sulfur.[4] In 1988 1,3,2-benzodithiaphosphenium salts were first isolated as air-sensitive, yellow-to-orange crystalline solids which were fully characterized as 10π aromatic cationic heteronaphthalenic systems, consistent with the Huckel 4*n*+2 rule.[4-5]

4.1.2 Cyclic inter-pnictogen compounds

Inter-pnictogen compounds containing a coordinate bond between pnictogen elements (Pn = N; P; As; Sb; Bi) in their molecular frameworks have been explored in the design for materials with new properties.[6] The Pn→Pn homo-atomic coordination chemistry is basically illustrated by the following reaction consisting of the combination of a $PnPh_3$, R_2PnCl, and a halide abstracting agent (*e.g.*, A = $Me_3SiOSO_2CF_3$, $AlCl_3$, $GaCl_3$). Firstly, the cation (Lewis acceptor) is immediately formed *via* the heterolytic cleavage of the Pn-Cl bond assisted by the interaction between the chlorine center and the halide abstracting agent. The Pn→Pn coordination of the $PnPh_3$ (Lewis donor) to the positive center R_2Pn^+ (Lewis acceptor) proceeds subsequently to deliver the inter-pnictogen salt $[Ph_3Pn\text{-}PnR_2][anion]$.[7]

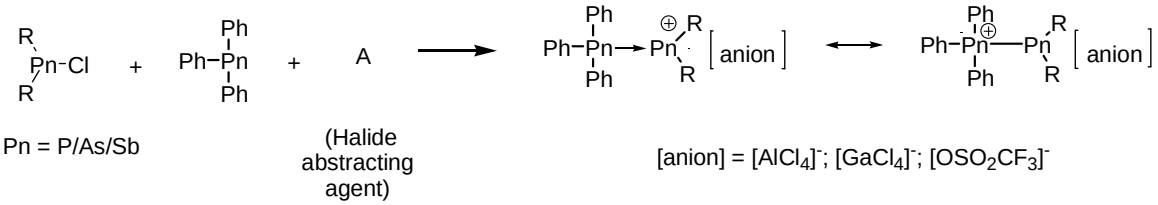

Scheme 4.1. Preparation of inter-pnictogen compounds.[8]

In these systems the adduct can be variously described in terms of two alternative structures; in the case of Pn = P either a phosphenium cation with a dative covalent phosphine or as a phosphonium cation with a covalently bonded phosphino group, PR_2 (Scheme 4.1).

4.1.3 Project aims

In this work, the formation of phosphenium, arsenium, and stibenium cations based on C/S/P, C/S/As, C/S/Sb, and C/N/P heterocyclic systems was investigated. All compounds (Scheme 4.2) were characterized by NMR spectroscopy and several of them by means of X-ray diffraction and analytical methods.

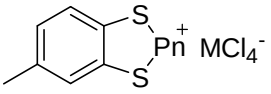

[**2**][MCl_4] (Pn = P)
[**9**][MCl_4] (Pn = As)
[**10**][MCl_4] (Pn = Sb)
M = Al or Ga

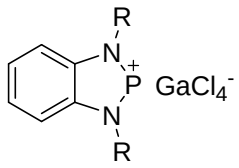

[**4**][$GaCl_4$] (R = H)
[**7**][$GaCl_4$] (R = CH_3)

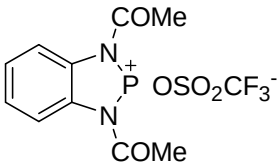

[**6**][OSO_2CF_3]

Scheme 4.2. Salts based on C/S/P, C/S/As, C/S/Sb, and C/N/P heterocyclic systems.

In addition the synthesis of inter-pnictogen compounds including coordinate bonds between P←P (phosphenium-phosphine), P←As (phosphenium-arsine), P←Sb (phosphenium-stibine), As←P (arsenium-phosphine), and Sb←P (stibenium-phosphine) are reported (Scheme 4.3). They can be prepared in a one-step reaction using a halide abstracting agent ($AlCl_3$ or $GaCl_3$) to activate P–Cl, or As-Cl, or Sb-Cl bonds in the presence of triphenylphosphine, or triphenylarsine, or triphenylstibine.[9] The flexibility and simplification of these procedures promises to provide good opportunities for the widespread development of inter-pnictogen structures as well as for the development of new inorganic materials.

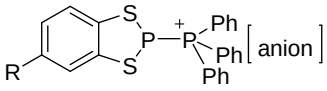

[**1**·PPh_3] [anion] (R = H)
[**2**·PPh_3] [anion] (R = CH_3)

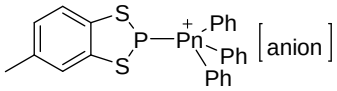

[**2**·$PnPh_3$] [anion] (Pn = As, Sb)
[anion] = $[AlCl_4]^-$; $[GaCl_4]^-$

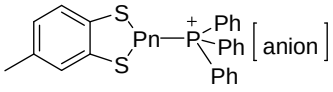

[**9**·PPh_3] [anion] (Pn = As)
[**10**·PPh_3] [anion] (Pn = Sb)

Scheme 4.3. Inter-pnictogen Pn-Pn structures.

4.2 Results and Discussion

4.2.1 Syntheses of As-chloro-dithiaarsole and Sb-chloro-dithiastibole, [9]Cl and [10]Cl

*4.2.1.1 Syntheses of [**9**]Cl and [**10**]Cl*

The syntheses of [**9**]Cl and [**10**]Cl were performed using similar procedures to those of [**1**]Cl and [**2**]Cl.[10] Condensation of toluene-3,4-dithiol with arsenic trichloride/antimony trichloride afforded the *As*-chloro-dithiaarsole [**9**]Cl, and *Sb*-chloro-dithiastibole [**10**]Cl as yellow solids in high yields (82-85%). Both were characterized by NMR spectroscopy and analytical methods. The molecular structure of [**9**]Cl was determined by single-crystal X-ray diffraction and found to be the same as that reported by Kisenyi *et al.*[10a] although the quality of the structure described here is significantly improved (R_1= 0.021 based on all data).

*4.2.1.2 Crystal structure of [**9**]Cl*

The crystal structure of [**9**]Cl adopts the monoclinic space group $P2_1/c$ with one molecule in the asymmetric unit (Figure 4.1). In general, its heterocyclic geometry is similar to those of the *P*-chloro-dithiaphospholes and *P*-chloro-diazaphospholes, *i.e.* the heterocycle is folded and the chlorine atom lies out of the heterocyclic plane (Figure 4.1). The replacement of P by As in [**2**]Cl gives rise to some changes in bond lengths and bond angles within the heterocyclic structure; while some bond lengths in [**2**]Cl (S-C 1.766(2)-1.767(2) Å, C-C 1.390(2) Å) are unchanged when compared to [**9**]Cl (S-C 1.761(1)-1.764(1) Å, C-C 1.394(2) Å), the increased covalent radius of As leads to increases in both Pn-Cl and Pn-S bond lengths when P is replaced by the heavier pnictogen; *cf.* P-Cl (2.1103(7) Å) and P-S (2.0921(6)-2.0932(7) Å) *vs.* As-Cl (2.2497(5) Å) and As-S (2.2113(4)-2.2163(4) Å). While the As-Cl bond (2.2497(5) Å) in [**9**]Cl is longer than normal As-Cl bonds (*e.g.* 2.161 Å in $AsCl_3$),[11] the As-S bonds (2.2113(4)-2.2163(4) Å) are equivalent to the conventional As-S bond length (2.25 Å).[12] Compared to other arsenic(III) systems containing analogous $AsClS_2$ cores such as 5-chloro-l,4,6,5,-

oxadithiarsocane[13] (As-S 2.259, 2.247 Å; As-Cl 2.268 Å) and 2-chloro-1,3,6,2-trithiarsocane[14] (As-S 2.268, 2.248 Å; As-Cl 2.356 Å), [**9**]Cl has shorter As-S and As-Cl bond lengths.

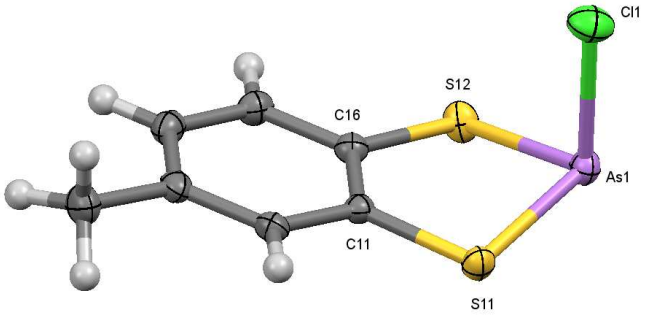

Figure 4.1. Molecular structure of [**9**]Cl with thermal ellipsoids drawn at 50% probability for non-H atoms.

Akin to [**1**]Cl, [**2**]Cl, [**5**]Cl, [**6**]Cl and [**7**]Cl, compound [**9**]Cl also contains a tri-coordinate geometry with angles close to 90^{o} (range 92.45– 99.86^{o}). The sum of bond angles at As is about 292^{o} which is less than the range values of the S/P analogues (299-300^{o}) and close to that expected for a non-hybridised As centre (270^{o}) which is as expected on descending the group. Resembling [**2**]Cl, [**9**]Cl has a non-planar heterocycle which is folded about the S-S vector with a fold angle of 23.60^{o}, smaller than that within the [C_2S_2PCl] unit in [**2**]Cl (26.06^{o}).

The packing of [**9**]Cl reveals a short intermolecular contact between As and the benzo group of a neghbouring molecule [$d_{As\cdots cent}$ = 3.25 Å] which propagate through the solid state to form a one-dimensional chain motif (Figure 4.2). Such As$\cdots$arene$_{\pi}$ contacts have been observed elsewhere and proposed to be structure-directing.[15]

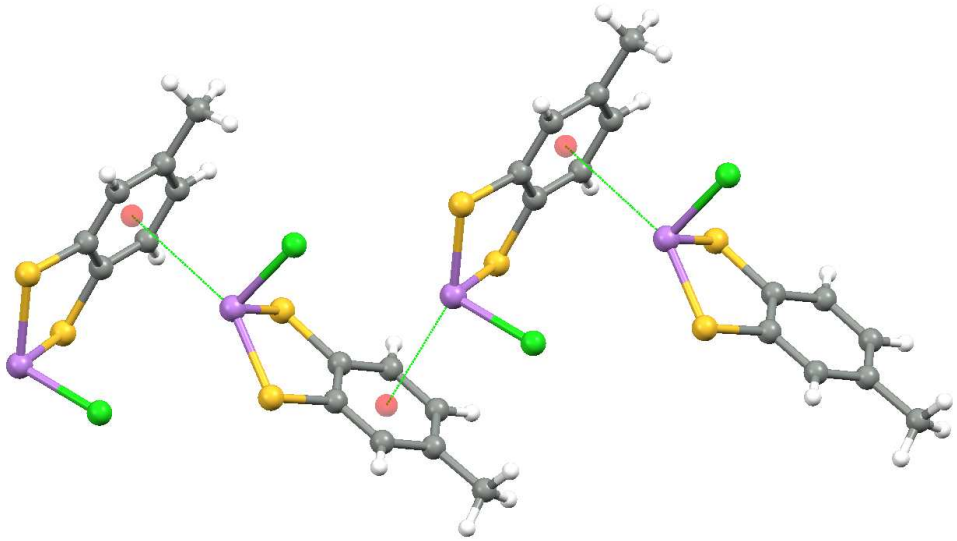

Figure 4.2. Solid state packing of [**9**]Cl showing the As···arene$_\pi$ interactions.

4.2.2 Syntheses of dithia-phosphenium, arsenium and stibenium cations

4.2.2.1 Syntheses of phosphenium, arsenium, and stibenium cations

Reaction of the chloro-compounds [**2**]Cl (Chapter 2), [**4**]Cl, [**6**]Cl, [**7**]Cl (Chapter 3), [**9**]Cl, and [**10**]Cl with MCl_3 (M = Al, Ga) or $Me_3SiOSO_2CF_3$ in CH_2Cl_2 or MeCN followed by evaporation of the resultant solution afforded the corresponding $MCl_4/OSO_2CF_3^-$ salts of the dithiaphosphenium cation **2**$^+$ (yellow-to-orange), dithia-arsenium cation **9**$^+$ (red), dithiastibenium **10**$^+$ (dark red), and diazaphosphenium cations **4**$^+$ (yellow), **6**$^+$ (yellow) and **7**$^+$ (purple) (Scheme 4.2). These were isolated as extremely air-sensitive solids which decomposed after long-term storage in the glove-box. Methylene chloride appears to be an appropriate solvent for most of these reactions because it is non-coordinating but has a satisfactorily high dielectric constant to dissolve the salts.[16]

In solution, as expected, the existence of the positive charge and the low coordination number on P atom is the root of deshielding chemical shifts of phosphenium cations.[16] The chemical shifts of the phosphenium ions ([**4**][$GaCl_4$] δ_P 212.6 ppm, [**6**][OSO_2CF_3] δ_P 219.2 ppm, and [**7**][$GaCl_4$] δ_P 217.5 ppm) are ~ 65-92 ppm downfield in comparison to

those of the corresponding *P*-chloro precursors ([**4**]Cl δ_P 142.4 ppm, [**6**]Cl δ_P 127.1, and [**7**]Cl δ_P 153.1 ppm), consistent with previous observations.[16] Conversely the dithiaphosphenium cations $\mathbf{1}^+$ and $\mathbf{2}^+$ seemingly exhibited an ***upfield*** shift, appearing around 55 ppm. This seemingly anomalous behaviour was alluded to by Burford who first prepared such dithiaphosphenium cations.[4b,c] Their studies revealed the ^{31}P NMR shift was very sensitive to concentration with 'free' $\mathbf{1}^+$ and $\mathbf{2}^+$ cations evident around ~410 ppm at high dilution but were sometimes broad and they proposed formation of aggregates such as $[\mathbf{1}_2Cl]^+$ at higher concentration. Notably more recent work by Russell characterised $[\{(RC)_4P\}_2Cl]^+$ which appeared in the region 70-100 ppm, *i.e.* upfield with respect to the parent chloro-phosphine.[17] This is in good agreement with the peak observed at 57 ppm which we tentatively attribute to $[\mathbf{2}_2Cl]^+$. Thus it would seem that an equilibrium is present in which the dithiaphosphenium is present only at high dilution (Scheme 4.4). ^{31}P NMR studies at different concentrations failed to identify free phosphenium cation in this case.

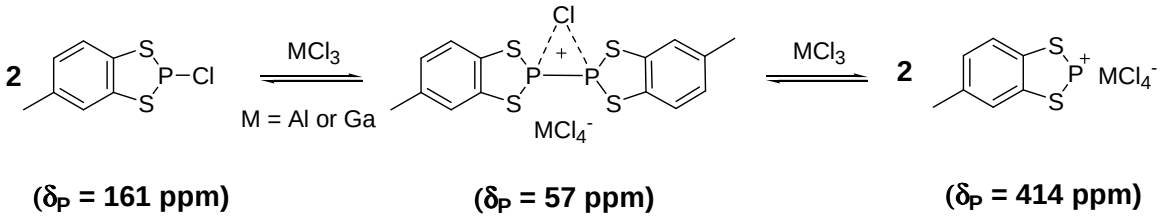

Scheme 4.4. Equilibrium between [**2**]Cl, $[\mathbf{2}_2Cl]^+$ and $\mathbf{2}^+$.

Notably treatment of [**2**]Cl (161 ppm) with $AlCl_3$ afforded a single peak at 57 ppm, consistent with formation of $[\mathbf{2}_2Cl]^+$. Subsequent treatment of $[\mathbf{2}_2Cl]^+$ with THF regenerated [**2**]Cl and the adduct $AlCl_3 \cdot 2THF$, confirming that the reversible nature of the first step. Conversely the solid state structure of the phosphenium cation [**2**][$GaCl_4$] was determined by X-ray diffraction and is described below.

*4.2.2.2 Structures of [**2**][$GaCl_4$], [**7**][$GaCl_4$][18] and [**9**][$GaCl_4$]*

Crystals of $[C_7H_6S_2P][GaCl_4]$ and $[C_7H_6S_2As][GaCl_4]$ were grown by slow evaporation of anhydrous CH_2Cl_2 solutions while crystals of $[C_6H_4(NMe)_2P][GaCl_4]$ were formed by

slow evaporation of a MeCN solution under N_2. Single-crystal X-ray structure studies were carried out for compounds [**2**][$GaCl_4$], [**7**][$GaCl_4$] and [**9**][$GaCl_4$]. Selected bond lengths, and bond angles are listed in Table 4.1.

a. Crystal structure of [2][$GaCl_4$]

Compound [**2**][$GaCl_4$] crystallised in the monoclinic space group *P2₁/c* with one molecule in the asymmetric unit and the molecular structure of [**2**][$GaCl_4$] is illustrated in Figure 4.3.

Compared to the "envelope shape" of the five-membered ring in [**2**]Cl (fold angle of 26.06°), the heterocycle in [**2**][$GaCl_4$] is almost planar (fold angle 0.48°). The $\mathbf{2}^+$ cation possesses shorter P-S (2.027(2)-2.033(2)Å) bonds than those of its neutral precursor [**2**]Cl (P-S 2.0921(6)-2.0932(7)Å) but the S-C and C-C bond lengths are the same within experimental error (3 esd's). The P-S bond lengths in [**2**][$GaCl_4$] lies in between P=S double bond (mean 1.908(8) Å in P_4S_{10}) and P-S single bonds (mean 2.097(8) Å).[4c] As mentioned in Chapter 2 and 3 such bond shortening in the cation can be explained in terms of ring planarity which optimizes $p\pi$-$p\pi$ bonding in the C_2S_2P ring, enhancing the bond order and leading to shorter bonds. Conversely the exocyclic P-Cl bond in [**2**]Cl disrupts π-bonding affording longer P-S and C-S bonds and permits the P atom to distort out of C_2S_2 plane.[19] The P-S bond shortening in $\mathbf{2}^+$ also results in an enlargement of S-P-S angle (98.37(8)°) in comparison to that of [**2**]Cl (95.43(2)°). The bond lengths and angles within [**2**][$GaCl_4$] (P-S 2.027(2)- 2.033(2)Å, S-C 1.736(6)-1.749(5) Å, C-C 1.409(8)Å and S-P-S 98.37(8)°) are comparable to those of [**1**][$AlCl_4$] (P-S 2.015(3)-2.016(3) Å, S-C 1.711(6)-1.728(5) Å, C-C 1.383(7) Å and S-P-S 97.59(10)°).[4c]

The closest cation···anion P···Cl contact is 3.326(2) Å, significantly longer than the covalent P-Cl bond in [**2**]Cl (2.1103(7) Å), but shorter than the sum of the van der Waals radii (3.55 Å), confirming the ionic nature of the structure. Unlike the only other previously reported dithiaphosphenium cation, [**1**][$AlCl_4$],[4c] which exhibits alternating cation-anion layers perpendicular to the crystallographic *b* axis, the packing pattern of [**2**][$GaCl_4$] has no layer-like order (Figure 4.3).

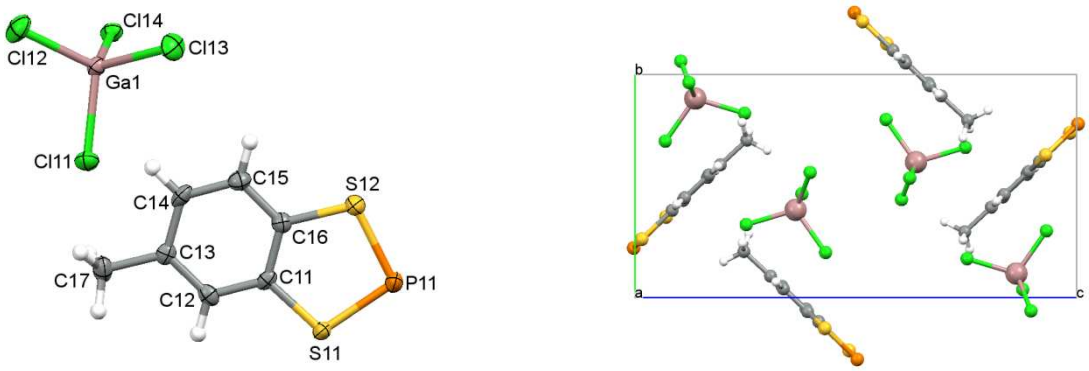

Figure 4.3. Crystal structure (left) and unit cell packing (right) for [**2**][$GaCl_4$]. Thermal ellipsoids drawn at 50% probability for non-H atoms.

b. Crystal structure of [7][$GaCl_4$][18]

The crystal structure of [**7**][$GaCl_4$] has higher symmetry than that of [**2**][$GaCl_4$], crystallising in the orthorhombic space group *Pbca* with one molecule in the asymmetric unit (Figure 4.4). In general, bond lengths and bond angles of [**7**][$GaCl_4$] (P-N 1.650(2)-1.654(2) Å, N-C 1.384(2)-1.385(2) Å, C-C 1.397(2) Å, and N-P-N 91.33(7)^o) fall within the normal range of values reported for monocyclic-1,3,2-diazaphosphenium cations.[20]

Compared to [$C_2(^t$BuN$)_2$P][X] (X = BF_4, PF_6)[20] for which N-P-N are 90.38(7)^o and 90.71(11)^o, respectively, [**7**][$GaCl_4$] possesses a larger N-P-N angle of 91.33(7)^o. An increase of N-P-N angle in $\mathbf{7}^+$ can be understood on the basic of P-N bond length shortening (1.650(2)-1.654(2) Å) in comparison to those of [$C_2(^t$BuN$)_2$P]$^+$ (mean 1.662 Å). On the other hand, the N-P-N angle in $\mathbf{7}^+$ is smaller than that in the unstrained, acyclic cation [(^{i}Pr$_2$N$)_2$P]$^+$ (N-P-N 114.8(2)^o).[16]

All of the cation-anion interactions, which are less than the sum of the van der Waals' radii, occur between the chlorine atoms (Cl4, Cl1, Cl3) of the anion and some atoms (P1, H3 on C3, C7) of the cation. The closest P···Cl contacts occur between P1 and Cl4 atoms (3.452-3.457 Å) and link molecules into a one-dimensional chain structure (Figure 4.4).

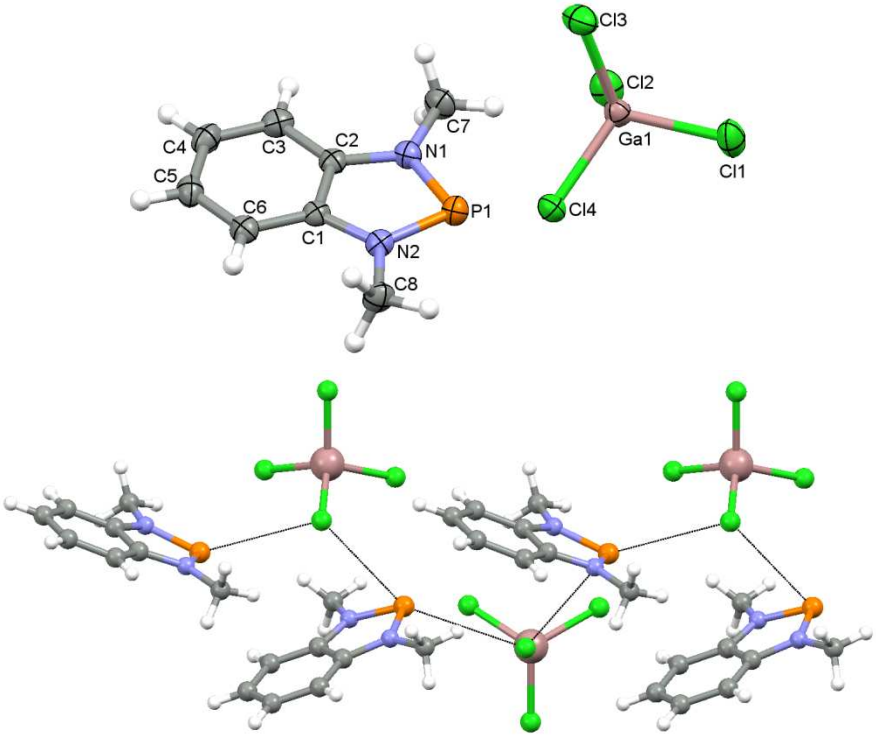

Figure 4.4. Molecular structure of [**7**][$GaCl_4$][18] (top) with thermal ellipsoids for non-H atoms drawn at the 50% probability level; (bottom) propagation of cation-anion P···Cl contacts in the solid state.

c. Crystal structure of [9][$GaCl_4$]

The salt [**9**][$GaCl_4$] crystallises in the monoclinic space group $P2_1/m$ with two half molecules of $\mathbf{9}^+$ and $GaCl_4^-$ in the asymmetric unit, with each located on a mirror plane (Figure 4.5).

The abstraction of the chlorine atom from [**9**]Cl to generate [**9**][$GaCl_4$] alters the heterocyclic [C_2S_2As] structure. Most notably the structure of $\mathbf{9}^+$ is rigorously planar in relation to [**9**]Cl (fold angle of 23.60°). In addition the positive charge of $\mathbf{9}^+$, leads to some bond shortening with respect to [**9**]Cl (As-S from 2.2113(4)-2.2163(4) Å in [**9**]Cl to 2.1414(9)-2.151(1) Å for $\mathbf{9}^+$; S-C from 1.761(1)-1.764(1) Å in [**9**]Cl to 1.727(3)-1.734(3) Å in $\mathbf{9}^+$). The reduction of the As-S and S-C bond lengths in $\mathbf{9}^+$ can be explained as the result of planarity which optimizes $3p_\pi$-$4p_\pi$ bonding between the heavier *p*-block

elements. The S-As-S bond angle expands from 92.45(1)^{o} in [**9**]Cl to 93.38(3)-94.82(3)^{o} in [**9**][$GaCl_4$].

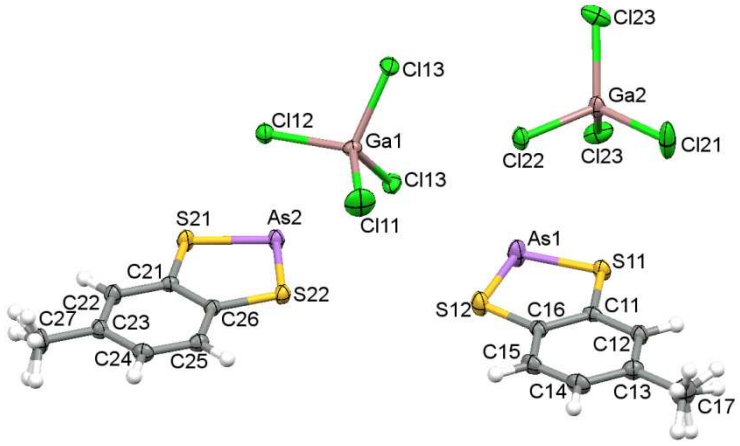

Figure 4.5. The two crystallographically independent molecules of [**9**][$GaCl_4$] with thermal ellipsoids drawn at 50% for non-H atoms.

While [**9**]Cl exhibits short intermolecular As···arene$_\pi$ contacts, [**9**][$GaCl_4$] exhibits a web of As···Cl contacts with each of the two crystallographically independent As centres forming multiple As···Cl contacts (3.295 – 3.560 Å) less than the sum of the van der Waals radii (3.80 Å). Both [**9**][$GaCl_4$] and [**7**][$GaCl_4$] form supramolecular chains formed *via* Pn···Cl contacts. However the web of As···Cl contacts (Figure 4.6) appears more extensive than in [**7**][$GaCl_4$] (Figure 4.4) with inter-chain As···Cl contacts in addition to intrachain contacts. These cation-anion contacts in [**9**][$GaCl_4$] are the root of a macrostructure comprising layers perpendicular to the crystallographic *c* axis (Figure 4.6). Layers of cations are separated by 7.015(2) Å equivalent to the crystallographic *b*-axis. The phosphenium salt [$C_6H_4S_2P$][$AlCl_4$] also adopts a layered structure with cation···anion contacts (Figure 4.6).[4c]

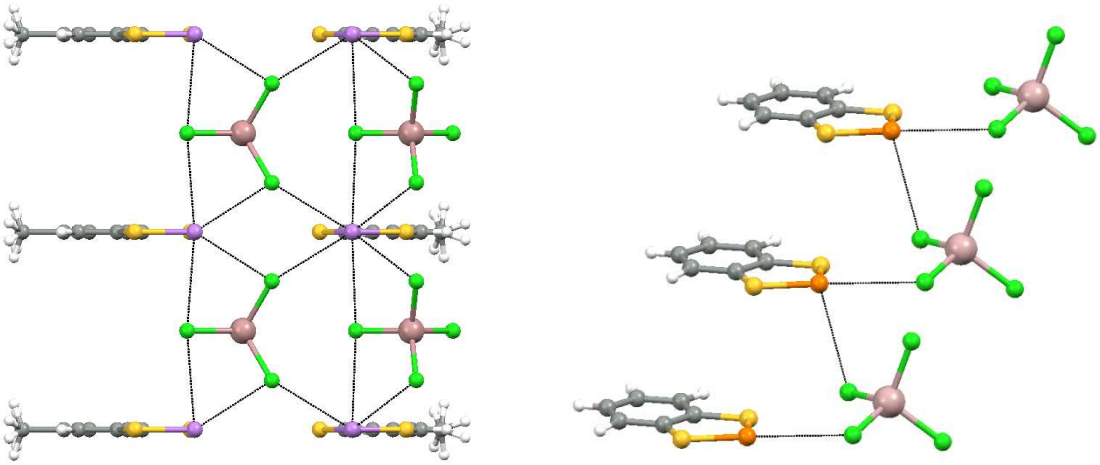

Figure 4.6. (left) Propagation of As···Cl contacts in the structure of [**9**][$GaCl_4$]; (right) propagation of P···Cl contacts in [**1**][$AlCl_4$].

d. Analysis and comparison of structures and bonding in [2][$GaCl_4$], [7][$GaCl_4$],[18] [9][$GaCl_4$] and [9]Cl

A summary of the heterocyclic geometries of [**2**][$GaCl_4$], [**7**][$GaCl_4$], [**9**][$GaCl_4$] and [**9**]Cl are presented in Table 4.1. Chlorine atom abstraction to form phosphenium or arsenium cations would appear to lead to a marked reduction in the folding of the heterocyclic framework and some shortening of the Pn-E bond lengths, consistent with a move towards more multiple bond character.

The heterocycles become approximately or completely planar with folding angles close to 0 (0^o in [C_2S_2As], 0.83^o in [C_2S_2P], and 1.46^o in [C_2N_2P]). This phenomenon is also observed in similar cations from previous studies. It is argued that the planarity of these systems implies the involvement of the heterocenters in a 10π electron environment (C=C, two lone pairs from N or S, and the vacant 3*p* orbitals from P or As), facilitating an effective delocalization of the positive charge.[4-5]

Table 4.1. Selected bond lengths (Å), bond angles and fold angles (°) of heterocycles in [**2**][$GaCl_4$], [**7**][$GaCl_4$],[18] [**9**][$GaCl_4$] and [**9**]Cl.

[2][$GaCl_4$]	**[7][$GaCl_4$][18]**	**[9][$GaCl_4$]**	**[9]Cl**
P-S	P-N	As-S	As-S
2.027(2)	1.650(2)	2.1414(9)	2.2163(4)
2.033(2)	1.654(2)	2.146(1)	2.2113(4)
		2.146(1)	
		2.151(1)	
S-C	N-C	S-C	S-C
1.736(6)	1.384(2)	1.727(3)	1.761(1)
1.749(5)	1.385(2)	1.731(2)	1.764(1)
		1.734(3)	
		1.734(2)	
C-C	C-C	C-C	C-C
1.409(8)	1.397(2)	1.399(4)	1.394(2)
		1.397(3)	
S-P-S	N-P-N	S-As-S	S-As-S
98.37(8)	91.33(7)	94.82(3)	92.45(1)
		93.38(3)	
		Fold angle /°	
0.83	1.46	0	23.60
		0	

4.2.3 Syntheses and spectroscopic analysis of inter-pnictogen compounds

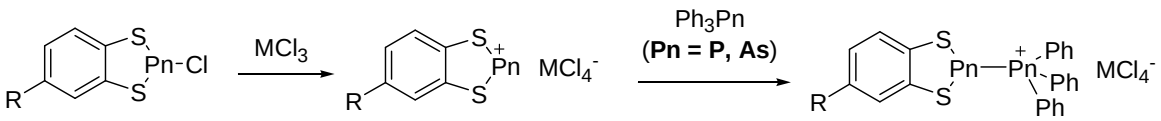

R = H or CH_3
M = Al or Ga

Scheme 4.5. Preparation of inter-pnictogen compounds.

In order to obtain inter-pnictogen compounds, previous reports suggested one-pot procedures in which a mixture of Pn-Cl and a halide abstracting agent are stirred in CH_2Cl_2 for 1-2 h at room temperature, then $PnPh_3$ is added and the reaction mixture stirred for a further 1-2 h.[8-9] However, in our hands, when using Ph_3P, this methodology

afforded an extra singlet appeared at δ_P 5.0-6.0 ppm in the ^{31}P NMR spectra which was indentified as [$Ph_3P\rightarrow MCl_3$] (M = Ga, Al). This was confirmed through NMR studies of the reaction of Ph_3P (δ_P -4.0) with MCl_3 in CH_2Cl_2 or toluene in 24 h. This suggests that the rate of chloride abstraction from the Pn-Cl bond is comparable with the rate of $Ph_3P\rightarrow MCl_3$ adduct formation.

To avoid this problem, Pn-Cl and a Lewis acid ($AlCl_3$ or $GaCl_3$) were reacted in toluene for 24 h, resulting in a biphasic mixture, reflecting separation of the ionic salt from the toluene solvent. A toluene solution of $PnPh_3$ (Pn = P, As, Sb) was subsequently added and the mixture stirred for a further 24 h. The orange-red oily products obtained after removing the upper-layer solvent appeared to be stable in solution but very unstable as solids, decomposing rapidly on storage even in the glove-box. No crystals could be obtained for X-ray diffraction even though many recrystallization approaches were attempted. Nevertheless ^{31}P NMR of these reactions provided some useful insight into the chemical reactivity of these pnictogen cations.

Initial studies clearly reveal that $\mathbf{2}^+$ has some Lewis acidity; reaction of [**2**][$AlCl_4$] (generated *in situ* from [**2**]Cl and $AlCl_3$) with several soft donors, Ph_3E (E = P, As, Sb) affords 1:1 complexes which were characterised by ^{31}P NMR. The ^{31}P NMR of complexes between $\mathbf{1}^+$ or $\mathbf{2}^+$ with Ph_3P exhibit AX-type spectra with two doublets indicating the bonding P←P between two unequivalent phosphorus atoms: [**1**·PPh_3][$AlCl_4$] (δ_P 7.6, 48.7; $^1J_{PP}$ = 442 Hz); [**2**·PPh_3][$AlCl_4$] (δ_P 7.9, 52.3; $^1J_{PP}$ = 444 Hz); and [**2**·PPh_3][$GaCl_4$] (δ_P 7.8, 51.7; $^1J_{PP}$ = 447 Hz). These coupling constants are similar to those of [Ph_3P-P=$CSiMe_3$][$AlCl_4$] (δ_P 20.2, 300.5; $^1J_{PP}$ = 450Hz),[21] and [$Ph_2P(Cl)$-PPh_2][$GaCl_4$] (δ_P 75.5, -0.9; $^1J_{PP}$ = 381.0 Hz),[22] consistent with P-Pn bond formation.

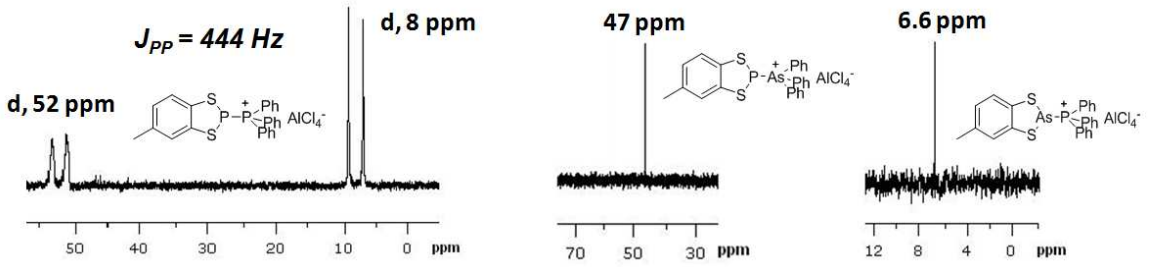

Figure 4.7. ^{31}P NMR spectra of [**2**·PPh_3][$AlCl_4$], [**2**·$AsPh_3$][$AlCl_4$], and [**9**·PPh_3][$AlCl_4$] complexes.

Table 4.2. ^{31}P NMR chemical shifts of adducts of heterocyclic cations with Ph_3E (E = P, As, Sb).

	Colour	**δ_P(ppm)**	**$^1J_{PP}$ (Hz)**	**δ_P of cation (ppm)**
[**1**·PPh_3][$AlCl_4$]	Yellow	7.6 (d), 48.7 (d)	442	56.1 (s)
[**2**·PPh_3][$AlCl_4$]	Orange	7.9 (d), 52.3 (d)	444	58.4 (s)
[**2**·PPh_3][$GaCl_4$]	Yellow	7.8 (d), 51.7 (d)	447	57.2 (s)
[**2**·$AsPh_3$][$AlCl_4$]	Red	47.1 (s)	-	58.4 (s)
[**2**·$SbPh_3$][$GaCl_4$]	Yellow-orange	48.8 (s)	-	57.2 (s)
[**9**·PPh_3][$GaCl_4$]	Red	6.1 (s)	-	-
[**9**·PPh_3][$AlCl_4$]	Orange	6.6 (s)	-	-
[**10**·PPh_3][$GaCl_4$]	Dark red	5.7 (s)	-	-

When the Lewis base Ph_3P is replaced by Ph_3As or Ph_3Sb, a singlet is observed in the ^{31}P NMR spectra. However similar trends in the chemical shift of the phosphenium centre are observed for [**2**·PPh_3]$^+$, [**2**·$AsPh_3$]$^+$, and [**2**·$SbPh_3$]$^+$. For instance, δ_P of [**2**][$AlCl_4$] moves from 58.4 to 52.3 ppm or to 56.8 ppm upon coordination with PPh_3 or $AsPh_3$, and δ_P of [**2**][$GaCl_4$] shifts from 57.2 to 48.8 ppm upon formation of the adduct [**2**·$SbPh_3$][$GaCl_4$]. In addition, δ_P of the Lewis base PPh_3 (δ_P -4.0) shifts to 7.9 ppm, 6.1-6.6 ppm and 5.7 ppm upon coordination to **2**$^+$, **9**$^+$, and **10**$^+$, respectively (Figure 4.7). Actually, the ^{31}P chemical shifts of As←P bonds in [**9**·PPh_3][$AlCl_4$] (δ_P 6.6 ppm) and [**9**·PPh_3][$GaCl_4$] (δ_P

6.1 ppm) are similar to the previously reported adduct [$C_{12}H_9NAs$-PPh_3][OTf] (δ_P 6 ppm).[23] Besides, the Sb←PPh_3 bond exhibits a resonance at δ_P 5.7 ppm which is comparable with similar Sb←PPh_3 adducts such as Cl_3Sb←PPh_3 and $PhCl_2Sb$←PPh_3 complexes[24] both of which occur at 5.6 ppm. In these systems the 1:1 nature of the adduct was confirmed by the integrals of the ^{1}H NMR resonances for the phenyl rings in relation to the methyl group (and aromatic H) of the phosphenium/arsenium cation.

4.2.4 Theoretical calculations

4.2.4.1 Computational studies on phosphenium cations

Geometry-optimised DFT calculations were undertaken using the B3LYP functional and 6-311G*+ basis set. Natural Bond Orbital (NBO) calculations were employed to compare the partial charges and bond orders between *P*-chloro-benzodithiaphosphole or *P*-chloro-benzodiazaphosphole and its corresponding cation. A summary of the bond orders is presented in Table 4.3 and partial charges in Table 4.4.

Table 4.3. Bond orders in the heterocyclic structures obtained from NBO analysis at B3LYP/6-311G*+ level in some chlorophospholes and their equivalent phosphenium cations.

Bond	**P-Cl**	**P-S** or **P-N**	**N-C_{endo}** or **S-C**	**C-C**	**N-C_{exo}**
1$^+$	-	0.97 & 1.66	0.97 & 1.44	0.97	-
[**1**]Cl	0.90	0.95	0.97	0.97	-
2$^+$	-	0.97 & 1.66	0.97 & 1.44	0.97	-
[**2**]Cl	0.90	0.95	0.97	0.97	-
4$^+$	-	0.98 & 1.68	0.98 &1.52	0.97	-
[**4**]Cl	0.86	0.96	0.98	0.97	-
[**5**]Cl	0.91	0.95	0.97	0.97	0.95
6$^+$	-	0.97& 1.64	0.98 &1.47	0.97	1.06
[**6**]Cl	0.90	0.95	0.97	0.97	0.95
7$^+$	-	0.87 & 1.36	0.98 &1.51	0.97	0.99
[**7**]Cl	0.85	0.96	0.97	0.97	0.99
8$^+$	-	0.98 & 1.64	0.98 & 1.51	0.97	0.98
[**8**]Cl	0.84	0.96	0.97	0.97	0.98

These NBO studies (based on DFT/B3LYP/6-311G*+ calculations)[20] of the chlorophospholes validate the presence of P-S, P-N and C-C single bonds around the heterocyclic ring and an exocyclic P-Cl single bond, in agreement with previous studies by Gudat.[13] These data clearly point to disruption of the π-system in $[C_2S_2P]$ and $[C_2(NR)_2P]$ units in the chloro-functionalised substituents, leading to a non-planar heterocycle. On the other hand, the phosphenium cations reflect significant p_π-p_π bonding between P and S in dithiaphospholes (bond order 1.66), P and N in diazaphospholes (bond order 1.36-1.68), S and C (bond order 1.44), N-C_{endo} (bond order 1.47-1.52).

Table 4.4. Atomic partial charges (δ) gained from the Natural Population Analysis (B3LYP/6-311G*+)[25] of the heterocycles in the synthesized chlorophospholes and their corresponding cations.

	P	**Cl**	**N** or **S**	**C**	$\Delta\delta_{P\text{-}Cl}$
1$^+$	0.50	-	0.30	-0.21	-
[**1**]Cl	0.51	-0.33	0.07	-0.20	0.84
2$^+$	0.48	-	0.30[a]	-0.21[a]	-
[**2**]Cl	0.50	-0.33	0.07[a]	-0.21[a]	0.83
4$^+$	1.17	-	-0.80	0.14	-
[**4**]Cl	1.18	-0.46	-0.89	0.13	1.64
[**5**]Cl	1.25	-0.36	-0.77	0.14	1.61
6$^+$	1.18	-	-0.72	0.15[a]	-
[**6**]Cl	1.20	-0.36	-0.77	0.14	1.56
7$^+$	1.15	-	-0.65	0.15	-
[**7**]Cl	1.21	-0.48	-0.75	0.15	1.69
8$^+$	1.14	-	-0.65	0.15	-
[**8**]Cl	1.21	-0.49	-0.75	0.15	1.70
$C_2(NPh)_2PCl$[26]	1.17	-0.42	-0.68	-0.08	1.58
$C_2(N^tBu)_2PCl$[26]	1.20	-0.53	-0.71	-0.09	1.72

([a]Average values)

Further supporting evidence for the presence of π-electron delocalization in the rings of phosphenium cations can be achieved from a comparison between exocyclic and endocyclic C-N bond lengths in **7**$^+$. The exocyclic C-N bonds (1.468-1.474 Å) can be judged as pure single bonds since π interactions between CH_3 group and diazaphosphenium rings are absent. This is in agreement with the NBO calculations in

that all the N-C_{exo} bond orders fall into a range of 0.95-0.99. However, the endocyclic C-N bonds appear to be comparatively shorter (1.384-1.385 Å). It is actually intermediate between single and double bonds (for instance in imine 1,5-diazabicyclo(4.3.0)non-5-ene: C-N single bond 1.465 Å, C=N double bond 1.279 Å).[27] The bond shortening may be attributed to partial double-bond character resulting from π delocalization in the diazaphosphenium rings.

The elimination of Cl^- makes phosphenium cation isoelectronic with other heavy-atom equivalents of *N*-heterocyclic carbenes, simultaeously offering a P lone pair plus a vacant *p*-orbital (conjugated to the C/S framework). Therefore, the phosphenium cation might be both a σ-donor and π-acceptor.[16,28] The donor capacity of various systems of phosphenium cations has been widely examined in terms of ligands for transition metals (primarily with group 6 and 8 metals, or with rhodium).[29] A series of η^5-cyclopentadienyl (Cp) molybdenum,[30] and tungsten complexes,[30-31] as well as a Cp-free complex of manganese[32] have been synthesized through reactions of neutral halophosphines with anionic transition-metal fragments.

Notably chloride ion abstraction does not significantly change the charge on the group 15 element itself but the other heteroatom bonded to it, *e.g.* removal of Cl^- from [**1**]Cl (P +0.50, S +0.07) forms $\mathbf{1}^+$ (P +0.51, S +0.30). The net positive charge on the pnictogen, however, likely reduces its donor capacity.

Based on the difference of atomic partial charges $\Delta\delta_{P\text{-}Cl}$ between P and Cl, it can be concluded that (a) P−Cl bonds in *S*-heterocyclic phospholes are substantially less polar than those in *N*-heterocyclic ones; (b) the electron withdrawing/donating nature of *N*-substituents influences P-Cl bond polarity. The $^{\delta+}P-Cl^{\delta-}$ interactions appear to be more ionic when *N*-substituents are placed in the order: -COMe < -COOMe < -H < -Me < -Et with ethyl offering the strongest bond polarity. This is consistent with strongly electron-withdrawing groups drawing electron density from the P centre which then enhances P-Cl covalency, leading to a reduction in ionicity. This observation is consistent with the features of *N*-monoheterocyclic phospholes previously reported.[26] Indeed *N*-alkyl chlorophospholes derived from four-membered (P−N−C−N) and five-membered

(P−N−C=C−N) C/N/P heterocycles have been proposed as the most appropriate candidates for halide abstraction because of their more polar P-Cl bonds.[26] Indeed strongly electron-releasing groups are expected to stabilise phosphenium centres leading to a move from covalent P-Cl to ionic $P^{\delta+}\cdots Cl^{\delta-}$ and a concomitant P-Cl bond lengthening. In order to probe this further, a correlation between the electron donating/releasing properties of the *exo* R group attached to the heterocyclic N and the P-Cl bond length was examined. In this context we employed the Hammett parameters σ_m and σ_p as potential estimates of the electronic effects of the R group.[33] Figure 4.8 illustrates the correlations of the P-Cl bond length with σ_m and σ_p parameters. While both provide good correlations, the R^2 value (1.00 for a perfect correlation) is marginally better for the σ_m parameter, reflecting a through bond electronic effect rather than stabilisation by resonance.

Table 4.5. Data to construct Hammett correlation of P-Cl bond length. Hammett parameters taken from reference {33}.

Substituent	**$d_{P\text{-}Cl}$/Å**	**σ_m**	**σ_p**
-COMe	2.1267	0.38	0.5
-COOMe	2.121	0.37	0.45
-H	2.26	0	0
-Me	2.297	-0.07	-0.17
-Et	2.30	-0.07	-0.15

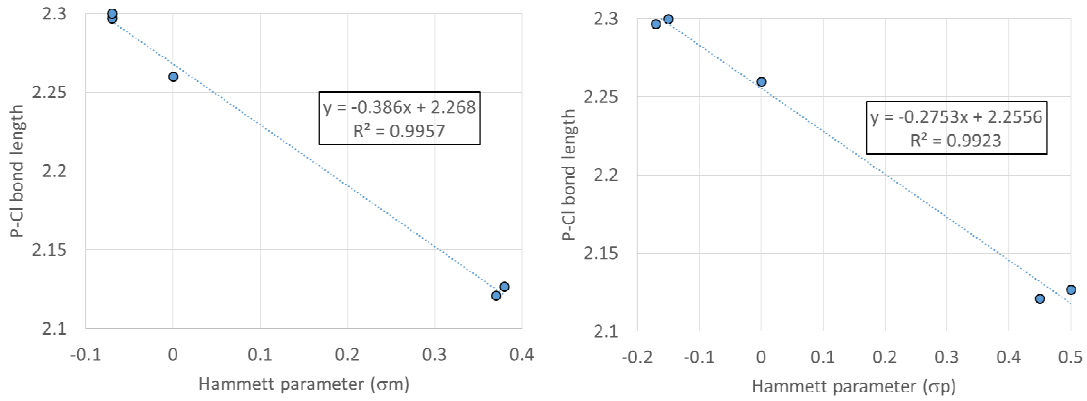

Figure 4.8. Correlation of P-Cl bond length with the Hammett parameter σ_m (left) and σ_p (right)

An examination of the LUMOs of the series of *N*-heterocyclic phosphenium cations (Figure 4.9) reveal exensive π-delocalisation in which the exocyclic R group not only adjusts delocalisation to the NR group but also to the benzo-fused substituent. For R = H, Me and Et there is no evident delocalisation to the exocyclic R group but for the acetyl derivative there is clear delocalisation to the acetyl carbonyl, leading to a much lower LUMO, *i.e.* the acetyl derivative is anticipated to be a substantially stronger Lewis acid. In addition 1e^- reduction to generate a radical is more favourable for the acetyl derivative.

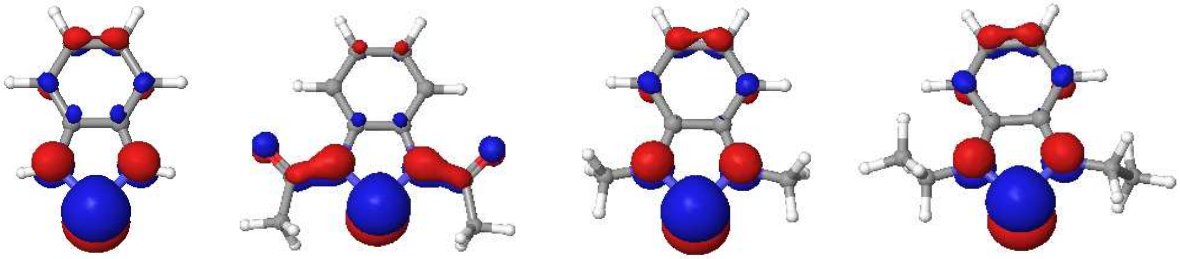

4$^+$ (-7.35) **6**$^+$(-7.84) **7**$^+$ (-6.91) **8**$^+$ (-6.75)

Figure 4.9. LUMOs (B3LYP/6-311G*+) of some *N*-heterocyclic phosphenium cations and their orbital energies (eV), in parentheses.

Notably the π-delocalisation afforded by the acetyl group also reduces the π-delocalisation to the benzo ring whereas electron-donating groups lead to larger coefficients on the benzo-ring.

4.2.4.2 Computational studies on periodic trends between phosphenium, arsenium and stibenium cations

Conventional all-electron B3LYP/6-311G*+ calculations which take into account additional diffuse and polarisation terms necessary for 'softer' 3p elements clearly replicate structural variations within the series of phosphenium cations discussed in the previous section. In order to examine heavier group 15 elements (which are not parameterised within the 6-311G basis set within Jaguar), a number of effective core potential (ECP) basis sets were examined. These ECP basis sets implement an effective

nuclear charge to accommodate the core electrons and nucleus and explicitly considers just the outer valence electrons. In order to establish an appropriate basis set to model trends within group 15 ECPs which reproduced the B3LYP/6-311G*+ computations were considered appropriate. *Ab initio* DFT/B3LYP/LACV3P methods have been applied to calculate geometric data (bond lengths, bond angles), thermodynamic stability, standard enthalpies which reflect the total energetic content, as well as the standard free energies for six-memberred hetero-aromatic rings containing group 15 elements (N, P, As, Sb, Bi).[34] The LACV3P*+ basis set is selected in these studies because it is fully parameterized for all the group 15 elements. It has been confirmed that DFT/B3LYP/LACV3P calculations can deliver a reliable estimation of the geometry.[35]

In order to evaluate the dependence of theoretical calculations on basis sets, geometry-optimized calculations and Natural Population Analysis of $\mathbf{2}^{+}$ and [**2**]Cl were carried out using both B3LYP/6-311G*+ and B3LYP/LACV3P*+ basis set and functionals. The results obtained (Table 4.6) show that the atomic partial charges and bond orders derived from these basis sets are the same, proving that the LACV3P*+ basis set replicates well the all-electron approach.

Table 4.6. Comparison of atomic partial charges (δ) and bond orders gained from the Natural Population Analysis of the heterocycles in *S*-heterocyclic phosphole, phosphenium cation and its congeners.

	Pn	**Cl**	**S**	**C**	$\Delta\delta_{\mathbf{Pn\text{-}Cl}}$	**Pn-S**	**Pn-Cl**	**S-C**	**C-C**
$\mathbf{2}^{+b}$	0.48	-	0.30[a]	-0.21[a]	-	0.97; 1.66	-	0.97; 1.44	0.97
$\mathbf{2}^{+c}$	0.48	-	0.30[a]	-0.21[a]	-	0.97; 1.66	-	0.97; 1.44	0.97
[**2**]Cl[b]	0.50	-0.33	0.07[a]	-0.21[a]	0.83	0.95[a]	0.90	0.97[a]	0.97
[**2**]Cl[c]	0.50	-0.33	0.07[a]	-0.20[a]	0.83	0.95[a]	0.90	0.97[a]	0.97
$[\mathbf{9}]^{+c}$	0.66	-	0.21[a]	-0.21[a]	-	0.97; 1.65	-	0.97	1.52
[**9**]Cl[c]	0.71	-0.41	0.01[a]	-0.21[a]	1.12	0.95[a]	0.88	0.97[a]	0.97
$[\mathbf{10}]^{+c}$	1.00	-	0.06[a]	-0.21[a]	-	0.97; 1.68	-	0.98; 1.47	0.97
[**10**]Cl[c]	1.09	-0.51	-0.13[a]	-0.20[a]	1.60	0.96[a]	0.89	0.97[a]	1.58

(Pn = P/As/Sb; [a]Average values; [b]B3LYP/6-311G*+;[25c]B3LYP/LACV3P*+[35])

Similar to $\mathbf{2}^+$ and $\mathbf{7}^+$, all calculations demonstrate the presences of p_π-p_π bonding between Pn and S, as well as C and C or S and C atoms in the heterocycles of $\mathbf{9}^+$ and $\mathbf{10}^+$.

Lowest unoccupied molecular orbitals (LUMOs) of the abovementioned cations which interact directly with an electron pair in Cl^- to generate the Pn−Cl (Pn = P/As/Sb) bonds are particularly studied in the nature of bonding with corresponding Pn-chloro precursors.

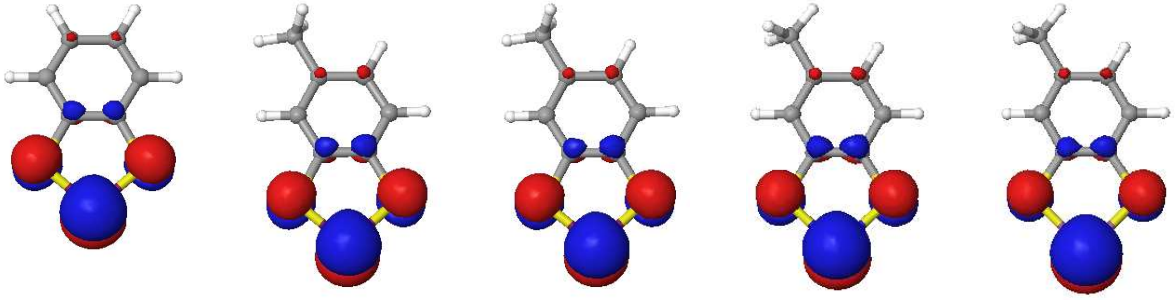

$\mathbf{1}^+$ (-8.41)[a] $\mathbf{2}^+$ (-8.25)[a] $\mathbf{2}^+$ (-8.24)[b] $\mathbf{9}^+$ (-8.40)[b] $\mathbf{10}^+$ (-8.24)[b]

Figure 4.10. LUMOs calculated by B3LYP ([a]6-311G*+; [b]LACV3P*+) of *S*-heterocyclic phosphenium cations and their congeners, and their orbital energies (eV), in parentheses.

Reassuringly, LUMOs of $\mathbf{2}^+$ obtained from two different basis sets (6-311G*+ and LACV3P*+) are comparable (Figure 4.10) and within the group 15 series almost invariant at the B3LYP/LACV3P*+ level of theory, though notably the Lewis acidity (LUMO energy) in the series varies in the order $\mathbf{2}^+ < \mathbf{9}^+ > \mathbf{10}^+$ and in agreement with the partial charge of the pnictogen (Table 4.6).

A comparison of the bonding in $C_7H_6S_2Pn^+$ reveals subtle differences in bonding on descending the group. The NBO structures (best Lewis structure) for each derivative coupled with their NBO partial charges and bond orders are presented in Figure 4.11. Notably the most stable resonance form varies in each case. On descending the group there is a steady increase in the positive charge on the pnictogen (in agreement with the increasing electropositive nature of the pnictogen) and a decrease in the Wiberg bond index reflecting poorer π-bonding on descending the group (Wiberg bond orders: P-S 1.33, As-S 1.26 and Sb-S 1.16). Notably the NBO partial charges on the S centre

decrease on descending the group. This leads to a near constant charge on the S_2Pn unit of +1.07 (Pn = P), +1.08 (Pn = As) and +1.11 (Pn = Sb) suggesting that bonding within the phenylene ring is somewhat invariant. An analysis of the second order perturbation (deviations from the best localised Lewis structure) indicate that the only significant perturbations (> 50 kcal/mol) are associated with π-delocalisation within the aromatic core for $C_7H_6S_2P^+$ and $C_7H_6S_2Sb^+$ to stabilise the formal negative charge. In the case of $C_7H_6S_2Sb^+$ there are additional significant perturbations associated with delocalisation of the lone pair on the C centre to Sb-S π* and C-C π* orbitals. Notably there is no perturbation energy greater than 50 kcal/mol for $C_7H_2S_2As^+$.

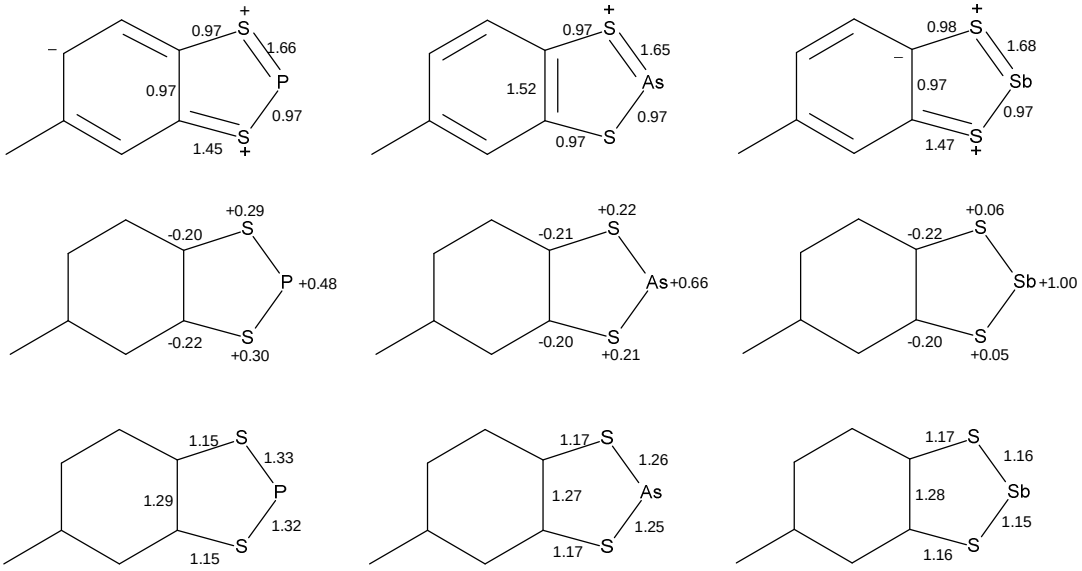

Figure 4.11. (top) NBO bond orders and best resonance structure derived from the NBO analysis for the $C_7H_6S_2Pn^+$ ring; (middle) NBO partial charges around the heterocyclic ring; (bottom) Wiberg bond orders

Replacement of S by NMe leads to substantial changes in the charge distribution (Figure 4.12), substantially enhancing the electropositive nature of the P^+ centre with the N atoms possessing a partial negative charge and leading to a small positive charge at the benzo ring carbons. The resonance form for the diazaphosphenium cation exhibits the same resonance structure as the dithiastibenium cation. Notably the Wiberg bond index for the

P-N bond is even lower than that for S-Sb suggesting very limited multiple bond character and a strongly polar ionic contribution to stability. All second order perturbations in the NBO analysis of $C_6H_4(NMe)_2P^+$ (> 50 kcal/mol) were associated with stabilisation of the formal C lone pair *via* delocalisation to the C=C π* and C=N π* orbitals.

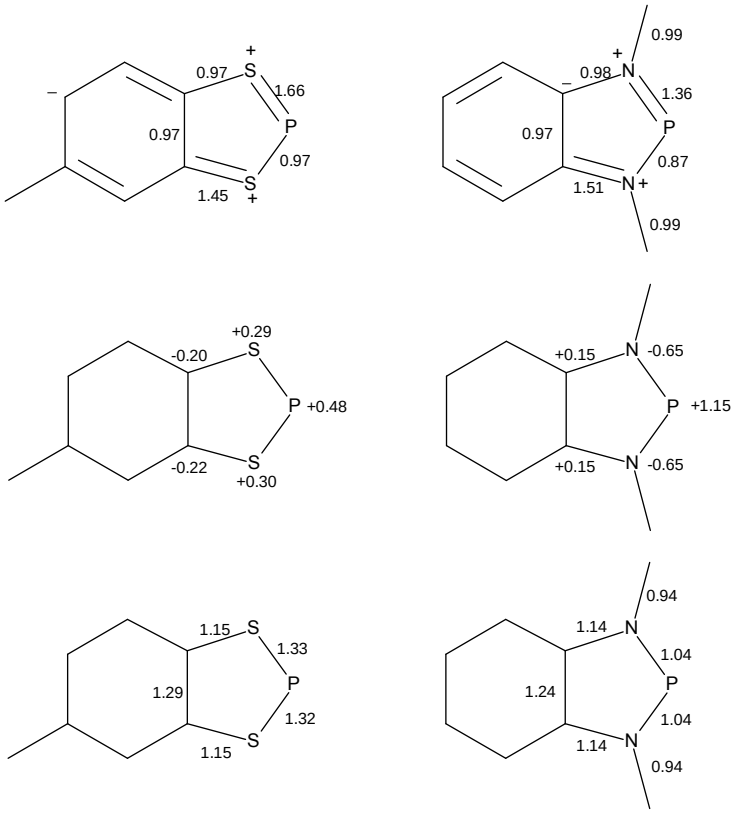

Figure 4.12. (top) NBO bond orders and best resonance structure derived from the NBO analysis for the $C_7H_6S_2P^+$ and $C_6H_4(NMe)_2P^+$ cationic rings ; (middle) NBO partial charges around the heterocyclic ring; (bottom) Wiberg bond orders

4.3 Conclusions

The bonding in bicyclic benzodithiaphosphenium, benzodithiaarsenium and benzo-diazaphosphenium cations differs significantly from the precursor chloro-phosphines/arsines. The latter are best described in terms of a localised bonding structure

whereas the cations exhibit planar five-membered ring structures in which there is π-delocalisation affording 10π-electron species isolobal with *N*-heterocyclic carbenes.

These cationic species are formally amphoteric, possessing both a lone pair and vacant orbital. Computational studies reveal the Lewis acidity (LUMO energy) is sensitive to the nature of the ring and the pnictogen; within the series $C_6H_4S_2Pn^+$ the order of Lewis acidity is As > P ~ Sb. Within the series of diazaphospheniums, $C_6H_4(NR)_2P^+$, the Lewis acidity can be tuned by the electron-withdrawing/releasing nature of the R group.

A series of new inter-pnictogen complexes based on S/P, S/As, and S/Sb cations have been synthesized from the *P*-chloro-benzodithiaphosphole, *As*-chloro-benzodithiaarsole, and *Sb*-chloro-benzodithiastibole by treatment with a Lewis acid, followed by addition of Ph_3Pn (Pn = P, As, Sb) which affords 1:1 adducts which were characterised by multinuclear NMR.

4.4 Experimental

All reagents were used as received without any further purification unless otherwise noted: toluene-3,4-dithiol, $AlCl_3$, $GaCl_3$, $AsCl_3$, $SbCl_3$(Sigma-Aldrich).

4.4.1 Preparation of $[C_7H_6S_2P][AlCl_4]$, [2][AlCl$_4$]

A solution of $C_7H_6S_2PCl$ (synthesized in Chapter 2) (1.00 g; 4.53 mmol) in CH_2Cl_2 (20 mL) was added dropwise to a solution of $AlCl_3$ (0.604 g; 4.53 mmol) in CH_2Cl_2 (10 mL) under N_2. The resulting orange mixture was stirred at room temperature overnight. The solvent was then removed *in vacuo* to give an orange solid. Yield: 1.45 g (90%).

^{1}H NMR (300 MHz, CD_2Cl_2) δ_H 8.51 (d, $^3J_{HH}$ = 8.7 Hz, 1H, aromatic CH), 8.43 (s, 1H, aromatic CH), 7.89 (d, $^3J_{HH}$ = 8.7 Hz, 1H, aromatic CH), 2.71 (s, 3H, CH_3).

^{13}C NMR(75.5MHz, CD_2Cl_2) δ_C 152.80, 149.58, 143.61, 132.96, 127.88 (d, $^2J_{PC}$ = 5.1 Hz, aromatic S<u>C</u>), 127.60 (d, $^2J_{PC}$ = 4.2 Hz, aromatic S<u>C</u>), 21.74.

^{31}P{^{1}H} NMR (121.5 MHz, CD_2Cl_2) δ_P 58.38 (s).

Found ($[C_7H_6S_2P][AlCl_4]$ requires): C = 23.21% (23.75); H = 1.41% (1.71).

Melting point: 101-102 ^{o}C.

4.4.2 Preparation of $[C_7H_6S_2P][GaCl_4]$, [2][$GaCl_4$]

A solution of $C_7H_6S_2PCl$ (synthesized in Chapter 2; 0.500g; 2.27 mmol) in CH_2Cl_2 (10 mL) was added dropwise to a solution of $GaCl_3$ (0.399g; 2.27 mmol) in CH_2Cl_2 (10 mL) under N_2. The resulting yellow orange solution was stirred at room temperature for 2 hours. The solvent was then removed *in vacuo* to give a yellow-orange solid. Yield: 0.840g (93%). Crystals were obtained by slow evaporation of a CH_2Cl_2 solution of the product in a Schlenk flask under N_2.

^{1}H NMR (300 MHz, CD_2Cl_2) δ_H7.90 (d, $^{3}J_{HH}$ = 9.75 Hz, 1H, aromatic CH), 7.82 (s, 1H, aromatic CH), 7.39 (d, $^{3}J_{HH}$ = 9.75 Hz, 1H, aromatic CH), 2.50 (s, 3H, CH_3).

^{13}C NMR (75.5 MHz, CD_2Cl_2) δ_C 142.81, 140.05, 132.31, 130.33, 127.74 (d, $^{2}J_{PC}$ = 5.1 Hz, aromatic S<u>C</u>), 127.40 (d, $^{2}J_{PC}$ = 4.2 Hz, aromatic S<u>C</u>), 21.66.

^{31}P{^{1}H} NMR (121.5 MHz, $CDCl_3$) δ_P 57.2 (s).

Found ($[C_7H_6S_2P][GaCl_4]$ requires): C = 21.36% (21.19); H = 1.68% (1.52).

Melting point: 80-81 °C.

4.4.3 Preparation of $C_7H_6S_2AsCl$, [9]Cl[10]

To a solution of toluene-3,4-dithiol (1.000 g; 6.4 mmol) in CH_2Cl_2 (40 mL) was added arsenic trichloride (1.160 g; 6.4 mmol). The reaction mixture was stirred at reflux under N_2 at 40^{o}C for 1.5 h. Solvent was removed *in vacuo* to afford a pale yellow solid (1.389g; 5.25 mmol; 82%).The product was recrystallized by cooling a saturated MeOH solution to -20 ^{o}C for 24 h to give suitable crystals for X-ray diffraction.

^{1}H NMR (300 MHz, $CDCl_3$) δ_H 7.48 (d, $^{3}J_{HH}$ = 8.1 Hz, 1H, aromatic CH), 7.42 (s, 1H, aromatic CH), 7.04 (d, $^{3}J_{HH}$ = 8.1 Hz, 1H, aromatic CH), 2.37 (s, 3H, CH_3).

^{13}C NMR (75.5 MHz, $CDCl_3$) δ_C 139.55, 136.60, 136.08, 127.44, 127.34, 126.61, 20.85.

Found ($C_7H_6AsClS_2$ requires): C = 32.00% (31.77); H = 2.16% (2.29).

Melting point: 81-82 ^oC.

4.4.4 Preparation of $[C_7H_6S_2As][AlCl_4]$, [9][$AlCl_4$]

A solution of $C_7H_6S_2AsCl$ (1.00 g; 3.78 mmol) in CH_2Cl_2 (20 mL) was added dropwise to a solution of $AlCl_3$ (0.504 g; 3.78 mmol) in CH_2Cl_2 (10 mL) under N_2. The resulting red solution was stirred at room temperature overnight. The solvent was then removed *in vacuo* to give an orange-red solid. Yield: 1.34 g (89%).

^{1}H NMR (300 MHz, CD_2Cl_2) δ_H 8.31 (d, $^3J_{HH}$ = 8.25 Hz, 1H, aromatic CH), 8.22 (s, 1H, aromatic CH), 7.75 (d, $^3J_{HH}$ = 8.25 Hz, 1H, aromatic CH), 2.66 (s, 3H, CH_3).

^{13}C NMR (75.5 MHz, CD_2Cl_2) δ_C150.20, 146.91, 141.14, 130.92, 128.61, 128.27, 21.32.

Found ($[C_7H_6S_2As][AlCl_4]$ requires): C = 21.09% (21.13); H = 1.80% (1.52).

Melting point: 122-124 ^oC.

4.4.5 Preparation of $[C_7H_6S_2As][GaCl_4]$, [9][$GaCl_4$]

A solution of $C_7H_6S_2AsCl$ (0.500g; 1.89 mmol) in CH_2Cl_2 (10 mL) was added dropwise to a solution of $GaCl_3$ (0.333g; 1.89 mmol) in CH_2Cl_2 (10 mL) under N_2. The resulting red solution was stirred at room temperature in 2 hours. The solvent was then removed *in vacuo* to give an orange-red solid. Yield: 0.807g (97 %). Crystals were obtained by slow evaporation of a saturated CH_2Cl_2 solution of the product in Schlenk flask under N_2.

^{1}H NMR (300 MHz, CD_2Cl_2) δ_H 7.89 (d, $^3J_{HH}$ = 8.25 Hz, 1H, aromatic CH), 7.82 (s, 1H, aromatic CH), 7.40 (d, $^3J_{HH}$ = 8.25 Hz, 1H, aromatic CH), 2.51 (s, 3H, CH_3).

^{13}C NMR (75.5 MHz, CD_3CN) δ_C 140.66, 137.73, 137.15, 128.24, 128.05, 127.44, 20.68.

Found ($[C_7H_6S_2As][GaCl_4]$ requires): C = 18.52% (19.08); H = 1.64% (1.37).

Melting point: 128-129 ^{o}C.

4.4.6 Synthesis of $C_7H_6S_2SbCl$, [10]Cl[10]

To a solution of toluene-3,4-dithiol (1.000g, 6.4 mmol) in CH_2Cl_2 (40 mL) was added $SbCl_3$ (1.460 g, 6.4 mmol). The reaction mixture was stirred at reflux under N_2 for 1 h. The resulting yellow solution was cooled on an ice-water bath but no precipitate appeared. The solvent was removed *in vacuo* to give a yellow solid (1.70 g, 85%).

^{1}H NMR (500 MHz, $CDCl_3$) δ_H 7.45 (d, $^{3}J_{HH}$ = 8.2 Hz, 1H, aromatic CH), 7.39 (s, 1H, aromatic CH), 6.92 (d, $^{3}J_{HH}$ = 8.2 Hz, 1H, aromatic CH), 2.34 (s, 3H, CH_3).

^{13}C NMR (75.5 MHz, CD_2Cl_2) δ_C 140.54, 137.07, 136.39, 130.59, 129.90, 127.09, 20.59.

Found ($C_7H_6ClS_2Sb$ requires): C = 26.52% (26.99); H = 1.65% (1.94).

Melting point: 142–143 ^{o}C.

4.4.7 Synthesis of $[C_7H_6S_2Sb][GaCl_4]$, [10][$GaCl_4$]

A solution of $C_7H_6S_2SbCl$ (0.800g, 2.57 mmol) in CH_2Cl_2 (30 mL) was added dropwise to a solution of $GaCl_3$ (0.452g, 2.57 mmol) in CH_2Cl_2 (10 mL) under N_2. The resulting red solution was stirred at room temperature in 2 hours. The solvent was then removed *in vacuo* to give a dark red solid. Yield: 1.201g (96%).

^{1}H NMR (300 MHz, CD_3CN) δ_H 7.37 (d, $^{3}J_{HH}$ = 8.1 Hz, 1H, aromatic CH), 7.33 (s, 1H, aromatic CH), 6.89 (d, $^{3}J_{HH}$ = 8.1 Hz, 1H, aromatic CH), 2.28 (s, 3H, CH_3).

^{13}C NMR (75.5 MHz, CD_3CN) δ_C 141.61, 138.12, 136.23, 130.86, 130.29, 126.98, 20.34.

Found ($[C_7H_6S_2Sb][GaCl_4]$ requires): C = 16.40% (17.24); H = 1.57% (1.24).

Melting point: 110-111 ^{o}C.

4.4.8 Synthesis of [$C_7H_6S_2Sb$][$AlCl_4$], [10][$AlCl_4$]

A solution of $C_7H_6S_2SbCl$ (1.00 g, 3.21 mmol) in CH_2Cl_2 (40 mL) was added dropwise to a solution of $AlCl_3$ (0.428 g, 3.21 mmol) in CH_2Cl_2 (10 mL) under N_2. The resulting red solution was stirred at room temperature overnight. The solvent was then removed *in vacuo* to give a dark red sticky solid. Yield: 0.91 g (64%).

^{1}H NMR (300 MHz, CD_2Cl_2) δ_H 8.60 (d, $^3J_{HH}$ = 8.7 Hz, 1H, aromatic CH), 8.50 (s, 1H, aromatic CH), 7.99 (d, $^3J_{HH}$ = 8.7 Hz, 1H, aromatic CH), 2.75 (s, 3H, CH_3).

^{13}C NMR (75.5 MHz, CD_2Cl_2) δ_C 145.42, 141.94, 140.65, 135.07, 134.44, 126.51, 22.18.

Found ([$C_7H_6S_2Sb$][$AlCl_4$] requires): C = 18.60% (18.90); H = 1.54% (1.36).

Melting point:165-166 ^oC.

4.4.9 Preparation of [$C_6H_4(NH)_2P$][$GaCl_4$], [4][$GaCl_4$]

A solution of $GaCl_3$ (0.306 g, 1.74 mmol) in MeCN (5 mL) was added dropwise to a suspension of $C_6H_4(NH)_2PCl$ (synthesized in Chapter 3, 0.300 g, 1.74 mmol) in MeCN (5 mL). The yellow solution was left to stir at RT for 2h. The solvent evaparated *in vacuo* to give a yellow solid. Yield: 0.450 g (74%).

^{1}H NMR (300 MHz, CD_3CN) δ_H 12.38 (s, broad, 2H, NH), 7.81-7.85 and 7.62-7.65 (m, AA′BB′ aromatic CH).

^{13}C NMR (75.5 MHz, CD_3CN) δ_C 138.35 (d, $^2J_{PC}$ = 6.2 Hz, PN<u>C</u>), 128.24, 116.24.

^{31}P{^{1}H} NMR (121.5 MHz, CD_3CN) δ_P 212.55 (s)

Found ([$C_6H_4(NH)_2P$][$GaCl_4$] requires): C = 20.53% (20.67); H = 1.92% (1.73); N = 7.98% (8.04).

Melting point: 137-138 ^oC.

4.4.10 Preparation of $[C_6H_4(NCOCH_3)_2P][OSO_2CF_3]$, [6][OTf]

A solution of $Me_3SiOSO_2CF_3$ (0.520 g, 2.34 mmol) in MeCN (5 mL) was added dropwise to a solution of $C_6H_4(NCOCH_3)_2PCl$ (synthesized in Chapter 3, 0.500 g, 1.95 mmol) in MeCN (5 mL). The yellow solution was left to stirred at RT overnight. Volatiles were evaporated *in vacuo* to give a yellow solid. Yield: 0.505 g (70%).

^{1}H NMR (300 MHz, CD_3CN) δ_H 8.22-8.25 (m, 2H, ring C_6H_4), 7.21-7.26 (m, 2H, ring C_6H_4), 2.65 (d, $^4J_{PH}$ = 5.4 Hz, 6H, $COCH_3$).

^{13}C NMR (75.5 MHz, CD_3CN) δ_C169.82, 155.48, 128.53, 117.05, 115.26, 27.37.

^{31}P{^{1}H} NMR (121.5 MHz, CD_3CN) δ_P 219.19 (s).

Found ($[C_6H_4(NCOCH_3)_2P][OSO_2CF_3]$ requires): C = 35.88% (35.68); H = 2.98% (2.72); N = 7.65% (7.57).

4.4.11 Preparation of $[C_6H_4(NCH_3)_2P][GaCl_4]$, [7][$GaCl_4$]

A solution of $GaCl_3$ (0.176 g, 1.00 mmol) in MeCN (5 mL) was added dropwise to a solution of $C_6H_4(NCH_3)_2PCl$ (synthesized in Chapter 3, 0.20 g, 1.00 mmol) in MeCN (5 mL). The purple solution was stirred for 1 h at room temperature. Volatiles were removed to give a purple solid (0.295 g,78%) which was recrystallized from MeCN to yield suitable crystals of $[C_6H_4(NCH_3)_2P][GaCl_4]$ for X-ray diffraction.

^{1}H NMR (300 MHz, $CDCl_3$) δ_H 7.81 (m, 2H, aromatic CH), 7.78 (m, 2H, aromatic CH), 4.13 (d, $^3J_{PH}$ = 10.71 Hz, 6H, NCH_3).

^{13}C NMR (75.5 MHz, CD_3CN) δ_C 140.01 (d, $^2J_{PC}$ = 5.59 Hz, heterocyclic PNC), 128.14 (s, aromatic), 114.50 (s, aromatic), 34.10(d, $^2J_{PC}$ = 16.76 Hz, $PNCH_3$).

^{31}P{^{1}H} NMR (121.5 MHz, CD_3CN) δ_P 214.41.

Found ($[C_6H_4(NCH_3)_2P][GaCl_4]$ requires): C = 25.38% (25.51); H = 2.81% (2.68); N = 7.62% (7.44).

Melting point: 265-266 ^{o}C.

4.4.12 General procedure for the preparation of inter-pnictogen complexes

Equimolar quantities of $AlCl_3$ or $GaCl_3$ (1 mmol) and $C_7H_6S_2PnCl$ (Pn = P/As/Sb) (1 mmol in 10 mL of toluene) were combined and stirred at RT overnight. A solution of $PnPh_3$ (1 mmol in 10 mL of toluene) was then added and stirred for a further 24 hours to yield a biphasic mixture (the top layer was usually pale yellow, and the bottom layer was yellow/orange/red). The upper solvent phase was decanted. Solvent removal from the bottom residue afforded very viscous orange-to-red oils, and no precipitation when using layering methods. Yield: [**1**·PPh_3][$AlCl_4$] (71%); [**2**·PPh_3][$AlCl_4$] (75%); [**2**·PPh_3][$GaCl_4$] (68%); [**2**·$AsPh_3$][$AlCl_4$] (78%); [**2**·$SbPh_3$][$GaCl_4$] (63%); [**9**·PPh_3][$GaCl_4$] (66%); [**9**·PPh_3][$AlCl_4$] (72%); [**10**·PPh_3][$GaCl_4$] (65%).

*4.4.12.1 Data for [**1**·PPh_3][$AlCl_4$]*

^{1}H NMR (300 MHz, CD_2Cl_2) δ_H 7.72-7.77 (m, 3H, aromatic CH in PPh_3), 7.63-7.68 (m, 6H, aromatic CH in PPh_3), 7.58-7.60 (m, 6H, aromatic CH in PPh_3), 7.18-7.22 and 7.01-7.04 (dd and dd, $^{3}J_{HH}$ = 6.0 Hz, $^{4}J_{HH}$ = 3.3 Hz, AA'BB', aromatic CH).

^{13}C NMR (75.5 MHz, CD_2Cl_2) δ_C 135.80 (d, $^{3}J_{PC}$ = 3.32 Hz, PPh_3), 135.15, 134.34 (d, $^{2}J_{PC}$ = 7.40 Hz, PPh_3), 130.80 (d, $^{1}J_{PC}$ = 10.72 Hz, P<u>C</u> in PPh_3), 128.49 (s, PPh_3), 126.14, 117.78.

^{31}P{^{1}H} NMR (202.5 MHz, CD_2Cl_2) δ_P 48.75 (d, $^{1}J_{PP}$ = 442 Hz, heterocycle C_2S_2P),7.63 (d, $^{1}J_{PP}$ = 442 Hz, PPh_3).

*4.4.12.2 Data for [**2**·PPh_3][$AlCl_4$]*

^{1}H NMR (300 MHz, $CDCl_3$) δ_H 7.81-7.89 (m, 3H, aromatic CH in PPh_3), 7.72-7.74 (m, 6H, aromatic CH in PPh_3), 7.67-7.70 (m, 6H, aromatic CH in PPh_3), 7.14 (d, $^{3}J_{HH}$ = 7.7 Hz, 1H, aromatic CH), 6.92 (s, 1H, aromatic CH), 6.71 (d, $^{3}J_{HH}$ = 7.7 Hz, 1H, aromatic CH), 2.27 (s, 3H, CH_3).

^{13}C NMR (75.5 MHz, CD_2Cl_2) δ_C 138.47, 137.46, 136.06 (d, $^3J_{PC}$ = 2.87 Hz, PPh_3), 135.75, 134.15 (d, $^2J_{PC}$ = 5.81 Hz, PPh_3), 130.77 (d, $^1J_{PC}$ = 10.57 Hz, PC in PPh_3), 130.50 (s, PPh_3), 122.21, 115.41, 114.24, 20.73.

^{31}P{^{1}H} NMR (202.5 MHz, CD_2Cl_2) δ_P 52.30 (d, $^1J_{PP}$ = 444 Hz, heterocycle C_2S_2P),7.92 (d, $^1J_{PP}$ = 444 Hz, PPh_3).

*4.4.12.3 Data for [**2**·PPh_3][$GaCl_4$]*

^{1}H NMR (500 MHz, CD_2Cl_2) δ_H 7.75-7.80 (m, 3H, aromatic CH in PPh_3), 7.68-7.73 (m, 6H, aromatic CH in PPh_3), 7.63-7.66 (m, 6H, aromatic CH in PPh_3), 7.12 (d, $^3J_{HH}$ = 7.5 Hz, 1H, aromatic CH), 7.01 (s, 1H, aromatic CH), 6.85 (d, $^3J_{HH}$ = 7.5 Hz, 1H, aromatic CH), 2.23 (s, 3H, CH_3).

^{31}P{^{1}H} NMR (202.5 MHz, CD_2Cl_2) δ_P 51.73 (d, $^1J_{PP}$ = 447 Hz, heterocycle C_2S_2P), 7.81 (d, $^1J_{PP}$ = 447 Hz, PPh_3).

*4.4.12.4 Data for [**2**·$AsPh_3$][$AlCl_4$]*

^{1}H NMR (500 MHz, CD_2Cl_2) δ_H 7.72-7.75 (m, 3H, aromatic CH in $AsPh_3$), 7.59-7.62 (m, 6H, aromatic CH in $AsPh_3$), 7.49-7.50 (m, 6H, aromatic CH in $AsPh_3$), 7.16 (d, $^3J_{HH}$ = 7.5 Hz, 1H, aromatic CH), 7.04 (s, 1H, aromatic CH), 6.91 (d, $^3J_{HH}$ = 7.5 Hz, 1H, aromatic CH), 2.23 (s, 3H, CH_3).

^{13}C NMR (75.5 MHz, CD_2Cl_2) δ_C 138.25, 135.05, 133.43, 132.60, 131.42, 130.90, 130.63, 128.87, 128.63, 126.28, 21.32.

^{31}P{^{1}H} NMR(202.5 MHz, $CDCl_3$) δ_P 47.11 (s, heterocycle C_2S_2P).

*4.4.12.5 Data for [**2**·$SbPh_3$][$GaCl_4$]*

^{1}H NMR (300 MHz, $CDCl_3$) δ_H 7.63-7.66 (m, 3H, aromatic CH in $SbPh_3$), 7.42-7.45 (m, 6H, aromatic CH in $SbPh_3$), 7.33-7.36 (m, 6H, aromatic CH in $SbPh_3$), 7.18 (d, $^3J_{HH}$ = 7.8 Hz, 1H, aromatic CH), 7.06 (s, 1H, aromatic CH), 6.93 (d, $^3J_{HH}$ = 7.8 Hz, 1H, aromatic CH), 2.34 (s, 3H, CH_3).

$^{31}P\{^{1}H\}$ NMR(121.5 MHz, $CDCl_3$) δ_P 48.80 (s, heterocycle C_2S_2P).

*4.4.12.6 Data for [**9**·PPh_3][$AlCl_4$]*

^{1}H NMR (500 MHz, CD_2Cl_2) δ_H 7.95-7.99 (m, 3H, aromatic CH in PPh_3), 7.73-7.79 (m, 6H, aromatic CH in PPh_3), 7.56-7.65 (m, 6H, aromatic CH in PPh_3), 7.03 (d, $^{3}J_{HH}$ = 7.5 Hz, 1H, aromatic CH), 6.91 (s, 1H, aromatic CH), 6.79 (d, $^{3}J_{HH}$ = 7.5 Hz, 1H, aromatic CH), 2.22 (s, 3H, CH_3).

^{13}C NMR (75.5 MHz, CD_2Cl_2) δ_C 138.03, 137.11, 135.38 (d, $^{3}J_{PC}$ = 3.32 Hz, PPh_3), 134.19 (d, $^{2}J_{PC}$ = 8.61 Hz, PPh_3), 130.65 (d, $^{1}J_{PC}$ = 12.08 Hz, P<u>C</u> in PPh_3), 128.53 (s, PPh_3), 127.18, 126.42, 118.62, 117.85, 20.39.

$^{31}P\{^{1}H\}$ NMR (202.5 MHz, CD_2Cl_2) δ_P 6.63 (s, PPh_3).

*4.4.12.7 Data for [**9**·PPh_3][$GaCl_4$]*

^{1}H NMR (300 MHz, CD_2Cl_2) δ_H 7.70-7.74 (m, 3H, aromatic CH in PPh_3), 7.62-7.63 (m, 6H, aromatic CH in PPh_3), 7.54-7.60 (m, 6H, aromatic CH in PPh_3), 7.01 (d, $^{3}J_{HH}$ = 9.1 Hz, 1H, aromatic CH), 6.89 (s, 1H, aromatic CH), 6.77 (d, $^{3}J_{HH}$ = 9.1 Hz, 1H, aromatic CH), 2.18 (s, 3H, CH_3).

^{13}C NMR (75.5 MHz, CD_2Cl_2) δ_C 138.04, 137.18, 135.37 (d, $^{3}J_{PC}$ = 3.32 Hz, PPh_3), 134.23 (d, $^{2}J_{PC}$ = 8.61 Hz, PPh_3), 130.67 (d, $^{1}J_{PC}$ = 12.08 Hz, P<u>C</u> in PPh_3), 128.54 (s, PPh_3), 127.21, 126.44, 118.68, 117.91, 20.41.

$^{31}P\{^{1}H\}$ NMR(202.5 MHz, $CDCl_3$) δ_P 6.05 (s, PPh_3).

*4.4.12.8 Data for [**10**·PPh_3][$GaCl_4$]*

^{1}H NMR (300 MHz, $CDCl_3$) δ_H 7.81-7.85 (m, 3H, aromatic CH in PPh_3), 7.70-7.72 (m, 6H, aromatic CH in PPh_3), 7.58-7.63 (m, 6H, aromatic CH in PPh_3), 7.39 (d, $^{3}J_{HH}$ = 8.1 Hz, 1H, aromatic CH), 7.32 (s, 1H, aromatic CH), 6.88 (d, $^{3}J_{HH}$ = 8.1 Hz, 1H, aromatic CH), 2.31 (s, 3H, CH_3).

^{13}C NMR (75.5 MHz, $CDCl_3$) δ_C 137.39, 136.01 (d, $^3J_{PC}$ = 2.87 Hz, PPh_3), 134.30 (d, $^2J_{PC}$ = 9.06 Hz, PPh_3), 130.33 (d, $^1J_{PC}$ = 12.23 Hz, P<u>C</u> in PPh_3), 127.84 (s, PPh_3), 123.01, 122.15, 116.22, 115.10, 113.97, 20.67.

^{31}P{^{1}H} NMR(121.5 MHz, $CDCl_3$) δ_P 5.70 (s, PPh_3).

4.5 References

1. Denk, M.; Lennon, R.; Hayashi, R.; West, R.; Belyakov, A. V.; Verne, H. P.; Haaland, A.; Wagner, M.; Metzler, N., *J. Am. Chem. Soc.* **1994**, *116* (6), 2691-2692.

2. Carmalt, J. C.; Lomeli, V., *Chem. Commun.* **1997**, *0* (21), 2095-2096.

3. Bansal, R. K.; Grupta, N.; Collier, S. J., Product class 15: dithiaphospholes and their analogues. 2004; Vol. 13, pp 641-646.

4. (a) Burford, N.; Royan, B. W., *J. Chem. Soc., Chem. Commun.* **1989**, *0* (1), 19-21; (b) Burford, N.; Royan, B. W.; Linden, A.; Cameron, T. S., *J. Chem. Soc., Chem. Commun.* **1988**, *0* (13), 842-844; (c) Burford, N.; Royan, B. W.; Linden, A.; Cameron, T. S., *Inorg. Chem.* **1989**, *28* (1), 144-150; (d) Burford, N.; Royan, B. W.; White, P. S., *J. Am. Chem. Soc.* **1989**, *111* (10), 3746-3747.

5. Burford, N.; Parks, T. M.; Royan, B. W.; Richardson, J. F.; White, P. S., *Can. J. Chem.* **1992**, *70* (3), 703-709.

6. Chivers, T.; Manners, I., Inorganic Rings and Polymers of the *p*-Block Elements: From Fundamentals to Applications. The Royal Society of Chemistry: Cambridge, UK, 2009; pp 212-276.

7. Conrad, E.; Burford, N.; McDonald, R.; Ferguson, M. J., *J. Am. Chem. Soc.* **2009**, *131* (46), 17000-17008.

8. Burford, N.; Ragogna, P. J., *J. Chem. Soc., Dalton Trans.* **2002**, *0* (23), 4307-4315.

9. (a) Burford, N.; Ragogna, P. J.; McDonald, R.; Ferguson, M. J., *J. Am. Chem. Soc.* **2003**, *125* (47), 14404-14410; (b) Conrad, E.; Burford, N.; McDonald, R.; Ferguson, M. J., *Inorg. Chem.* **2008**, *47* (8), 2952-2954; (c) Conrad, E.; Burford, N.; McDonald, R.; Ferguson, M. J., *J. Am. Chem. Soc.* **2009**, *131* (14), 5066-5067.

10. (a) Kisenyi, J. M.; Willey, G. R.; Drew, M. G. B.; Wandiga, S. O., *J. Chem. Soc., Dalton Trans.* **1985**, (1), 69-74; (b) Baudler, M.; Moog, A.; Glinka, K.; Kelsch, U., *Z. Naturforsch., B* **1973**, *28*, 363-369.

11. (a) Klapoetke, T. M., The vibrational spectrum of arsenic trichloride. In *Main Group Metal Chemistry*, 1997; Vol. 20, pp 81-83; (b) Lide, D. R., *CRC Handbook of Chemistry and Physics (88th 2007-2008 edition)*. CRC Press: **2007**.

12. (a) Pauling, L., *The Nature of the Chemical Bond and the Structure of Molecules and Crystals: An Introduction to Modern Structural Chemistry*. Cornell University Press: **1960**; (b) Pauling, L., *Mineral. Soc. Am. Spec. Pap.* **1981**, *3* (1170), 125-131.

13. Dräger, M., *Z. Anorg. Allg. Chem.* **1975**, *411* (1), 79-89.

14. Dräger, M., *Chem. Ber.* **1974**, *107* (8), 2601-2611.

15. (a) Vickaryous, W. J.; Herges, R.; Johnson, D. W., *Angew. Chem. Int. Ed. Engl.* **2004**, *43* (43), 5831-5833; (b) Schmidbaur, H.; Bublak, W.; Huber, B.; Müller, G., *Angew. Chem. Int. Ed. Engl.* **1987**, *26* (3), 234-236; (c) Probst, T.; Steigelmann, O.; Riede, J.; Schmidbaur, H., *Chem. Ber.* **1991**, *124* (5), 1089-1093; (d) Schmidbaur, H.; Nowak, R.; Steigelmann, O.; Müller, G., *Chem. Ber.* **1990**, *123* (6), 1221-1226.

16. Cowley, A. H.; Kemp, R. A., *Chem. Rev.* **1985**, *85* (5), 367-382.

17. Slattery, J. M.; Fish, C.; Green, M.; Hooper, T. N.; Jeffery, J. C.; Kilby, R. J.; Lynam, J. M.; McGrady, J. E.; Pantazis, D. A.; Russell, C. A.; Willans, C. E., *Chem. Eur. J.* **2007**, *13* (24), 6967-6974.

18. Dunmore, A., Cooperation work in 59-410: Synthesis and Reactivity of Benzodiazaphospholes: Towards Diazaphospholyl Radicals. University of Windsor, Windsor, **2014**.

19. Gudat, D.; Haghverdi, A.; Hupfer, H.; Nieger, M., *Chemistry – A European Journal* **2000**, *6* (18), 3414-3425.

20. Gudat, D.; Haghverdi, A.; Hupfer, H.; Nieger, M., *Chem. Eur. J.* **2000**, *6* (18), 3414-3425.

21. David, G.; Niecke, E.; Nieger, M.; Radseck, J.; Schoeller, W. W., *J. Am. Chem. Soc.* **1994**, *116* (5), 2191-2192.

22. Weigand, J. J.; Burford, N.; Decken, A., *Eur. J. Inorg. Chem.* **2008**, *2008* (28), 4343-4347.

23. Burford, N.; Ragogna, P. J.; Sharp, K.; McDonald, R.; Ferguson, M. J., *Inorg. Chem.* **2005**, *44* (25), 9453-9460.

24. Chitnis, S. S.; Burford, N.; McDonald, R.; Ferguson, M. J., *Inorg. Chem.* **2014**, *53* (10), 5359-5372.

25. Reed, A. E.; Weinstock, R. B.; Weinhold, F., *J. Chem. Phys.* **1985**, *83* (2), 735-746.

26. Brazeau, A. L.; Hänninen, M. M.; Tuononen, H. M.; Jones, N. D.; Ragogna, P. J., *J. Am. Chem. Soc.* **2012**, *134* (11), 5398-5414.

27. Savoca, A. C.; Urgaonkar, S., 1,5-Diazabicyclo[4.3.0]non-5-ene. In *Encyclopedia of Reagents for Organic Synthesis*, John Wiley & Sons, Ltd: 2001.

28. Gudat, D., *Coord. Chem. Rev.* **1997**, *163* (0), 71-106.

29. (a) Abrams, M. B.; Scott, B. L.; Baker, R. T., *Organometallics* **2000**, *19* (24), 4944-4956; (b) Gudat, D., *Eur. J. Inorg. Chem.* **1998**, *1998* (8), 1087-1094; (c) Nakazawa, H., *J. Organomet. Chem.* **2000**, *611* (1–2), 349-363.

30. Reisacher, H.-U.; McNamara, W. F.; Duesler, E. N.; Paine, R. T., *Organometallics* **1997**, *16* (3), 449-455.

31. Lang, H.; Leise, M.; Schmitzer, A., *J. Organomet. Chem.* **1995**, *489* (1–2), 77-81.

32. Lang, H.; Leise, M.; Emmerich, C., *J. Organomet. Chem.* **1991**, *418* (1), C9-C13.

33. Hansch, C.; Leo, A.; Taft, R. W., *Chem. Rev.* **1991**, *91* (2), 165-195.

34. (a) Hay, P. J.; Wadt, W. R., *J. Chem. Phys.* **1985**, *82* (1), 299-310; (b) Wadt, W. R.; Hay, P. J., *J. Chem. Phys.* **1985**, *82* (1), 284-298; (c) Hay, P. J.; Wadt, W. R., *J. Chem. Phys.* **1985**, *82* (1), 270-283.

35. Medeleanu, M.; Mracec, M.; Pop, O. R.; Mocanu, L.; Mracec, M., *Rev. Roum. Chim.* **2014**, *59* (11-12), 1077-1087.

CHAPTER 5

EXPLORATION OF HETEROCYCLIC CHEMISTRY OF BENZODITHIAPHOSPHOLES AND BENZODIAZAPHOSPHOLES

5.1 Introduction

5.1.1 P-N bond-containing heterocyclic materials

The discovery of the first organophosphorus compound in 1897 (Me_3P prepared from methyl chloride and calcium phosphide) ignited the study of phosphorus-containing compounds. However, more recent developments in phosphorus chemistry rapidly escalated due to the introduction of ^{31}P NMR spectroscopy and solid state structure determination by X-ray crystallography since the 1950s.[1]

In the most general sense, heterocyclic compounds are central to many chemical and biological processes. More recently the incorporation of main group elements into organic structures has become increasingly important in next generation molecular electronics such as conducting poly(thiophene) and poly(pyrrole)[2] and light-emitting materials such as those derived from boron-containing compounds such as BODIPY.[3] Therefore, scientists have been attempting to understand and develop the chemistry of heterocyclic compounds to improve our quality of life.[4]

Many P-N bond-containing ligands have been prepared and employed to stabilize a variety of transition metals over the past years.[5] This results from several unique advantages of these ligands, *e.g.* some moieties such as P/N and P/O primarily perform as reversible binding donors to a metal center,[6] therefore, offering or protecting temporarily a vacant coordination site, essential for many catalytic processes.[7] A number of diphosphinoamine $RN(PPh_2)_2$ (PNP) ligands have been publicized in terms of their catalytic ability for the Suzuki-Heck cross-coupling.[8] Additionally, their Pd complexes have also proved to be excellent catalysts.[8b,c] The reaction between an aldehyde and a functionalized-phosphine tertiary amine results in the insertion of carbon fragments into

the P^{III}-N bonds or the cleavage of P^{III}-N bond.[5a,b,6] For example, Priya *et al.* reported the first insertion of C-fragments from aldehydes into the P-N bonds of phosphinoamines to generate α-amino phosphonates.[9] When treated with paraformaldehyde, the P^{III}-N bond can undergo CH_2 insertion, and then oxidation of P^{III} to P^{V}. A number of mono- and bis(phosphino) amines have been found to display similar reactivities towards many different aldehydes and ketones.[10] Such insertion reactions might contribute significantly to the preparation and isolation of phosphine oxide derivatives which offer prospective herbicidal, antimicrobial, and neuroactive reagents.[6,11]

At the present time, phosphorus chemistry is considered to be one of the most important research areas due to its many applications within the pharmaceutical and cosmetics industries, as well as agriculture. In addition, many phosphine-based complexes are indispensable catalysts in industrial processes.[1] Therefore, a greater understanding of P-based chemistry offers potential to promote developments in these areas and scientists continue to explore more novel phosphorus-based compounds to enrich the library of phosphorus chemistry.

5.1.2 Project objectives

In the route to explore new P-N involving ligands, I have been inspired to develop novel structures based on a variety of heterocylic S/P, S/As, and N/P systems. This chemistry has developed from the reactivity of the P-Cl and As-Cl bonds in *P*-chloro-dithiaphospholes and *P*-chloro-dithiaarsoles and the related *P*-chloro-diazaphospholes. In particular the potential to utilise the reactivity of the P-Cl (or As-Cl) bond to transfer the heterocyclic ring to make more complex structures has been explored. Here the synthesis and structural studies on some unusal heterocyclic compounds with various structures containing two or three heterocycles are described. These comprise the paddle-wheel complexes $N[\mathbf{2}]_3$ and $N[\mathbf{9}]_3$, as well as the systematic synthesis of $C_6H_4(NR[\mathbf{5}])_2$ which was initially prepared fortuitously during attempted reduction of $C_6H_4(NR)_2PCl$ (Chapter 3).

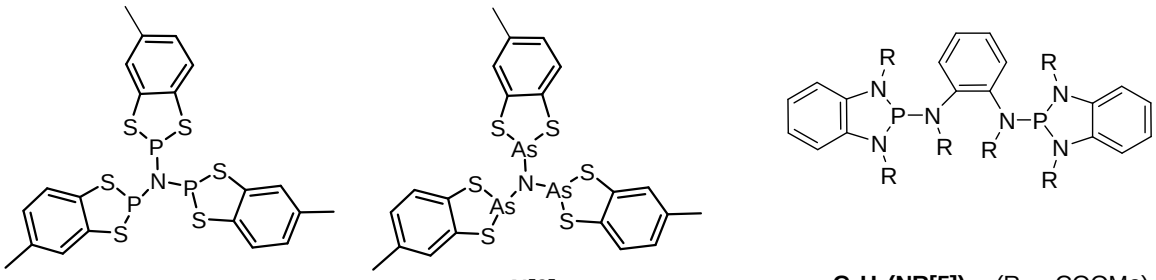

5.2 Results and Discussion

5.2.1 Paddle-wheel structures of five-membered dithiaphosphole and dithiaarsole rings

5.2.1.1 Syntheses of N[2]$_3$ and N[9]$_3$

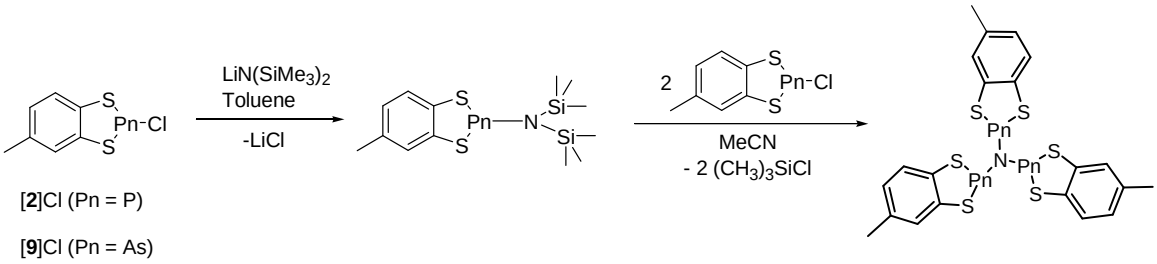

Scheme 5.1. Synthesis of $N(C_7H_6S_2Pn)_3$.

Precursors $C_7H_6S_2PnN(SiMe_3)_2$ (Pn = P or As) were readily obtained in quantitative yields (by NMR) as spectroscopically pure colorless-to-yellow oils *via* metathesis of the chloride salts [**2**]Cl or [**9**]Cl with lithium bis(trimethylsilyl)amide in a 1:1 mole ratio. However condensation of these silyl derivatives with further [**2**]Cl or [**9**]Cl depended upon solvent. Attempts to achieve the second and third Pn-N bond formation *via* condensation of two equivalents of [**2**]Cl or [**9**]Cl with $C_7H_6S_2PnN(SiMe_3)_2$ in toluene at 120-130^{o}C proved unsuccessful. ^{31}P NMR revealed that the second and third substitutions of $SiMe_3$ by $C_7H_6S_2Pn$ at N atom (*i.e.* the elimination of Me_3SiCl) did not reach completion even at these elevated temperatures over periods of 3-5 days. A range of other solvents were investigated and eventually MeCN was found to be the most suitable solvent not only for the substitution reactions but also, fortuitously, for product

purification. In particular, all starting materials and by-product, $(CH_3)_3SiCl$, are soluble in MeCN, whereas $(C_7H_6S_2Pn)_3N$ (Pn = P, As) precipitates from solution. Isolation by filtration followed by recrystallization provided suitable crystals for X-ray diffraction.

Similar reactivity was explored for the antimony derivative but continued to prove elusive. Firstly, both the starting material $C_7H_6S_2SbCl$ and intermediate $C_7H_6S_2SbN(SiMe_3)_2$ appear insoluble in MeCN. Last but not least, the product is very sensitive to air and light, its yellow colour turns into brownish in the course of cooling down the reaction mixture and isolating it through filtration. Previous studies by Wright amongst others have shown that certain complexes of the heavier pnictogens such as phosphinidines are prone to disproportionation leading to the formation of Zintl phases.[12]

5.2.1.2 Structures and bonding of $N(C_7H_6S_2Pn)_3$

Single X-ray diffraction was carried out for compounds $N(C_7H_6S_2P)_3$ and $N(C_7H_6S_2As)_3$. Crystallographic data are presented in Appendix 6.

a. Crystal structure of $N(C_7H_6S_2P)_3$

White needle crystals of $N(C_7H_6S_2P)_3$ were grown by cooling a concentrated CH_2Cl_2 solution at -20 ^oC. It crystallises in the rhombohedral space group *P-3* with a third of a molecule in the asymmetric unit, with the N atom located on the crystallographic 3-fold axis. Crystals of $N(C_7H_6S_2P)_3$ selected for X-ray diffraction were persistently hampered by merohedral twinning and the data reported here is the best refinement based on several full data collections.

The five-membered rings of N[**2**]$_3$ have an analogous "envelope" geometry to the previously-studied C_2S_2P-containing compounds [**2**]X (X = Cl, Br, I), with a fold angle of 20.66^o (*cf* other structures which fall in the range 19.62-26.06^o (see Table 5.1). The P-S (2.105(2)-2.125(2) Å) bond lengths in N[**2**]$_3$ are slightly longer than other [**2**]X derivatives (P-S mean 2.086 Å). The greater uncertainty on the S-C and C-C bond lengths means that all derivatives are the same within experimental error and no meaningful comparison can be drawn. As with other [**2**]X derivatives, these geometric parameters

coupled with folding of the heterocycle are consistent with a loss of π-delocalisation when compared to [**2**][$GaCl_4$]. Although there is some variation in both SPS bond angle and P-S distance there is no clear correlation evident between these two parameters.

Table 5.1. Selected bond lengths [Å] and angles [°] of some heterocyclic C_2S_2P-containing compounds. Fold angle [°] is angle between [SCCS] and [SPS] planes.

	P-X	**P-S**	**S-C**	**C-C**	**S-P-S**	**Fold angle/^{o}**
[**2**]Cl [a]	2.1103(7)	2.0932(7) 2.0921(6)	1.767(2) 1.766(2)	1.390(2)	95.43(2)	26.06
[**2**]Br [a]	2.304(3)	2.079(3) 2.078(3)	1.772(9) 1.761(9)	1.39(1)	96.1(1)	24.27
[**2**]I [a]	2.5687(8)	2.0861(9) 2.090(1)	1.759(3) 1.757(2)	1.395(4)	96.16(4)	19.62
[**2**][$GaCl_4$] [b]	-	2.027(2) 2.033(2)	1.736(6) 1.749(5)	1.409(8)	98.37(8)	0.83
N[**2**]$_3$	1.7274(2)	2.105(2) 2.125(2)	1.782(6) 1.768(2)	1.377(8)	94.39(9)	20.66

[a, b] *Data from Chapter 2, and Chapter 4, respectively.*

The exocyclic P-N bond lengths (1.7274(2) Å) falls into the range of normal P-N single bonds (1.70-1.77Å).[13] The P1-N1-P1 (119.81^o) is very close to 120^o expected for sp^2 hydridization at the 'hub' N1 atom with N1 displaced just 0.076 Å from the plane defined by the three P1 atoms with the N atom adopting a trigonal planar geometry. Notably the three-fold rotation axis places the three pendant methyl groups all on the same side of the molecule with respect to the P_3N plane and there was no evidence for disorder of the methyl groups over the alternative site.

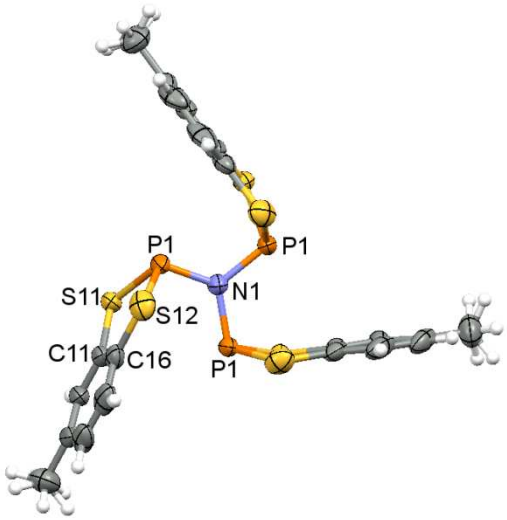

Figure 5.1. Molecular structure of $N(C_7H_6S_2P)_3$ determined from single crystal X-ray diffraction with thermal ellipsoids drawn at the 50% probability level for non-H atoms.

Along the crystallographic *c* axis molecules of $N(C_7H_6S_2P)_3$ molecules adopt an alternating stacked structure with inter-layer N···N separations of 4.354 and 6.892 Å (Figure 5.2). The shorter N···N contacts are associated with an aggregation process with a series of six symmetry equivalent S···S contacts between molecules (3.512 Å) which are marginally shorter than the sum of the van der Waals' radii (3.60 Å) and which form a chair-like supramolecular conformation of S atoms (Figure 5.3). There are no close contacts between these 'dimers' along the three-fold axis. These columns then adopt a hexagonal array.

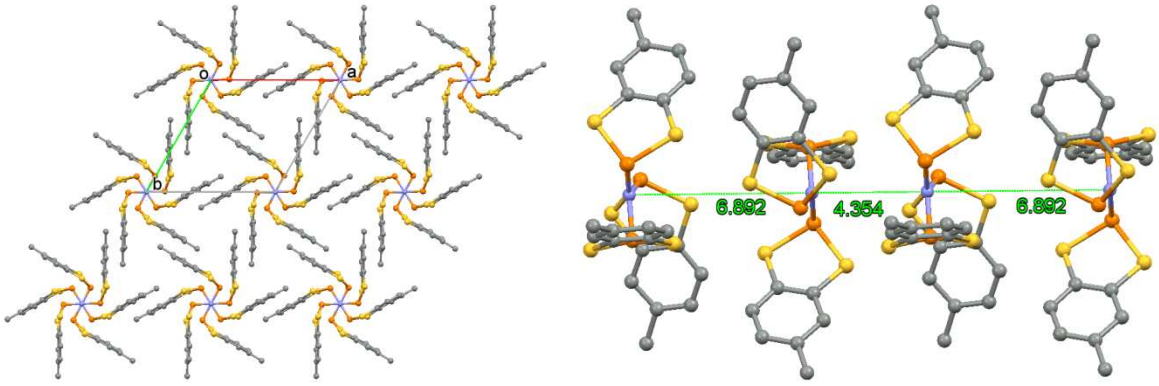

Figure 5.2. Crystal packing for $N(C_7H_6S_2P)_3$ viewed parallel to the *c*-axis (left) showing the three-fold symmetry axis; and the alternating N···N separation which propagates parallel to the *c*-axis.

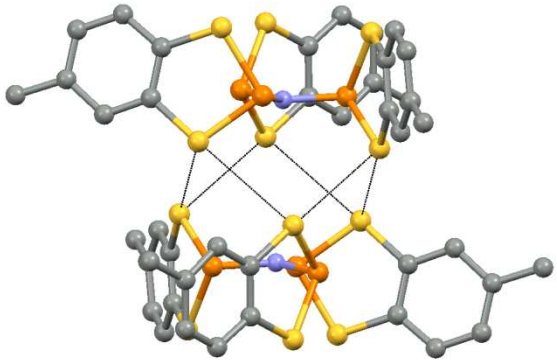

Figure 5.3. S…S contacts between molecules of N[**2**]$_3$

b. Crystal structure of $N(C_7H_6S_2As)_3$

Yellow crystals of $N(C_7H_6S_2As)_3$ were grown by cooling a concentrated CH_2Cl_2 solution to -20 ^oC. The molecule adopts the triclinic space group *P-1* with one molecule in the asymmetric unit. The structure is similar to $N(C_7H_6S_2P)_3$ described above but now the pendant methyl groups are located on different sides with respect to the As_3N plane, leading to a lowering of the crystallographic symmetry. In other respects the molecule adopts a similar geometry and packing arrangement to N[**2**]$_3$. Although the five-membered units of N[**9**]$_3$ preserve the "envelope" geometry of its precursor [**9**]Cl, the

fold angles (mean 14.52^{o}) are significantly smaller than that of [**9**]Cl (23.60^{o}). The six As-S bonds (2.237(3), 2.245(3), 2.265(3), 2.226(3), 2.247(3), 2.239(2) Å) in N[**9**]$_3$ are all lengthened in comparison to those in [**9**]Cl (2.2163(4)-2.2113(4)Å). The heterocyclic S-C and C-C bonds are the same within experimental error (Table 5.2). Although the lengthening of the As-S bonds in N[**9**]$_3$ (with respect to [**9**]Cl) likely renders a reduction in S-As-S bond angles (91.46(9), 91.1(1), 91.54(9)^{o}), the studies on the corresponding dithiaphospholes (discussed previously) indicate that there is no direct correlation with the fold angle and the Pn-S bond length.

Table 5.2. Selected bond lengths [Å] and angles [°] of some heterocyclic C_2S_2As-containing compounds. Fold angle [°] is angle between [SCCS] and [SAsS] planes.

	As-S	**S-C**	**C-C**	**S-As-S**	**Fold angle/^{o}**
[**9**]Cl [a]	2.2163(4)	1.761(1)	1.394(2)	92.45(1)	23.60
	2.2113(4)	1.764(1)			
N[**9**]$_3$	2.237(3)	1.752(8)	1.38(1)	91.46(9)	14.07
	2.245(3)	1.756(8)	1.37(2)	91.1(1)	14.66
	2.265(3)	1.75(1)	1.38(1)	91.54(9)	14.83
	2.226(3)	1.748(9)			
	2.247(3)	1.771(8)			
	2.239(2)	1.75(1)			

[a]*Data from Chapter 4*

The As1-N1 1.849(9), As2-N1 1.850(6), As3-N1 1.875(7)Å bond lengths at the core of the structure are comparable to the conventional As^{III}-N^{III} ones (mean 1.858Å).[13] The As1-N1-As2 117.8(4)^{o}, As1-N1-As3 115.7(4)^{o}, As2-N1-As3 117.7(4)^{o} bond angles are close to 120^{o} anticipated for sp^2 hydridization at N1. This is also supported by the fact that N1 is close to being coplanar with the three bonded As atoms (displacement from the As_3 plane is just 0.320 Å). Therefore, the N1 atom here similarly possesses trigonal planar geometry, analogous to the nitrogen in the aforementioned P-based derivatives.

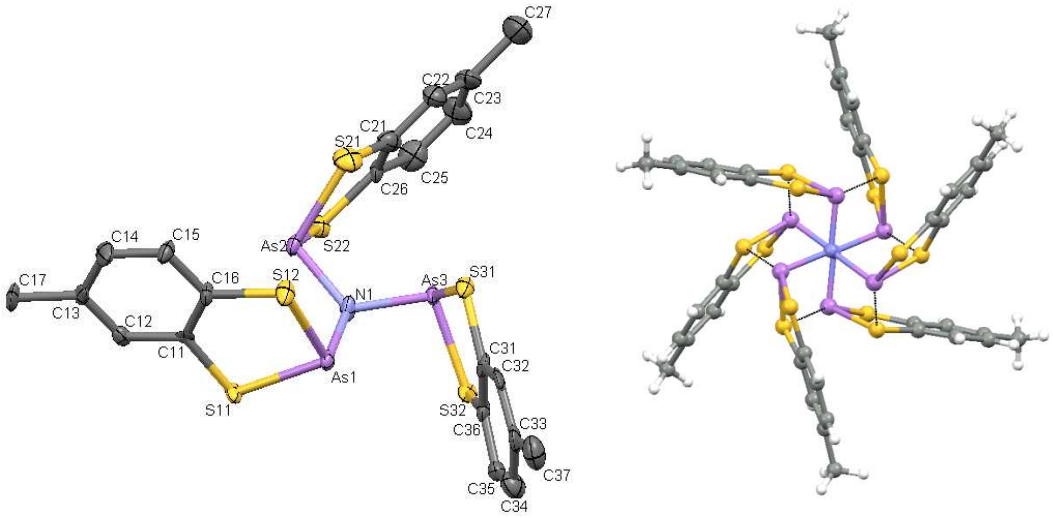

Figure 5.4. (left) Molecular structure of $N(C_7H_6S_2As)_3$ determined from single crystal X-ray diffraction. Thermal ellipsoids drawn at 50% probability and H atoms omitted for clarity; (right) pairs of molecules linked through As···S contacts.

In contrast to $N(C_7H_6S_2P)_3$ its crystal structure has lower symmetry with two molecules existing in the triclinic *P-1* unit cell. For $N(C_7H_6S_2As)_3$ two molecules form a dimer with a shorter N···N separation (3.761 Å) than in $N(C_7H_6S_2P)_3$. Here the two molecules are linked *via* a set of six S···S contacts (3.443 – 3.588 Å) forming a supramolecular chair conformation analogous to the S···S contacts in $N[\mathbf{2}]_3$ (3.512 Å). Notable however the replacement of P with As leads to a set of S···As contacts (3.482 – 3.498 Å) which are significantly less than the sum of the van der Waals radii (3.85 Å) (Figure 5.5) and arguably contribute more significantly to the association in the solid state.

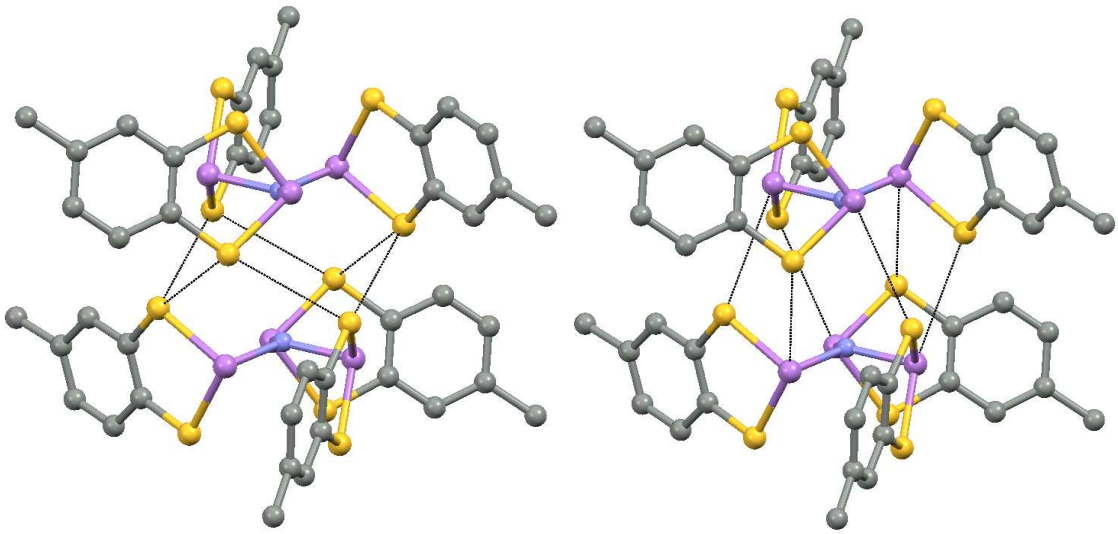

Figure 5.5. Aggregation of $N(C_7H_6S_2As)_3$ to form dimers can be considered to be driven by S···S contacts (left) or S···As contacts (right). H atoms omitted for clarity.

In the case of $N[\mathbf{9}]_3$ the next pair of molecules are laterally displaced away from the non-crystallographic 3-fold axis with no significant contacts along the "stacking direction", reminiscent of $N[\mathbf{2}]_3$.

c. Analysis and comparison of structures and bonding in $N(C_7H_6S_2Pn)_3$

X-ray crystallography reveals that to some extent the $N(C_7H_6S_2P)_3$ and the $N(C_7H_6S_2As)_3$ adopt similar fashions of spatially atomic arrangements within the "paddle-wheel" shapes. Their crystal structures consist of molecular units $N(C_7H_6S_2Pn)_3$, therefore they might be interpreted as tertiary amines NR_3 with three large $C_7H_6S_2Pn$ substituents. Each molecule consists of three 1,3,2-benzodithiaphosphole or 1,3,2-benzodithiaarsole rings connected to a central nitrogen atom as shown in Figures 5.1 and 5.4. Although many species including a central nitrogen atom surrounded by three phenyl rings have been reported, these are unprecedented examples of structurally characterized pnictogen compounds bearing an analogous model.

The structures show that the central nitrogen atom is located on a (crystallographic) three-fold axis and is almost coplanar with the three pnictogen atoms (P/As), consistent

with an essentially trigonal planar sp^2 geometry. There is an expected increase in Pn-N bond length on descending the group 15 due to the increase in covalent radius on descending the group. As a consequence the exocyclic P-N bond (1.727 Å) is shorter than the As-N bond (1.849-1.875 Å). This leads to greater steric congestion at the central N atom which, in turn, leads to a marked rotation of the heterocyclic ring planes from the central NPn_3-plane. Notably the dihedral angle for the P derivative (88.17°) is larger than that for the As derivative (82.54°, 82.94°, 83.77°; mean 83.08°) consistent with the greater steric demand associated with the shorter P-N bond. The crystal structures of $N(C_7H_6S_2Pn)_3$ resemble that of $N(C_3N_3)_3Cl_6$ (tris(2,4-dichloro-1,3,5-triazine)amine, TDT)[14] although the three C_3N_3 rings in TDT are inclined at smaller dihedral angles (34.33°) with respect to the central C_3N plane.

These kinds of "paddle-wheel" shapes might be assumed to inherit the geometric characteristics of phosphorus/arsenic atoms from their corresponding precursors $C_7H_6S_2PnCl$, *i.e.* the nitrogen atom replaces the chlorine atom, and Pn-N bonds locate at flagpole positions against the heterocyclic rings. Indeed, the Pn atoms adopt neutral tricoordinate pnictogen (σ^3-Pn) in pyramidal structures with local 3-fold (C_{3v}) symmetry about the pnictogen. The electronic structure of this geometry is traditionally considered to be associated with an energetically high-lying nitrogen lone pair.[15]

5.2.1.3 Spectroscopic studies of paddle-wheel molecules

a. $^{31}P\{^1H\}$ NMR of $N[2]_3$

Table 5.3. $^{31}P\{^1H\}$ NMR chemical shifts of starting materials and product.

Compound	$C_7H_6S_2PCl$	$C_7H_6S_2PN(SiMe_3)_2$	$N(C_7H_6S_2P)_3$
δ_P (ppm)	161.4	94.4	86.8

The $^{31}P\{^1H\}$ NMR of $N(C_7H_6S_2P)_3$ exhibits a singlet, reflecting the chemical equivalence of the three ^{31}P centres in solution. The chemical shift is substantially different compared to [**2**]Cl but relatively close to intermediate [**2**]$N(SiMe_3)_2$ as expected for a molecule with

a similar first coordination environment at the P centre (see Chapter 2). Using the methodology established in Chapter 2 and the ^{31}P NMR data for $Me_2PN(SiEt_3)_2$[16] we can estimate σ_{para} for the $N(SiEt_3)_2$ group around 10.5 which gives a predicted ^{31}P shift for [**2**]$N(SiMe_3)_2$ in the 74 ppm region. Although there is some discrepancy here between calculated and observed chemical shifts, it is clearly in the right region of the ^{31}P NMR spectrum and it is evident that the σ_{para} values for amino groups, R_2N, are very sensitive to the nature of R [compare σ_{para} values for $N(SiEt_3)_2$ and NMe_2 at 10.5 and 61.5 respectively].

b. Time-of-flight mass spectrometry (TOF-MS)

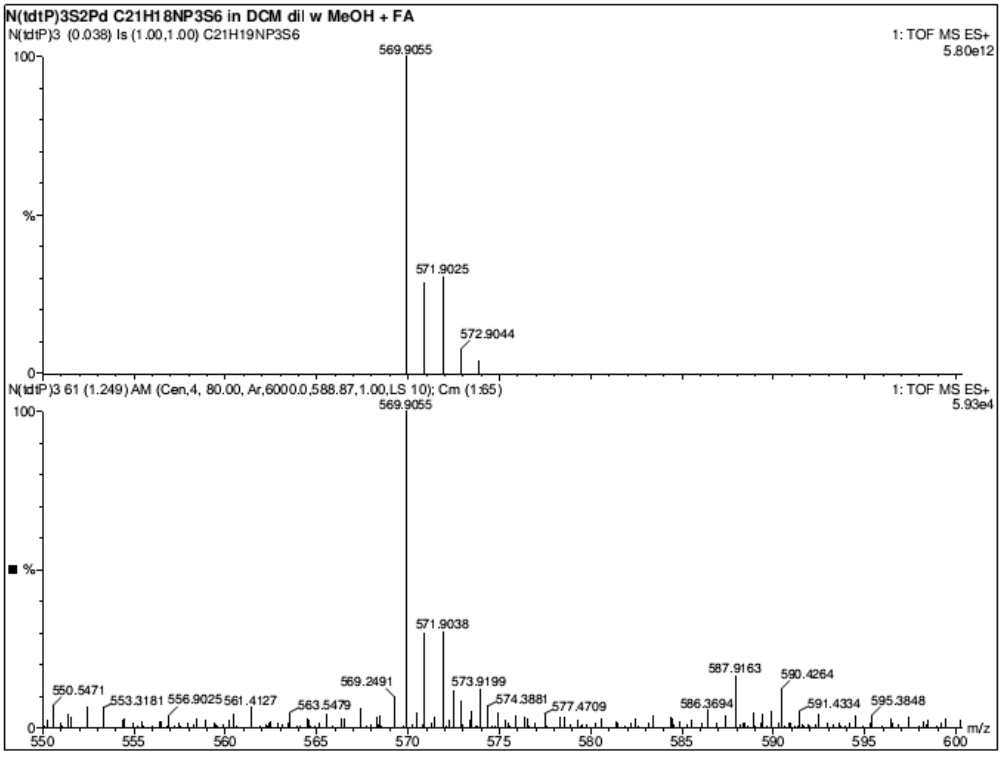

Figure 5.6. A comparison of the calculated (top) and experimental (bottom) TOF-MS spectrum of $[N(C_7H_6S_2P)_3 + H]^+$.

To characterize structures of the paddle-wheel molecules $N(C_7H_6S_2Pn)_3$, electrospray TOF-MS was employed to verify their molecular weights. The sample was dissolved in CH_2Cl_2, diluted with MeOH and formic acid added. A molecular ion for $(M+H)^+$ was

observed at M = 569.9055 (theoretical value M = 569.6856) in good agreement with the calculated $(M+H)^+$ ion (M = 569.9055) to within 5 ppm mass accuracy and confirmed by the good agreement with the expected isotope distribution pattern.

Similar approaches to identify the molecular ion derived from $N(C_7H_6S_2As)_3$ proved unsuccessful, with the dominant ion observed matching that for $C_7H_6S_2As^+$ group (M = 228.9221). This indicates that the arsenic derivative is significantly more labile with respect to cleavage of the N-Pn bond. It can be confirmed by the conventional bond dissociation energies (enthalpy change ΔHf_{298} kJ/mol) for a bond A-B which is broken through the reaction AB → A + B with values refer to the gaseous state and at 298 K (As-N 582(126) kJ/mol; P-N 617(21) kJ/mol).[17]

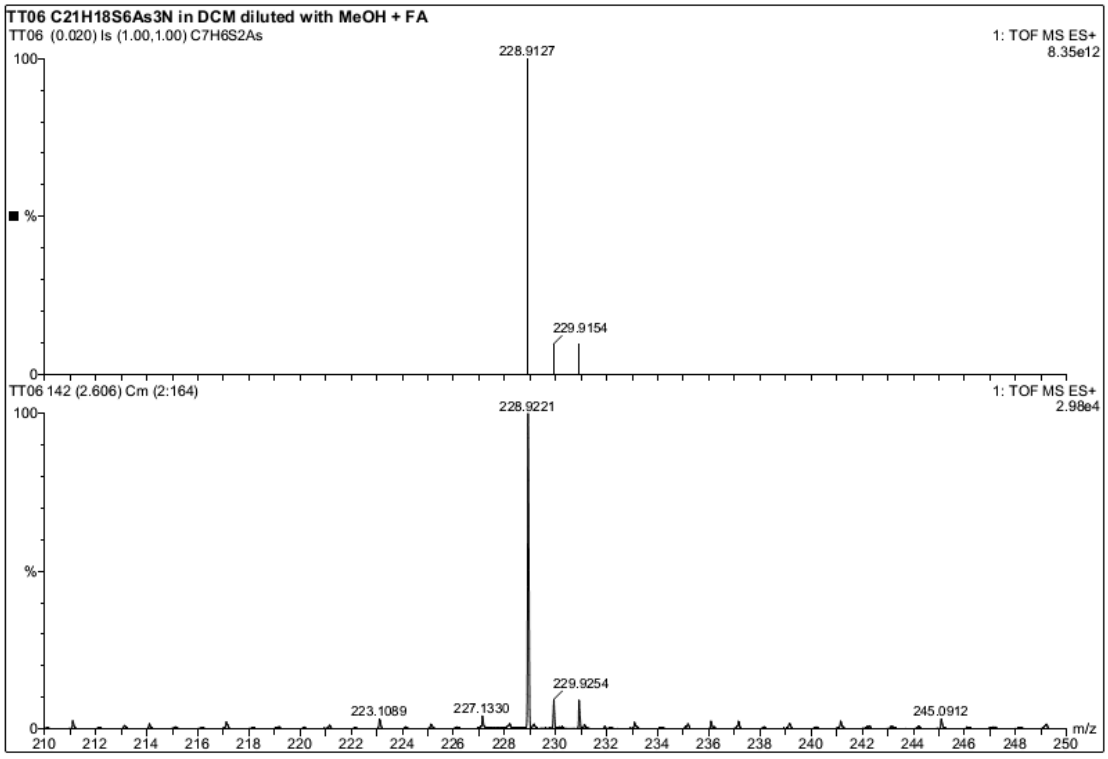

Figure 5.7. A comparison of the simulated spectrum (upper panel) to the observed spectrum (lower panel) of $N(C_7H_6S_2As)_3$, reflecting fragmentation to form $C_7H_6S_2As^+$.

5.2.1.4 Theoretical calculations

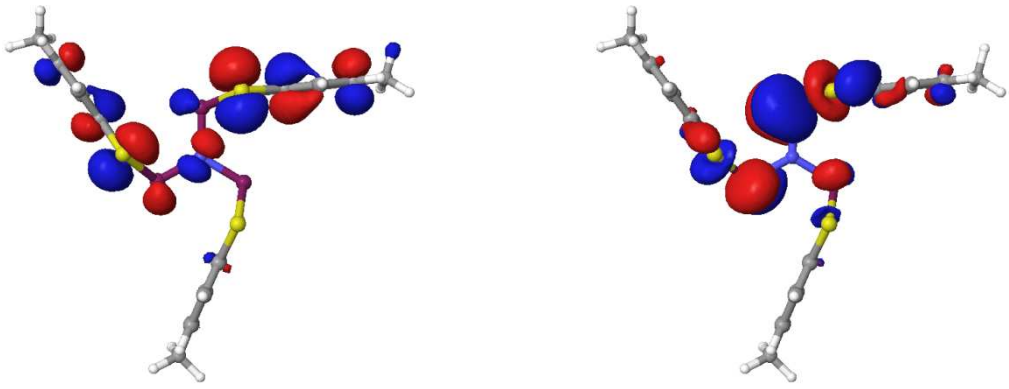

E = -5.950 eV E = -1.318 eV

Figure 5.8. (Left) Highest occupied molecular orbital (HOMO) and (right) Lowest unoccupied molecular orbital (LUMO) orbitals of N[**2**]$_3$ from DFT/B3LYP/6-311G*+ calculations.

Geometry-optimised DFT calculations were undertaken on the P-based system using the B3LYP functional and 6-311G*+ basis set.[18] An Natural Bond Orbital (NBO) analysis was employed to identify the frontier orbitals, partial charges, and hybridization on the structure.[19] The frontier orbitals of N[**2**]$_3$ are illustrated in Figure 5.8. It is clear that the HOMO is not associated with the non-bonding N lone pair but rather a linear combination of π MOs on two of the three heterocycles with a small contribution from the bridging N atom. Conversely the LUMO would appear to arise from a non-bonding combination of orbitals based on the NP_3 unit (with some additional delocalisation to the heterocyclic σ-framework). It is noteworthy in this context that the near orthogonal orientation of the heterocyclic ring to the NP_3 plane should permit π-donation of the N lone pair into the P-S σ* orbitals which should lead to P-S bond lengthening. While this is clearly evident in N[**2**]$_3$, similar arguments can be applied to [**2**]Cl, [**2**]Br and [**2**]I but the effects are less evident in these cases. In this context it is noteworthy that the methoxy derivative [**5**]OMe (Chapter 3) is arranged to maximise such π-type interactions between the *exo*-methoxy group and the heterocycle. Indeed a comparison of the P-N bonds in [**5**]Cl with [**5**]OMe and [**5**]$_2$O reveal marked lengthening on replacement of Cl by the

stronger π-donor O. However NBO studies is ambiguous about the degree of π-delocalisation to the heterocycle from the exo P-X group

An NBO analysis reveals that the N atom in N[**2**]$_3$ undergoes sp^2 hybridization an is involved in σ-bonding with three neighbouring P atoms, and possesses a N lone pair of *p*-character (Table 5.4).The partial charges on N and P atoms in N[**2**]$_3$ are -1.50420 and (+0.75881, +0.75881, +0.75881), suggesting a strongly polarised bonding model.

Structurally the geometry of N[**2**]$_3$ and N[**9**]$_3$ appear similar but the mass spectroscopy indicates weaker As-N bonding. In order to probe the bonding in N[**9**]$_3$ geometry-optimised DFT/B3LYP/LACV3P*+[20] calculations were undertaken, coupled with a subsequent NBO analysis.[19] Despite the similarities in structure there are subtle differences in the bonding patterns evident in the two systems. The frontier orbitals of N[**9**]$_3$ are illustrated in Figure 5.9 and are similar to those of N[**2**]$_3$ with the HOMO still localized on the heterocyclic rings and the LUMO reflecting non-bonding π-character based on the As_3N core.

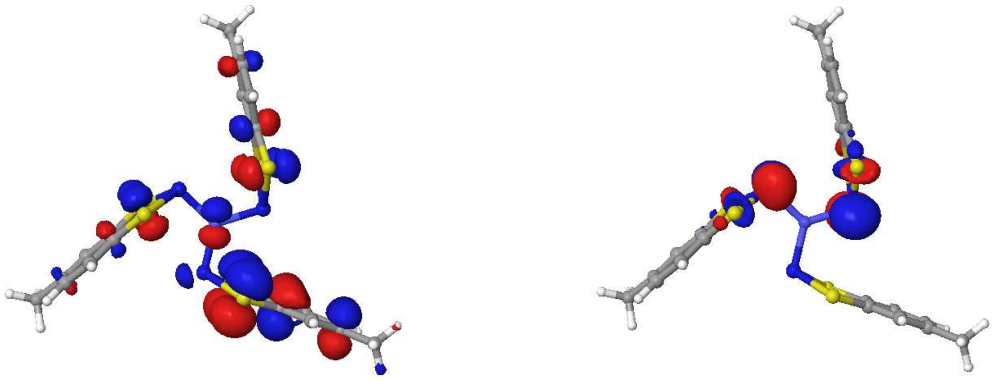

E = -5.904 eV E = -1.794 eV

Figure 5.9. (Left) Highest occupied molecular orbital (HOMO) and (right) Lowest unoccupied molecular orbital (LUMO) orbitals of N[**9**]$_3$ from DFT/B3LYP/LACV3P*+ calculations.

Despite such similarities in the frontier orbitals the NBO analysis provided an entirely different interpretation of the bonding for N[**9**]$_3$ with a complete absence of covalent N-

As bonds. The best Lewis structure of N[**9**]$_3$ might be described as three [$C_7H_6S_2As$] cations around a central [N] anion with four lone pairs located on one *s* and three *p* orbitals (Table 5.4). The partial charge on the N atom and the three As atoms are -1.62847 and (+0.95823, +0.95711, +0.95868), respectively, suggesting that the arsenic derivative might be considered more ionic in nature, *viz.* [$C_7H_6S_2As^+$]$_3$[N^{3-}].

Table 5.4. Natural Bond Orbital Analysis of bond orbitals in the heterocycles of N[**2**]$_3$ and N[**9**]$_3$.

	Bond orbital	**Coefficients / Hybrids**
[a]N[**2**]$_3$	LP (1) N3	s(0.00%) p 1.00(100.00%) d 0.00(0.00%)
	BD (1) P2-N3	(23.27%) 0.4823*P2 s(11.58%) p7.51(87.00%) d 0.12(1.42%) (76.73%) 0.8760*N3 s(33.31%) p 2.00(66.63%) d 0.00(0.06%)
[b]N[**2**]$_3$	LP (1) N3	s(0.00% p 1.00(100.00%) d 0.00(0.00%)
	BD (1) P2-N3	(23.27%) 0.4823* P2 s(11.58%) p 7.51(87.00%) d 0.12(1.42%) (76.73%) 0.8760*N3 s(33.31%) p 2.00(66.63%) d 0.00(0.06%)
[b]N[**9**]$_3$	LP (1) N1	s(0.00%) p 1.00(100.00%) d 0.00(0.00%)
	LP (2) N1	s(99.95%) p 0.00(0.01%) d0.00(0.05%)
	LP(3) N1	s(0.00%) p 1.00(99.97%) d 0.00(0.03%)
	LP (4) N1	s(0.00%) p 1.00(99.97%) d 0.00(0.03%)

[a]B3LYP-6-311G*+[19]; [b]B3LYP-LACV3P*+[20];LP: 1-center valence lone pair, BD: 2-center bond.

The deficiency in such an ionic perspective is reflected in the second order perturbation theory analysis within the NBO basis (Table 5.5) which indicates many significant interactions between the central N-anion and the As-containing cations (*ca.* 75-220 kcal/mol). The **9**$^+$ cations are amphoteric and therefore can act as Lewis acids and the most significant second order perturbations can be considered as lone pair donation from N1 to vacant orbitals on each As centre. This more extreme bonding perspective is not entirely unreasonable given the more electropositive nature of As over P giving rise to more polar As-N bonding *vs* P-N bonding.

Table 5.5. Summary of second-order perturbation theory analysis of the Fock matrix in NBO basis for N[**9**]$_3$.

Donor (L) NBO	Acceptor (NL) NBO	E(2) kcal/mol	E(NL)-E(L) a.u.	F(L,NL) a.u.
54. LP (2) N1	132. LV (2) As2	86.33	0.68	0.216
55. LP (3) N1	132. LV (2)As2	184.18	0.24	0.189
54. LP (2) N1	133. LV (2)As18	86.65	0.68	0.216
56. LP (4) N1	133. LV (2)As18	218.56	0.24	0.206
54. LP (2) N1	134. LV (2)As34	86.50	0.68	0.216
55. LP (3) N1	134. LV (2)As34	146.32	0.24	0.169
56. LP (4) N1	134. LV (2)As34	75.20	0.24	0.121

E(2): means energy of hyperconjugation interaction; L: Lewis; NL: non-Lewis
E(NL)-E(L): Energy difference between donor (L) and acceptor (NL) NBO orbitals
F(L,NL): the Fock matrix element between L and NL NBO orbitals
LP: 1-center valence lone pair; LV: unfilled valence nonbonding orbital of "lone vacancy"

5.2.2 Bifunctional diazaphosphole systems

5.2.2.1 Synthesis of bis-triamide compounds

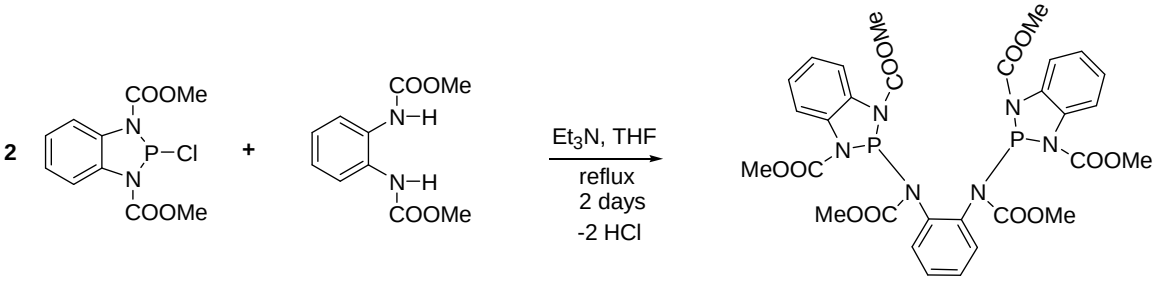

Scheme 5.2. Synthetic procedure for bis-triamide C_6H_4(N(COOMe)[**5**])$_2$

The initial formation of C_6H_4[NMe[**7**])$_2$ during attempted reduction of [**7**]Cl in Na/Toluene (Chapter 3) prompted us to examine the systematic synthesis of this compound.

Bis-triamide C_6H_4(N(COOMe)[**5**])$_2$ was readily accessed through the condensation reaction between *N*,*N′*-dimethylcarbamato-benzodiamine and [**5**]Cl in the presence of a

base such as Et_3N. The progress of this reaction was monitored by $^{31}P\{^1H\}$ NMR spectroscopy (Figure 5.10) due to the different chemical shifts of the starting material (δ_P 122.7 ppm) and product (δ_P 93.6 ppm). An intermediate appears at 79.7 ppm which can tentatively be assigned to [**5**]-$N(COOMe)C_6H_4N(COOMe)H$ in which just one of the two reactive NH groups has undergone condensation.

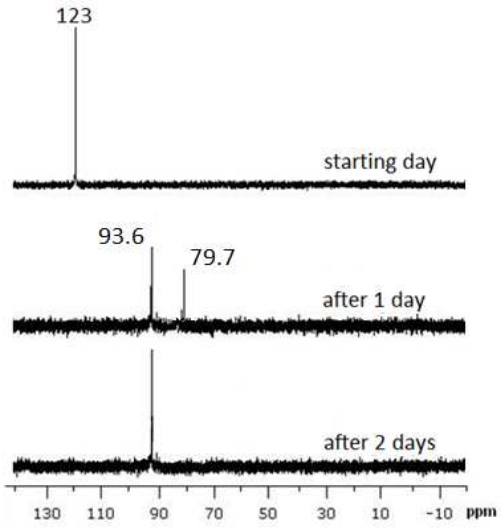

Figure 5.10. $^{31}P\{^1H\}$ NMR of the condensation process between $C_6H_4(NHCOOMe)_2$ and $C_6H_4(NCOOMe)_2PCl$.

Using this methodology $C_6H_4(N(COOMe)[\mathbf{5}])_2$ could be isolated in 70% yield. However attempts to prepare this compound in a one-pot process from the parent amine and PCl_3 in a 3:2 ratio (Scheme 5.3) proved unsuccessful. After 1-2 days the reaction yielded a mixture of unknown products: δ_P 78.8 (major), 82.9 and 92.8 (minor). To date attempts to separate these products have proved unsuccessful.

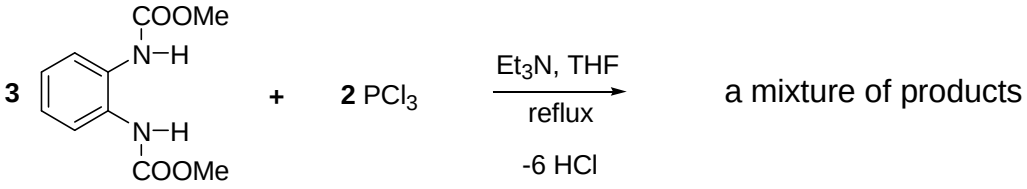

Scheme 5.3. An attempt to synthesize bis-triamide $C_6H_4(N(COOMe)[\mathbf{5}])_2$ *via* a one-step reaction.

5.2.2.2 Spectroscopic studies of bis-triamide compounds

a. Infrared (IR) spectra

An assessment of the IR spectra of bis-triamide $C_6H_4(N(COOMe)[\mathbf{5}])_2$ with the corresponding *N,N′*-dimethylcarbamato-benzodiamine indicates a notable structural change upon condensation, particularly the absence of the N-H stretching band (3312 $cm^{-1}$of $C_6H_4(NHCOOMe)_2$) in the IR spectrum of $C_6H_4(N(COOMe)[\mathbf{5}])_2$ provides direct evidence for the elimination of HCl between N-H and P-Cl bonds.

b. Nuclear Magnetic Resonance (NMR) spectra

Multinuclear NMR spectroscopy (^1H and ^{31}P) were employed to examine the structure of this derivative.

^{1}H NMR (in $CDCl_3$)

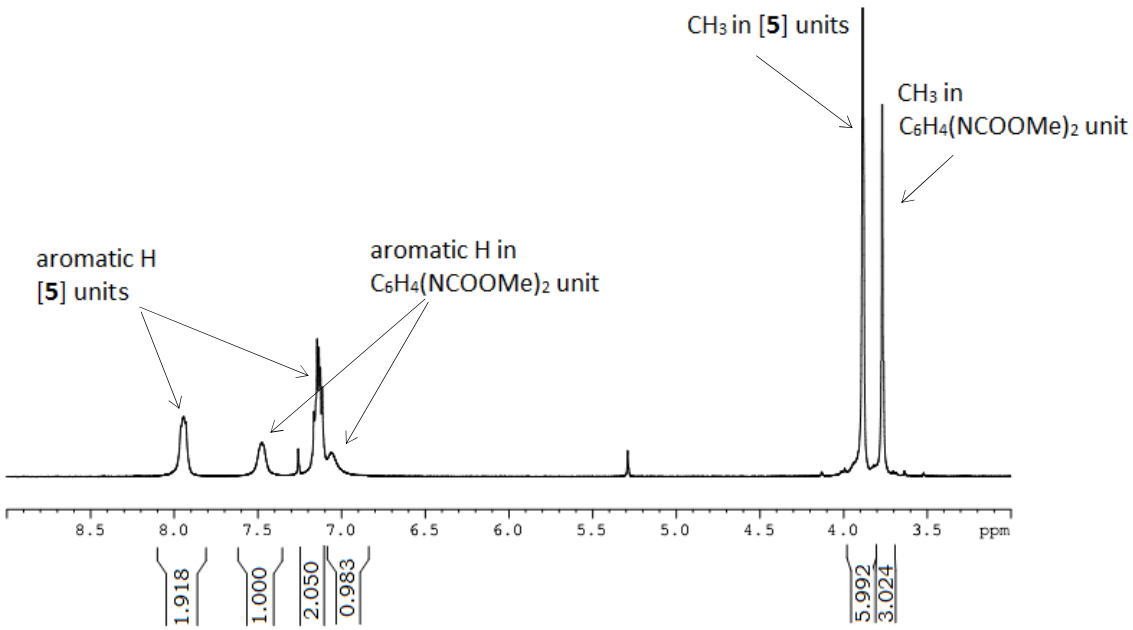

Figure 5.11. ^{1}H NMR of $C_6H_4(N(COOMe)[\mathbf{5}])_2$.

Two regions of aromatic protons in [**5**] and $C_6H_4(NCOOMe)_2$ units of the bis-triamide product exhibit distinguishable multiplets at δ_H 7.93-7.94 (4H, C_6H_4 ring in [**5**]) and 7.49-

7.51 (2H, C_6H_4 ring in $C_6H_4(NCOOMe)_2$). However, the other aromatic protons are partly overlapping around 7.12-7.17 (m, 4H, ring C_6H_4 in [**5**] units) and 7.06-7.09 (m, 2H, ring C_6H_4 in $C_6H_4(NCOOMe)_2$ unit). The methyl groups in both units are well resolved at 3.89 (s, 12H, $COOCH_3$ in [**5**] units) and 3.78 (s, 6H, $COOCH_3$ in $C_6H_4(NCOOMe)_2$ unit), respectively. The ratio of integrations is roughly (2:1:2:1:6:3), reflecting the relative ratio among the numbers of protons of all equivalent proton regions in the expected product (Figure 5.11).

^{31}P NMR

^{31}P NMR is one of the most effective tools to monitor the completion of the condensation reaction (see Figure 5.10) as well as to confirm the purity of the product because of a difference between δ_P values of P-Cl starting material and the product. $C_6H_4(NCOOMe)_2PCl$ and $C_6H_4(N(COOMe)[\mathbf{5}])_2$ display one singlet at δ_P 122.7 and 93.6 ppm, respectively, in both ^{31}P ^{1}H-coupled and decoupled spectra.

5.3 Conclusions

These studies reveal that it is possible to construct more complex architectures bearing dithiaphosphole, dithiaarsole and diazophosphole functional groups through simple salt elimination or condensation reactions. Several examples of such multifunctional structures have been characterised including those with two or three heterocylic $C_7H_6S_2Pn$ and $C_6H_4(NR)_2P$ systems.

DFT studies reveal the lone pair on N atom of the paddle-wheel compounds, $N(C_7H_6S_2P)_3$, is of *p*-character. While $N[\mathbf{2}]_3$ appears to be predominantly covalent, NBO analysis suggests more strongly polar bonding in $N[\mathbf{9}]_3$. While electrospray TOF-MS provides evidence for protonation (Pn = P) it does not discriminate between protonation at the N lone pair or elsewhere on the heterocyclic framework. Notably the As-based complexes seem less chemically stable and the heavier Sb derivatives could not be isolated.

5.4 Experimental

5.4.1 Preparation of $C_7H_6S_2PN(SiMe_3)_2$

A solution of *P*-chloro-5-methyl-1,3,2-benzodithiaphosphole [**2**]Cl (2.000 g; 9.06 mmol) in toluene (15 mL) was added dropwise to a cooled solution of $LiN(SiMe_3)_2$ (1.517 g; 9.06 mmol) in toluene (15 mL) at 0 ^oC in an ice bath under N_2. The mixture was then warmed up to RT and stirred at RT overnight. LiCl was filtered off. The solvent was removed from the filtrate *in vacuo* to afford a colorless oily product. Yield: 2.901g (93%).

^{1}H NMR (300 MHz, $CDCl_3$) δ_H 7.36 (d, $^3J_{HH}$ = 8.1 Hz, 1H, aromatic CH), 7.30 (s, 1H, aromatic CH), 6.94 (d, $^3J_{HH}$ = 8.1 Hz, 1H, aromatic CH), 2.34 (s, 3H,CH_3), 0.20 (d, $^2J_{SiH}$ = 3.3 Hz, 18H, $(SiMe_3)_2$).

^{13}C NMR (75.5 MHz, $CDCl_3$) δ_C 141.22, 137.74, 135.14, 126.33, 124.83 (d, $^2J_{PC}$ = 8.30 Hz, aromatic SC), 124.03 (d, $^2J_{PC}$ = 8.23 Hz, aromatic SC), 20.98, 4.26 (d, $^1J_{SiC}$ = 9.66 Hz, $(SiMe_3)_2$).

^{31}P NMR (202.5 MHz, $CDCl_3$) δ_P 94.37 (s).

5.4.2 Preparation of $N(C_7H_6S_2P)_3$

A solution of $C_7H_6S_2PN(SiMe_3)_2$ (0.300g; 0.87 mmol) in MeCN (10 mL) was added dropwise to a solution of $C_7H_6S_2PCl$ (0.383g; 1.74 mmol) in MeCN (10 mL) at 0 ^oC under N_2. The mixture was then warmed up to RT and heated at reflux overnight. The reaction mixture was cooled to RT and placed in ice bath for 3h to give white precipitate. MeCN was decanted. The white precipitate was washed with dry MeCN (2×10 mL). Yield: 0.431g (87%). Needle crystals were obtained by re-dissolving the white powder in a small quantity of CH_2Cl_2, and storing the solution at -20 ^oC.

^{1}H NMR (300 MHz, $CDCl_3$): δ_H7.42 (d, $^3J_{HH}$ = 8.1 Hz, 1H, aromatic CH), 7.37 (s, 1H, aromatic CH), 6.99 (d, $^3J_{HH}$ = 8.1 Hz, 1H, aromatic CH), 2.34 (s, 3H, CH_3).

^{13}C NMR (75.5 MHz, CD_2Cl_2): δ_C 139.96, 136.84, 136.33, 127.55, 125.33, 124.50, 21.00.

^{31}P NMR (202.5 MHz, C_6D_6): δ_P 86.75 (s).

Found ($C_{21}H_{18}NP_3S_6$ requires): C = 43.94% (44.27); H = 3.00% (3.18); N = 2.73% (2.46).

TOF MS ES+ (*m/z*):$[M+H]^+$ ion 569.9055 (theoretical value: 569.69)

Melting point: 154-155 ^oC.

5.4.3 Preparation of $C_7H_6S_2AsN(SiMe_3)_2$

A solution of *As*-chloro-5-methyl-1,3,2-benzodithiarsole (1.000 g; 3.78 mmol) in toluene (7 mL) was added dropwise to a cooled solution of $LiN(SiMe_3)_2$ (0.632 g; 3.78 mmol) in toluene (8 mL) at 0 ^oC in an ice bath under N_2. The mixture was then warmed up to RT and stirred at RT overnight. LiCl was filtered off. Solvent was removed from the filtrate *in vacuo* to give yellow oily product. Yield: 1.245 g (85%).

^{1}H NMR (500 MHz, $CDCl_3$) δ_H 7.32 (d, $^3J_{HH}$ = 8.1 Hz, 1H, aromatic CH), 7.27 (s, 1H, aromatic CH), 6.90 (d, $^3J_{HH}$ = 8.1 Hz,1H, aromatic CH), 2.34 (s, 3H,CH_3), 0.22 (s, 18H, $(SiMe_3)_2$).

5.4.4 Preparation of $N(C_7H_6S_2As)_3$

A solution of $C_7H_6S_2AsN(SiMe_3)_2$ (0.350 g; 0.90 mmol) in MeCN (10 mL) was added dropwise to a solution of $C_7H_6S_2AsCl$ (0.476 g; 1.80 mmol) in MeCN (10 mL) at 0 ^oC under N_2. The mixture was then warmed up to RT and heated at reflux overnight (80 ^oC). The reaction mixture was cooled to RT and placed in ice bath for 3h to give pale yellow precipitate. MeCN was decanted. The precipitate was washed with dry MeCN (2×10 mL). Yield: 0.607 g (96%). Crystals were obtained by re-dissolving the precipitate in CH_2Cl_2, and cooled at -20 ^oC.

^{1}H NMR (300 MHz, CD_2Cl_2) δ_H 7.35 (d, $^{3}J_{HH}$ = 8.1 Hz, 1H, aromatic CH), 7.30 (s, 1H, aromatic CH), 6.95 (d, $^{3}J_{HH}$ = 8.1 Hz, 1H, aromatic CH), 2.32 (s, 3H, CH_3).

^{13}C NMR (75.5 MHz, $CDCl_3$) δ_C 140.66, 137.12, 135.91, 126.92, 126.71, 125.98, 20.89.

Found ($C_{21}H_{18}NAs_3S_6$ requires): C = 34.93% (35.95); H = 2.43% (2.59); N = 1.91% (2.00).

TOF MS ES+ (*m/z*): 228.9221 ($C_7H_6S_2As$) (theoretical value: 229.17)

Melting point: 79-80 ^{o}C.

5.4.5 Preparation of bis-triamide compound $C_6H_4(N(COOMe)[5])_2$

A solution of $C_6H_4(NHCOOMe)_2$ (0.117 g, 0.52 mmol) and Et_3N (0.30 mL, 2.2 mmol) in THF (15 mL) was added dropwise to a solution of $C_6H_4(NCOOMe)_2PCl$ (0.300 g, 1.04 mmol) in THF (5 mL). The white cloudy mixture was stirred at reflux for 1-2 days. The reaction was monitored by $^{31}P\{^{1}H\}$ NMR and reaction continued until one singlet at *ca.* 93 ppm was observed. The resultant suspension was filtered and the solvent evaporated from the filtrate under vacuum to afford a white solid. Yield: 0.265 g (70%). Recrystallization of product was carried out through slow evaparation of a concentrated CH_2Cl_2 solution to give colourless crystals.

^{1}H NMR (300 MHz, $CDCl_3$) δ_H 7.93-7.94 (m, 4H, ring C_6H_4 in $[C_6H_4(NCOOMe)_2P]$ units), 7.49-7.51 (m, 2H, ring C_6H_4 in $C_6H_4(NCOOMe)_2$ unit), 7.12-7.17 (m, 4H, ring C_6H_4 in $[C_6H_4(NCOOMe)_2P]$), 7.06-7.09 (m, 2H, ring C_6H_4 in $C_6H_4(NCOOMe)_2$), 3.89 (s, 12H, $COOCH_3$ in $[C_6H_4(NCOOMe)_2P]$), 3.78 (s, 6H, $COOCH_3$ in $C_6H_4(NCOOMe)_2$).

^{13}C NMR (75.5 MHz, $CDCl_3$) δ_C 152.72 (d, $^{2}J_{PC}$= 16.3 Hz, PN<u>C</u>O), 131.45 (d, $^{2}J_{PC}$ = 8.7 Hz, heterocyclic PN<u>C</u>), 123.87(s, aromatic), 116.24 (s, aromatic), 53.86 (s, CH_3).

^{31}P{^{1}H} NMR (121.5 MHz, $CDCl_3$) δ_P 93.62 (s).

IR ν_{max} (cm^{-1}): 2956 (w), 1725 (m), 1697 (m), 1484 (m), 1437 (m), 1357 (m), 1301 (m), 1289 (m), 1234 (m), 1205 (m), 1089 (m), 1059 (m), 1001 (m), 783 (m), 769 (m), 757 (m), 636 (m), 488 (m).

Found ($C_{30}H_{30}N_6O_{12}P_2$ requires): C = 49.73% (49.46); H = 4.39% (4.15); N = 12.09% (11.54).

Melting point: 139-140 ^{o}C.

5.5 References

1. Konieczny, M.; Sosnovsky, G., *Chem. Rev.* **1981**, *81* (1), 49-77.

2. (a) Goward, G. R.; Leroux, F.; Nazar, L. F., *Electrochim. Acta* **1998**, *43* (10–11), 1307-1313; (b) He, L.-Y.; Urrego-Riveros, S.; Gates, P. J.; Näther, C.; Brinkmann, M.; Abetz, V.; Staubitz, A., *Tetrahedron* **2015**, *71* (33), 5399-5406; (c) Hu, S.; Ma, L.; Wang, H.; Zhang, L.; Zhao, Y.; Wu, G., *RSC Adv.* **2015**, *5* (40), 31947-31953; (d) Orchard, B. J.; Freidenreich, B.; Tripathy, S. K., *Polymer* **1986**, *27* (10), 1533-1541; (e) Oriakhi, C. O.; Lerner, M. M., *Mater. Res. Bull.* **1995**, *30* (6), 723-729.

3. (a) Mukherjee, S.; Thilagar, P., *J. Mater. Chem. C* **2015**; (b) Shaikh, A. C.; Ranade, D. S.; Thorat, S.; Maity, A.; Kulkarni, P. P.; Gonnade, R. G.; Munshi, P.; Patil, N. T., *Chem. Commun.* **2015**; (c) Tanaka, K.; Chujo, Y., *Macromol. Rapid Commun.* **2012**, *33* (15), 1235-1255.

4. Gupta, N., Recent Advances in the Chemistry of Diazaphospholes. In *Phosphorus Heterocycles II*, Bansal, R. K., Ed. Springer Berlin Heidelberg: 2010; Vol. 21, pp 175-206.

5. (a) Balakrishna, M. S.; Reddy, V. S.; Krishnamurthy, S. S.; Nixon, J. F.; Laurent, J. C. T. R. B. S., *Coord. Chem. Rev.* **1994**, *129* (1–2), 1-90; (b) Balakrishna, M. S.; Panda, R.; Mague, J. T., *Inorg. Chem.* **2001**, *40* (22), 5620-5625; (c) Chandrasekaran, P.; Mague, J. T.; Balakrishna, M. S., *Inorg. Chem.* **2005**, *44*

(22), 7925-7932; (d) Chandrasekaran, P.; Mague, J. T.; Balakrishna, M. S., *Inorg. Chem.* **2006**, *45* (17), 6678-6683; (e) Ly, T. Q.; Woollins, J. D., *Coord. Chem. Rev.* **1998**, *176* (1), 451-481; (f) Mandal, S. K.; Venkatakrishnan, T. S.; Sarkar, A.; Krishnamurthy, S. S., *J. Organomet. Chem.* **2006**, *691* (13), 2969-2977; (g) Chandrasekaran, P.; Mague, J. T.; Balakrishna, M. S., *Organometallics* **2005**, *24* (15), 3780-3783.

6. Biricik, N.; Kayan, C.; Gümgüm, B., *Helv. Chim. Acta.* **2014**, *97* (8), 1158-1164.

7. (a) Sun, Z.; Zhu, F.; Wu, Q.; Lin, S.-a., *Appl. Organomet. Chem.* **2006**, *20* (3), 175-180; (b) Leadbeater, N. E.; Marco, M., *Chem. Rev.* **2002**, *102* (10), 3217-3274.

8. (a) Biricik, N.; Meric, N.; Kayan, C.; Ozgen, Z.; Ekerazizoglu, S.; Gumgum, B., *Turk. J. Chem.* **2015**, 1-8; (b) Biricik, N.; Durap, F.; Kayan, C.; Gümgüm, B.; Gürbüz, N.; Özdemir, İ.; Ang, W. H.; Fei, Z.; Scopelliti, R., *J. Organomet. Chem.* **2008**, *693* (16), 2693-2699; (c) Biricik, N.; Kayan, C.; Gümgüm, B.; Fei, Z.; Scopelliti, R.; Dyson, P. J.; Gürbüz, N.; Özdemir, İ., *Inorg. Chim. Acta* **2010**, *363* (5), 1039-1047.

9. Priya, S.; Balakrishna, M. S.; Mague, J. T., *Inorg. Chem. Commun.* **2001**, *4* (8), 437-440.

10. (a) Priya, S.; Balakrishna, M. S.; Mague, J. T.; Mobin, S. M., *Inorg. Chem.* **2003**, *42* (4), 1272-1281; (b) Priya, S.; Balakrishna, M. S.; Mobin, S. M., *Polyhedron* **2005**, *24* (13), 1641-1650; (c) Chandrasekaran, P.; Mague, J. T.; Balakrishna, M. S., *Tetrahedron Lett.* **2007**, *48* (30), 5227-5229.

11. Kafarski, P.; Mastalerz, P., *Beitr. Wirkstofforsch.* **1984**, (21), 1-12.

12. Hopkins, A. D.; Wood, J. A.; Wright, D. S., *Coord. Chem. Rev.* **2001**, *216–217*, 155-172.

13. Allen, F. H.; Kennard, O.; Watson, D. G.; Brammer, L.; Orpen, A. G.; Taylor, R., *J. Chem. Soc., Perkin Trans. 2* **1987**, (12), S1-S19.

14. Vodak, D. T.; Kim, K.; Iordanidis, L.; Rasmussen, P. G.; Matzger, A. J.; Yaghi, O. M., *Chem. Eur. J.* **2003**, *9* (17), 4197-4201.

15. Gilheany, D. G., *Chem. Rev.* **1994**, *94* (5), 1339-1374.

16. Samuel, R. C.; Kashyap, R. P.; Krawiec, M.; Watson, W. H.; Neilson, R. H., *Inorg. Chem.* **2002**, *41* (26), 7113-7124.

17. Cottrell, T. L., *The Strengths of Chemical Bonds (Butterworths Scientific Publications)*. 2nd ed.; Academic Press/Butterworths: London, **1958**.

18. Gudat, D.; Haghverdi, A.; Hupfer, H.; Nieger, M., *Chem. Eur. J.* **2000**, *6* (18), 3414-3425.

19. Reed, A. E.; Weinstock, R. B.; Weinhold, F., *J. Chem. Phys.* **1985**, *83* (2), 735-746.

20. Medeleanu, M.; Mracec, M.; Pop, O. R.; Mocanu, L.; Mracec, M., *Rev. Roum. Chim.* **2014**, *59* (11-12), 1077-1087.

CHAPTER 6

CATIONIC POLYMERIZATION OF CYCLIC ETHERS BY PHOSPHENIUM CATIONS AND THEIR ANALOGUES

6.1 Introduction

6.1.1 Cationic ring-opening polymerization (CROP) of cyclic ethers

The ring-opening polymerization (ROP) of cyclic ethers has been extensively investigated in the literature.[1] Polyethers derived from the polymerization of cyclic ethers are of particular interest in polymer chemistry because their main chains possess high level of polarisability and flexibility. They play important roles as key additives in producing thermoplastic elastomers, such as polyesters (Hytrel ®) and polyurethanes (Spandex).[1a,1h,1k,2]

Mechanisms of ROP are varied and include cationic ring opening polymerisation (CROP), anionic ring opening polymerisation (AROP), ring-opening metathesis polymerisation (ROMP) and (free) radical ring opening polymerisation (RROP).[1b,1e,1h-m,1o,3] Amongst common cationic initiators Bronsted acids are common,[1a,1c] although carbenium cations, R_3C^+,[3d,4] and onium ions, R_3O^+,[5] are also known to act as cationic polymerisation catalysts. Particularly relevant to these studies is the use of Lewis acids as ring opening polymerisation catalysts.[1c,d,1g,1j,1n] In this regard PF_4^+ (generated from PF_5)[1f] has been studied in detail and other strongly cationic *p*-block centres are known to catalyze such CROP processes including 1,3,2,4-dithiadiazolium cations with a large partial positive charge at sulfur[6] and $TeBr_4$ in the presence of Ph_3P.[7] Similar Lewis acid-base pairs such as $R_2PH/B(C_6F_5)_3$ have also been shown to polymerise THF.[8] Studies on the reactivity of Lewis acidic phosphenium cations have recently been reviewed and revealed electron acceptor character of the P^{III} centre,[9] as observed elsewhere in this thesis.

6.1.2 Project aims

To the best of my knowledge there have been no reports of phosphenium cations and their analogues as catalysts for CROP reactions. In this work the CROP of cyclic ethers (THF, dioxane, propylene oxide) was explored using a range of phosphenium cations as Lewis acid catalysts and monitored by ^{1}H NMR spectroscopy with the calculated percentages of polymer conversion based on integration of the distinctive protons in the ^{1}H NMR spectra. The catalytic properties of the following cations were examined in these studies:

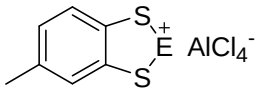

[**2**][$AlCl_4$] (E = P)

[**9**][$AlCl_4$] (E = As)

[**10**][$AlCl_4$] (E = Sb)

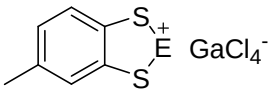

[**2**][$GaCl_4$] (E = P)

[**9**][$GaCl_4$] (E = As)

[**10**][$GaCl_4$] (E = Sb)

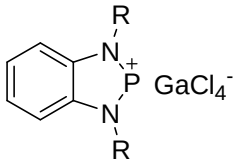

[**4**][$GaCl_4$] (R = H)

[**7**][$GaCl_4$] (R = Me)

6.2 Results and Discussion

6.2.1 Cationic Ring Opening Polymerisation (CROP) of THF

6.2.1.1 CROP of THF using [2][$GaCl_4$]

Initial attempts to crystallise [**2**][$GaCl_4$] from THF at room temperature afforded viscous gels over 1-2 hours, alerting us to the potential for polymerisation of THF in these systems. These led to further studies to probe this reactivity.

a. Polymerisation at room temperature

CROP of THF initiated by [**2**][$GaCl_4$] was studied at room temperature with a ratio of 0.906 mmol of [**2**][$GaCl_4$]: 50 mL (616 mmol) of THF (0.15 mol% catalyst). At room temperature the magnetic stir bar failed to rotate after 1-2 h due to the formation of a viscous solution. ^{1}H NMR spectroscopy proved to be an indispensable and effective method to monitor the CROP of THF due to the distinctive chemical shifts of the α- and

β-methylene protons in THF and poly(THF). In addition the polymer conversion can be determined from the relative integrals of these protons, while an upper limit of the number-average molecular weight (M_n) of poly(THF) can be estimated by ^{1}H NMR end-group analysis.[10]

^{1}H NMR studies reveal the signals of the α- and β-methylene protons of THF shift upfield upon addition of [**2**][$GaCl_4$], indicating the formation of poly(THF): δ_H 1.55-1.61 (2H, m, C$\underline{H_2}$CH_2O) and 3.37-3.39 (2H, m, CH_2C$\underline{H_2}$O) *cf* pure THF 1.81-1.84 (2H, m, C$\underline{H_2}$CH_2O), 3.70-3.73 (2H, m, CH_2C$\underline{H_2}$O) (Figure 6.1, left). Integration of the ^{1}H NMR data revealed *ca*. 9% conversion to poly(THF) after 1 h, increasing to 78% over 24 h.

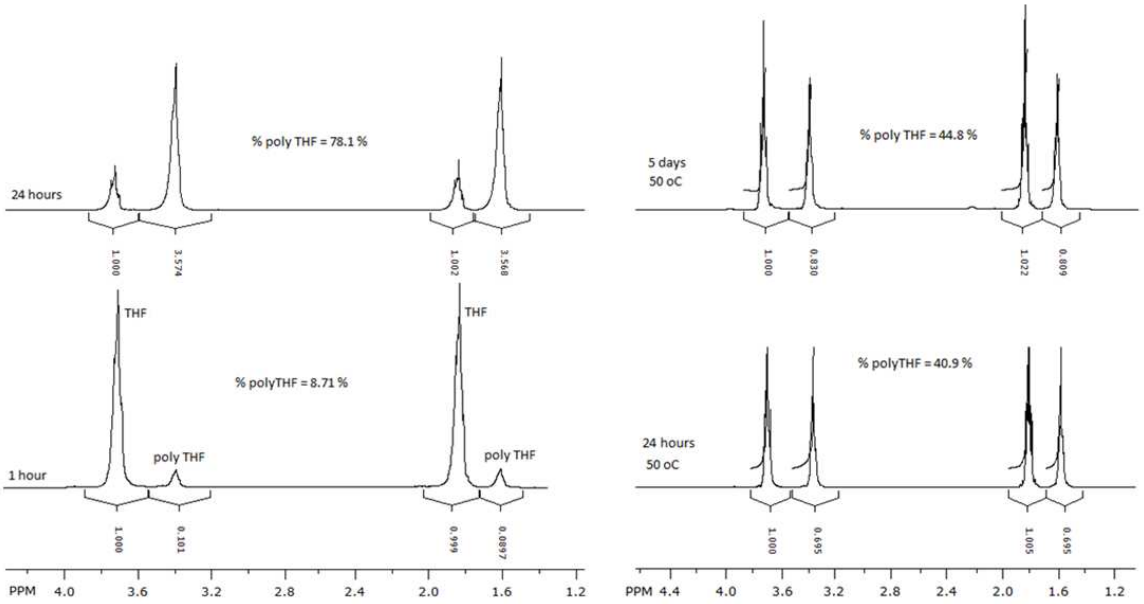

Figure 6.1. ^{1}H NMR of mixture (0.906 mmol of [**2**][$GaCl_4$] : 50 mL of THF) at RT (left) and at 50 ^oC (right).

Notably the $^{31}P\{^1H\}$ NMR spectrum of the reaction between [**2**][$GaCl_4$] and THF also exhibits a new resonance (δ_P 124.4 ppm, singlet) downfield in comparison to "[**2**][$GaCl_4$]" (δ_P 57.2 ppm), indicating a change in geometry/coordination number at the phosphorus centre. A comparison of chemical shifts between [**2**]X and PX_3 (Table 6.1) shows a good correlation (Figure 6.2) dependent upon the nature of X (see Chapter 2), consistent with the additive nature of chemical shift and substituents in structurally

similar compounds in ^{31}P NMR spectroscopy.[11] Based on the chemical shifts presented in Table 6.1, the ^{31}P NMR of [**2**]OR would be expected to appear in the 95 – 150 ppm range consistent with coordination of THF to the ^{31}P centre, most likely in ring-opened form. Indeed the experimental value appears to fit extremely well within the correlation values shown in Figure 6.2.

Table 6.1. Comparison of ^{31}P NMR chemical shifts of PX_3 and [**2**]X compounds.

PX_3	**PCl_3**	**PBr_3**	**PI_3**	**$P(NMe_2)_3$**	**$P(OMe)_3$**
	220[12]	228[12]	178[12]	122[13]	140[13]
[2]X	**[2]Cl**	**[2]Br**	**[2]I**	**[2]N(SiMe$_3$)$_2$**	**[2]OR**
	161.4[a]	163.6 [a]	155.4 [a]	94[b]	124.4*

* The experimental value for [**2**][$GaCl_4$] in THF; [a]from Chapter 2; [b]from Chapter 5.

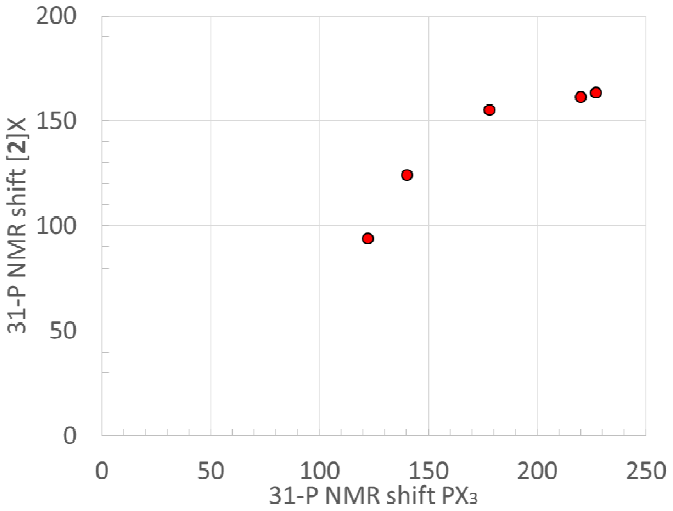

Figure 6.2. Correlation of ^{31}P NMR chemical shifts for PX_3 and [**2**]X compounds.

Control experiments to support the suggestion that the polymerization of THF is catalyzed by coordination to the phosphenium cation, **2**$^+$, were undertaken. Reactions between (a) Lewis-acidic $GaCl_3$ and THF, and (b) [**2**]Cl and THF were studied for 24 h at RT. Spectroscopic studies revealed no signal for poly(THF) in the ^{1}H NMR spectra of either reaction mixture. In addition, there is a singlet around δ_P 161.4 ppm in the ^{31}P{^{1}H} NMR spectrum of the mixture of [**2**]Cl and THF, proving [**2**]Cl (δ_P 161.4 ppm) is inert in

THF. Polymerisation of THF would therefore appear to occur *via* initial coordination of THF to $\mathbf{2}^+$ to form an oxonium ion. (Scheme 6.1).

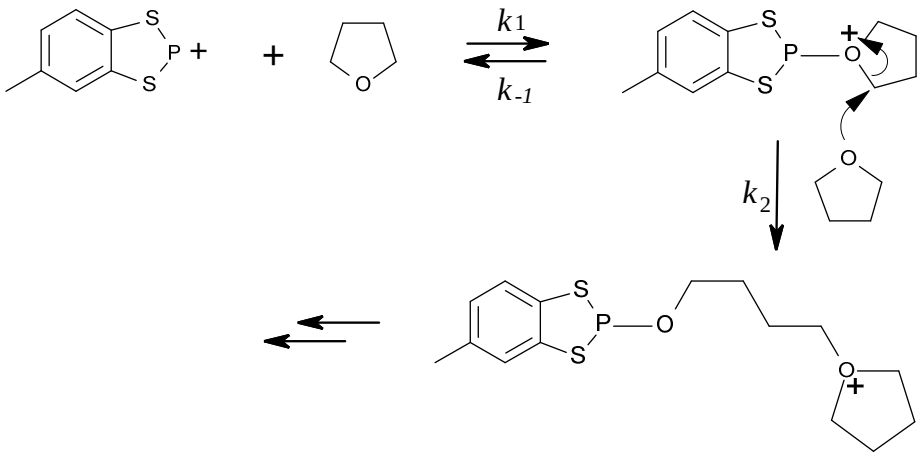

Scheme 6.1. Key steps in the polymerization of THF by $[\mathbf{2}]^+$; coordination of THF to $\mathbf{2}^+$ and chain-growth process *via* S_N2 mechanism.

b. Computational Studies on THF binding to $\mathbf{2}^+$

B3LYP/6-311G*+ geometry optimisations on $\mathbf{2}^+$, THF and the adduct $[\mathbf{2}\cdot\text{THF}]^+$ were made within Jaguar to examine both the energetics of THF binding as well as the effect of THF coordination on the heterocyclic ring and charge distribution. The P-O bond length in the geometry-optimised adduct is 2.19 Å, somewhat longer than a conventional P-O single bond (1.63 Å)[14] but shorter than a van der Waals' contact (3.32 Å). Zero point energy corrected thermodynamic calculations reveal that association is moderately favourable (ΔH_{rxn} = -60 kJ.mol^{-1}) albeit entropically disfavoured (ΔS = - 145 J.K.mol^{-1}). These data are in broad agreement with the qualitative perspectives discussed in the last section. Adduct formation leads to a modest weakening of the P-S bonds (Wiberg bond index decreases from 1.34 in $\mathbf{2}^+$ to 1.28 in $[\mathbf{2}\cdot\text{THF}]^+$) and formation of a weak adduct (Wiberg bond index for P-O = 0.26). Similarly slight weakening of the THF C-O bonds is detected (bond order = 0.92 in free THF, decreasing to 0.80 upon coordination).

Table 6.2. Partial charges, bond lengths and Wiberg bond indices for various pnictogen cation…THF adducts. [Thermodynamic parameters calculated at 298 K].

		$[\mathbf{2}\cdot\mathbf{THF}]^+$	$[\mathbf{9}\cdot\mathbf{THF}]^+$	$[\mathbf{10}\cdot\mathbf{THF}]^+$	$[\mathbf{4}\cdot\mathbf{THF}]^+$	$[\mathbf{7}\cdot\mathbf{THF}]^+$
Partial charge	Pn	+0.64	+0.85	+1.23	+1.29	+1.27
	O	-0.63	-0.66	-0.69	-0.64	-0.64
	$C_{(next\text{-}to\text{-}O)}$	-0.028 -0.025	-0.018 -0.022	-0.020 -0.024	-0.025 -0.025	-0.025 -0.026
Bond length	Pn-O	2.19	2.22	2.30	2.45	2.64
	O-C	1.48	1.48	1.48	1.46	1.46
	ΔH_{rxn}	-59.5	-69.1	-86.0	-44.9	-47.1
	ΔS_{rxn}	-145.1	-145.2	-153.6	-129.0	-91.9
	ΔG_{rxn}	-16.9	-26.4	-40.85	-7.0	-20.1
Wiberg bond index	Pn-O	0.26	0.25	0.23	0.13	0.08
	C-O	0.80	0.82	0.82	0.86	0.88

c. Effect of temperature on CROP of THF by [2][$GaCl_4$]

In contrast to the reaction undertaken at ambient temperature, there was no trace of poly(THF) after 1 h when the same reaction was performed at 50 ^oC. However build-up of poly(THF) occurred over extended periods with *ca*. 41% conversion after 24 h and 45% after 5 days (Figure 6.1, right). This observation seems somewhat counter-intuitive since rate constants are expected to increase with increasing temperature.[15] In addition at elevated temperatures the viscosity of the poly(THF) is decreased which would facilitate faster diffusion times of the THF to the active site. However this is possible in systems where the reverse process becomes more favourable than the forward reaction at elevated temperatures. For example, we would anticipate K_1 (= k_1/k_{-1}) for THF binding to be less favourable at elevated temperatures due to the increase in entropy upon dissociation. Thus when the rate of dissociation of $[\mathbf{2}\cdot THF]^+$ is greater than the rate of ring-opening/propagation, polymeriation is inhibited. Such behaviour is reminiscent of the CROP of α-methyl styrene[16] in which chain-breaking processes have a lower activation energy than the propagation rate. In order to probe this, we examined the effect of catalyst concentration on THF polymerisation.

d. Dependence of polymer conversion on catalyst concentration

The influence of catalyst concentrations on polymer conversion was initially examined at two different concentrations for comparison purposes: 9.06 mM (equivalent to [**2**][$GaCl_4$]:THF = 0.453:616 or 0.074 mol%), and 18.12 mM (equivalent to [**2**][$GaCl_4$]:THF = 0.906:616 or 0.15 mol%). The ^{1}H NMR spectra were recorded over certain periods of time, and polymer conversions determined based on the ^{1}H NMR integration values of different proton groups in THF and poly(THF).

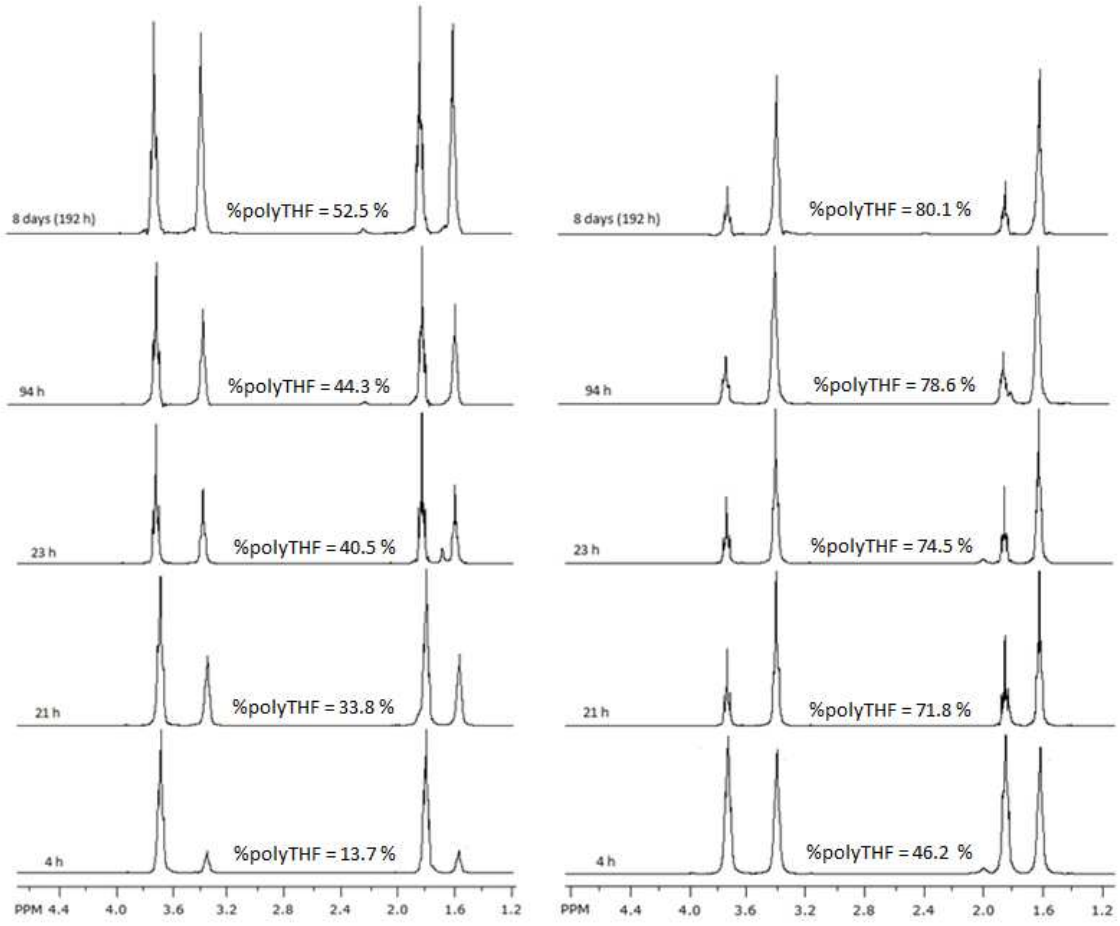

Figure 6.3. ^{1}H NMR spectra of CROP of THF at RT by 9.06 mM (left) and 18.12 mM (right) of [**2**][$GaCl_4$].

As the reaction progressed, the degree of viscosity of the reaction mixture increased, and a gradual increase in conversion of THF into poly(THF) was observed based on the ^{1}H

NMR spectra. Normally, the whole colorless reaction solutions solidified after 1 - 2 days at which point little variation in the THF : poly(THF) ratio was observed consistent with a system where diffusion through the viscous poly(THF) solution becomes extremely slow.

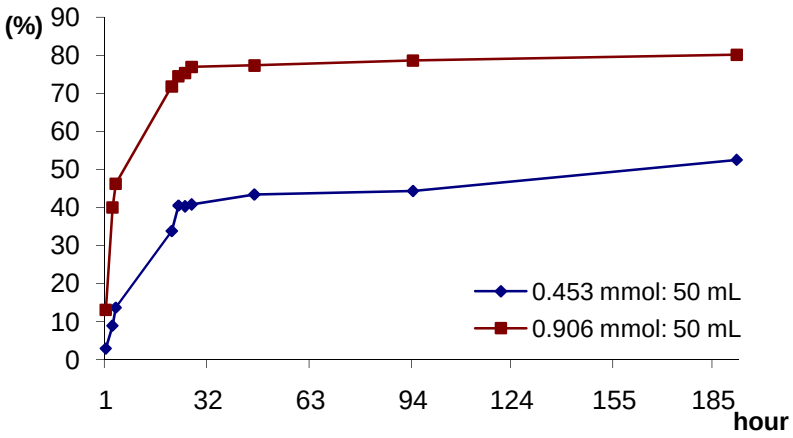

Figure 6.4. Poly(THF) conversion *vs.* time at different concentrations of [**2**][$GaCl_4$].

The polymerization of THF was monitored until the extent of conversion of THF remained constant. After 8 days, [**2**][$GaCl_4$] converts THF into poly(THF) with the yields of 52.5% and 80.1% at 9.06 mM and 18.12 mM, respectively. The increase of poly(THF) at higher concentration of [**2**][$GaCl_4$] can be explained according to the fundamental mechanisms for CROP.[1k] It suggests that one initiator will create an active polymer chain to which a new monomer will attach to the positively charged end of the chain to extend the polymer chain. Thus the number of active sites responsible for initiating polymerization is proportional to the amount of [**2**][$GaCl_4$] catalyst (assuming first order kinetics) and the initial rate would be proportional to the concentration of [**2**][$GaCl_4$]. Therefore, doubling concentration should afford a doubling of the rate which is qualitatively observed. However after the initial reaction onset, the mixture containing more [**2**][$GaCl_4$] will afford more poly(THF) and become viscous quicker leading to a slowing of the kinetics. Comparable results were achieved by Aouissi *et al*. in the CROP of THF using 12-tungstophosphoric acid.[1a]

e. Dependence of polymer conversion on reaction time

The time dependence of the conversion is demonstrated in Figures 6.3 and 6.4. Based on the slope of the conversion curves, it can be concluded that the polymer conversion rate is highest within the first 1-2 hours of the reaction. Thereafter, the rate decreases, attributed to the increasing viscosity of the solution, until the conversion reaches a stable value. On average, the bulk of the polymer is produced during the first 24 hours of the polymerization. The complex nature of the reaction rate which varies as a function of both viscosity and catalyst concentration precluded quantitative studies.

Table 6.3. Dependence of polymer conversion on reaction time at different catalyst concentrations of [**2**][$GaCl_4$].

Time (hours)	Polymer conversion (%) at 9.06 mM	Polymer conversion (%) at 18.12 mM	Rate 1 (9.06 mM)	Rate 2 (18.12 mM)	Ratio of rates
1.5	2.96	13.1	1.97	8.73	4.43
3	8.93	40.0	2.98	13.33	4.48
4	13.7	46.2	3.43	11.55	3.37
21	33.8	71.8	1.61	3.42	2.12
23	40.5	74.5	1.76	3.24	1.84
25	40.3	75.3	1.61	3.01	1.87
27	40.8	76.9	1.51	2.85	1.88
46	43.4	77.3	0.94	1.68	1.78
94	44.3	78.6	0.47	0.84	1.77
192	52.5	80.1	0.27	0.42	1.53

Rate (polymer reaction rate) = %poly(THF)/h; Ratio of rates = Rate 2/Rate 1

f. Dependence of polymer conversion on CH_2Cl_2 solvent

All of the above-mentioned CROP reactions used neat THF as both solvent and reagent. To study the influence of other solvent on the CROP of THF, a CH_2Cl_2 solution of catalyst was employed. Here [**2**][$GaCl_4$] was prepared *in situ* from [**2**]Cl and $GaCl_3$, the solvent was not removed and THF added.

An initial 9.06 mM solution of $[C_7H_6S_2P][GaCl_4]$ at room temperature (*i.e.* ([**2**][$GaCl_4$]: THF : CH_2Cl_2) = (0.453 mmol : 25 mL : 25 mL)) was used. Although the concentration of catalyst is the same with aforementioned case (*i.e.* 0.453 mmol : 50 mL of THF), the THF monomer to catalyst ratio here is reduced by two times. After 1 hour, the colourless CROP reaction is not viscous and there is no trace of poly(THF) by ^{1}H NMR spectroscopy. After five days, there is just *ca.* 17% poly(THF) in the reaction mixture.

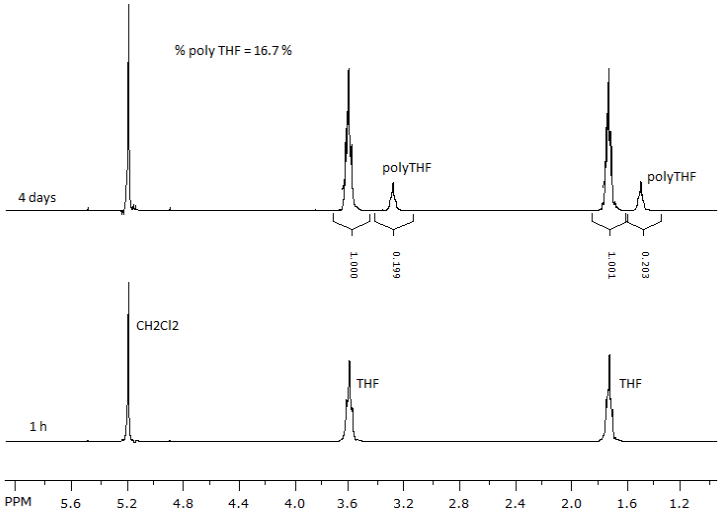

Figure 6.5. ^{1}H NMR spectra of CROP mixture ($[C_7H_6S_2P][GaCl_4]$: THF : CH_2Cl_2) = (0.453 mmol : 25 mL : 25 mL) at RT.

g. Attempted CROP by [2][$AlCl_4$]

Attempted polymerization of THF using [**2**][$AlCl_4$] was undertaken at RT with *ca*. 0.3 mmol of [**2**][$AlCl_4$] dissolved in 15 mL of THF. No glutinous solutions were formed after 6 hours and no resonances attributable to poly(THF) were detected. Even though both [**2**][$AlCl_4$] and [**2**][$GaCl_4$] contain the same $\mathbf{2}^+$ cation, their catalytic performances in CROP are dramatically different. This is likely due to the known displacement reaction:[17]

$$AlCl_4^- + THF \longrightarrow AlCl_3{\cdot}n\text{THF} + Cl^-$$

Thus, in the case of [**2**][$AlCl_4$], addition of THF is likely to afford [**2**]Cl which has been shown to be inactive in THF polymerisation. Displacement of Cl^- from $GaCl_4^-$ is

seemingly less favourable. This is supported by the observation of a singlet in the ^{31}P NMR around 161 ppm, diagnostic of [**2**]Cl. In addition crystals of $AlCl_3 \cdot 2THF$ were isolated from attempts to crystallise [**2**][$AlCl_4$] from THF.

h. Number-average molecular weight, M_n

The CROP mechanism assumes each catalyst will generate one 'living' polymer chain. In the case of [**2**][$GaCl_4$] the methyl substituent on the cation has a resonance ($\delta_H \sim 2.25$ ppm) readily distinguishable from the protons of the $\{CH_2CH_2CH_2CH_2O\}_{\boldsymbol{n}}$ (δ_H 1.55-1.61 and 3.37-3.39 ppm) repeat unit. Therefore, the average repeat unit $\boldsymbol{n}$ and the number-average molecular weight ($\mathbf{M_n}$) can be estimated by ^1H NMR spectroscopy *via* end-group analysis.[10]

The detail calculations are explained below:

$$Integral\ per\ proton = \frac{Sum\ of\ CH_3\ proton\ integrals}{3}$$

$$Number\ of\ repeating\ monomer\ units\ \boldsymbol{n} = \frac{Sum\ of\ ((CH_2)_4O)\ proton\ integrals}{8 * (integral\ per\ proton)}$$

$$= 0.375 * \frac{Sum\ of\ ((CH_2)_4O)\ proton\ integrals}{Sum\ of\ CH_3\ proton\ integrals}$$

$$\boldsymbol{M_n} = (Formula\ weight\ of\ C_7H_6S_2P) + (Formula\ weight\ of\ repeating\ unit)(\boldsymbol{n})$$

$$= 185.23 + 72.11(\boldsymbol{n})$$

The CROP of THF by [**2**][$GaCl_4$] affords poly(THF) with the number-average molecular weight ($\mathbf{M_n}$) in a range of 1897-3163, dependent upon polymerization conditions (Table 6.4).

i. Comparison of the CROP of THF using [2][$GaCl_4$] and $H_3PW_{12}O_{40}$

The best THF conversion accomplished by [**2**][$GaCl_4$] (concentration of 18.12 mM stored at room temperature) afforded poly(THF) with conversion of 78% over 24 hours.

Recently the CROP of THF, catalyzed by the Brønsted acid $H_3PW_{12}O_{40}\cdot 13H_2O$,[1a] has been reported with a conversion of *ca.* 63% at 20 ºC in two hours, suggesting that this acid is more active than [**2**][$GaCl_4$]. However the Brønsted acid requires acetic anhydride as a mandatory initiator for polymerization. The molecular weights of the polymers reported here 1897-3163 have comparable molecular weights to those synthesized by the latter catalyst (1360-4535).[1a]

6.2.1.2 Attempted CROP of THF using other main group heterocyclic cations

Given the success of [**2**][$GaCl_4$] in polymerising THF we set about expanding the range of potential cations capable of driving this polymerisation and also the range of substrates (Section 6.2.2).

a. Comparison of CROP of THF by [$C_7H_6S_2E$][$GaCl_4$] (E = P/As/Sb)

The cationic polymerization of THF using [$C_7H_6S_2E$][$GaCl_4$] (E = P, As, Sb) was attempted at concentrations of 20 mM ([$C_7H_6S_2E$][$GaCl_4$]:THF) = (0.3 mmol:15 mL = 0.3:185 mmol = 0.16 mol%) and monitored by ^{1}H NMR (Figure 6.6). After 96 hours, the resultant colourless solution catalyzed by [**2**][$GaCl_4$] offered a gelatinous solution with *ca*. 80% conversion to poly(THF) whereas the heavier pnictogen analogues [$C_7H_6S_2As$][$GaCl_4$] and [$C_7H_6S_2Sb$][$GaCl_4$] appeared fluid with their ^{1}H NMR data reflecting negligible quantities (*ca.* 1.4–2%) of poly(THF) formed in these reaction mixtures.

The lack of catalytic activity may be due to facile elimination of THF from the cationic centre prior to ring opening, or a larger activation barrier to initial ring-opening of the coordinated THF. DFT calculations indicate that initial THF binding becomes more favourable (Table 6.2) on descending the group consistent with the increasing partial charge on descending group 15, with little change in the entropy term. Conversely the Pn-O Wiberg bond index decreases down the group and notably the C-O bond of the THF molecule is not weakened as extensively as with the lighter P analogue (Table 6.2) suggesting a larger activation energy to ROP.

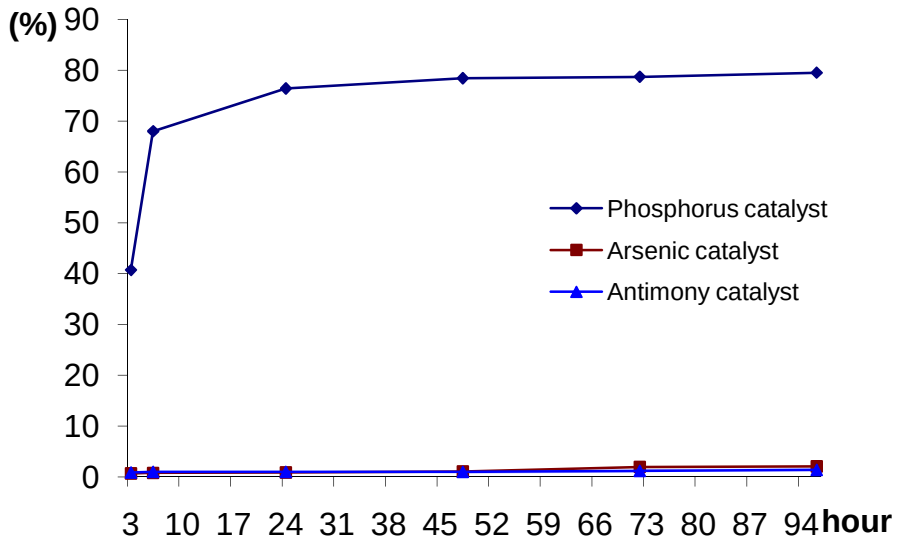

Figure 6.6. Comparison between poly(THF) conversions *vs.* time for $[C_7H_6S_2E][GaCl_4]$ catalysts.

b. CROP of THF by $[C_6H_4(NR)_2P][GaCl_4]$ (R = H or Me)

Given the inability of the heavier pnictogens to efficiently catalyse the CROP of THF, diazaphophenium cations were examined which offer a substantial formal P^+ charge (+1.15 to +1.17, Table 4.4). Initial studies revealed that $[C_6H_4(NH)_2P][GaCl_4]$ exhibited rather poor CROP characteristics with *ca*. 2% conversion to poly(THF) at *ca*. 20 mM. However, at 25 mM concentration polymer conversion was much enhanced with 10.9% conversion after 1 day and 13.3% conversion after 8 days. Notably $[C_6H_4(NH)_2P][GaCl_4]$ (δ_P 212.5 ppm) like [**2**][$GaCl_4$] reacts with THF to form an adduct, evidenced by a singlet at 120.9 ppm in the $^{31}P\{^1H\}$ NMR, suggesting O-coordination to the P centre, *cf.* (^{t}BuN)$_2$P-OEt (δ_P 100.4 ppm).[18] Conversely $[C_6H_4(NMe)_2P][GaCl_4]$ does not polymerize THF at all, although there is a marked shift in the $^{31}P\{^1H\}$ NMR spectrum indicating the absence of $[C_6H_4(NMe)_2P][GaCl_4]$ (δ_P 214.4 ppm) and the formation of new unknown phosphorus species (δ_P 17.1(s) and 5.9 (s) ppm). The difference in reactivity between these two salts may be the potential for $[C_6H_4(NH)_2P]^+$ to undergo elimination of H^+ which could act as a Bronsted acid catalyst for this process. However there was no ^{31}P

NMR evidence for the formation of neutral $C_6H_4(NH)PN$ suggesting this is not a particularly favourable process.

Table 6.4. Summary of the polymerization of THF by different phosphenium catalysts.

Catalyst	Concentration (mmol/L)	Reaction conditions	% conversion	*n*	M_n (g/mol)
[**2**][$GaCl_4$]	9.06	RT, 4 days (THF:CH_2Cl_2 = 1:1)	16.7	-	-
	9.06	RT, 8 days	52.5	23.74	1897
	18.12	RT, 8 days	80.1	41.30	3163
	18.12	50 ^oC, 5 days	44.8	25.50	2024
[**4**][$GaCl_4$]	20.0	RT, 8 days	2.0	-	-
	25.0	RT, 1 day	10.9	-	-
	25.0	RT, 8 days	13.3	-	-
$H_3PW_{12}O_{40}\cdot 13H_2O$[1a]	5.40	RT, 2h, acetic anhydride/cat. = 0.2	63	-	1360-4535

6.2.2 Attempted CROP of propylene oxide or 1,4-dioxane

A large range of cyclic ethers are known to undergo CROP reactions to form polyethers.[1b,1e,1h,1j-m,1o,3b,c,3f,19] In order to examine the substrate scope [**2**][$GaCl_4$] was employed to polymerize propylene oxide and 1,4-dioxane at RT with concentrations of 20 mM (propylene oxide and dioxane serve as monomers and solvents for their reactions, 0.3 mmol catalyst per 15 mL of monomer). The solution of [**2**][$GaCl_4$] turned colourless immediately and NMR spectroscopy was used to examine the reactivity. Upon reacting with THF, propylene oxide, and 1,4-dioxane "[$C_7H_6S_2P$][$GaCl_4$]" (δ_P 57.2 ppm) exhibits a singlet, shifted downfield to 124.4 ppm, 127.4 ppm, and 124.9 ppm respectively consistent with formation of a P-O bond. These S_2PO chemical shifts are similar to but a little lower than similar heterocylic structures previously reported (136.7 ppm,[20] 150.6 ppm[21]). However, no viscous solutions were formed over a 1-hour period and additional NMR studies (after 3, 6 and 48 h) provided no evidence for the formation of poly(ethers).

This would suggest that initial O-coordination is facile but there is a large energy barrier to ring-opening for propylene oxide and 1,4-dioxane.

6.3 Conclusions

A series of studies on the catalytic ability of heterocyclic phosphenium, arsenium, and stibenium salts for CROP of cyclic ethers have been undertaken. These reveal that among the systems tested [**2**][$GaCl_4$] exhibits the highest reactivity with the heavier As and Sb analogues showing limited catalytic activity. Although the ^{31}P NMR data clearly reveal coordination of the substrate to the phosphenium centre, only THF underwent polymerisation with no catalytic activity in CROP towards propylene oxide or dioxane. The polymerization of THF by [**2**][$GaCl_4$] is suppressed at elevated temperature indicating dissociation of the adduct, but at ambient temperatures up to 80% conversion was determined with molecular weights comparable with those reported for the Brønsted acid $H_3PW_{12}O_{40}$.[1a]

6.4 Experimental

***General procedure of ring-opening polymerization**:*

To create a polymerization reaction with a desired concentration of the catalyst, a certain amount (in mL) of cyclic ether (THF, or propylene oxide, or dioxane) was delivered into a Schlenk flask or a sealed 20 mL-disposable vial containing a calculated amount (in g) of test catalyst. This solution was stirred under N_2 at a specific temperature (RT or 50 ^oC). The concentrations in this work covered a range values: 9.06 mM, 18.12 mM, 20 mM, and 25 mM.

With [$C_7H_6S_2E$][MCl_4] (E = P/As/Sb; M = Ga/Al), and [$C_6H_4(NH)_2P$][$GaCl_4$]: the yellow-to-red colour of the catalysts disappeared immediately after adding cyclic ether. Regularly, the resulting colourless solutions became more and more viscous after 1-2 h of stirring; therefore the stir bars could not rotate. ^1H NMR spectra were taken after appropriate periods of time to monitor the polymerization process.

With [$C_6H_4(NMe)_2P][GaCl_4]$: the purple colour was maintained throughout these studies and the reaction mixtures were not gelatinous.

^{1}H NMR (300 MHz, $CDCl_3$): δ_H 1.55-1.61 (2H, m, poly(THF) $C\underline{H_2}CH_2O$); 1.81-1.84 (2H, m, THF $C\underline{H_2}CH_2O$); 3.37-3.39 (2H, m, poly(THF) $CH_2C\underline{H_2}O$); and 3.70-3.73 (2H, m, THF $CH_2C\underline{H_2}O$).

^{31}P{^{1}H} NMR (121.5 MHz, $CDCl_3$):

$[C_7H_6S_2P][GaCl_4]$ in THF: δ_P 124.4 (s)

$[C_7H_6S_2P][AlCl_4]$ in THF: δ_P 161.1 (s) (consistent with $[C_7H_6S_2P]Cl$)

$[C_7H_6S_2P][GaCl_4]$ in propylene oxide: δ_P 127.4 (s)

$[C_7H_6S_2P][GaCl_4]$ in dioxane: δ_P 124.9 ppm (s)

$[C_6H_4(NH)_2P][GaCl_4]$ in THF: δ_P 120.9 (s)

$[C_6H_4(NMe)_2P][GaCl_4]$ in THF: δ_P 17.11 (s) and 5.92 (s).

6.5 References

1. (a) Aouissi, A.; Al-Deyab, S. S.; Al-Shahri, H., *Molecules* **2010**, *15* (3), 1398-1407; (b) Bednarek, M.; Biedroń, T.; Kahłużyński, K.; Kubisa, P.; Pretula, J.; Penczek, S., *Macromol. Symp.* **2000**, *157* (1), 1-12; (c) Cataldo, F., *Eur. Polym. J.* **1996**, *32* (11), 1297-1302; (d) Dagorne, S.; Normand, M.; Kirillov, E.; Carpentier, J.-F., *Coord. Chem. Rev.* **2013**, *257* (12), 1869-1886; (e) Grath James, E. M., Ring-Opening Polymerization: Introduction. In *Ring-Opening Polymerization*, American Chemical Society: 1985; Vol. 286, pp 1-22; (f) Hoene, R.; Reichert, K.-H. W., *D. Makromol. Chem.* **1976**, *177* (12), 3545-3570; (g) Hrkach, J. S.; Matyjaszewski, K., *Macromolecules* **1990**, *23* (18), 4042-4046; (h) Jayakannan, M.; Ramakrishnan, S., *Macromol. Rapid Commun.* **2001**, *22* (18), 1463-1473; (i) Kubisa, P., Cationic Polymerization of Heterocyclics. In Cationic Polymerizations. Matyjaszewski, K., Ed, Ed. Marcel Dekker: New York, NY,

USA: 1996; pp 437-553; (j) Navarro-Llobet, D., Studies of the ring-opening polymerization of cyclic ethers and esters by coordinate catalysis. 3054367, Indiana University, Ann Arbor, **2002**; (k) Nuyken, O.; Pask, S., *Polymers* **2013**, *5* (2), 361-403; (l) Penczek, S.; Kubisa, P., Cationic Ring-Opening Polymerization. In Ring-Opening Polymerization. Brunelle, D.J., Ed. ed.; Hanser Publishers: Munich, Germany: 1993; pp 13-86; (m) Ravve, A., Ring-Opening Polymerizations. In *Principles of Polymer Chemistry*, Springer New York: 2012; pp 253-327; (n) You, L.; Hogen-Esch, T. E.; Zhu, Y.; Ling, J.; Shen, Z., *Polymer* **2012**, *53* (19), 4112-4118; (o) Young, R. J.; Lovell, P. A., Introduction to Ring-Opening Polymerization. In *Introduction to Polymers, Third Edition*, Taylor & Francis: 2011; pp 169-189.

2. (a) Chow, H.-F.; Chan, I. Y.-K.; Mak, C. C.; Man-Kit, N., *Tetrahedron* **1996**, *52* (12), 4277-4290; (b) Dale, J., *Tetrahedron* **1993**, *49* (39), 8707-8725; (c) Rozhanskii, I. L.; Tomita, I.; Endo, T., *Polymer* **1999**, *40* (6), 1581-1591; (d) Stephen Clark, J.; Elustondo, F.; Trevitt, G. P.; Boyall, D.; Robertson, J.; Blake, A. J.; Wilson, C.; Stammen, B., *Tetrahedron* **2002**, *58* (10), 1973-1982.

3. (a) Chivers, T.; Manners, I., Inorganic Rings and Polymers of the *p*-Block Elements: From Fundamentals to Applications. The Royal Society of Chemistry: Cambridge, UK, 2009; pp 212-276; (b) Coulembier, O.; Dubois, P.; Raquez, J. M., Handbook of Ring-Opening Polymerization. Wiley-VCH, Weinheim, Bergstraße: 2008; (c) Kamber, N. E.; Jeong, W.; Waymouth, R. M.; Pratt, R. C.; Lohmeijer, B. G. G.; Hedrick, J. L., *Chem. Rev.* **2007**, *107* (12), 5813-5840; (d) Kennedy, J. P.; Marechal, E., Carbocationic Polymerization. John Wiley & Sons: New York, NY, USA: 1982; pp 95-97; (e) Mark, J. E.; Allcock, H. R.; West, R., *Inorganic polymers 2nd Edn* Oxford University Press: New York, **2005**; (f) Richards, D. H., Ring-Opening Polymerization in the Synthesis of Block Copolymers. In *Ring-Opening Polymerization*, American Chemical Society: 1985; Vol. 286, pp 87-95.

4. Olah, G. A., *D. Makromol. Chem.* **1974**, *175* (4), 1039-1064.

5. (a) Higashimura, T.; Aoshima, S.; Sawamoto, M., *Makromol. Chem. Macromol. Symp.* **1988**, *13-14* (1), 457-471; (b) Matyjaszewski, K., *Makromol. Chem. Macromol. Symp.* **1992**, *60* (1), 107-117; (c) Zhu, Q. Q.; Schnabel, W., *Eur. Polym. J.* **1997**, *33* (8), 1325-1331.

6. Banister, A. J.; Luke, A. W., *J. Polym. Sci. A* **1992**, *30* (12), 2653-2656.

7. Kunnari, S. M.; Oilunkaniemi, R.; Laitinen, R. S.; Ahlgren, M., *J. Chem. Soc., Dalton Trans.* **2001**, (23), 3417-3418.

8. Welch, G. C.; Masuda, J. D.; Stephan, D. W., *Inorg. Chem.* **2006**, *45* (2), 478-480.

9. Bayne, J. M.; Stephan, D. W., *Chem. Soc. Rev.* **2015**.

10. Izunobi, J. U.; Higginbotham, C. L., *J. Chem. Educ.* **2011**, *88* (8), 1098-1104.

11. (a) Ernst, L., *Magn. Reson. Chem.* **2006**, *44* (12), 1135-1135; (b) Quin, L. D.; Williams, A. J., *Practical interpretation of P-31 NMR spectra and computer-assisted structure verification*. Advanced Chemistry Development: Toronto, Ontario, **2004**.

12. (a) Gutowsky, H. S.; McCall, D. W., *J. Chem. Phys.* **1954**, (22), 162-164; (b) Emsley, J. W.; Feeney, J.; Sutcliffe, L. H., *High Resolution Nuclear Magnetic Resonance Spectroscopy*. Elsevier Science: **2013**.

13. (a) Bruker Almanac_Chemical shifts. 1991; (b) Berger; Braun; Kalinowski, *NMR Spektroskopie der Nicht-Metallen_Chemical shifts and couplings*. Georg Thieme Verlag: Stuttgart, **1993**.

14. Lide, D. R., *CRC Handbook of Chemistry and Physics (88th 2007-2008 edition)*. CRC Press: **2007**.

15. Silberberg, M., *Principles of General Chemistry*. McGraw-Hill Companies,Incorporated: **2009**.

16. Plesch, P. H., *The Chemistry of Cationic Polymerisation*. Pergamon Press: Germany, **1963**.

17. Banister, A. J.; Hauptman, Z. V.; Kendrick, A. G.; Small, R. W. H., *J. Chem. Soc., Dalton Trans.* **1987**, (4), 915-924.

18. Burck, S.; Gudat, D.; Nieger, M.; Du Mont, W.-W., *J. Am. Chem. Soc.* **2006**, *128* (12), 3946-3955.

19. Ivin, K. J., *Polymer Handbook*. Wiley: **1975**.

20. Swamy, K. C. K.; Holmes, J. M.; Day, R. O.; Holmes, R. R., *J. Am. Chem. Soc.* **1990**, *112* (16), 6092-6094.

21. Olesiak, M.; Okruszek, A., *Phosphorus Sulfur Silicon Relat. Elem.* **2009**, *184* (6), 1548-1560.

CHAPTER 7

CONCLUSIONS AND FUTURE WORK

In conclusion, this dissertation deals with a series of different derivatives of the dithiazolyl heterocycle in which N is replaced by isoelectronic heavier *p*-block elements (Pn = P, As, Sb) and S by isolobal NR groups. The main themes are concentrated on reactivity of Pn-Cl bonds towards the syntheses and characterizations of five-membered heterocyclic [C_2S_2P] dithiaphospholes and [$C_2(NR)_2P$] diazaphospholes and their heavier *p*-block analogues (As/Sb).

The reduction of P-Cl bonds leads to trivalent P(II) P-P bonded dimers which have a large dimerization enthalpy. The first structure of a dithiaphospholyl dimer is described and found to dimerise *via* 2*c*,2e^- P-P bond formation rather than 4*c*,2e^- bonding typically observed for DTA dimers. Experimental and computational studies reveal dimerization is strongly favoured. Halogenation affords the corresponding *P*-halogeno-1,3,2-benzodithiaphospholes all of which are the first structurally characterised examples of benzodithiaphospholes with P-Cl, P-Br and P-I bonds. Unlike the dithiaphospholes, the reduction of *P*-halogeno-benzodiazaphospholes proved more diverse, depending on reducing reagents, solvent, and reaction time. Although ^{31}P NMR data indicated formation of the reduced products, these were often accompanied by other species arising from oxidation, degradation of the R group or ring fragmentation.

Treatment of these Pn-Cl systems with Lewis acids MCl_3 leads to Lewis acidic phosphenium, arsenium and stibenium cations which form adducts with P and O donors. Structural studies reveal these cationic rings adopt planar five-membered ring geometries which facilitate π-bonding between these heavier *p*-block elements affording 10π-electron structures in which the pnictogen is amphoteric.

Pn-Cl bond metathesis leads to new structures such as the P and As paddlewheels $N(C_7H_6S_2Pn)_3$, as well as the diazaphosphenium derivative, $(C_6H_4(NCOOMe)_2P)$-$N(COOMe)C_6H_4N(COOMe)$-$(P(NCOOMe)_2C_6H_4)$.

The salt $[C_7H_6S_2P][GaCl_4]$ is efficient for the CROP of THF but arsenic and antimony analogues have low activity. Notably $[C_6H_4(NH)_2P]^+$ has modest activity and $[C_6H_4(NMe)_2P]^+$ shows no activity. The reactivity of $AlCl_4^-$ salts differs from the $GaCl_4^-$ salts due to formation of stable $AlCl_3$.2THF and reformation of the parent phosphenium chloride salt which is inactive towards cationic polymerisation.

Future work

This research has identified and structurally characterised the first dithiaphosphole dimer containing P(II) and which is found to exhibit a $2c,2e^-$ P-P σ-bond. Preliminary studies revealed this bond was susceptible to oxidation with halogenating agents but a more expansive study of its chemistry would be desirable. Can these dithiaphospholes undergo oxidation with group 16 elements O_2, S_8 or Se to form terminal P=E or bridging P-E-P units (E = O, S, Se) in an analogous fashion to the reactivity of P-P bonds in P_4?[1] In addition these systems are potentially capable of undergoing oxidative addition to low valent transition metals in an analogous fashion to disulfides, RSSR [2].[2] The chemistry of P(II) is predominantly limited to a series of compounds of formula P_2X_4 (X= F, Cl, Br, I, CN)[1] so the development of this dithiaphosphole chemistry will be an interesting comparison to these derivatives. For example P_2I_4 reacts with S_8 to form $P_2I_4S_2$ with terminal P=S bonds.[1] This thesis focused on two simple dithiaphospholes, $[C_6H_4S_2P]_2$ and $[C_7H_6S_2P]_2$ but approaches to diversify the chemistry to access a wider range of benzo-functionalised derivatives would expand the potential to tailor the electronic and steric demands of the substituents to see how this affects reactivity (and radical stability). In this context recent work by S. Kosnik [Macdonald group, U. Windsor] in conjunction with the Rawson group has shown that oxidative addition of tetrathiocins $[4,5\text{-}(MeO)_2C_6H_2S_2]_2$ to P(I) salts leads to formation of the dimethoxy-functionalised benzo-dithiaphosphole (Figure 7.1), offering an alternative synthetic strategy to access these heterocycles.

Figure 7.1. Molecular structure of $[(MeO)_2C_6H_2S_2P]_2$ (courtesy of S. Kosnik).

The absence of a signal in the ^{31}P NMR spectrum of $[C_7H_6S_2P]^+$ (+415 ppm) at ambient temperature (only evident at -80 ^oC, Figure 7.2) suggests a complex equilibrium in solution which is also sensitive to the ratio of *P*-chloro-dithiaphosphole and Lewis acid. Clearly at ambient temperature free phosphenium cations are not present in significant quantities and so it is less clear what active species is present when considering the reactivity of such dithiaphosphenium cations, *e.g.* CROP. Functionalisation of the benzodithiaphosphole may permit some of these species to be isolated in the solid state, providing a greater insight into the reactivity of these heterocycles. Although the phosphenium cations appeared capable of polymerising THF, less success was achieved with propylene oxide and dioxane. A wider range of substatres can be examined including ε-caprolactone[2] and $(NPCl_2)_3$[3] which are also known to undergo CROP.

Crystallographic studies on the paddlewheel compounds $(C_7H_6S_2Pn)_3N$ reveal two different conformations and it would be interesting to repeat these studies to identify if they form as a mixture of two isomers (PXRD) or as a single isomer which would suggest some potential differences in the mechanistic pathway. In addition these compounds offer the potential to act as tripodal neutral S_3 donors analogous to 9-ane-S_3 $(C_6H_{12}S_3)$[4] to metal centres yet their coordination chemistry is unexplored.

Although the reactivity of the diazaphospholes in part mimics that of the dithiaphospholes, reduction of the diazaphospoholes appears more problematic and sensitive to reducing conditions. Alternative mild reducing agents such as Mg(I) reagents developed by Jones[5] may prove to be efficient $1e^-$ reducing agents for these derivatives. Previous work[6] has shown that these diazaphospholes exhibit weaker dimerization enthalpies for sterically demanding NR substituents and further work should combine the

potential for further π-delocalisation coupled with the established steric protection to inhibit dimerization.

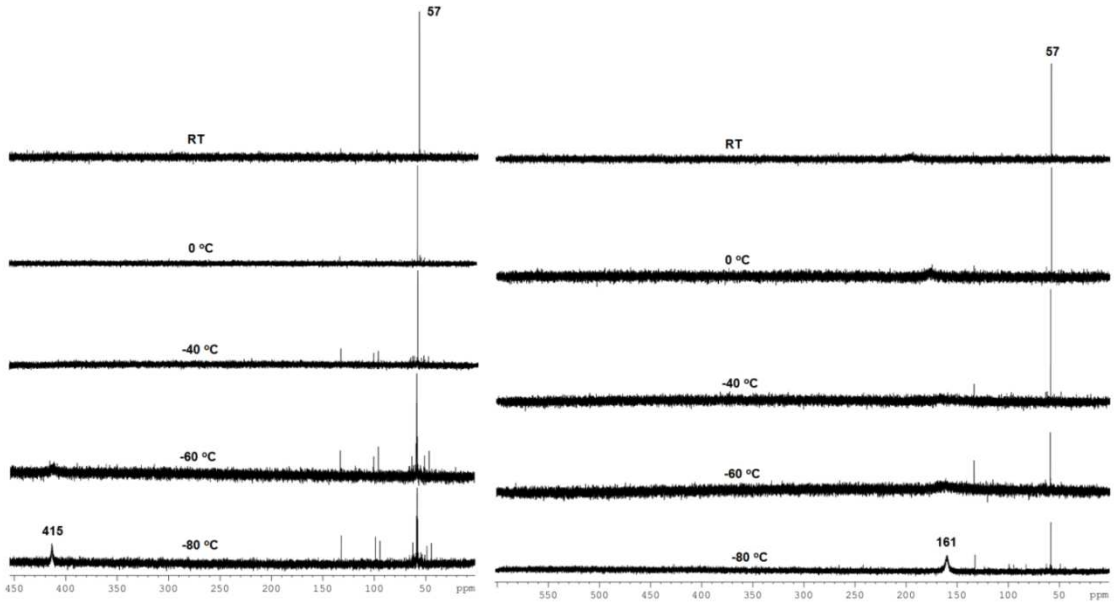

Figure 7.2. (Left) $C_7H_6S_2PCl$:$GaCl_3$ (1:1) (50 mg of $C_7H_6S_2PCl$) in CD_2Cl_2 (2 mL); (right) $C_7H_6S_2PCl$:$GaCl_3$ (2:1) (50 mg of $C_7H_6S_2PCl$) in CD_2Cl_2 (2 mL).

References

1. Greenwood, N. N.; A. Earnshaw, A., *Chemistry of the Elements*. Pergamon Press, Oxford: 1986.

2. Liu, Y.-C.; Ko, B.-T.; Lin, C.-C., *Macromolecules* **2001**, *34* (18), 6196-6201.

3. Zhang, Y.; Huynh, K.; Manners, I.; Reed, C. A., *Chem.Commun.* **2008**, (4), 494-496.

4. Todd, A. M.; Swinburne, A. N.; Goeta, A. E.; Steed, J. W., *New J. Chem.* **2013**, (37), 89-96.

5. Ma, M.; Stasch, A.; Jones, C., *Chem. Eur.J.* **2012**, (18), 10669 - 10676.

6. Edge, R.; Less, R. J.; McInnes, E. J. L.; Muther, K.; Naseri, V.; Rawson, J. M.; Wright, D. S., *Chem. Commun.* **2009**, *0* (13), 1691-1693.

APPENDICES

Appendix 1. Crystallographic data for [**1**]Cl, [**2**]X (X = Cl; Br; I), and (**1**)$_2$.

	[1]Cl	**(1)$_2$**	**[2]Cl**	**[2]Br**	**[2]I**
Empirical Formula	$C_6H_4ClPS_2$	$C_{12}H_8P_2S_4$	$C_7H_6ClPS_2$	$C_7H_6BrPS_2$	$C_7H_6IPS_2$
Formula Weight	206.63	342.36	220.66	265.12	312.11
Temperature/K	173(2)	173(2)	173(2)	173(2)	173(2)
Wavelength/Å	0.71073	0.71073	0.71073	0.71073	0.71073
Crystal System	monoclinic	monoclinic	monoclinic	monoclinic	monoclinic
Space Group	$P2_1/n$	$P2_1/n$	$P2_1/c$	$P2_1/c$	$P2_1/c$
a/Å	6.0177(11)	7.2588(15)	7.9354(13)	8.1085(18)	9.6746(10)
b/Å	17.011(3)	6.1271(12)	15.016(3)	8.4527(19)	12.2785(13)
c/Å	8.0037(14)	15.846(3)	7.5386(13)	13.436(3)	8.3822(9)
α/°	90.00	90.00	90.00	90.00	90.00
β/°	97.1936(18)	104.17(3)	91.7942(17)	91.7942(17)	102.7120(10)
γ /°	90.00	90.00	90.00	90.00	90.00
V/Å^3	812.9(3)	683.3(2)	897.844	919.6(4)	971.31(18)
Z	4	2	4	4	4
Density calc./g·cm^{-3}	1.688	1.664	1.632	1.915	2.134
Abs. coeff., μ/mm^{-1}	1.094	0.905	0.996	5.028	3.825
F(000)	416	348	448	520	592
Crystal size/mm^3	0.18 × 0.15 × 0.14	0.18 × 0.16 × 0.08	0.27 × 0.17 × 0.15	0.18 × 0.16 × 0.08	0.28 × 0.23 × 0.18
θ range for data collection/°	2.39-28.15	3.58-28.24	2.57 – 28.31	3.75-28.17	2.16-28.26
Index ranges	$-7 \le h \le +7$ $-22 \le k \le +22$ $-10 \le l \le +10$	$-9 \le h \le +9$ $-8 \le k \le +8$ $0 \le l \le +20$	$-10 \le h \le +10$ $-19 \le k \le +19$ $-9 \le l \le +9$	$-10 \le h \le +10$ $-11 \le k \le +11$ $0 \le l \le +17$	$-12 \le h \le +12$ $-15 \le k \le +15$ $-10 \le l \le +10$
Reflections Collected	8905	3367	9944	3939	10893
R_{int}	0.0517	0.0428	0.0485	0.0630	0.0332
Independent Reflections	1902	3347	2123	2142	2273
Data/restraints/parameters	1902/0/91	3347/0/83	2123/0/101	2142/0/101	2273/0/101
Goodness of fit (S) (all)	1.048	1.020	1.046	1.121	1.037
R_1 and wR_2 (I> 2σ(I)]	0.0332, 0.0827	0.0628, 0.1579	0.0304, 0.0766	0.0855, 0.2130	0.0250, 0.0635
R_1 and wR_2 (all data)	0.0370, 0.0857	0.0807, 0.1675	0.0335, 0.0790	0.1148, 0.2279	0.0269, 0.0649
Residual peak/hole (e−/Å^3)	+0.47, -0.21	+0.69, -0.44	+0.49, -0.27	+1.37, -2.27	+1.69, -0.47
Structure code	TT01	TT02	TT06	TT07	TT05

Appendix 2. License Agreement with Royal Society of Chemistry provided by Copyright Clearance Center to reproduce figure in Chapter 3.

ROYAL SOCIETY OF CHEMISTRY LICENSE TERMS AND CONDITIONS

Aug 28, 2015

This is a License Agreement between Thao Tran ("You") and Royal Society of Chemistry ("Royal Society of Chemistry") provided by Copyright Clearance Center ("CCC"). The license consists of your order details, the terms and conditions provided by Royal Society of Chemistry, and the payment terms and conditions.

All payments must be made in full to CCC. For payment instructions, please see information listed at the bottom of this form.

License Number	3697651134169
License date	Aug 28, 2015
Licensed content publisher	Royal Society of Chemistry
Licensed content publication	Chemical Communications (Cambridge)
Licensed content title	Formation of a new class of 7π radicals via sterically induced P–P bond cleavage of the dimers [(CH)2(NR)2P]2
Licensed content author	Ruth Edge,Robert J. Less,Eric J. L. McInnes,Kristine Müther,Vesal Naseri,Jeremy M. Rawson,Dominic S. Wright
Licensed content date	Feb 13, 2009
Issue number	13
Type of Use	Thesis/Dissertation
Requestor type	academic/educational
Portion	figures/tables/images
Number of figures/tables /images	1
Format	print and electronic
Distribution quantity	10
Will you be translating?	no
Order reference number	None
Title of the thesis/dissertation	Heavy p-block analogues of thiazyl radicals
Expected completion date	Dec 2015
Estimated size	200
Total	0.00 CAD

Appendix 3. Crystallographic data for [**5**]Cl, [**6**]Cl, [**7**]Cl, and [**8**]OCl.

	[5]Cl	**[6]Cl**	**[7]Cl**	**[8]OCl**
Empirical Formula	$C_{10}H_{10}ClN_2O_4P$	$C_{10}H_{10}ClN_2O_2P$	$C_8H_{10}ClN_2P$	$C_{10}H_{14}ClN_2OP$
Formula Weight	288.62	256.62	200.60	244.65
Temperature/K	150(2)	150(2)	173(2)	150(2)
Wavelength/Å	0.71073	0.71073	0.71073	0.71073
Crystal System	monoclinic	triclinic	orthorhombic	orthorhombic
Space Group	$P2_1/c$	P-1	$P2_12_12_1$	Pbca
a/Å	8.2892(10)	8.3151(5)	5.8257(8)	8.3820(4)
b/Å	8.7581(10)	9.0480(5)	10.0332(14)	15.7453(7)
c/Å	16.863(2)	9.4371(5)	16.210(2)	17.3537(8)
α/°	90.00	64.292(2)	90.00	90.00
β/°	100.340(6)	71.834(2)	90.00	90.00
γ /°	90.00	63.772(2)	90.00	90.00
V/Å^3	1204.4(3)	567.49(6)	947.5(2)	2290.29(18)
Z	4	2	4	8
Density calc./g·cm^{-3}	1.592	1.502	1.406	1.419
Abs. coeff., μ/mm^{-1}	0.458	0.463	0.517	0.448
F(000)	592	264	416	1024
Crystal size/mm^3	0.50 × 0.20 × 0.18	0.30 × 0.15 × 0.13	0.12 × 0.11 × 0.07	0.47 × 0.04 × 0.03
θ range for data collection/°	2.46 - 30.23	2.42 - 26.37	2.39 - 27.81	2.48 - 24.99
Index ranges	$-11 \le h \le +11$ $-12 \le k \le +11$ $-20 \le l \le +23$	$-8 \le h \le +10$ $-10 \le k \le +11$ $-11 \le l \le +11$	$-7 \le h \le +7$ $-12 \le k \le +13$ $-20 \le l \le +21$	$-9 \le h \le +9$ $-18 \le k \le +18$ $-20 \le l \le +20$
Reflections Collected	10042	7070	9861	16610
R_{int}	0.0359	0.0199	0.0520	0.0603
Independent Reflections	3484	2297	2118	2010
Data/restraints/parameters	3484/0/165	2297/42/147	2118/0/111	2010/0/138
Goodness of fit (S) (all)	1.130	1.103	1.200	1.482
R_1 and wR_2 ($I > 2\sigma(I)$]	0.0511, 0.1189	0.0263, 0.0709	0.0387, 0.0940	0.1083, 0.1918
R_1 and wR_2 (all data)	0.0597, 0.1228	0.0275, 0.0716	0.0412, 0.1000	0.1111, 0.1929
Residual peak/hole (e^-/Å^3)	+0.50, -0.48	+0.26, -0.23	+0.44, -0.22	+0.48, -0.52
Structure code	TT2103	jmrcolplatesp	JH12	AD03

Appendix 4. Crystallographic data for [**5**]$_2$O, C_6H_4(NMe[**7**])$_2$, [**5**]OMe.

	[5]$_2$O	**C_6H_4(NMe[7])$_2$**	**[5]OMe**
Empirical Formula	$C_{20}H_{20}N_4O_9P_2$	$C_{24}H_{30}N_6P_2$	$C_{11}H_{13}N_2O_5P$
Formula Weight	522.34	464.48	284.20
Temperature/K	150(2)	173(2)	173(2)
Wavelength/Å	0.71073	0.71073	0.71073
Crystal System	monoclinic	monoclinic	orthorhombic
Space Group	C2/c	C2/c	Pnma
a/Å	22.700(4)	25.454(4)	8.5140(5)
b/Å	16.826(4)	8.5115(14)	11.8714(7)
c/Å	13.049(2)	10.9147(18)	12.6840(8)
α/°	90.00	90.00	90.00
β/°	116.152(8)	91.272(2)	90.00
γ /°	90.00	90.00	90.00
V/Å^3	4473.8(14)	2364.2(7)	1282.01(13)
Z	12	4	4
Density calc./g·cm^{-3}	1.551	1.305	1.472
Abs. coeff., μ/mm^{-1}	0.256	0.209	0.233
F(000)	2160	984	592
Crystal size/mm^3	0.30 × 0.15 × 0.13	0.30 × 0.26 × 0.22	0.31 × 0.11 × 0.04
θ range for data collection/°	2.65 - 25.00	1.60 - 28.19	2.88 - 26.42
Index ranges	$-22 \le h \le +26$ $-19 \le k \le +19$ $-13 \le l \le +15$	$-33 \le h \le +33$ $-11 \le k \le +10$ $-13 \le l \le +13$	$-10 \le h \le +10$ $-14 \le k \le +14$ $-15 \le l \le +15$
Reflections Collected	5675	13090	15385
R_{int}	0.0410	0.0440	0.0210
Independent Reflections	3529	2792	1380
Data/restraints/parameters	3529/0/303	2792/0/149	1380/0/93
Goodness of fit (S) (all)	1.153	1.056	1.078
R_1 and wR_2 ($I > 2\sigma(I)$]	0.1021, 0.2138	0.0416, 0.1114	0.0355, 0.0843
R_1 and wR_2 (all data)	0.1488, 0.2368	0.0463, 0.1181	0.0465, 0.0912
Residual peak/hole (e−/Å^3)	+0.90, -0.40	+0.34, -0.28	+0.23, -0.35
Structure code	jmrphosdim	TT09A	Thao18

Appendix 5. Crystallographic data for [**2**][$GaCl_4$], [**7**][$GaCl_4$], [**9**][$GaCl_4$], and [**9**]Cl.

	[2][$GaCl_4$]	**[7][$GaCl_4$]**	**[9]Cl**	**[9][$GaCl_4$]**
Empirical Formula	$C_7H_6Cl_4GaPS_2$	$C_8H_{10}Cl_4GaN_2P$	$C_7H_6AsS_2Cl$	$C_7H_6AsCl_4Ga\ S_2$
Formula Weight	396.73	376.67	264.63	440.68
Temperature/K	153(2)	173(2)	150(2)	150(2)
Wavelength/Å	0.71073	0.71073	0.71073	0.71073
Crystal System	monoclinic	orthorhombic	monoclinic	monoclinic
Space Group	$P2_1/c$	Pbca	$P2_1/c$	$P2_1/m$
a/Å	8.0083(16)	13.840(3)	6.0319(5)	11.409(4)
b/Å	9.2891(19)	10.993(2)	15.6876(14)	7.015(2)
c/Å	18.572(4)	18.396(3)	9.6731(6)	17.742(6)
α/°	90.00	90.00	90.00	90.00
β/°	96.23(3)	90.00	90.601(8)	102.483(3)
γ /°	90.00	90.00	90.00	90.00
V/Å^3	1373.41	2798.9(9)	915.28(13)	1386.4(8)
Z	4	8	4	4
Density calc./g·cm^{-3}	1.919	1.788	2.007	2.111
Abs. coeff., μ/mm^{-1}	3.166	2.818	4.395	5.390
F(000)	776	1488	544	848
Crystal size/mm^3	0.30 × 0.30 × 0.30	0.30 × 0.20 × 0.15	0.66 × 0.27 × 0.17	0.30 × 0.03 × 0.02
θ range for data collection/°	2.21 - 28.44	2.21 - 27.92	2.47 - 30.69	1.95 - 27.54
Index ranges	$-10 \le h \le +10$ $-12 \le k \le +12$ $-4 \le l \le +24$	$-17 \le h \le +18$ $-14 \le k \le +14$ $-24 \le l \le +24$	$-8 \le h \le +8$ $-22 \le k \le +22$ $-13 \le l \le +13$	$-14 \le h \le +14$ $-9 \le k \le +9$ $-22 \le l \le +22$
Reflections Collected	3320	27923	25149	15899
R_{int}	0.0590	0.0484	0.0245	0.0385
Independent Reflections	3320	3220	2772	3426
Data/restraints/para-meters	3320/0/138	3220/0/147	2772/0/102	3426/0/177
Goodness of fit (S) (all)	1.062	1.076	1.260	1.019
R_1 and wR_2 ($I > 2\sigma(I)$]	0.0464, 0.1087	0.0253, 0.0640	0.0191, 0.0467	0.0221, 0.0605
R_1 and wR_2 (all data)	0.0607, 0.1186	0.0290, 0.0667	0.0212, 0.0484	0.0252, 0.0625
Residual peak/hole (e^-/Å^3)	+0.77, -0.83	+0.40, -0.26	+0.53, -0.32	+0.54, -0.42
Structure code	TT24	AD03	TT2048c	TT42

Appendix 6. Crystallographic data for N[**2**]$_3$, N[**9**]$_3$.

	N[2]$_3$	**N[9]$_3$**
Empirical Formula	$C_{21}H_{18}N\,P_3S_6$	$C_{21}H_{18}As_3NS_6$
Formula Weight	569.63	701.48
Temperature/K	150(2)	150(2)
Wavelength/Å	0.71073	0.71073
Crystal System	trigonal	triclinic
Space Group	P-3	P-1
a/Å	12.134(2)	11.277(7)
b/Å	12.134(2)	11.671(7)
c/Å	11.246(2)	12.023(7)
α/°	90.00	76.122(9)
β/°	90.00	67.953(7)
γ /°	120.00	87.177(8)
V/Å^3	1434.0(5)	1422.4(15)
Z	2	2
Density calc./g·cm^{-3}	1.319	1.638
Abs. coeff., μ/mm^{-1}	0.655	3.954
F(000)	584	692
Crystal size/mm^3	0.14 × 0.13 × 0.04	0.13 × 0.05 × 0.02
θ range for data collection/°	1.81-27.53	1.95-27.49
Index ranges	$-15 \le h \le +15$ $-15 \le k \le +15$ $0 \le l \le +14$	$-13 \le h \le +14$ $-14 \le k \le +15$ $0 \le l \le +15$
Reflections Collected	6447	6382
R_{int}	0.0353	0.0000
Independent Reflections	2214	6382
Data/restraints/parameters	2214/0/96	6382/0/273
Goodness of fit (S) (all)	1.255	1.136
R_1 and wR_2 (I> 2σ(I)]	0.0993, 0.2888	0.0836, 0.1573
R_1 and wR_2 (all data)	0.1054, 0.2888	0.1184, 0.1676
Residual peak/hole ($e-$/Å^3)	+1.39, -0.49	+1.07, -1.81
Structure code	TT22	TT43

VITA AUCTORIS

NAME:	Thao Thi Phuong Tran
PLACE OF BIRTH:	Vietnam
YEAR OF BIRTH:	1981
EDUCATION:	Hochiminh City University of Technology, B.Sc., Vietnam, 2004
	Hochiminh City University of Technology, M.Sc., Vietnam, 2007
	University of Windsor, PhD, Canada, 2015